Signalling and Regulation of the Glucagon-like Peptide-1 Receptor

Thesis submitted for the degree of Doctor of Philosophy
at the University of Leicester

by

Jing Lu BSc

Department of Cell Physiology and Pharmacology
University of Leicester

May 2014

Signalling and Regulation of the Glucagon-like Peptide-1 receptor

Following nutrient ingestion, glucagon-like peptide 1 (GLP-1) secreted from intestinal L-cells mediates anti-diabetic effects, most notably stimulating glucose-dependent insulin release from pancreatic β-cells but also inhibiting glucagon release, promoting satiety and weight reduction and potentially enhancing or preserving β-cell mass. These effects are through the GLP-1 receptor (GLP-1R) which is a therapeutic target in type 2 diabetes. The present study focused on desensitisation and re-sensitisation of GLP-1R-mediated signalling and interactions of orthosteric and allosteric ligands. Data demonstrate GLP-1R desensitisation and subsequent re-sensitisation following removal of extracellular ligand with ligand-specific features. Following GLP-1-mediated desensitisation, re-sensitisation is dependent on receptor internalisation, endosomal acidification and receptor recycling. Re-sensitisation is also dependent on endothelin converting enzyme-1 (ECE-1) activity, possibly through proteolysis of GLP-1 in endosomes, facilitating disassociation of receptor-β-arrestin complexes leading to GLP-1R recycling and re-sensitisation. ECE-1 activity also regulates GLP-1-induced activation of extracellular signal regulated kinase (ERK) and generation of cAMP possibly through a G protein independent/β-arrestin dependent mechanism. By contrast, following GLP-1R activation by the orthosteric agonist, exendin-4, or allosteric agonist, compound 2, re-sensitisation was slow and independent of ECE-1 activity. Thus, different ligands depend on different events during GLP-1R trafficking which could be important for re-sensitisation and signalling, particularly that mediated by scaffolding around β-arrestin.

As the GLP-1R is targeted therapeutically at orthosteric and allosteric sites, this study examined activation of the GLP-1R by orthosteric and allosteric agonists and in particular interactions between ligands of these sites. Challenging the GLP-1R with the allosteric ligand, compound 2, along with GLP-1 9-36 amide, a low affinity, low efficacy metabolite of GLP-1 7-36 amide, results in synergistic receptor activation. This may be important for therapeutic approaches with allosteric ligands, as metabolites of GLP-1 may be present *in vivo* at concentrations higher than the classic endogenous ligand. Indeed this could present a novel therapeutic approach.

ACKNOWLEDGEMENTS

Firstly, I would like to express my sincerest appreciation and thanks to my supervisor Dr Gary Willars. You have given me great trust, encouragement and support during my PhD study. Thank you for your each advice for the progress of my project. Thank you for all your contribution to help with my talk preparation and thesis correction. All the things I learnt from you are priceless and will be enormously helpful for the development of my future career.

I would also like to acknowledge my committee members Dr Terry Herbert and Dr Nina Storey for their contributions towards the project and my progress.

Special thanks go to Dr Yan Huang and Dr Naichang Li who have provided me with scientific advice and support on my project. I have learnt brilliant experimental techniques and research skills from you. Thanks also go to group members Khaled, Omar, Manish and Neil.

I am also very grateful for the support of the Advanced Imaging Facility from Dr. Kees Staatman (Department of Biochemistry, University of Leicester). I would also like to thank Dr. Jianling Xie, Dr. Gabrielle Le Provost, Dr. Craig Nash, Xuechan Zhao, Qi Cheng and all my friends in CPP for your never ending support.

Finally, I would like to thank my Mum and Dad for understanding me and both financially and mentally supporting me during my PhD study. I would never have been able to finish the study without your company through the internet. I would also like to thank my grandparents especially my grandma. You will always live in my heart.

Without these people, this thesis would never have been possible. Thank you all.

ABBREVIATIONS

$[Ca^{2+}]_i$	concentration of intracellular Ca^{2+}
[^{3}H]-cAMP	[2,8-^{3}H]-adenosine 39, 59-cyclic phosphate, ammonium salt
3D	3 dimensional
AC	adenylyl cyclase
ACE	angiotensin-converting enzyme
ANOVA	analysis of variance
AP	adaptor protein complex
β-arrestin1-GFP	GFP-tagged β-arrestin1
β-arrestin2-GFP	GFP-tagged β-arrestin2
β_1AR	β_1-adrenoceptor
β_2AR	β_2-adrenoceptor
$AT_{1A}R$	angiotensin II type 1A receptor
AT_1R	angiotensin II type 1 receptor
AT_2R	angiotensin II type 2 receptor
ATI	angiotensin I
ATII	angiotensin II
ATP	adenosine-5'-triphosphate
big ET	big endothelin-1
bp	base pair
BRET	bioluminescence resonance energy transfer
BSA	bovine serum albumin
$Ca^{2+}{}_i$	intracellular Ca^{2+}
cAMP	cyclic adenosine 3', 5'-monophosphate
CaM	calmodulin (calcium-modulated protein)
CCPs	clathrin-coated pits
cDNA	complementary DNA
CGRP	calcitonin gene-related peptide
CHL	Chinese hamster lung
CHO	Chinese hamster ovary
CHO-GLP-1R	Chinese hamster ovary cells expressing GLP-1R
CICR	Ca^{2+}-induced Ca^{2+} release
CK-I	casein kinase-I

CK-II	casein kinase-II
CLR	calcitonin receptor-like receptor
CREB	cAMP-responsive element binding-protein
CRF	corticotropin-releasing factor
CRF_1	corticotropin-releasing factor receptor 1
DAG	diacylglycerol
DMEM	Dulbecco's modified Eagle medium
DMSO	dimethyl sulfoxide
DNA	deoxyribonucleic acid
dNTPs	deoxynucleotide triphosphates
DPP-IV	dipeptidyl peptidase IV
D_1R	dopamine D_1 receptor
D_2R	dopamine D_2 receptor
DTT	dithiothreitol
EC_{50}	concentration given 50% of the maximal response
ECE	endothelin-converting enzyme
ECE-1	endothelin-converting enzyme-1
ECE-1a	endothelin-converting enzyme-1 isoform a
ECE-1b	endothelin-converting enzyme-1 isoform b
ECE-1c	endothelin-converting enzyme-1 isoform c
ECE-1d	endothelin-converting enzyme-1 isoform d
ECE-1a-mCherry	C-terminal mCherry-tagged ECE-1a
ECE-1b-mCherry	C-terminal mCherry-tagged ECE-1b
ECE-1c-GFP	C-terminal GFP-tagged ECE-1c
ECE-1c-mCherry	C-terminal mCherry-tagged ECE-1c
ECE-1d-mCherry	C-terminal mCherry-tagged ECE-1d
ECE-2	endothelin-converting enzyme-2
ECL	extracellular loop
EDTA	ethylenediaminetetraacetic acid
EEA1	early endosomal antigen 1
ELISA	enzyme-linked immunosorbent assay
EGF	epidermal growth factor
EGFP	enhanced green fluorescence protein
EGFR	epidermal growth factor receptor
Epac	exchange protein directly activated by cAMP

ER	endoplasmic reticulum
ERK	extracellular signal-regulated kinase
ET-1	endothelin-1
ET_A	endothelin receptor type A
ET_B	endothelin receptor type B
FCS	fetal calf serum
FLAG-ECE-1	N-terminal FLAG epitoge-tagged ECE-1
FU	fluorescence units
G418	Geneticin
G6PDH	glucose-6-phosphate dehydrogenase
$GABA_B$	type B receptor for gamma-aminobutyric acid
GDM	gestational diabetes mellitus
GDP	guanosine diphosphate
GEF	guanine nucleotide exchange factor
GFP	green fluorescence protein
GFP-ECE-1a	N-terminal terminal GFP-tagged ECE-1a
GFP-ECE-1b	N-terminal terminal GFP-tagged ECE-1b
GFP-ECE-1c	N-terminal terminal GFP-tagged ECE-1c
GIP	gastric inhibitory polypeptide
GIP-R	gastric inhibitory polypeptide receptor
GLP-1	glucagon-like peptide-1
GLP-1R	glucagon-like peptide-1 receptor
GLP-1R-GFP	C-terminal GFP-tagged GLP-1R
GLP-2	glucagon-like peptide-2
GLUT	glucose transporter
GPCR	G protein-coupled receptor
GRK	G protein-coupled receptor kinase
GRP	G protein-coupled receptor phosphatase
GRPP	glicentin-related pancreatic peptides
GTP	guanosine triphosphate
HA	hemagglutinin
HbA_{IC}	glycosylated hemoglobin
HEK293	human embryonic kidney 293 cell line
HEK-GLP-1R	HEK293 cells expressing GLP-1R
HEK-GLP-1R-EGFP	HEK293 cells expressing C-terminal EGFP-tagged GLP-1R

HPLC	high-performance liquid chromatography
HUVEC	human umbilical vein endothelial cells
IBMX	3-isobutyl-1-methylxanthine
ICL	intracellular loop
IIGI	isoglycemic intravenous glucose infusion
IP_3	inositol 1, 4, 5 trisphosphate
IP_3R	inositol 1, 4, 5 trisphosphate receptor
IP1	intervening peptide-1
IP2	intervening peptide-2
IRS	insulin receptor substrate
JNK	c-Jun N-terminal kinases
K_{ATP}	ATP-sensitive potassium channel
K_V	voltage-dependent K^+ channel
KHB	Krebs'-HEPES buffer
KHB-BSA	KHB containing 0.1% *w:v* BSA
KNRK	Kirsten murine sarcoma virus-transformed rat kidney cells
LB	Luria-Bertani
MAPK	mitogen-activated protein kinase
MEM	minimum essential *medium*
MPGF	major proglucagon fragment
mRNA	messenger RNA
mTOR	mammalian target of rapamycin
MWt	molecular weight
NEB	New England Biolabs
NEP	neutral endopeptidase-24.11
NFAT	nuclear factor of activated T-cells
NF-κB	nuclear factor kappa-light-chain-enhancer of activated B cells
NHS	National Health Service
NK_1R	neurokinin 1 receptor
NTD	amino terminal extracellular ($-NH_2$) domain
OD	optical density
OGTT	oral glucose tolerance test
p90RSK	p90 ribosomal S6 kinase
PAGE	polyacrylamide gel electrophoresis
PAR1	protease-activated receptor 1

PBS	phosphate buffered saline
PC	prohormone convertase
PC1	prohormone convertase 1
PC2	prohormone convertase 2
PC3	prohormone convertase 3
PCR	polymerase chain reaction
PDE	phosphodiesterase
PDX-1	pancreatic and duodenal homeobox factor-1
pEC_{50}	negative logarithm of the concentration given 50% of the maximal response
PIP_2	phosphatidylinositol 4, 5-bisphosphate
PKA	protein kinase A
PKB	protein kinase B
PKC	protein kinase C
PLC	phospholipase C
PLCβ	β isoform of phospholipase C
PMA	phorbol 12-myristate 13-acetate
PP-1β	protein phosphatase-1β
PP-2A	protein phosphatase type 2A
pro-ET	pro-endothelin
PTH	parathyroid hormone
PTHR	parathyroid hormone receptor
PTHrP	parathyroid hormone-related peptide
PVDF	polyvinylidene fluoride
RAMP1	receptor activity-modifying protein 1
RE	restriction endonucleases
RGS	regulators of G protein signalling
rh	recombinant human
Rho-GLP-1 7-36 amide	N-terminal rhodamine-labeled GLP-1 7-36 amide
RNA	ribonucleic acid
RPMI1640	Roswell Park Memorial Institute medium 1640
RT	room temperature
RT-PCR	reverse transcription polymerase chain reaction
RyR	ryanodine receptor
S.E.M.	standard error of the mean

SGLT	sodium-glucose co-transporter
siRNA	small interfering RNA
SP	substance P
TCA	trichloroacetic acid
TM	transmembrane domain
TSH	thyroid-stimulating hormone
TZD	thiazolidinedione
Ucn1	urocortin 1
UV	ultraviolet
VDCC	voltage-dependent Ca^{2+} channel
VIP	vasoactive intestinal peptide
$VPAC_2$	type 2 receptor for vasoactive intestinal peptide
V2R	vasopressin type 2 receptor
WHO	World Health Organization

PUBLICATION

Peer-reviewed publication:

Li, N., **Lu, J**. and Willars, G.B. (2012) Allosteric modulation of the activity of the glucagon-like eptide-1 (GLP-1) metabolite GLP-1 9-36 amide at the GLP-1 receptor. *PLoS ONE* 7 e47936 1-10

Selway, J., Rigatti, R., Storey, N., **Lu, J.**, Willars, G.B. and Herbert, T.P. (2011) Evidence that Ca^{2+} within the microdomain of the L-type voltage gated Ca^{2+} channel activates ERK in MIN6-cells in response to glucagon-like peptide-1. *PLoS ONE* 7 e330004 1-10

Abstracts:

Lu J, Li NC, Willars GB (2012) Signalling by the glucagon-like peptide-1 (GLP-1) receptor: interactions between the ago-allosteric agent ‘compound 2' and the major GLP-1 metabolite, GLP-1 9-36 amide. pA_2 Online 10 (4) 089P

Lu J, Willars GB (2013) Endothelin-converting enzyme-1 regulates the re-sensitisation of signalling by the glucagon-like peptide-1 receptor. Acta Pharmacologica Sinica 34 Suppl. S8.29

Lu J, Willars GB (2014) Ligand-dependent desensitization and re-sensitization of GLP-1R has been accepted for the publication on pA_2 Online.

TABLE OF CONTENTS

CHAPTER 1 General Introduction

1.1. Diabetes

Diabetes is a group of metabolic diseases characterized by hyperglycemia induced by defects of insulin secretion, insulin action or both (American Diabetes Association, 2011). Uncontrolled diabetes may lead to acute and life-threatening issues (Van Ness-Otunnu and Hack, 2013, Umpierrez and Kitabchi, 2003) whereas long-term diabetes is associated with the development of secondary complications (Sheikh-Ali et al., 2013, Pinhas-Hamiel and Zeitler, 2007, Barnett, 2005). According to the World Health Organization (WHO), globally, there were approximately 285 million people with diabetes in 2010 and the number is expected to reach 438 million by 2030. In the UK in 2009, 2.6 million people had diagnosed diabetes and this number may increase to more than 4 million by 2025 according to Diabetes UK. Diabetes not only reduces life quality, but also brings a huge burden on healthcare costs. It was reported in 2012 by Diabetes UK that the NHS's annual spending on diabetes in the UK would increase from £9.8 billion to £16.9 billion over the next 25 years which would be 17% of its entire budget. The report also suggested that the cost of treating diabetic complications might be double from the current total of £7.7 billion to £13.5 billion by 2035 (Diabetes, 2012).

Insulin is released from granules in β-cells of the pancreatic islets of Langerhans in response to increased blood glucose concentration (Maechler, 2012). Insulin is the main hormone controlling intermediary metabolism and triggers the uptake and storage of blood glucose by muscle, liver and fat. In patients with diabetes, an absolute or relative insufficiency of insulin impairs the control of glucose homeostasis resulting in an elevated plasma glucose level compared to that in healthy subjects (Niswender, 2011, Edelman et al., 1990, Moore et al., 2012). The WHO defines the current diagnostic criteria for diabetes as a fasting plasma glucose concentration ≥ 7.0 mmol/L and a level of ≥ 11.1 mmol/L 2 h after a 75 g oral glucose load.

1.1.1. Type 1 and type 2 diabetes

The major forms of diabetes are type 1 and type 2, other specific types of diabetes and gestational diabetes mellitus (GDM). Type 1 diabetes is characterized by a cellular-mediated autoimmune destruction of the pancreatic β-cells, usually leading to absolute insulin deficiency. The proportion of patients with type 1 diabetes accounts for 5-10% of the total (American Diabetes Association, 2011). This type of diabetes is generally considered to be caused by genetic predisposition and possibly environmental factors such as viral infections, immunization, diet, vitamin D deficiency and perinatal factors (Knip et al., 2005, Morahan, 2012). Type 1 diabetes normally occurs in childhood and adolescence although it could happen at any age (Groop and Pociot, 2014). Treatment of patients with type 1 diabetes is by the injection of insulin. Type 2 diabetes, a major type of diabetes accounting for approximately 90-95% of total cases, is characterized by insulin resistance, which usually leads to relative insulin deficiency without β-cell destruction (American Diabetes Association, 2011). The causes of type 2 diabetes are not clearly defined, but is often associated with obesity, which itself generally causes insulin resistance (Virally et al., 2007). In fact, insulin-evoked glucose disposal is impaired in obese subjects (Reaven, 2013). This type of diabetes usually develops fairly slow and patients are often undiagnosed for many years. At the early stages, as insulin resistance appears, a healthy pancreas is able to compensate by increasing insulin secretion and β-cell mass (Araújo et al., 2013). However, as the disease advances, there is a progressive decline in β-cell function and mass resulting from increased β-cell death by apoptosis and decreased β-cell proliferation (Puff et al., 2011, Butler et al., 2003). This results in a loss of the compensatory mechanism and β-cells fail to respond to the growing requirement for insulin leading to hyperglycemia. The treatments for the patients with type 2 diabetes are diverse and will be described in **section 1.1.3.**. Other specific types of diabetes result from causes such as genetic defects in insulin action, exocrine pancreas dysfunction and drug or chemical-induced side effects and GDM happens during pregnancy. These two types of diabetes represent a very small proportion of total diabetes cases (American Diabetes Association, 2011).

1.1.2. Symptoms and complications

Under hyperglycemic conditions, the ability of the kidney to reabsorb glucose is exceeded and it spills over into the urine. This causes an osmotic diuresis (polyuria) followed by increased drinking (polydipsia). The inability of insulin-sensitive cells to take up glucose results in the metabolism of fat which induces weight loss, which in turn, leads to increased eating (polyphagia). Uncontrolled diabetes can lead to acute problems including diabetic ketoacidosis that results from the increased breakdown of fat to acetyl-CoA and hyperosmolar hyperglycemic syndrome. Both of these conditions are life-threatening (De Beer et al., 2008).

Long-term diabetes is virtually always associated with the development of secondary complications including macrovascular diseases (eg. coronary artery disease and peripheral artery disease) and microvascular diseases (eg. nephropathy, neuropathy and retinopathy) which is a result of microvascular changes. Diabetic retinopathy may be the most common complication of diabetes and may lead to blindness (Fong et al., 2004). The exact mechanisms leading to these complications are complex and not fully understood. Diabetes associated abnormalities in energy production could be a key factor in the development of diabetic complications (Forbes and Cooper, 2013). In addition, inhibition of glucose-6-phosphate dehydrogenase (G6PDH) by high glucose levels may lead to oxidative stress and the accumulation of sorbitol increased as a consequence of flux of glucose through aldose reductase which may result in osmotic stress that contribute to the development of diabetic complications (Singh et al., 2011, Forbes and Cooper, 2013, Zhang et al., 2000).

1.1.3. Current treatments for type 2 diabetes

Oral hypoglycaemic agents for treating type 2 diabetes include metformin, sulfonylureas, thiazolidinediones (TZDs) and α-glucosidase inhibitors like acarbose. They show great clinical benefits in various aspects when used either singly or in combination although many have adverse effects. Metformin improves insulin

sensitivity by increasing glucose uptake and utilization in skeletal muscle. It also inhibits hepatic glucose production, although the mechanism is unclear (Wiernsperger and Bailey, 1999, Chai et al., 2012). The side effects of metformin include anorexia and gastrointestinal disturbances such as diarrhoea and nausea (Hirst et al., 2012). Sulfonylureas stimulate insulin secretion by inhibition of β-cell K_{ATP} channels (Panten et al., 1996). However, chronic treatment with sulfonylureas is commonly associated with impairment of its acute insulintropic action (Takahashi et al., 2007). It can also cause hypoglycaemia as insulin release is evoked independently of the prevailing plasma glucose concentration (Lapane et al., 2013). The α-glucosidase inhibitors block glucose absorption, but the unabsorbed glucose is fermented by coliform bacteria in the gastrointestinal tract producing gas in the intestines (Garber, 2010). TZDs are also insulin sensitizers but show adverse effects such as a decrease in bone density (Garber, 2010).

As the disease progresses and β-cell function and mass are reduced, the oral agents fail to maintain the glycemic control. Treatment with insulin is then required for these patients. However, insulin therapy is commonly associated with wide excursions of blood glucose levels including hypoglycaemia. It is also associated with weight gain and possibly colorectal cancer (Chiasson, 2009).

1.2. The incretin-based therapies for type 2 diabetes

The incretin effect was defined following experiments that showed orally ingested glucose evokes much higher insulin release than intravenous glucose injection despite identical blood glucose concentrations. Indeed, the incretin effect can account for up to 70% of glucose-induced insulin release in healthy subjects (Deacon and Ahrén, 2011, Nauck et al., 1986). However, in patients with type 2 diabetes, the incretin effect is largely impaired **(Fig 1.1.)** (Bagger et al., 2011).

1.2.1. GIP and GLP-1

In 1970, the first incretin hormone, glucose-dependent insulinotropic polypeptide or gastric inhibitory polypeptide (GIP), was found by Brown and colleagues (Brown and Pederson, 1970). It was then reported that GIP has the ability to stimulate insulin secretion at physiological doses in a glucose-dependent manner (Ding and Gromada, 1997). GIP is released from K-cells in the proximal small intestine and targets the GIP receptor (GIP-R). However, more than 50% of the incretin effect remains after removal of GIP (Ebert et al., 1983). Other peptides were then identified including glucagon-like peptide-1 (GLP-1), which has considerable insulinotropic activities at physiological levels (Kreymann et al., 1987, Mojsov et al., 1987). GLP-1 not only stimulates insulin release from pancreatic β-cells in a glucose-dependent manner, but also promotes the transcription of proinsulin and insulin biosynthesis. It also shows both anti-apoptotic and pro-proliferative effects on β-cells (Farilla et al., 2002, Farilla et al., 2003). In addition, other anti-diabetic effects include the inhibition of glucagon secretion from pancreatic α-cells, suppression of gastric emptying and appetite reduction (Garber, 2010). All these effects are mediated via binding to its receptor, the GLP-1 receptor (GLP-1R), which will be described later **(section 1.3.3.)**. Type 2 diabetes is associated with a progressive decrease in β-cell mass and function, an increase in glucagon release and is often associated with obesity (Butler et al., 2003, Li et al., 2013a, Eckel et al., 2011) suggesting that targeting the GLP-1 systems may be a valuable therapeutic approach. Indeed, in patients with type 2 diabetes, the incretin effect is reduced due to a reduction in GLP-1 but not GIP secretion (Vilsbøll et al., 2001). However, the insulintropic effects of GLP-1 are largely preserved in type 2 diabetes. In contrast, the incretin effects of GIP are severely impaired even if the concentration is increased to the pharmacological range (Vilsbøll et al., 2002). Therefore, the GLP-1 system (both the ligand and receptor) have developed into targets for the treatment of type 2 diabetes.

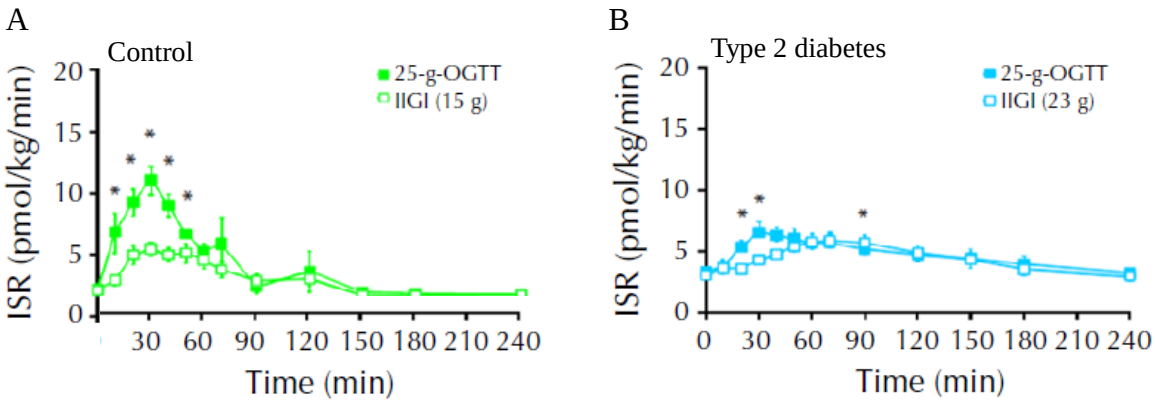

Fig 1.1. Impaired regulation of the incretin effects in patients with type 2 diabetes. Insulin secretion rates (ISR), defined as picomoles insulin secreted per minute per kilogram body weight, in healthy control subjects **(A)** and patients with type 2 diabetes **(B)** following 25 g oral glucose loads (closed symbols: OGTT, oral glucose tolerance test) or corresponding isoglycemic intravenous glucose infusion (open symbols: IIGI).. *, $p < 0.05$. Adapted from Bagger et al., 2011.

1.2.2. GLP-1 synthesis and secretion

The mRNA of proglucagon, transcribed from the proglucagon gene is translated into the proglucagon peptide, which produces different peptides by differential post-translational processing that differs in different tissues. Prohormone convertase (PC) enzymes are responsible for this tissue-specific processing of proglucagon. In pancreatic α-cells, proglucagon is generally cleaved by PC2 and produces glicentin-related pancreatic peptides (GRPP), glucagon, intervening peptide-1 (IP1) and the major proglucagon fragment (MPGF). MPGF is further cleaved by PC1/3, yielding GLP-1 (**Fig 1.2.A**) (Lee and Jun, 2014). In gut and brain, GLP-1 is produced by the cleavage of proglucagon by PC1/3 associated with the production of other peptides including GRPP, oxyntomodulin, intervening peptide-2 (IP2) and GLP-2 (**Fig 1.2.B**) (Lee and Jun, 2014).

GLP-1 is mainly secreted from intestinal L-cells in response to nutrient ingestion such as fats, proteins and carbohydrates (Perfetti and Merkel, 2000). The secretion of GLP-1 shows a biphasic pattern in response to feeding, with an early phase initiating within minutes and lasting for 30-60 min and a second phase lasting for 1-3 h after a meal (Sinclair and Drucker, 2005). GLP-1 secretion is regulated via a complex mechanism. First and foremost, it is regulated via a glucose-sensing mechanism. Both metabolizable sugar and non-metabolizable sugar can trigger GLP-1 release by closure of K_{ATP} channels and stimulation of sodium-glucose co-transporters (SGLTs) respectively in L-cells (Gribble et al., 2003). Given that there are a lot more L-cells in the distal gut than proximal gut, it is proposed that the early phase of GLP-1 secretion may result from the indirect stimulation of L-cells. An indirect neutrally-mediated signalling in non-L-cells of the proximal gut is proposed to indirectly stimulate GLP-1 release from L-cells of the distal gut (Chandra and Liddle, 2012). Nevertheless, although the proportion of L-cells in the proximal gut is relatively small, a model of direct stimulation is supported by the suggestion that glucose induced activation of gustducin-coupled sweet receptors expressed in proximal L-cells leads to GLP-1 secretion from the same L-cells (Jang et al., 2007). Additionally, GLP-1 is released in

response to the stimulation of many GPCRs in the intestine. For example, GPR119 is activated by natural lipid amides and GPR40, GPR120 and TGR5 (bile acid receptor) can be stimulated by fatty acids (Whalley et al., 2011, Lee and Jun, 2014). Stimulation of these receptors activates PC1 promoters and enhances GLP-1 release from intestinal L-cells (Whalley et al., 2011). Moreover, PC1 is also found in pancreatic α-cells and GLP-1 secretion has been reported in pancreatic α-cell lines and human islets (Whalley et al., 2011). Interestingly, elevated GLP-1 secretion but impaired glucagon secretion from pancreatic α-cells and islets were determined in response to supra-physiological glucose levels and this was associated with an increased level of PC1 expression. Expression of GPR119, GPR120 and TGR5 was also observed in αTC1-6 cells where the activity of the PC1 promoter was up-regulated by a TGR5 agonist. Furthermore, GLP-1 secretion was promoted in response to TGR5 stimulation while glucagon secretion was inhibited (Whalley et al., 2011). GLP-1 secretion from α-cells is also enhanced in islets with damaged β-cells which may be a consequence of the up-regulation of PC1 (Whalley et al., 2011, Nie et al., 2000). Therefore, the level of GLP-1 secretion from pancreatic α-cells is predominantly dependent on the expression of PC1 which could be regulated by GPCRs.

Following post-translation processing of proglucagon to generate GLP-1 1-37, this is further processed to generate GLP-1 7-37 and COOH-terminally amidated GLP-1 1-36 amide and GLP-1 7-36 amide (Kreymann et al., 1987). GLP-1 7-37 and GLP-1 7-36 amide are the two major bioactive forms of GLP-1 with GLP-1 7-36 amide being largely responsible for the incretin effects of GLP-1 following a meal (Edwards et al., 1999).

The range of biological effects of GLP-1, coupled with the preservation of its insulinotropic effect in type 2 diabetes, suggest that GLP-1 would be a suitable therapy. However, GLP-1 requires injection. Furthermore, it is rapidly degraded in the body by dipeptidyl peptidase IV (DPP-IV, also known as CD26) and has a short half-life of only 1-2 min (Kieffer et al., 1995). DPP-IV cleaves the two N-terminal amino acid residues

generating GLP-1 9-37 or GLP-1 9-36 amide **(Fig 1.2.C)**, which are generally considered to be either inactive or even antagonists of the GLP-1R (Hansen et al., 1999). For these reasons, GLP-1 analogues have been developed that are insensitive to DPP-IV. DPP-IV inhibitors have also been developed. DPP-IV resistant GLP-1 analogues or DPP-IV inhibitors are used as mono-therapies or in combination with other oral anti-diabetic agents. These are discussed below.

A. Pancreatic α-cells

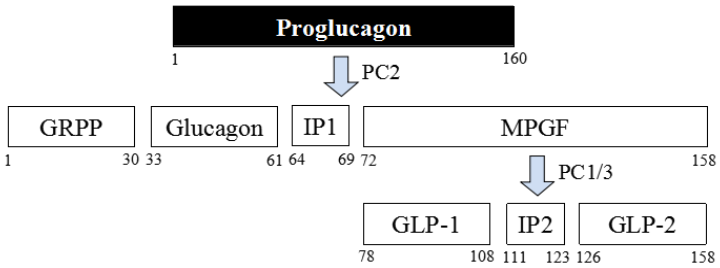

B. Intestinal L-cells and brain

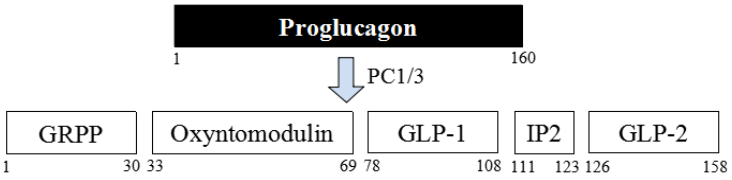

C.

DPP-IV

GLP-1 7-37 HAEGTFTSDVSSYLEGQAAKEFIALLVKGRG

GLP-1 7-36 amide HAEGTFTSDVSSYLEGQAAKEFIALLVKGR amide

GLP-1 9-37 EGTFTSDVSSYLEGQAAKEFIALLVKGRG

GLP-1 9-36 amide EGTFTSDVSSYLEGQAAKEFIALLVKGR amide

Fig 1.2. The post-translational process of proglucagon and GLP-1. A. In pancreatic α-cells, proglucagon peptide (1-160) can be cleaved by PC2 and produces the peptides glicentin-related pancreatic peptides (GRPP, 1-30), glucagon (33-61), intervening peptide-1 (IP1, 64-69) and major proglucagon fragment (MPGF, 72-158). MPGF can be further cleaved by PC1/3 yielding GLP-1 (78-108), intervening peptide-2 (IP2, 111-123) and GLP-2 (126-158). **B.** In intestinal L-cells and brain, proglucagon can be processed by PC1/3 and produces GRPP, oxyntomodulin (33-69), GLP-1, IP2 and GLP-2. **C**. GLP-1 7-37 and GLP-1 7-36 amide can be cleaved by dipeptidyl peptidase IV (DPP-IV) to generate the metabolites GLP-1 9-37 and GLP-1 9-36 amide respectively. The cleavage site is indicated by the arrow and the continued dashed line. Picture A and B are adapted from Lee and Jun, 2014.

1.2.3. GLP-1 analogues and DDP-IV inhibition

There are two GLP-1 analogues registered for the treatment of type 2 diabetes, exenatide and liraglutide. Exenatide is a synthetic version of exendin-4, a hormone found in the saliva of the Gila monster. This peptide shares 53% amino acid homology with GLP-1. Importantly exendin-4 has a glycine residence at the position equivalent to 8 in GLP-1 where it is an alanine. As a consequence, exenatide is somewhat resistant to DDP-IV cleavage and has a longer half-life in the body than GLP-1 (Sinclair and Drucker, 2005) allowing twice daily injection. A once-weekly formulation of exenatide has been developed (long-acting release; LAR). Liraglutide (NN2211) shares 97% sequence homology to GLP-1 with only one amino acid substitution ($Lys^{34}Arg$) and the addition of an acyl group linked to Lys^{26} leading to the extension of half-life to 10-12 h, which allows once-daily treatment (Juhl et al., 2002). Both exenatide and liraglutide efficiently reduce glycosylated hemoglobin (HbA_{IC}) level demonstrating improved control and prevent hypoglycemia. Cardiovascular safety is always a concern associated with long-term drug treatment for diabetes. The more traditional anti-diabetic agents such as TZDs, sulfonylureas and insulin have been reported to have adverse cardiovascular effects (Singh et al., 2013). Interestingly, native GLP-1 shows cardioprotective effects (Petrie, 2013, Mannucci and Rotella, 2008) and treatment with GLP-1 analogues impacts on many cardiovascular risk factors. For example, both exenatide and liraglutide have benefits including weight loss, blood pressure reduction and an improvement in fasting lipids levels (Petrie, 2013). However, both exenatide and liraglutide are associated with gastro-intestinal-related side effects, commonly inducing nausea. Although these therapies can offer improved diabetic control and a low risk of hypoglycemia due to the glucose-dependence of GLP-1R-mediated insulin release, these therapies still require injection. Additionally, prolonged treatment with especially exenatide may increase the risk of pancreatitis (Garber, 2010).

An alternative to GLP-1 analogues is to extend the life of endogenous GLP-1 using DPP-IV inhibitors. Clinically-used DPP-IV inhibitors (eg. sitagliptin, saxagliptin and

linagliptin) double the level of circulating GLP-1 and can prolong the half-life of GLP-1 analogues. DPP-IV inhibitors also efficiently reduce the HbA_{IC} levels and effectively limit postgrandial hyperglycemia (Petrie, 2013). As DPP-IV inhibitors are orally active, they are much more convenient for clinical use. They have also been reported to have some cardioprotective effects but have limited effects on weight loss and blood pressure reduction (Petrie, 2013). Incretin-based therapies including GLP-1 analogues and DPP-IV inhibitors have significant advantages in treating type 2 diabetes not only with respect of reducing plasma glucose levels, but also in preventing side effects including hypoglycemia and cardiovascular disease.

1.2.4. Small-molecule agonists of the GLP-1R

The imperfections of treatment with GLP-1 analogues or DPP IV inhibitors have encouraged the search for small-molecule and orally active drugs that mimic the physiological functions of GLP-1. By high-throughput screening of large chemical libraries, several small-molecular agonists have been discovered, including compound 2 (6,7-dichloro-2-methylsulfonyl-2-N-tert- butylaminoquinoxaline) (Knudsen et al., 2007), compound B (4-(3-(benzyloxy) phenyl)-2-(ethylsulfinyl)-6-(trifluoromethyl) pyrimidine) (BETP) (Sloop et al., 2010) and Boc5 (1,3-bis [[4-(tert-butoxy-carbonylamino) benzoyl]amino]-2,4-bis[3-methoxy-4-(thiophene-2-carbonyloxy)-phenyl]cyclobutane-1, 3-dicarboxylic acid) (Chen et al., 2007). Both compound 2 and compound B do not compete with GLP-1 for binding and have intrinsic efficacy (ago-allosteric agonists). They stimulate insulin secretion in pancreatic islets in a glucose-dependent manner (Knudsen et al., 2007, Sloop et al., 2010). However, whether they have other anti-diabetic effects such as weight loss and β-cell survival is unclear. Boc5, the first non-peptidic GLP-1R agonist, stimulates glucose-dependent insulin releases and inhibits food intake in diabetic mice (Chen et al., 2007, Su et al., 2008). However, the binding site of Boc5 is unclear. It is proposed to bind in the extracellular region of the GLP-1R and may overlap to some extent with the orthosteric binding site (Wootten et al., 2013). Additionally, both compound 2 and compound B can promote Boc5-mediated

responses suggesting distinct binding sites (Wootten et al., 2013). The pharmacological perspective of allosteric agonists of the GLP-1R will be discussed further below.

1.3. G protein-coupled receptors (GPCRs)

The G protein-coupled receptors (GPCRs) or 7-transmembrane domain receptors constitute the largest family of plasma membrane receptors. They are involved in many diseases and are targets for around 40% of drugs. This type of receptor regulates various functions including metabolism, secretion, electrical activity, shape and motility of most cells in response to neurotransmitters, hormones, ions and sensory stimuli (Stevens et al., 2013). GPCRs consist of seven transmembrane α helices with an extracellular N-terminal domain and an intracellular C-terminal domain joined by a series of extracellular and intracellular loops. These receptors conduct signalling via coupling to heterotrimeric G proteins. However, it has been apparent for many years that some receptors which do not consist of 7 transmemebrane helices can also activate signalling via G proteins (Patel, 2004). The following will focus on GPCRs (7-transmemebrane domain receptors).

1.3.1. GPCR classification

This super-family of receptors can be classified into three families based on sequence similarities including the length of the extracellular N terminus. Family A is the largest family which accounts for ~85% of the GPCR genes. These receptors are also called rhodopsin-like receptors and have a short extracellular N terminal tail. Ligands bind to the transmembrane helices or to extracellular loops. Receptors for most amine neurotransmitter and many neuropeptides belong to this family. Family B receptors, also called the secretin/glucagon receptor family, have an intermediate extracellular N terminal tail length comprising the ligand-binding domain. The receptors for peptide hormones including secretin and glucagon are in this family. The smallest family, family C, contains metabotropic glutamate receptors, gamma-aminobutyric acid type B ($GABA_B$) receptors and Ca^{2+}-sensing receptors. These receptors have a long extracellular N terminal tail containing ligand binding domain.

1.3.2. The activation and classification of G proteins

Heterotrimeric G proteins consist of three subunits, α, β, γ, with the α subunit being responsible for binding guanine nucleotides. At the resting state, G proteins are assembled as a heterotrimer with GDP bound to the α subunit. G proteins (α, β, γ) associate with the cell membrane due to palmitoylation. When a GPCR is activated by ligand binding, the conformation of the receptor changes resulting in high affinity for a G protein. The G protein binds with the activated receptor causing GDP to disassociate from the α subunit with the subsequent binding of GTP as a consequence of the activity of guanine nucleotide exchange factors (GEF), which in this case is the GPCR. This results in the disassociation of α-GTP from the βγ complex. The released α-GTP and βγ diffuse in the place of the membrane and interact with various enzymes and ion channels. Such interaction with α subunits can result in either activation or inhibition dependent on the specific Gα subunit. Each α subunit has intrinsic GTPase activity which hydrolyzes GTP to GDP. The interaction with effectors or regulators of G protein signalling (RGS) proteins can increase the activity of the intrinsic GTPase (Sowa et al., 2000, Magalhaes et al., 2012). The α-GDP then disassociates from the effectors and reunites with βγ complex awaiting the next round of activation **(Fig 1.3)**.

There are more than 20 subtypes of α subunits with four main classes; $G\alpha_s$, $G\alpha_{i/o}$, $G\alpha_q$ and $G\alpha_{12/13}$. They show binding selectivity to both receptors and effectors allowing specificity of coupling, although a number of receptors have been shown to be promiscuous in terms of G protein coupling. Both $G\alpha_s$ and $G\alpha_i$ interact with adenylyl cyclase (AC) causing activation and inhibition respectively. Activation of AC increases cyclic adenosine 3', 5'-monophosphate (cAMP) production which in turn activates protein kinase A (PKA), cAMP-gated ion channels and Epac (exchange proteins directly activated by cAMP) therefore regulating cellular functions (Gancedo, 2013, Gloerich and Bos, 2010). $G\alpha_q$ activates phospholipase C (PLC) which cleaves phosphatidylinositol 4, 5-bisphosphate (PIP_2) into inositol 1, 4, 5 trisphosphate (IP_3) and diacylglycerol (DAG) respectively stimulating Ca^{2+} release from the intracellular store

and activating protein kinase C (PKC) (Kadamur and Ross, 2013).

The Gβγ dimer was originally considered only to be required for the inactivation of the Gα subunit. However, it is clear that they modulate the activity of many intracellular effectors including PLCβ (Camps et al., 1992), specific AC isoforms (Tang and Gilman, 1991) and ion channels such as voltage-dependent Ca^{2+} channels (VDCC) (Ikeda, 1996), via direct interaction. There are 5 Gβ and 12 Gγ subunits which could form 60 possible combinations. They have specific tissue expression and show broad distribution in sub-cellular compartments including endosomes, mitochondria, endoplasmic reticulum (ER), Golgi apparatus, cytoplasm and the nucleus (Khan et al., 2013) suggesting diverse cellular roles.

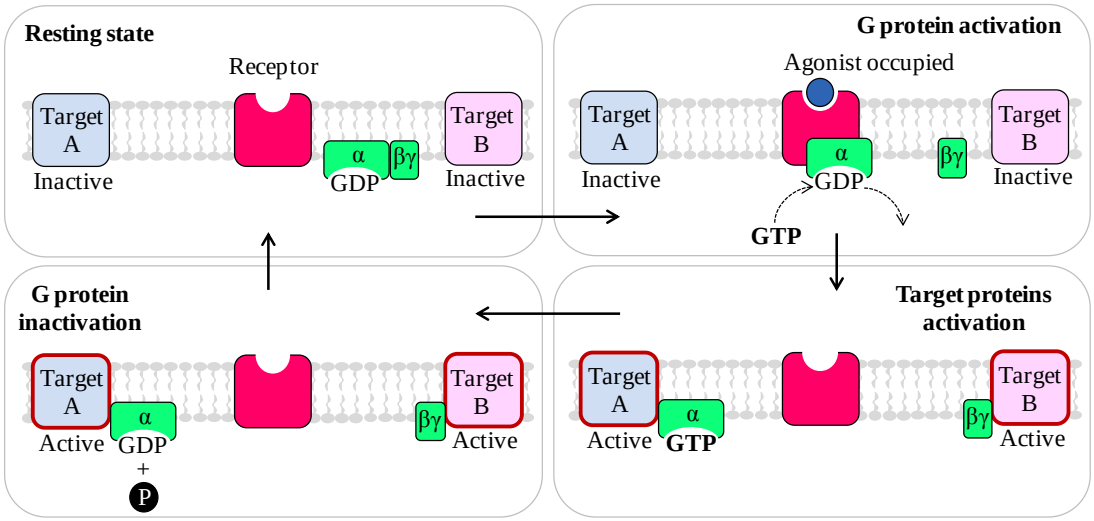

Fig 1.3. The activation of G proteins. In the resting state, heterotrimeric G proteins consisting of α, β and γ subunits distribute in the cell membrane due to palmitoylation. In response to agonist stimulation, the GPCR undergoes a conformational change, facilitating binding of the G protein. The subsequent conformational change of the G protein results in disassociation of GDP and binding of GTP. The binding of GTP causes disassociation of the α subunit from the βγ complex, both of which are then able to interact with effector molecules (Targets A/B). The increased GTPase activity of the α subunit then hydrolyzes GTP to GDP leading to the recombination of the G protein complex.

1.3.3. GLP-1R

1.3.3.1. The distribution and structure of GLP-1R

In addition to the pancreas, the GLP-1R is also found in lung, brain, kidney, stomach and heart in Man (Wei and Mojsov, 1995). The wide distribution of GLP-1R highlights potentially diverse functions of GLP-1 beyond lowing plasma glucose level. Therefore understanding the structure-based activation of GLP-1R is essential.

The GLP-1R is a member of Family B GPCRs and as such has a typical 7-transmembrane domain (TM_{1-7}) structure with 3 extracellular loops (ECL_{1-3}), 3 intracellular loops (ICL_{1-3}), an amino terminal extracellular ($-NH_2$) domain (NTD) and an intracellular carboxyl (-COOH) terminus. Commonly for Family B GPCRs, the endogenous ligand binds to the receptor following the 'two domain model' in which the C-terminus of the peptide interacts with the NTD of the receptor and the N-terminus of the ligand subsequently interacts with the core domain of the receptor including both the ECL and the TM (Hoare, 2005). Similar to other Family B GPCRs, there are 6 highly conserved cysteine residues located in the NTD of the GLP-1R to form three disulfide bonds which are critical for binding of the endogenous ligand. Denaturing the NTD results in a complete loss of affinity for GLP-1 (Bazarsuren et al., 2002). Nevertheless, GLP-1 binds with the isolated NTD of the GLP-1R with a reduced affinity (Xiao et al., 2000) implying the core domain also contributes to GLP-1 binding. By contrast, the complete removal of the core domain had no impact on exendin-4 binding (López de Maturana et al., 2003) suggesting the binding of exendin-4 may not rely on the core domain. Furthermore, both the removal of N-terminal His^7 of the ligand GLP-1 7-37 (GLP-1 8-37) or the inclusion of the full N-terminus of the ligand (GLP-1 1-37) results in more than 300-fold lower affinity (Mojsov, 1992). By contrast, the N-terminal truncated exendin-4 (up to 8 amino acids) maintains high affinity (Al-Sabah and Donnelly, 2003). To date a number of residues of the receptor have been reported to be responsible for the binding of the N-terminus of GLP-1, including Lys^{197} and Asp^{198}

(TM_2/ECL_1), Lys^{202} and Asp^{215} (ECL_1), Arg^{227} and Lys^{288} (TM_4/ECL_2) and Arg^{310} (TM_5) (Xiao et al., 2000, López de Maturana and Donnelly, 2002, Al-Sabah and Donnelly, 2003, Coopman et al., 2011). Although evidence for the interaction between exendin-4 and the core domain of the GLP-1R is limited **(see above)**, a study has reported that mutation of residues including Tyr^{152} (TM_1), Arg^{190} (TM_2) and Tyr^{235} (TM_3) reduced the affinities of GLP-1 7-36 amide and exendin 9-39 amide to similar extents (Coopman et al., 2011) implying these residues have general structural functions.

The GLP-1R is primarily coupled to $G\alpha_s$-containing heterotrimeric G proteins to mediate signalling through the generation of cAMP, although coupling to other G proteins has been reported (Montrose-Rafizadeh et al., 1999, Coopman et al., 2010, Hällbrink et al., 2001). Residues in ICL_3 and ICL_3/TM_5 regions have been shown critical for efficient signalling. Mutation of ^{334}LysLeuLys^{336} in IC_3 and Val^{327}, Ile^{328} and Val^{331} at the junction of ICL_3/TM_5 of the rat GLP-1R significantly reduces cAMP production without influencing GLP-1 binding and receptor expression (Takhar et al., 1996, Mathi et al., 1997). Residues of Lys^{197} (TM_2), Tyr^{284} (ECL_2) and Arg^{310} (TM_5) have more profound impact on potency than affinity of GLP-1 (Coopman et al., 2011) suggesting these residues are critical for receptor activation. Additionally, there is a residue located on ECL_1 and others located on ECL_2 that have been reported to be important for agonist binding and/or efficacy (Heller et al., 1996, Koole et al., 2012). Although GLP-1 1-36 amide shows lower affinity than GLP-1 7-36 amide at the GLP-1R, they both show similar intrinsic activity in cAMP generation (Koole et al., 2012). However, the metabolite, GLP-1 9-36 amide, generated by the hydrolysis of GLP-1 7-36 amide by DPP-IV, displays low affinity and weak activity (Montrose-Rafizadeh et al., 1997) suggesting that His^7 of the ligand is essential in both binding and function. Interestingly, although the N-terminus of exendin-4 is not critical for binding, it does play an important role in activity. Importantly, the N-terminal truncated version of GLP-1 7-36 amide, exendin 9-39 amide, is actually an antagonist of the GLP-1R with high affinity (Montrose-Rafizadeh et al., 1997) again highlighting the importance of the N-terminus of the ligand in receptor activation.

Knowledge about the binding sites for allosteric ligands is limited. In contrast to the endogenous ligand, both compound 2 and compound B activates the NTD-truncated version of GLP-1R suggesting they interact with the core domain (Huang, 2010, Sloop et al., 2010). Compound 2 acts via $G\alpha_s$ and generates cAMP with a lower activity than GLP-1 7-36 amide (Coopman et al., 2010). Given that the allosteric ligands can modulate the affinity and/or efficacy of orthosteric agonists **(section 1.7 and Chapter 5)**, knowledge of the binding sites could contribute significantly to our understanding of the GLP-1R.

1.3.3.2. GLP-1R-mediated signalling

1.3.3.2.1. cAMP

Following GLP-1 binding, the coupling of $G\alpha_s$ to the receptor induces the activation of AC. This subsequently stimulates the production of the second messenger, cAMP (Perfetti and Merkel, 2000, Delmeire et al., 2003) **(Fig 1.4.)**, which is the main mediator leading to acute insulin secretion in β-cells. Importantly, GLP-1-mediated cAMP generation is glucose-dependent. In the presence of a high concentration of glucose (20 mM) which itself does not influence cAMP production, GLP-1 produces a significantly enhanced level of cAMP in β-cells compared to that seen at a low concentration of glucose (1.4 mM) (Delmeire et al., 2003). The production of cAMP is tightly regulated by the balance between the activities of AC and cyclic nucleotide phosphodiesterases (PDEs) that hydrolyze cAMP (Cooper, 2003). Among the 11 families of PDEs, PDE 3B is reported to play major role in limiting GLP-1-induced insulin secretion in β-cells (Doyle and Egan, 2007). A novel approach in measuring cellular level of cAMP using a fluorescent biosensor determined that GLP-1 evoked oscillations in cAMP in a concentration-dependent manner in β-cells (Dyachok et al., 2006). Oscillations occurred more frequently with low concentrations (0.3-1 nM) of GLP-1 whereas the response was increased and sustained with high concentrations (Dyachok et al., 2006). Increased levels of cAMP activate both PKA and Epac1/2 **(Fig 1.4.)**, which regulate various down-stream aspects of signalling in β-cells **(see below)**. The transduction of the

activity of the GLP-1R through the actions of PKA and Epac1/2 are essential for glucose-dependent insulin release in β-cells (Hashiguchi et al., 2006, Seino et al., 2009) **(see below)**.

1.3.3.2.2. $Ca^{2+}{}_i$

Particularly important that both PKA and Epac regulate the increase in $[Ca^{2+}]_i$, which occurs through Ca^{2+} influx through the activation of Ca^{2+}-induced Ca^{2+} release (CICR) from the intracellular stores and/or plasma membrane VDCC depending on the cell type. In β-cell expressing L-type VDCC, the GLP-1R-mediated increase in $Ca^{2+}{}_i$ is through both of these mechanisms **(Fig 1.4.)** and the activation of CICR requires the rapid increase of $[Ca^{2+}]_i$ through VDCC. Indeed, GLP-1-induced CICR fails to occur in the presence of a VDCC inhibitor (Gromada et al., 2004). The rapid increase in $[Ca^{2+}]_i$ is driven by glucose-induced VDCC opening in β-cells. Indeed, the GLP-1-stimulated $[Ca^{2+}]_i$ increase only occurred in the presence of glucose which was blocked by VDCC antagonists (MacDonald et al., 2002a). In β-cells glucose is taken up mainly through the activity of glucose transporter 2 (GLUT2) leading to an enhanced production of ATP through mitochondrial metabolism. The increased ratio of ATP/ADP results in the closure of K_{ATP} channels causing depolarization of the plasma membrane which therefore cause the opening of L-type VDCC. This leads to Ca^{2+} influx from the extracellular fluid **(Fig 1.4.)**. The plasma membrane is subsequently repolarized by the opening of the voltage-dependent K^+ channels (K_V). GLP-1 further promotes Ca^{2+} influx through VDCC via both facilitating the closure of K_{ATP} channels by PKA-mediated phosphorylation and deactivating the K_V in a PKA-dependent manner **(Fig 1.4.)** although the exact mechanisms are unclear (Gromada et al., 1997, Light et al., 2002, MacDonald et al., 2002b). GLP-1R activation also stimulates CICR from intracellular stores through both the IP_3 receptor (IP_3R) and the ryanodine receptor (RyR). The activation of IP_3R is through a PKA-dependent phosphorylation (Dyachok and Gylfe, 2004) and it is through an Epac-dependent mechanism for RyR activation (Kang et al., 2003). Activation of the GLP-1R evoked an increase in $[Ca^{2+}]_i$, which also

oscillated coincident with those of cAMP, highlighting the coordinated relationship. The cAMP response induced by GLP-1 was abolished by removing extracellular Ca^{2+} and incubation with EGTA (Dyachok et al., 2006). Moreover, CICR did not occur in the absence of cAMP-elevating agents (forskolin, GPCR agonists or cAMP analogues) despite increasing $[Ca^{2+}]_i$ by uncaging Ca^{2+} (Kang et al., 2005).

1.3.3.2.3. ERK and PI3 kinase

The GLP-1R also regulates mitogen-activated protein kinase (MAPK) pathways, particularly extracellular signal-regulated kinases 1 and 2 (ERK1/2). Glucose activates ERK1/2 in β-cells and GLP-1 potentiates such activation (Briaud et al., 2003). Glucose/GLP-1-activation of ERK is blocked by inhibition of either PKA or VDCC illustrating a cAMP/PKA-dependent and Ca^{2+}-dependent pathway (Gomez et al., 2002, Arnette et al., 2003). Evidence relating to the source of Ca^{2+} for ERK activation is conflicting, which might be due to the different cell lines used. In INS-1E cells, glucose/GLP-1-induced ERK activation is regulated by Ca^{2+} influx through both VDCC and CICR whereas in MIN6 cells, this appears independent of CICR (Arnette et al., 2003, Selway et al., 2012). The increased $[Ca^{2+}]_i$ activates calmodulin-dependent protein kinases (CaM kinases), enhancing affinity for calmodulin. Indeed, it was shown that glucose/GLP-1-evoked ERK activation is blocked by a calmodulin antagonist (Arnette et al., 2003), although the mechanisms of Ca^{2+}-mediated ERK activation are unclear **(Fig 1.4.)**. GLP-1 also activates ERK in a Raf-dependent mechanism via the small GTPase protein, Rap1, which can be activated by Epac (de Rooij et al., 1998, Kawasaki et al., 1998) **(Fig 1.4.)**. Thus in human islets, activation of ERK was associated with the co-immunoprecipitation of Rap1 and B-Raf, rather than Ras and Raf-1 (Trümper et al., 2005). However GLP-1 alone in the absence of glucose also activates ERK but in a VDCC-independent manner in β-cells (Quoyer et al., 2010, Briaud et al., 2003). Recently, it was suggested that GLP-1 can stimulate ERK by a G protein-independent but β-arrestin-dependent mechanism **(section 1.6.1.)**. Whether this is the mechanism responsible for GLP-1-induced ERK activation in the absence of glucose is unknown.

ERK activation plays positive roles in regulating glucose-mediated insulin gene transcription and β-cell proliferation and survival (Briaud et al., 2003, Costes et al., 2006, Lawrence et al., 2005).

Additionally, the GLP-1R regulates PI3 kinases through a number of complex mechanisms. One possibility is through transactivation of epidermal growth factor (EGF) receptors leading to the activation of PI3 kinase (Buteau et al., 2003) **(Fig 1.4.)**. The activated PI3 kinases further activate protein kinase B (PKB) and mammalian target of rapamycin (mTOR) (Lawlor and Alessi, 2001, Kwon et al., 2004). PKB is a regulator of β-cell proliferation and survival (Bernal-Mizrachi et al., 2001, Tuttle et al., 2001) and mTOR plays a role in β-cell proliferation (Kwon et al., 2004).

1.3.3.2.4. Insulin secretion

Insulin is a hormone synthesized in the ER and stored in vesicles in pancreatic β-cells. The glucose-induced initial increase of $[Ca^{2+}]_i$ triggers fusion of these insulin-containing vesicles with the plasma membrane followed by insulin release via an exocytotic process **(Fig 1.4.)**. The molecular mechanism by which Ca^{2+} triggers insulin exocytosis is complex and has been well reviewed (Lang, 1999, Rorsman and Renström, 2003). The enhanced increase in the $[Ca^{2+}]_i$ by activation of the GLP-1R thereby leads to potentiation of glucose-triggered acute insulin secretion. Indeed, in rat pancreas, GLP-1 induces little insulin release at low concentrations of glucose whereas it stimulates a strong insulin secretion at higher glucose concentrations, and this release is greater than that in response to glucose alone (Göke et al., 1993). This mechanism is important in preventing hypoglycaemia in the fasting state (Qualmann et al., 1995). Recently, it was suggested that glucose-mediated insulin secretion is positively regulated by the activation of ERK1/2 in MIN6 cells via phosphorylation of synapsin I, a protein associated with insulin secretory granules (Longuet et al., 2005). Furthermore, GLP-1 has a chronic effect on promoting insulin synthesis and secretion by regulating a number of transcription factors **(Fig 1.4.)**. For example, the increased level of $[Ca^{2+}]_i$ activates calcineurin (CaM kinase 2B), activating nuclear factor of activated T-cells

(NFAT) which is a key regulator of insulin gene transcription (Lawrence et al., 2001). PKA also activates cAMP-responsive element binding-protein (CREB) that subsequently activates the insulin receptor substrate 2 (IRS2) promoter thereby increasing the expression of IRS2 (Jhala et al., 2003) which is involved in regulating β-cell growth and survival (White, 2003). PDX-1 (pancreatic and duodenal homeobox factor-1) activity promotes both insulin gene transcription and β-cell growth and survival (Rafiq et al., 1998, Li et al., 2005). The mRNA level of PDX-1 is enhanced in response to GLP-1 treatment in a PKA-dependent mechanism, which also promotes the nuclear translocation of PDX-1 in β-cells (Stoffers et al., 2000, Wang et al., 2001). In addition, ERK1/2 has been shown to promote the activity of both Beta2/NeuroD and PDX-1 by phosphorylation which stimulate the insulin gene promoter to potentiate insulin gene transcription in β-cells (Lawrence et al., 2008, Khoo et al., 2003).

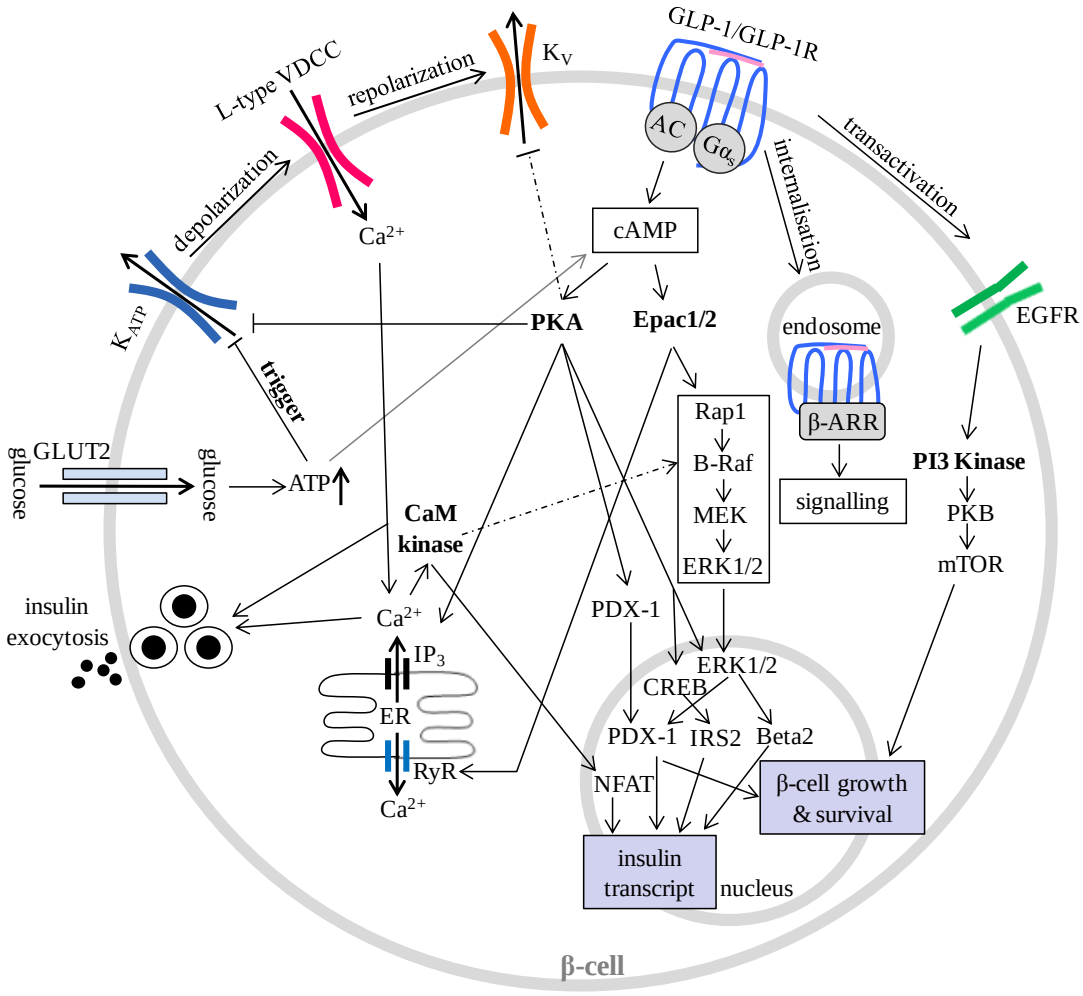

Fig 1.4. GLP-1R activation in pancreatic β-cells. Glucose is taken up via GLUT2 to stimulate the production of ATP which results in closure of K_{ATP} channels leading to plasma membrane depolarization and the subsequent activation of L-type VDCCs. The glucose-triggered increase of $[Ca^{2+}]_i$ results in insulin secretion via exocytosis. The activation of the GLP-1R by ligand binding amplifies glucose-triggered insulin secretion via several processes. Firstly, the coupling to $G\alpha_s$ activates AC which catalyzes the conversion of ATP to cAMP which then activates PKA and Epac1/2. PKA facilitates the closure of K_{ATP} channels and inactivates K_V channels, thereby potentiating Ca^{2+} influx through L-type VDCCs. Secondly, both PKA and Epac1/2 are required for CICR from the ER via IP_3Rs and RyRs respectively further potentiating the increase in $[Ca^{2+}]_i$. Furthermore, activation of PKA activates ERK1/2, CREB and PDX-1, which are important for either insulin gene transcription or β-cell growth and survival. The activation of ERK1/2 also requires Ca^{2+}-induced activation of CaM kinase and the

activation of Epac1/2 which allows the activation of Rap1 leading to a Raf-dependent ERK activation. CaM kinase also activates NFAT in the nucleus, enhancing insulin gene transcription. In addition, the activation of the GLP-1R transactivates the EGFR **(see below)** leading to the activation of PI3 kinase which further activates PKB and mTOR leading to β-cell growth and survival. Recently, signalling from the endocytosed GLP-1R has been reported which will be described below. Mechanisms that have not been well demonstrated are shown by dashed lines.

1.4. GPCR desensitisation and internalisation

1.4.1. GPCR phosphorylation and β-arrestin recruitment

Generally receptor-mediated signalling during prolonged or repeated administration of an agonist undergoes desensitisation (Hausdorff et al., 1990). Such desensitisation may be either homologous or heterologous. Homologous desensitisation refers to the loss of response of the receptors that agonists act on whereas heterologous desensitisation refers to the simultaneous reduction of responsiveness at multiple receptors even in absence of agonist (Kelly et al., 2008).

Once an agonist binds to its receptor, an activated receptor conformation is stabilized. In addition to facilitating G protein coupling, the receptor becomes a substrate for phosphorylation by one or more of the seven members of the G protein-coupled receptor kinase (GRK) family. These kinases are serine/threonine kinases and phosphorylate GPCRs generally on the 3rd ICL and/or C-terminal tail.. The phosphorylated GPCR also has a high affinity for β-arrestin proteins which sterically hinders G protein interaction facilitating its uncoupling to the receptor (Gurevich and Gurevich, 2006). Thus, receptor phosphorylation by GRKs and β-arrestin binding jointly result in homologous receptor desensitisation. For example, homologous desensitisation of the β_2-adrenergic receptor (β_2AR) is mediated by phosphorylation of the C-terminal tail by GRK2 (Lefkowitz et al., 1998). The phosphorylated β_2AR recruits β-arrestin proteins preventing the coupling and activation of $G\alpha_s$. GPCRs can also be phosphorylated by PKA or PKC generally in the 3rd intracellular loop further leading to impaired coupling of G proteins to the activated receptor. Both PKA and PKC are activated by many GPCRs and they are not highly substrate selective. Other receptors not occupied and activated by an agonist can therefore also be phosphorylated causing heterologous desensitisation.

1.4.2. GPCR internalisation

In addition to mediating receptor desensitisation by uncoupling the G proteins, β-arrestins mediate receptor internalisation which further facilitates desensitisation. β-arrestins serve as adapters interacting with clathrin and the β2-adaptin subunit of the clathrin adaptor AP-2 (adaptor protein complex-2) leading to the receptor/arrestin complex associating with clathrin-coated pits (CCPs). Newly formed CCPs gradually invaginate and are pinched off from the plasma membrane by the GTPase dynamin to form an endocytotic vesicle leading to receptor internalisation. These coated vesicles are then targeted within endosomes to allow receptor recycling to the plasma membrane in a process that includes receptor dephosphorylation. Alternatively, the internalised GPCRs are degraded in lysosomes. Phosphorylation of GPCRs by GRKs is a critical step for β-arrestin binding and receptor internalisation for many GPCRs. An example to illustrated this is, a mutant β_2-adrenergic receptor (Y326A) that is a poor substrate for GRK2 and shows little agonist-induced receptor internalisation. The internalisation can, however, be restored by either GRK2 or β-arrestin overexpression (Ferguson et al., 1995).

In addition to β-arrestin/clathrin-dependent receptor internalisation, a β-arrestin-independent route of internalisation may occur under some situations. Caveolae, a specialised type of lipid raft, may mediate endocytosis of some GPCRs in a β-arrestin-/clathrin-independent manner. For example, the internalisation of the vasoactive intestinal peptide (VIP) receptor 2 ($VPAC_2$), a member of the Family B GPCRs, is via a caveolae machinery which may depend on cell type. Both disruption and knockdown of caveolin-1, a major component of caveolae, inhibit VIP-evoked $VPAC_2$ receptor internalisation (Mahavadi et al., 2013). In addition, caveolin-1 contributes to $VPAC_2$ receptor desensitisation as deletion of caveolin-1 inhibited VIP-induced $VPAC_2$ receptor desensitisation (Mahavadi et al., 2013). The mechanism of caveolae-mediated endocytosis could be through the activation of the Src kinase pathway following receptor activation causing tyrosine phosphorylation of caveolin-1

and subsequent dynamin-dependent caveolar endocytosis (Li et al., 1996, Minshall et al., 2000, Mahavadi et al., 2013, Shajahan et al., 2004).

1.4.3. GLP-1R desensitisation

The GLP-1R undergoes both homologous desensitisation in response to ligand stimulation and heterologous desensitisation in response to PKC activation (Widmann et al., 1996b). For example, in βTC3 mouse insulinoma cells, the GLP-1-evoked $[Ca^{2+}]_i$ increase returned to basal levels within 4-5 min in the continued presence of ligand. The duration of ligand action was extended to 7 min by treatment with a PKC inhibitor. Pre-treatment with phorbol 12-myristate 13-acetate (PMA) to activate PKC also inhibited the GLP-1-evoked Ca^{2+} response (Gromada et al., 1996) highlighting that PKC is able to cause GLP-1R desensitisation. Furthermore, exposure to GLP-1 for 5 min followed by 5 min recovery reduced the Ca^{2+} response to a second exposure by approximately 70%, which was enhanced by inhibition of PKC (Gromada et al., 1996). Although GLP-1 stimulates AC to generate cAMP, GLP-1-evoked GLP-1R desensitisation is not mediated by PKA (Gromada et al., 1996). The impact of chronic GLP-1R activation on desensitisation has also been examined in INS-1E cells. Here, 1 h pre-treatment resulted in GLP-1-mediated desensitisation of the cAMP response for up to 96 h before full recovery. In contrast, GLP-1R desensitisation following pre-treatment with exendin-4 did not recover after 96 h pre-treatment. Both GLP-1 and exendin-4-mediated GLP-1R desensitisation were promoted by PMA pre-incubation (Baggio et al., 2004). The role of GRK in GLP-1R desensitisation is unclear.

The removal of the last 33 amino acids of the GLP-1R C-terminal tail abolished receptor phosphorylation and abolished both homologous and heterologous desensitisation (Widmann et al., 1996a, Widmann et al., 1996b). Moreover, the serine doublet at position 431/432 was shown to be the major phosphorylation sites for PKC-mediated GLP-1R phosphorylation and positions 441/442, 444/445 and 451/452 were the major phosphorylation sites following GLP-1R stimulation (Widmann et al., 1996b, Widmann et al., 1997). Indeed, alanine substitution of 431/432 abolished

PMA-mediated desensitisation of the cAMP response. Also GLP-1 pre-treatment for 15 min mediated a 50% reduction of cAMP production in response to re-challenge. However, mutation of all three phosphorylation serine doublets markedly reduced the extent of desensitisation (Widmann et al., 1997) highlighting the phosphorylation-mediated GLP-1R desensitisation.

1.4.4. GLP-1R internalisation

An early study using a Chinese hamster lung (CHL) fibroblast cell line stably expressing the rat GLP-1R showed that in response to GLP-1, the GLP-1R internalised into endosomes with a half-life of 2-3 min (Widmann et al., 1995). Receptor-dependent degradation of ^{125}I-labelled GLP-1 was also observed suggesting that GLP-1 may internalise with the receptor and be degraded in an intracellular compartment.

For the majority of GPCRs, receptor phosphorylation is responsible for receptor internalisation. Mutation of PKC phosphorylation sites at the serine doublet 431/432 of the GLP-1R did not influence internalisation. However, mutation of the GLP-1R phosphorylation sites at 441/442, 444/445 and 451/452 suppressed GLP-1-induced GLP-1R internalisation (Widmann et al., 1997) suggesting that phosphorylation mediates not only GLP-1R desensitisation, but also receptor internalisation. Furthermore, the region of the C-terminal tail close to transmembrane domain VII is also of importance in mediating agonist-dependent GLP-1R internalisation (Vazquez et al., 2005).

The mechanism of GLP-1R internalisation may be cell type-dependent. In CHL fibroblast cells, GLP-1-induced GLP-1R internalisation was mainly via a clathrin-dependent machinery (Widmann et al., 1995), which was confirmed in CHO cells expressing recombinant GLP-1R (CHO-GLP-1R) (Vazquez et al., 2005). Furthermore, co-immunoprecipitation studies demonstrate that β-arrestin1 binds to the GLP-1R in response to GLP-1 stimulation in INS-1E cells (Sonoda et al., 2008). However, GLP-1-induced GLP-1R internalisation is not influenced by β-arrestin1

knockdown. Also the desensitisation of GLP-1-mediated insulin release was similar in control and β-arrestin1 knockdown cells (Sonoda et al., 2008). Moreover, GLP-1-induced recruitment of both β-arrestin1 and β-arrestin2 were determined by bioluminescence resonance energy transfer (BRET) in CHO-GLP-1R cells (Wootten et al., 2013). However in another study GLP-1 failed to cause the re-distribution of β-arrestin2-GFP in HEK-GLP-1R cells (Syme et al., 2006) although the recruitment of β-arrestin1 was not investigated. Importantly, in the same cell line expressing GFP-tagged GLP-1R (GLP-1R-GFP), it was demonstrated that the GLP-1R associated with caveolin-1 and that this interaction is necessary for constitutive cycling of the receptor from intracellular compartments to the cell membrane and that this is necessary for efficient GLP-1R signalling (Syme et al., 2006). Moreover, the GLP-1R internalised in response to exendin-4 co-localized with caveolin-1 (Syme et al., 2006) and similar results were found in MIN6 cells transiently expressing GLP-1R-GFP. Although HEK293 cells express high levels of endogenous β-arrestin which may cause difficulties when investigating its recruitment in overexpression systems (Ménard et al., 1997), potential differences in the mechanisms of GLP-1R internalisation might be due to the different cell lines. Alternatively, it is possible that both clathrin/β-arrestin- and caveolin-1-dependent endocytosis occur following GLP-1R activation. Indeed the neurokinin 1 receptor (NK_1R), belonging to Family A GPCRs, has been shown to internalise by mechanisms requiring dynamin, β-arrestin and caveolin-1 although the latter was to a lesser extent (Kubale et al., 2007).

1.5. GPCR re-sensitisation

1.5.1. Internalisation may be required for GPCR dephosphorylation and re-sensitisation

Receptor phosphorylation induces receptor desensitisation and results in receptor internalisation. Both of these processes may result in desensitisation and highlight that subsequent re-sensitisation requires receptor dephosphorylation or, of course, the plasma membrane insertion of newly synthesized receptors or receptors from a reserve

pool. Many receptor types have been shown to dephosphorylate and recycle to the plasma membrane. It has been suggested that receptor internalisation is required for receptor dephosphorylation within the intracellular compartments, leading to receptor recycling and re-sensitisation. The β_2AR is phosphorylated in response to agonist stimulation. and dephosphorylated after 20 min recovery in agonist-free media (Anborgh et al., 2000). Inhibition of β_2AR internalisation prevents both receptor dephosphorylation and recovery (Pippig et al., 1995). An *in vitro* assay examining the dephosphorylation of GRK2-phosphorylated β_2AR by a G protein-coupled receptor phosphatase (GRP), a membrane-associated form of protein phosphatase type 2A (PP-2A), showed no dephosphorylation at pH 7.0 but clear dephosphorylation at acidic pH (maximum at pH 4.85). This suggests that the phosphorylated β_2AR is targeted to endosomes where the acidic pH facilitates dephosphorylation. The mechanism might be that the conformation of the receptor is changed by the altered pH to increase its sensitivity to GRP (Krueger et al., 1997) or that if the ligand is bound to the receptor, dissociation of ligand within the acidic endosomal compartment allows the receptor to adopt a phosphatase-sensitive conformation. Inhibition of endosomal acidification by an inhibitor of the vacuolar H^+/ATPase, bafilomycin A_1 or monensin, blocked recycling and re-sensitisation of many receptors including β_2AR, transfferrin receptors, NK_1R and EGFR (Moore et al., 1999, Presley et al., 1997, Grady et al., 1995, Wang et al., 2002). These highlight that receptor internalisation and endosomal acidification is required for receptor dephosphorylation, recycling and re-sensitisation.

Internalisation is not, however, the only mechanism of receptor dephosphorylation. It has been reported that some phosphorylated receptors are rapidly dephosphorylated by protein phosphatase(s) at or near the plasma membrane directly following receptor activation. These different mechanisms of receptor dephosphorylation might occur at different phosphorylation sites. For example, Ser^{341}/Ser^{343} of sst_{2A} somatostatin receptor undergo a slow process of dephosphorylation which requires receptor internalisation whereas ^{353}TTETQRT^{359} is rapidly dephosphorylated by protein phosphatase-1β (PP-1β) at or near the plasma membrane (Ghosh and Schonbrunn, 2011). Although the

mechanism of rapid dephosphorylation is not fully understood, it has been reported to be associated with β-arrestin. For example, the co-immunoprecipitation demonstrated an interaction between β-arrestin1 and PP-1β and knockdown of β-arrestin1 inhibited sst_{2A} receptor dephosphorylation. In contrast, dephosphorylation of this receptor was not regulated by β-arrestin2 (Kliewer and Schulz, 2013) implying distinct functions of the β-arrestin isoforms. Moreover, the reduced activity of PP-1β resulted in an elevated receptor phosphorylation at the plasma membrane and enhanced β-arrestin-dependent ERK activation (Pöll et al., 2011). This form of GPCR-mediated β-arrestin-dependent signalling will be discussed below. Additionally, although the internalised NK_1R can undergo internalisation, dephosphorylation, recycling and re-sensitisation (Grady et al., 1995), there is a large amount of desensitised NK_1Rs that remain at the cell surface. These non-internalised NK_1R is dephosphorylated by PP-2A also in association with β-arrestin1 (Murphy et al., 2011). Thus, rapid receptor dephosphorylation requires the scaffolding function of β-arrestin to recruit protein phosphatase(s) which in return prevent other forms of β-arrestin-dependent signalling.

1.5.2. GPCR re-sensitisation via receptor recycling

It is of interest that the rate of recycling considerably differs among GPCRs. For example, the thrombin receptor directly trafficked to lysosomes for degradation with little or no recycling to the cell surface (Trejo and Coughlin, 1999). Some receptors including the angiotensin II type 1A receptor ($AT_{1A}R$), recycle relatively slowly with only around 15% receptor recycling detected 1 h after removal of ligand (Anborgh et al., 2000). In contrast, the β_2AR is efficiently recycled back to the plasma membrane 1 h after removing the ligand (Tsao and von Zastrow, 2000).

There are several mechanisms involved in mediating GPCR recycling. One important factor is the stability of the receptor-β-arrestin complex. GPCRs have been classified into Class A and Class B according to the stability of their interaction with β-arrestin. Class A receptors (*e.g.* β_2AR, μ opioid receptor, endothelin 1 receptor and dopamine D_1 receptor (D_1R)) show transient interaction with β-arrestin at the cell surface and the

receptors internalise into vesicles without β-arrestin bound. In contrast, class B receptors (*e.g.* $AT_{1A}R$, vasopressin type 2 receptor (V2R), thyrotropin-releasing hormone and NK_1R) show high affinity for β-arrestin which traffics with the receptor into vesicles (Oakley et al., 1999, Shenoy and Lefkowitz, 2005). Receptors in these two classes also display distinct affinity for different isoform of β-arrestin. Class A receptors prefer to bind with β-arrestin2 whereas class B receptors bind equally to β-arrestin1 and β-arrestin2 (Oakley et al., 2000).

GPCR endocytosis either without or with β-arrestin bound leads to an either efficient or prolonged receptor recycling respectively **(Fig 1.5.)**. In HEK293 cells expressing recombinant β_2AR and equal amounts of β-arrestin1-GFP or β-arrestin2-GFP, challenge with isoproterenol induced both β-arrestin1-GFP and β-arrestin2-GFP re-distribution from the cytoplasm to the plasma membrane with a faster and greater translocation of β-arrestin2 than β-arrestin1 (Oakley et al., 2000). This binding of β-arrestin leads β_2AR to CCPs thereby mediating receptor internalisation. However, the β_2AR-β-arrestin complex disassociates quickly at or near the plasma membrane, so the receptor internalises without β-arrestin bound and efficiently recycles back to the plasma membrane (Oakley et al., 2000, Shenoy and Lefkowitz, 2003). In contrast, $AT_{1A}R$ belonging to Class B GPCR showed equal affinity for β-arrestin1-GFP and β-arrestin2-GFP. Furthermore, both β-arrestin isoforms internalised with the $AT_{1A}R$ into endosomes (Oakley et al., 2000, Oakley et al., 2001). Receptor recycling to the plasma membrane was minimal after removing the ligand (Anborgh et al., 2000). The factors that determine the stability of receptor-β-arrestin complex are discussed below.

1.5.2.1. Phosphorylation sites in the C-terminal tail of receptors

There is evidence to suggest that specific clusters of serine and threonine residues in the C-terminal tail of the receptor responsible for phosphorylation are critical in the formation of stable receptor-β-arrestin complexes. For example, the mutation of an STS cluster to AAA in the C-terminal tail of the neurotensin-1 receptor reduced agonist-induced receptor phosphorylation by 95%. This lack of phosphorylation allowed

the neurotensin-1 receptor to internalise and recruit β-arrestin2-GFP upon agonist stimulation but abolished the ability of the β-arrestin2-GFP couple and to internalise with the receptor (Oakley et al., 2001). Also, the mutation of serine or threonine residues in an SSLST or STLS cluster to alanine residues (AALAA or AALA) in the C-terminal domain of the $AT_{1A}R$ inhibited receptor phosphorylation by 67% and abolished the ability of β-arrestin2-GFP to internalise with the receptor to endocytic vesicles (Oakley et al., 2001). Furthermore, when the C-terminal tail of the $AT_{1A}R$ was replaced with that of the β_2AR, receptor recycling to the cell surface was demonstrated. In contrast, the replacement of C-terminal tail of β_2AR with the tail of $AT_{1A}R$ reduced β_2AR recycling to the plasma membrane (Anborgh et al., 2000). These data highlight the importance of specific clusters of serine and threonine phosphorylation residues in the C-terminal tail of receptors in mediating either the stability of the receptor-β-arrestin complex or the efficiency of receptor recycling.

1.5.2.2. β-arrestin ubiquitination

Ubiquitination is primarily considered as a posttranslation modification for protein degradation although it has now also been recognized as an essential process for the endocytosis, trafficking and lysosomal targeting of specific membrane proteins (Shenoy, 2007). It has been shown that the phosphorylation of GPCRs leads to not only the recruitment, but also ubiquitination of β-arrestin which in turn recruits ubiquitin ligases to further ubiquitinate other substrates including the receptor itself (Kommaddi and Shenoy, 2013). It has been shown the ubiquitinations of both β_2AR and V2R upon agoinsts stimulation are dependent on β-arrestin although it is not the case for CXCR4 chemokine receptor (Kommaddi and Shenoy, 2013). In addition, ubiquitination of β-arrestin is critical for its adaptor and scaffolding functions therefore regulating receptor internalisation and β-arrestin-dependent signalling (Shenoy et al., 2001, Shenoy et al., 2007). Protein ubiquitination can be reversed by deubiquitination and this is regulated by specific deubiquitinases (Shenoy, 2014). Therefore the stability of β-arrestin ubiquitination is regulated by a balance of ubiquitination and deubiquitination.

Importantly, ubiquitination of β-arrestin is responsible for its tight binding to the phosphorylated receptor and deubiquitination results in the disassociation of β-arrestin from the receptor (Shenoy et al., 2009). Thus, the differential trafficking of GPCRs and β-arrestin could be determined by the differential stability of β-arrestin ubiquitination. For example, upon recruitment by the phosphorylated receptor, either β_2AR (Class A), AT_{1A}R or V2R (Class B), β-arrestin2 is robustly ubiquitinated. However, the kinetics of deubiquitination differs among the receptors (Shenoy and Lefkowitz, 2003). Consistent with the transient interaction between β-arrestin2 and β_2AR, under these circumstances β-arrestin2 ubiquitination is transient, being deubiquitinated within 15 min. In contrast, activation of the AT_{1A}R or V2R induces a stable ubiquitination of β-arrestin2 consistent with the prolonged interaction between the AT_{1A}R or V2R and β-arrestin2 (Shenoy and Lefkowitz, 2003). Interestingly, the replacement of the C-terminal tail of β_2AR with that of the V2R resulted in a persistent ubiquitination of β-arrestin2 which stably interacted with the receptor and trafficked with the receptor into endosomes (Shenoy and Lefkowitz, 2003).

1.5.2.3. Agonist-dependence of receptor phosphorylation

The stability of the receptor-β-arrestin complex could be regulated by the nature of the agonist. It is now accepted that different receptor agonist can stabilize different conformations of the same receptor and this may expose different phosphorylation sites for GRKs thereby determining the stability of the receptor-β-arrestin complex. For example, CCL19 and CCL21 are two endogenous ligands for the chemokine GPCR CCR7. These agonists have equal binding affinity and similar efficacy and potency for $G_{i/o}$ protein activation (Sullivan et al., 1999). However, CCR7 is phosphorylated and desensitised to a greater extent upon CCL19 exposure compared to CCL21. In response to CCL19, CCR7 strongly interacted with β-arrestin2 which then re-distributes into endocytic vesicles. In contrast, only weak interaction between CCR7 and β-arrestin2 is detected following CCL21 stimulation and β-arrestin2 does not internalise into endocytic vesicles with the receptor (Zidar et al., 2009). Interestingly, CCL19

stimulation activates both GRK3 and GRK6 whereas only GRK6 is activated by CCL21 (Zidar et al., 2009), perhaps explaining the differential phosphorylation of the receptor following exposure to these different ligands.

1.5.2.4. The role of proteolysis within endosomes

Inside the endosomal compartment, there is more than one mechanism regulating the stability of the ligand-receptor-β-arrestin complex. Thus, the acidic environment of endosomes promotes receptor dephosphorylation and recycling possibly due to the conformational change (Krueger et al., 1997, Grady et al., 1995). More recently, and for a small number of ligands, it has been shown that proteases within the endosome, specifically endothelin-converting enzyme-1 (ECE-1), have the ability to hydrolyze internalised peptide ligands leading to the disassociation of receptor-β-arrestin complexes. Such proteases may therefore regulate the fate of endocytosed receptors. This will be further discussed below.

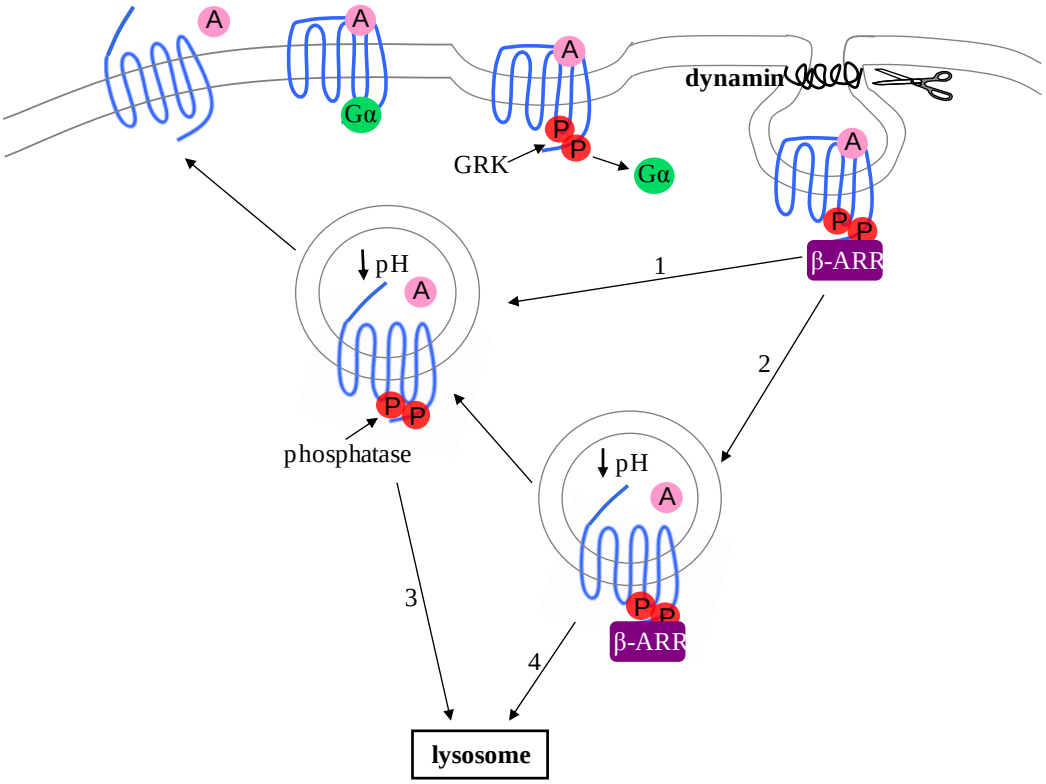

Fig 1.5. The general model of GPCR trafficking. The binding of an agonist promotes receptor-G-protein coupling and the subsequent regulation of effectors. Following activation, receptors are phosphorylated by GRKs leading to homologous receptor desensitisation. The phosphorylated GPCRs facilitate β-arrestin recruitment which targets the receptor/arrestin complex to CCPs. These CPPs are then pinched off from the plasma membrane by the GTPase dynamin to form a vesicle leading to internalisation of the receptor (route 1) or receptor-arrestin complex (route 2). Receptors internalise into endosomes either without β-arrestin bound leading to rapid receptor recycling or with β-arrestin bound leading to a longer recycling following receptor dephosphorylation. These two routes of trafficking can target the receptor to lysosomes for degradation upon chronic stimulation (route 3 and 4). A, agonist; β-ARR, β-arrestin.

1.5.3. Re-sensitisation via de novo receptor synthesis and a reserve pool of receptors

Stimulation with thrombin leads to the cleavage of protease-activated receptor 1 (PAR1) followed by internalisation. The internalised receptors were then sorted to lysosome for degradation (Trejo and Coughlin, 1999). Therefore, recovery of cell-surface PAR1 and therefore re-sensitisation must through other mechanisms. This could include *de novo* receptor synthesis and/or mobilization of receptors from a cytosolic 'reserve' pool. It has been found that PAR1 is constitutively cycled between the plasma membrane and cytosol in the absence of agonist (Shapiro et al., 1996, Paing et al., 2006) and following receptor endocytosis upon activation, recovery of the receptor requires uncleaved PAR1 moving from a cytosolic pool to the plasma membrane (Hein et al., 1994, Shapiro and Coughlin, 1998). Recovery of cell-surface receptor numbers may also require *de novo* protein synthesis. For example, re-sensitisation of the endogenous flagellin-receptor FLS2 is dependent on ligand-induced degradation and *de novo* synthesis of the receptor (Smith et al., 2013).

Although PARs represent a rather special case, the majority of GPCRs are desensitised as a consequence of phosphorylation following agonist stimulation, followed by receptor internalisation. Receptor re-sensitisation following internalisation can occur through at least three mechanisms: receptor recycling (requiring dephosphorylation); *de novo* receptor synthesis or; recruitment from a reserve (cytosolic) pool **(Fig 1.6.)**.

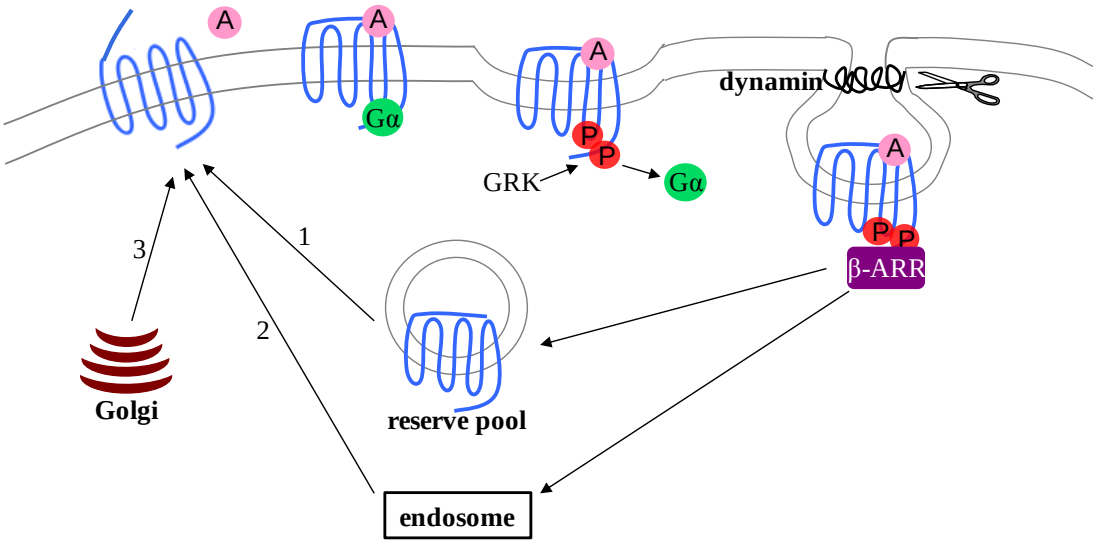

Fig 1.6. The general model of GPCRs re-sensitisation. As described in **Fig 1.5**, activated GPCRs undergo phosphorylation and internalisation leading to desensitisation. The re-sensitisation of GPCRs following internalisation may occur through one of three mechanisms. In most situations, receptors internalise and are trafficked to endosomes from where they can recycle to the plasma membrane following receptor dephosphorylation (see details in **Fig 1.6**) thereby allowing receptor re-sensitisation (route 2). In some situations, cellular re-sensitisation could also be due to receptor translocation from a reserve pool in the cytoplasm to the cell surface or from *de novo* receptor synthesis in the Golgi (route 1 and 3 respectively). A, agonist; β-ARR, β-arrestin.

1.5.4. GLP-1R re-sensitisation

There have only been a small number of studies that have examined GLP-1R re-sensitisation. One early study measuring Ca^{2+} responses as an index of receptor activation showed that pre-treatment with GLP-1 induced a rapid GLP-1R desensitisation followed by re-sensitisation within 1 h after removal of ligand (Gromada et al., 1996). Given that in addition to phosphorylation, receptor internalisation is also a process could influence receptor desensitisation, another early study using a radioligand binding assay to detect the changes of cell-surface receptor number showed that incubation with 10 nM GLP-1 at 4 ℃ for 5 h followed by 5 min re-warming induced a rapid loss of cell-surface GLP-1R of ~35% indicating receptor internalisation with recovery of binding within 1 h after removal of the extracellular GLP-1. This recovery was independent on *de novo* receptor synthesis (Widmann et al., 1995). However, it is unclear if the recovered cell-surface binding was from recycling or recruitment from reserve pool. Prolonged stimulation with GLP-1 can also lead to receptor internalisation and trafficking to lysosomes in β-cells (Kuna et al., 2013). However, re-sensitisation under this situation was not determined. Clearly, the mechanism of GLP-1R re-sensitisation needs to be further explored. Considering that there are a number of orthosteric and allosteric GLP-1R agonists have been synthesized to mimic the activity of GLP-1, whether these ligands could drive different process of receptor re-sensitisation is unclear.

1.6. GLP-1R-mediated G protein-independent/β-arrestin-dependent signalling

Apart from mediating receptor desensitisation and internalisation, β-arrestins also act as a scaffold, recruiting other intracellular molecules and leading to a diverse range of β-arrestin-dependent signalling pathways (Lefkowitz and Shenoy, 2005, Xiao et al., 2007, Xiao et al., 2010) including MAPKs (ERK, p38 kinases and c-Jun N-terminal kinases (JNK)), non-receptor tyrosine kinases, Akt, PI3 kinases and nuclear factor kappa-light-chain-enhancer of activated B cells (NF-κB). The mechanism is that the interaction of β-arrestin with the phosphorylated receptor results in conformational changes and posttranslational modifications of β-arrestin including dephoshorylation and ubiquitination, which facilitate the interaction with its binding partners including endocytic partners and signalling effectors (Lefkowitz and Shenoy, 2005). Therefore, the duration of β-arrestin-dependent signalling is dependent on the stability of the receptor-β-arrestin complex. The phosphorylation profile of the receptor is dependent on both the nature of the receptor and ligand. Different profiles of receptor phosphorylation may establish different structures of β-arrestin which may lead to specificity of β-arrestin-dependent signalling pathways. The signal transduction mediated by β-arrestin has been shown to be critical for many physiological functions such as cell proliferation, anti-apoptosis, cytoskeleton reorganization and protein synthesis (Murphy et al., 2009).

1.6.1. ERK/CREB

In response to GLP-1, the GLP-1R recruits β-arrestin1 (Sonoda et al., 2008). Although β-arrestin1 may not regulate GLP-1R internalisation (Sonoda et al., 2008) **(section 1.4.4.)**, it does, however, play an important role in regulating GLP-1R signalling. For example, in INS-1E cells, GLP-1 evoked rapid phosphorylation of both ERK1/2 and CREB, and this was greatly inhibited by knockout of β-arrestin1 (Sonoda et al., 2008). Further, the ability of GLP-1 to evoke insulin secretion under either low glucose or high glucose conditions was markedly inhibited in β-arrestin1 knockdown cells. This β-arrestin1-regulated insulin secretion evoked by GLP-1 is mediated through a

cAMP-dependent **(see below)**, but PKA-independent mechanism (Sonoda et al., 2008). GLP-1, therefore, mediates ERK1/2 activation through at least two mechanisms, a PKA-dependent **(section 1.3.3.2.3.)** and β-arrestin1-dependent process **(Fig 1.7.)**.

Interestingly, ERK activation through these two mechanisms shows temporal and spatial differences which contribute to different physiological functions. The GLP-1-evoked PKA-dependent ERK1/2 activation is rapid and transient. In contrast, the β-arrestin1-dependent pERK1/2 response is later and more sustained. Moreover, these activation mechanisms may result in different sub-cellular localization and therefore different functional consequences of activated ERK. Rapid ERK1/2 activation can be detected in both cytoplasm and nucleus in MIN6 cells whereas the sustained ERK1/2 activation is mainly cytosolic (Quoyer et al., 2010). The activated ERK1/2 translocated to the nucleus is mainly responsible for the activation of some transcription factors such as Beta2 and PDX-1 in β-cells (Khoo et al., 2003). However, in MIN6 cells and pancreatic islets, β-arrestin1-regulated pERK1/2 activates p90 ribosomal S6 kinase (p90RSK) which further phosphorylates the pro-apoptotic protein Bad facilitating its interaction with the scaffold protein 14-3-3 (Quoyer et al., 2010). The association of Bad and 14-3-3 prevents the translocation of Bad to mitochondria and also prevents the accumulation of apoptotic proteins on the mitochondrial membrane thereby inhibiting apoptosis (Bergmann, 2002, Datta et al., 2000, Yang et al., 1995, Adams and Cory, 2007). Knockdown of β-arrestin1 inhibited the anti-apoptotic effect of GLP-1 in MIN6 cells (Quoyer et al., 2010), which might therefore be related to the ability of GLP-1 to enhance β-cell survival.

1.6.2. c-Src

It has been described above that one mechanism involving GLP-1-induced β-cell proliferation is via the transactivation of the EGFR, which is dependent on the activation of the non-receptor-type tyrosine kinase c-Src (Buteau et al., 2003). Both the transactivation of the EGFR and cell proliferation were inhibited by inhibition of c-Src (Buteau et al., 2003). Interestingly, a recent study from the same group showed that

GLP-1-induced c-Src activation is dependent on β-arrestin1 as c-Src activation was abolished by knockdown of β-arrestin1 and the expression of a β-arrestin1 mutant that is unable to bind with c-Src impaired the proliferation in response to GLP-1(Talbot et al., 2012). The regulatory role of c-Src in GLP-1-mediated β-cell proliferation was further demonstrated by the expression of a kinase-dead c-Src mutant that abolished the proliferative action of GLP-1.

1.6.3. cAMP

As described above, the activation of G_s-coupled receptors leads to the production of cAMP. Although receptor phosphorylation, arrestin recruitment and internalisation are possible ways in which the signal could be reduced or terminated, there is some evidence to suggest that some GPCRs continuously generate cAMP even after receptor endocytosis possibly resulting from the prolonged association between receptor and G protein. This may also show some agonist specificity. For example, both parathyroid hormone (PTH) and PTH-related peptide (PTHrP) show similar kinetics and mechanisms of coupling and activation of $G\alpha_s$ in HEK293 cells expressing recombinant PTH receptor (PTHR). However, the disassociation and deactivation processes show temporal differences. In PTHrP-treated cells, $G\alpha_s$ rapidly disassociated from the receptor after removal of the extracellular ligand. This was followed by deactivation of $G\alpha_s$, whereas neither $G\alpha_s$ disassociation nor deactivation was detected after removal of PTH. PTH consistently evoked a more sustained cAMP response compared to PTHrP, which was blocked by a dominant negative dynamin mutant (Ferrandon et al., 2009). This cAMP response following endocytosis is also reported for other receptors including the thyroid-stimulating receptor (Calebiro et al., 2009) and sphingosine 1-phosphate receptor (Mullershausen et al., 2009). Notably, there is some evidence implying that the endocytosed GLP-1R may also be able to stimulate cAMP generation. Firstly, the internalised GLP-1/GLP-1R complex co-localized with adenylate cyclase (Kuna et al., 2013). Secondly, treatment with a dynamin inhibitor altered the exendin-4-mediated PKA substrate phosphorylation profile, inhibited the cAMP

response and blocked insulin secretion in β-cells (Kuna et al., 2013). Moreover, GLP-1-evoked cAMP production was also inhibited by β-arrestin1 knockdown (Sonoda et al., 2008). Taken together, these data suggest that the endocytosed GLP-1R may mediate persistent cAMP generation **(Fig 1.7.)**.

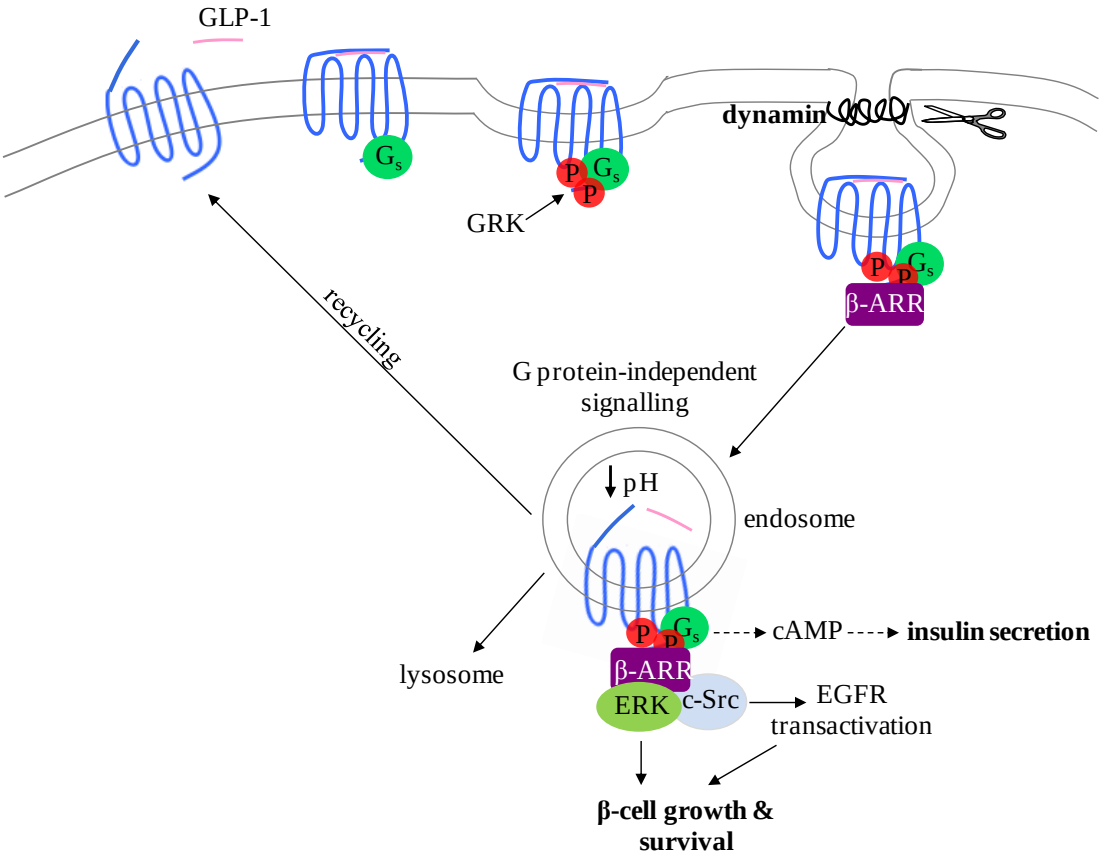

Fig 1.7. GLP-1R-mediated G protein-independent signalling. Upon receptor phosphorylation and β-arrestin recruitment, the receptor-β-arrestin complex targets to endosomes to be either recycled to the plasma membrane or degradated in lysosomes. β-arrestin acts as a scaffold to recruit ERK and c-Src leading to G protein-independent/β-arrestin-dependent signalling which is responsible for β-cell growth and survival. The endocytosed G_s may further activate AC leading to persistent cAMP generation which is critical for insulin secretion. It has been suggested to depend on β-arrestin, however the mechanism is unclear. Mechanisms that have not been well demonstrated are shown by dashed arrows.

1.7. Allosteric ligands of the GLP-1R

Allosteric ligands bind to GPCRs at sites distinct to the orthosteric binding sites to positively/negatively modulate the affinity and/or efficacy of endogenous agonists. Allosteric ligands which have intrinsic effects are called ago-allosteric agonists. The previously described small-molecule agonists for the GLP-1R, compound 2 and compound B, are ago-allosteric agonists that neither compete with ^{125}I-GLP-1 for binding nor are functionally inhibited by the orthosteric antagonist, exendin 9-39 amide. N-terminal truncation of the GLP-1R markedly reduces GLP-1 agonism but not that of either compound B (Sloop et al., 2010) or compound 2 (Huang, 2010) thereby demonstrating that these agonists interact with allosteric binding site(s). Both compound 2 and compound B stimulate cAMP generation and insulin release in a glucose-dependent manner, although show bell-shaped concentration-response curves with effects declining at high concentrations (Knudsen et al., 2007, Coopman et al., 2010, Sloop et al., 2010). This biphasic concentration-response curve may be due to toxicity (Coopman et al., 2010). There is evidence to suggest that these two ago-allosteric agonists activate the GLP-1R by different mechanisms. Indeed, the compound B-mediated cAMP response was increased additively by compound 2 which was also shown in cells expressing an N-terminally truncated GLP-1R (Cheong et al., 2012). Compound 2 enhances the affinity of the GLP-1R for GLP-1 in a concentration-dependent manner without changing the maximum efficacy of GLP-1 (Knudsen et al., 2007, Koole et al., 2010) although compound 2 can actually decrease the potency of GLP-1, possibly due to the toxicity (Coopman et al., 2010). However there is no evidence to suggest that compound B alters the affinity of the GLP-1R for GLP-1, although it has been reported to enhances the efficacy of GLP-1 (Cheong et al., 2012). Interestingly, the efficacy of compound 2-evoked cAMP generation is markedly enhanced by the GLP-1R orthosteric antagonist, exendin 9-39 amide, which in contrast, greatly inhibits the GLP-1-evoked cAMP response (Coopman et al., 2010, Cheong et al., 2012). However this potentiation is not detected for compound B (Cheong et al., 2012).

Furthermore, both compound 2 and compound B elevate Ca^{2+} in a concentration-dependent manner which show slower increases and longer-lasting effects compared to the GLP-1-evoked Ca^{2+} response. Indeed, the compound B-evoked Ca^{2+} response lasts longer than that of compound 2 (Cheong et al., 2012). Thus, a number of small-molecule agonists have been reported which interact with distinct allosteric sites of the GLP-1R, particularly leading to different mechanisms of activation. In addition, whether these ligands mediate GLP-1R trafficking through the same mechanisms as the orthosteric agonist and whether they behavior similarly in regulating β-arrestin-dependent signalling are unknown.

1.8. Endothelin-converting enzyme-1 (ECE-1)

1.8.1. ECE expression

Endothelin-converting enzymes (ECEs) belong to a family of membrane-bound zinc metalloproteases that are encoded by two distinct genes for ECE-1 and ECE-2 (Emoto and Yanagisawa, 1995). ECE-1 has a broader tissue distribution and is expressed at higher level than ECE-2. ECE-1 is abundantly expressed in endothelial cells *in vivo* and it is also expressed in non-vascular cells of many tissues including brain, lung, pancreas and adrenal gland (Xu et al., 1994, Takahashi et al., 1995, Korth et al., 1999) whereas ECE-2 is mainly present in neuroendocrine tissues (brain, pituitary and adrenal medulla) (Mzhavia et al., 2003). Furthermore, ECE-1 is active at both neutral and acidic pH and present both at the plasma membrane and in the intracellular compartments. By contrast, ECE-2 is optimally active at acidic pH and has an intracellular localization (Mzhavia et al., 2003, Pacheco-Quinto et al., 2013). Given that ECE-1 has activity against a range of substrates and has been suggested to regulate the signalling and trafficking of some GPCRs **(see below)**, the following sections will focus on ECE-1.

1.8.2. Sequence and distribution of ECE-1 isoforms

ECE-1 contains a single membrane-spanning region flanked by an N-terminal cytoplasmaic tail and a C-terminal catalytic ectodomain. The catalytic site is within the extracellular domain or within the lumen of organelles and vesicles (Pacheco-Quinto et al., 2013). Human ECE-1 has four isoforms which have identical C termini but differ in their N termini **(Fig 1.8.)**. This results from the use of different promoters from the same gene. The distinct sequence of each isoform in the N termini defines the sub-cellular distribution. Previous studies using immunofluoresence in transfected CHO cells have suggested that ECE-1a and ECE-1c are mainly targeted to the plasma membrane while ECE-1b is expressed predominantly inside the cell (Schweizer et al., 1997, Azarani et al., 1998) with ECE-1d displaying an intermediate distribution

between the plasma membrane and the inside of the cell (Valdenaire et al., 1999). Another study using AtT-20 neuroendocrine cells suggested the same distribution for ECE-1a, b and c, whereas ECE-1d was detected weakly on the plasma membrane, being present mainly inside the cells (Muller et al., 2003). This distribution of active ECE-1 is further defined by activity measurement for cell-surface ECE-1 and total ECE-1 for each isoform. When ECE-1 substrate McaBK2 was used, the percentages of the total cellular activity that was intracellular were shown to be around 19% for ECE-1a, 75% for ECE-1b, 53% for ECE-1c and 96% for ECE-1d in KNRK cells (Roosterman et al., 2007).

Although both ECE-1b and ECE-1d are present in the cytosol, these two isoforms are concentrated in different endosomal compartments (Muller et al., 2003). ECE-1d completely co-localizes with the transferrin receptor or internalised transferrin receptor (recycling endosome marker) whilst ECE-1b also partially co-localized with a rab7-GFP chimera or mannose-6-phosphate receptor (late endosome marker). However, neither ECE-1b nor ECE-1d co-localized with cathepsin D, Lamp-1 or lysotracker which are lysosome markers. A recent study using transfected ECE-1a-d with N-terminal GFP tags in KNRK cells showed that all the isoforms especially ECE-1b and ECE-1d co-localized with the early endosomal antigen 1 (EEA1) (Roosterman et al., 2007). The relative proportions of co-localization in these four isoforms were not compared and no other endosomal compartment marker was used.

ECE-1a, MRGVWPPPVSALLSALGMSTYKRATLDEEDLVDSLSEGDAYPNGLQVNFH

ECE-1b, MEALRESVLHLALQMSTYKRATLDEEDLVDSLSEGDAYPNGLQVNFH

ECE-1c, MPLQGLGLQRNPFLQGKRGPGLTSSPPLLPPSLQVNFH

ECE-1d, MMSTYKRATLDEEDLVDSLSEGDAYPNGLQVNFH

Fig 1.8. Sequences of human ECE-1a-d isoforms. Partial sequences of the N-termini of human ECE-1a-d. The residues in black in isoforms b, c or d are homologous to ECE-1a. Residues in other colors highlight the different sequences.

1.8.3. ECE-1 phosphorylation and trafficking

1.8.3.1. ECE-1 phosphorylation

In vitro evidence suggests that ECE-1 can be phosphorylated and that this is isoform specific. ECE-1 isoforms also show constitutive phosphorylation. One group immunopurified transfected N-terminal FLAG-tagged ECE-1 isoforms (FLAG-ECE-1) from CHO cells which were then incubated with various kinases including casein kinase-I (CK-I), casein kinase-II (CK-II), PKA or PKC in the presence of [γ-^{32}P]ATP (MacLeod et al., 2002). FLAG-ECE-1c was strongly phosphorylated by CK-I which was less active on FLAG-ECE-1b and FLAG-ECE-1d. Little or no phosphorylation was detected for FLAG-ECE-1a. By contrast, CK-II, PKA and PKC did not phosphorylate any of the isoforms (MacLeod et al., 2002). However, when wild-type ECE-1 isoforms were used, the degree of phosphorylation among the isoforms was more uniform compared to the FLAG-tagged versions although there was a phosphorylated form of ECE-1 found in human umbilical vein endothelin cells (HUVECs). This suggested that the FLAG epitope tag at the cytosolic tail may influence the phosphorylation status of the protein (MacLeod et al., 2002). As demonstrated in endothelial-like EA.hy926 cells, PKC is responsible for phosphorylation of endogenous ECE-1c including under basal conditions. In contrast, activation of PKA using di-butyryl cAMP did not affect ECE-1c phosphorylation in this cell (Smith et al., 2006). In CHO cells, PKC was also shown to phosphorylate C-terminal GFP-tagged ECE-1b (ECE-1b-GFP) and especially ECE-1a-GFP (Jafri and Ergul, 2006). The PKA activator, forskolin, also resulted in phosphorylation of ECE-1b-GFP but not ECE-1a-GFP illustrating that PKA may be involved in ECE-1b phosphorylation in some circumstances. There is no evidence for phosphorylation of wild-type ECE-1 a and b isoforms and limited research looking at the phosphorylation of the ECE-1d isoform.

1.8.3.2. ECE-1 trafficking

There is evidence to suggest that the trafficking of ECE-1 may be influenced by its phosphorylation status. Thus, treating EA.hy926 cells with PMA to activate PKC increased the amount of plasma membrane-bound ECE-1 without changing the total cellular amount (Kuruppu et al., 2010). Moreover, PMA treatment induced a significant increase of the activity of ECE-1 in the cell membrane, but did not influence the ECE-1 activity of the cell lysate. In order to investigate which ECE-1 isoform(s) contribute(s) to this effect, CHO cells were transfected with specific isoforms. Data suggested that PMA mediated phosphorylation induces the trafficking of ECE-1c to the cell surface (Kuruppu and Smith, 2012). In contrast, PMA treatment leads to a reduction of plasma membrane immunoreactivity of ECE-1a along with higher intracellular immunoreactivity (Jafri and Ergul, 2006). The PKC influence on the trafficking of other two isoforms, ECE-1b and ECE-1d, are less well investigated.

1.8.4. The regulation of ECE-1 expression level

1.8.4.1. Glucose

As the level of ET-1 is increased in hyperglycemia (Kuwaki et al., 1990) and ET-1 is the product of ECE-1 action on big ET-1, it is a logical hypothesis that the glucose concentration might influence the expression of ECE-1. This was first demonstrated in both EA.hy926 and HUVEC in which culturing the cells in high glucose (22.2 mM) for 5 days significantly promoted ECE-1 mRNA and protein expression compared to low glucose (5.5 mM) supplemented with 16.7 mM mannitol (Keynan et al., 2004). This effect was both time-dependent and glucose concentration-dependent. Interestingly, increasing the glucose concentration in the culture medium from 5.5 to 22.2 mM for 5 days increased the activity of PKC by 72% in EA.hy926 and 41% in HUVECs (Keynan et al., 2004). Furthermore PMA significantly increased ECE-1 expression. Moreover, the high glucose-induced increase in ECE-1 protein expression was abolished by a PKC inhibitor in both cells types (Keynan et al., 2004). Isoform-specific RT-PCR for ECE-1a,

b and c demonstrated that only the expression of isoform c increased in response to the increased glucose level (Keynan et al., 2004). The isoform of ECE-1d was not investigated in that study. Therefore, high concentrations of glucose result in up-regulation of ECE-1 expression possibly through a PKC-dependent mechanism. It has been reported that the activation of PKC promotes the expression of Ets-1 mRNA, a transcription factor of the ETS family, in EA.hy926 cells which might be responsible for the increased expression of ECE-1 (Orzechowski et al., 1998, Orzechowski et al., 2001).

1.8.4.2. ET-1

A study illustrated that the catalytic product of ECE-1 action on big ET, ET-1, regulates the expression of ECE-1. Thus, in SV-40-transformed rat pulmonary endothelial cells, treatment with ET-1 for 6 h reduced ECE-1 mRNA and protein expression (Naomi et al., 1998). Pre-incubation with endothelin receptor type B (ET_B) antagonist, BQ788, abolished the effect of ET-1 while endothelin receptor type A (ET_A) antagonist, BQ123, had no effect suggesting that the ET_B receptor mediates the ET-1-induced reduction of ECE-1 expression. This may be through PLC activation by ET_B leading to the elevation of $[Ca^{2+}]_i$ as the effect was mimicked by the calcium ionophore ionomycin. The regulation of specific isoforms by ET-1 was not investigated.

1.8.5. Catalytic function of ECE-1

The wide sub-cellular distribution of ECE-1 is consistent with a broad range of physiological functions. Cell-surface ECE-1 has been considered primarily to be the proteolytic cleavage of big ET to ET. The precursor of ET is synthesized in the ER. After the removal of the signal peptide, the pro-endothelins (pro-ETs) then undergo a two-step proteolytic process. Firstly, they are cleaved at conserved multibasic sites by furin and furin-like enzymes (Denault et al., 1995, Blais et al., 2002) and an intermediate, big ET, is then released. The second step is to convert the big ET to the 21 amino acid biologically active peptide, ET, by cleaving the Trp21-Val22 bond by

cell-surface ECE-1. Additionally, cell-surface ECE-1 hydrolyzes and inactivates the vasodilator peptide bradykinin in the extracellular fluid although ECE-1 has lower affinity for bradykinin than either ACE or NEP (Hoang and Turner, 1997). Therefore, cell-surface ECE-1 plays a role in the metabolism of some circulating peptides thereby either initiating or terminating cellular functions.

An understanding of possible roles of ECE-1 in endosomes has started to emerge. Some peptides including SP, bradykinin, angiotensin I (ATI), neurotensin and calcitonin gene-related peptide (CGRP) can be cleaved by ECE-1 with an acidic pH optimum. In contrast, peptides such as neuropeptide Y and angiotensin II (ATII) are poorly cleaved under acidic conditions (Johnson et al., 1999, Fahnoe et al., 2000, Roosterman et al., 2007, Padilla et al., 2007). For example, incubation of 250 μM CGRP with 415 nM recombinant human (rh) ECE-1 at either pH 7.4 or pH 5.5 for 0-720 min followed by HPLC separation and mass spectrometry demonstrated that CGRP was not degraded at pH 7.4 even at up to 360 min, but completely degraded within 240 min at pH 5.5 (Padilla et al., 2007) indicating the pH-dependence of ECE-1 function. Furthermore, rhECE-1 degraded CGRP in a concentration-dependent manner and was inhibited by the ECE-1 inhibitor, SM19712 **(section 1.8.6.)**. In similar experiments, ATI was degraded at pH 5.5 but there was no detectable degradation of ATII up to 480 min at either pH 7.4 or pH 5.5. Bradykinin was degraded by rhECE-1 at both pH 7.4 and pH 5.5 with degradation being completely inhibited by SM19712. Therefore, the function of ECE-1 is both peptide- and pH-dependent. Intracellular degradation was examined by incubation of HEK293 cells expressing recombinant receptor for CGRP, a heterodimer of the calcitonin receptor-like receptor (CLR) and receptor activity-modifying protein 1 (RAMP1), with ^{125}I-His^{8}-CGRP for 10 min to allow internalisation followed by acid wash and further incubation. Fractionation of cell lysates by HPLC demonstrated that the endocytosed CGRP was degraded and this was sensitive to both SM19712 and bafilomycin A_1, an inhibitor of vacuolar-type H^+-ATPase (Padilla et al., 2007) implying that the intracellular degradation of CGRP by ECE-1 may occur in endosomes, particularly as ECE-1 is present in endosomes,

co-localizing with endocytosed CGRP (Padilla et al., 2007). Moreover, inhibition of either ECE-1 or endosomal acidification prolonged the interaction between β-arrestins and CLR suggesting that ECE-1 regulated the recycling and re-sensitisation of the CLR (Padilla et al., 2007).

Studies have shown that endocytosed receptors can continue to signal by a G protein-independent or β-arrestin-dependent mechanism (Lefkowitz and Shenoy, 2005) **(section 1.6.)**. The degradation of endocytosed peptides in endosomes may facilitate disassociation of the ligand-receptor-arrestin complex thereby regulating β-arrestin-mediated events such as ERK activation. SP is degraded by endosomal ECE-1 and inhibition or knockdown of ECE-1 induced a prolonged interaction between the NK_1R and β-arrestins in endosomes (Roosterman et al., 2007). This may well influence ERK activation as sustained ERK activation is enhanced by either SM19712 or bafilomycin A_1 (Cottrell et al., 2009). SM19712 promoted ERK activation in both the cytosol and nucleus. In contrast, a C-terminally truncated NK_1R resulted in a weak and transient interaction with β-arrestins in response to SP and ECE-1 did not regulate ERK activation (Cottrell et al., 2009) implying that endosomal ECE-1 regulates SP-induced β-arrestin-mediated ERK activation. SP-induced ERK activation regulated a variety of functions including proliferation and anti-apoptosis. These have been reported to be facilitated by the formation of β-arrestin-dependent scaffolding complex (DeFea et al., 2000). However, ERK can also mediate cell death in the nervous system (Lu and Xu, 2006) and SP phosphorylates the transcription factor and nuclear receptor, Nur77, leading to cell death through β-arrestin-dependent ERK activation (Castro-Obregón et al., 2004). By terminating SP-induced β-arrestin-dependent ERK activation, ECE-1 prevents SP-mediated cell death of myenteric neurons (Cottrell et al., 2009).

1.8.6. Inhibition of ECE-1

ECE-1 degrades a number of peptides in either the extracellular fluid or endosomes thereby regulating signalling from membrane located or endocytosed receptors. Interestingly, elevated plasma ET-1 level is associated with heart disease,

hyperglycemia or hypertension. Therefore, a number of ECE-1 inhibitors have been developed. However, most are not selective. For example, the first ECE-1 inhibitor, phosphoramidon (IC_{50} = 3.5 μM for hrECE-1), inhibited the secretion of ET-1 from cultured endothelin cells (Ikegawa et al., 1990, Sawamura et al., 1990), the pressor and airway contractile responses of big ET-1 *in vivo* (Matsumura et al., 1990, Fukuroda et al., 1990) and the pathophysiological effects of big ET-1 (Matsumura et al., 1991, Grover et al., 1992, Vemulapalli et al., 1993). However, phosphoramidon has much higher affinity for NEP and a relatively low affinity for angiotensin-converting enzyme (ACE) (Kukkola et al., 1995). FR901533 is a selective ECE-1 inhibitor with an IC_{50} of 0.14 μM (Tsurumi et al., 1995) but it is unable to inhibit endogenous ET-1 production (Xu et al., 1994). Other inhibitors including PD 069185 and PD 159790 are cytotoxic and inhibit the production of both ET-1 and big ET-1 (Ahn et al., 1998).

SM19712, 4-chloro-*N*-[[(4-cyano-3-methyl-1-phenyl-1*H*-pyrazol-5-yl) amino] carbonyl] benzenesulfonamide monosodium salt, was found through the screening of the Sumitomo Pharmaceutical Library (Parent No. EP 885890). In an *in vitro* enzyme assay, phosphoramidon gave IC_{50} of 690 nM for rat ECE-1 while the IC_{50} for SM19712 was 42 nM (Umekawa et al., 2000). Furthermore, SM19712 did not inhibit NEP, ACE or nine other metalloprotease enzymes at up to 100 μM. Additionally, SM19712 did not influence the radioligand binding of receptors including AT_1R, AT_2R, ET_A, ET_B, EGFR and eight other receptors. *In vivo* studies showed that both phosphoramidon and SM19712 successfully suppress the pressor response induced by big ET-1 in anesthetized rats. Moreover, SM19712 inhibited the endogenous production of ET-1 in endothelin cells with an IC_{50} of 31 μM compared to 27 μM for phosphoramidon (Umekawa et al., 2000). Therefore, SM9712 is a highly selective inhibitor of ECE-1 at the concentrations used.

1.9. Aim

The current study will examine GLP-1R desensitisation and the subsequent re-sensitisation in both HEK-GLP-1R and INS-1E cells, looking at specific aspects of the mechanisms involved. In particular role of ECE-1 in regulating GLP-1-mediated signalling and re-sensitisation of the receptor will be investigated. Given that both GLP-1 analogues and small-molecule agonists are considered as valuable alternative strategies for the treatment of type 2 diabetes, in addition to investigating their activities, GLP-1R desensitisation and re-sensitisation and its regulation by ECE-1 will be examined, particularly to allow comparison with the endogenous ligand. The potential interaction between orthosteric and allosteric ligands of the GLP-1R will also be examined.

CHAPTER 2 Material and Methods

2.1. Materials

2.1.1. General chemicals, reagents and consumables

All the general chemicals, reagents and consumables were supplied by either Fisher Scientific (Loughborough, U.K.) or Sigma-Aldrich (Gillingham, U.K.) unless mentioned specifically. Tissue culture plasticware and the cover-slips were from Nunc (VWR International, Lutterworth, U.K.). Geiner ELISA strip-plates (96-well format) were purchased from Scientific Laboratory Supplies (Willford Industrial Estate, Nottingham, UK). All mammalian cell culture reagents including media, fetal calf serum (FCS), phosphate buffered saline (PBS), Geneticin (G418), streptomycin and penicillin sulphate were supplied by Invitrogen (Paisley, U.K.). Agarose powder was from Geneflow Ltd (Fradley, U.K.). Sterile plastic loops, Sterilin petri dishes and syringe filters were purchased from Appleton Woods (Birmingham, U.K.). Compound 2 was synthesised and provided by AstraZeneca UK (Alderley Edge, U.K.).

2.1.2. Peptides, antibodies, enzymes, primers, siRNA and cDNA

Peptides including GLP-1 7-36 amide, exendin-4 and exendin 9-39 amide were purchased from Bachem (Weil am Rhein, Germany). GLP-1 9-36 amide is from Tocris Bioscience (Bristol, U.K.). Rhodamine-labeled GLP-1 7-36 amide was purchased from Phoenix Pharmaceuticals, Inc. (Burlingame, U.S.A.). ^{125}I-Exendin 9-39 amide (2200 Ci/mmol) was from PerkinElmer Life and Analytical Sciences Ltd. (Buckinghamshire, U.K.).

Antibodies against phospho-ERK1/2, ERK1/2, ribosomal protein S6 were purchased from Santa Cruz Biotechnology, Inc. (Santa Cruz, CA). Antibody against ECE-1 was from GeneTex (Irvine, U.S.A). Antibody against EEA1 was obtained from BD Biosciences (Oxford, U.K.). Antibody against mCherry was from Novus Biologicals

(Cambridge, U.K.). Goat anti-rabbit IgG, HRP-linked antibody was from Cell Signaling (Herts, U.K.). Goat anti-mouse IgG, HRP-linked antibody was from Sigma-Aldrich (Gillingham, U.K.). Goat anti-mouse Alexa fluor 488 antibody was from Invitrogen (Paisley, U.K.)

The DNA polymerases, Taq and Phusion, restriction endonucleases (RE), T_4 DNA ligase and the relevant working buffers and supplements were purchased from New England Biolabs (Hitchin, U.K.). SuperScript III reverse transcriptase and all the primers were supplied by Invitrogen (Paisley, U.K.). ON-TARGET plus SMART pool consisted of four distinct siRNA duplexes of siRNA targeted to knockdown of human ECE-1 mRNA and the I.M.A.G.E cDNA of ECE-1a is from ThermoFisher Scientific (New Jersey, U.S.A.). Scrambled siRNA was from Invitrogen (Paisley, U.K.).

2.1.3. Specific reagents and kits

Fluo-4-acetoxymethyl ester (fluo-4-AM) and Lipofectamine RNAmaxi for siRNA transfection was purchased from Invitrogen (Paisley, U.K.). DNA ladder, dNTPs and pre-stained protein molecular size marker were from New England Biolabs (Hitchin, U.K.). Bradford reagent for protein determination was purchased from Sigma-Aldrich (Gillingham, U.K.). Acrylamide/*bis*-acrylamide stock solution (30%, *w:v*) was supplied by National Diagnostics (U.K.) Ltd (Hessle, U.K.). Polyvinylidene fluoride (PVDF) transfer membrane was purchased from Millipore (U.K.) Ltd (Watford, U.K.). ECL^+ reagents were from Amersham Biosciences (GE Healthcare U.K. Ltd, Chalfont, U.K.). [2,8-^{3}H]-adenosine 3', 5'-cyclic monophosphate, ammonium salt (^{3}H-cAMP; 40 Ci/mmol) was from Amersham Biosciences (GE Healthcare U.K. Ltd, Bucks., U.K.). Emulsifier Safe scintillation fluid was supplied by PerkinElmer Life and Analytical Sciences Ltd. (Buckinghamshire, UK). All the inhibitors, PDBu, ATP and Hoechst 33258 dye were from Sigma-Aldrich (Gillingham, U.K.). QIAGEN plasmid mini kits were obtained from QIAGEN (Crawley, U.K.). PCR clean-up gel extraction kits and plasmid Midi-prep kit were purchased from Macherey-Nagel (Duren, Germany).

2.2. Mammalian cell culture

2.2.1. Growth and maintenance

Wild-type HEK293cells and HEK293 cells expressing human recombinant GLP-1R (HEK-GLP-1R) were grown in Dulbecco's modified Eagle medium (DMEM) containing 5.5 mM or 25 mM glucose supplemented with 10% (*v:v*) fetal calf serum (FCS), 100 μg/mL streptomycin and 100 units/mL penicillin sulphate. Medium containing 5.5 mM glucose was also supplemented with 19.5 mM mannitol to maintain osmolarity. The C-terminal EGFP-tagged HEK-GLP-1R cells (HEK-GLP-1R-EGFP) were maintained in the same medium but with 200 μg/mL G418. INS-1E cells were cultured in RPMI1640 containing 11.1 mM glucose, supplemented with 5% heat-inactivated FCS, 100 μg/mL streptomycin, 100 units/mL penicillin sulphate, 50 μM β-mercaptoethanol, 10 mM HEPES and 1 mM sodium pyruvate. All cells were cultured at 37 ℃ in a 95% air/5% CO_2 humidified atmosphere.

2.2.2. Cell subculture

Adherent cells in either flasks or dishes were passaged at 70-100% confluence. Following aspiration of the culture medium, cells were washed gently with an appropriate volume of PBS to remove remaining FCS. Then 30 μL/cm^2 of trypsin-EDTA (0.05% *w:v* trypsin, 0.04% *w:v* EDTA in PBS) were added onto the cells to facilitate detachment. After being incubated at 37 ℃ for ~2 min or longer until the cells detached from the bottom, trypsination was terminated by adding growth medium. The cell suspension was then used for seeding appropriate plasticware for either continued culture or for experimental use.

2.2.3. Freezing cells for storage

Cells were grown to 70-80% confluence in flasks or dishes and harvested as described in **section 2.2.2**. Following cell harvesting, the cells suspension was centrifuged at 140 g for 4 min at room temperature (RT). After removing the supernatant, cells were

re-suspended in 1 mL of freezing medium (10% *v:v* dimethyl sulfoxide (DMSO) in FCS) and transferred into 2 mL cryotubes. The cryotubes were then placed in a cell freezing container for at least 4 h and then kept in liquid nitrogen until resuscitation.

2.2.4. Resuscitation of frozen cells

The frozen cells were immediately thawed at 37 ℃ once removed from liquid nitrogen. The 1 mL cell suspension was then transferred into a 30 mL sterile universal tube containing 9 mL fresh medium and centrifuged (140 g, 4 min, RT). The cell pellet was re-suspended in growth medium and transferred into a new flask or dish. The cells were then incubated at 37 ℃ in a 95% air/5% CO_2 humidified atmosphere to allow attachment and growth.

2.3. Poly-D-lysine coating

Where required, plasticware for cell growth was coated with 0.1% (*w:v*) poly-D-lysine hydrobromide. Before plating the cells, the plates were incubated with 250 μL/cm^2 of poly-D-lysine for at least 20 min at RT and then washed with 350 μL/cm^2 of PBS. After removing PBS, the plasticware was ready for use.

2.4. Transfection of cDNA plasmids or siRNA

2.4.1. cDNA plasmids transfection of HEK293 cells using the calcium phosphate method

Cells were plated into poly-D-lysine-coated 8-well strips, 24-well plates or 6-well plates with 25 mm cover-slips followed by incubation at 37 ℃ in a 95% air/5% CO_2 humidified atmosphere for 5-6 h to allow attachment (50-60% confluence). A mixture of 0.25 M Ca^{2+} and an appropriate amount of DNA (0.2 μg/well for 8-well strips, 0.4 μg/cm^2 for the plates) in H_2O was slowly added into an equal volume of 1.5 mM phosphate in H_2O drop by drop and mixed well. After 5-10 min incubation at RT, the Ca^{2+}-DNA-phosphate mixture was then added into each well (1:10 $v_{mixture}$:v_{medium}). The

cells were then incubated at 37 ℃ in a 95% air/5% CO_2 humidified atmosphere. After approximately 16 h, the medium was changed. After 36-48 h, the cells were used for treatment or harvested for immunoblotting.

2.4.2. siRNA transfection of HEK293 cells by Lipofectamine RNAmaxi

Cells were plated into poly-D-lysine coated 8-well strips or 24-well plates and left to attach for 5-6 h (50-60% confluence). The complete media (ie. with serum) was replaced with Opti-MEM (without serum; 100 µL and 500 µL for 8-well strips and 24-well plates respectively). The Lipofectamine RNAmaxi reagent was diluted in Opti-MEM (3:50 *v:v*) and another equal volume of Opti-MEM containing an appropriate amount of siRNA (5 pmol/well for 8-well strips and 10 pmol/well for 24-well plate for HEK293 cells) was prepared. The diluted siRNA was then added into the diluted reagent (1:1 *v:v*). After 20 min incubation at RT, the siRNA-lipid complex was added into each well (50 µL for 8-well strips and 100 µL for 24-well plates). The media was changed to fresh complete medium after approximately 16 h incubation. After 36-48 h the cells were used for treatment or harvested for immunoblotting.

2.5. Determination of protein concentration by Bradford assay

Protein standards were prepared by diluting BSA (1 mg/mL) in 0.1 M NaOH to the working concentrations of 0, 25, 50, 100, 125, 250, 375, 500, 625, 750 and 1000 µg/mL. All the protein test samples were also appropriately prepared and diluted in 0.1 M NaOH. A 2 µL aliquot of standards or samples was added into a 96-well plate followed by 200 µL of Bradford reagent diluted in H_2O (1:1, *v:v*). The reactions were incubated in the dark for 5 min at RT. After automatic shaking (600 rpm, 1 s), the absorbance was measured above 595 nm using a NOVOstar plate reader (BMG labtech, Aylesbury, UK). Standard curves were fit using GraphPad Prism 6 (GraphPad Software Inc., San Diego, CA, U.S.A.) and the protein concentrations of samples were generated by interpolation of the standard curve.

2.6. Determination of cAMP

2.6.1. Generation of cAMP by intact cells

Cells were seeded into 24-well plates pre-coated with 0.1% poly-D-lysine hydrobromide and cultured in their specific medium at 37˚C in a 95% air/5% CO_2 humidified atmosphere until more than 90% confluent. After washing twice and equilibrating for 10 min in Krebs'-HEPES buffer (KHB; 10 mM HEPES, 4.2 mM $NaHCO_3$, 11.7 mM D-glucose, 1.18 mM $MgSO_4 \cdot 7H_2O$, 1.18 mM KH_2PO_4, 4.69 mM KCl, 118 mM NaCl, and 1.3 mM $CaCl_2 \cdot 2H_2O$, pH 7.4), cells were stimulated with agonist at the required concentration in KHB with 0.1% (*w:v*) BSA in either the presence or absence of 500 µM 3-isobutyl-1-methylxathine (IBMX) for the required time. The response was terminated by aspiration off the buffer and addition of 400 µL of 0.5 M ice-cold trichloroacetic acid (TCA). The plate was then kept on ice for at least 20 min. The aqueous phase was neutralized by adding 500 µL of a freshly prepared oil mixture (1:1 *v:v* tri-n-octyl-amine and 1, 1, 2-trichlorotrifluoroethane) with 50 µL of 10 mM EDTA (pH 7.0). Samples were vortexed and left at RT for 12 min. After vortexing again, samples were microfuged (16,100 g, 4 min) and 200 µL of the upper aqueous was transferred to 50 µL of 60 mM $NaHCO_3$, which was used for subsequent determination of cAMP or stored at 4 ˚C for up to 7 days.

2.6.2. cAMP Assay

The concentration of cAMP in samples was determined by a competitive radioreceptor assay and calculated by comparison to a standard curve of 0 to 5 µM cAMP. A 50 µL aliquot of each standard and sample and 100 µL of [^{3}H]-cAMP (specific activity 40 Ci/mmol, 1 µL in 4 mL of 50 mM Tris-HCl/4 mM EDTA, pH 7.5) were mixed with 150 µL of binding protein (1 mL in 11 mL 50 mM Tris-HCl/4 mM EDTA) purified from bovine adrenal glands as previously described (Brown et al., 1971). The mixture was incubated on ice for at least 90 min. The free cAMP and free [^{3}H]-cAMP were absorbed by 250 µL charcoal solution (0.5% *w:v* charcoal, 0.2% *w:v* BSA, 50 mM Tris/4 mM

EDTA, pH 7.5) for 12 min, followed by vortexing and centrifugation (16,100 g, 4 min) at 4˚C (Coopman et al., 2010). The [^{3}H]-cAMP that was combined with the binding protein in 400 µL of the supernatant was counted by liquid-scintillation spectrometry in 4.2 mL Safeflour scintillant. The concentrations of cAMP in samples were calculated through interpolation of the standard curve and related to the amount of cellular protein as determined by Bradford assay **(section 2.5)**.

2.7. Determination and calibration of changes in the intracellular Ca^{2+} concentration ($[Ca^{2+}]_i$)

Cells were grown to approximately 90% confluence in 8-well ELISA strip plates pre-coated with 0.1% (*w:v*) poly-D-lysine. The standard protocol is that cells were washed twice with 100 µL KHB buffer and loaded with 2 µM fluo-4 in this buffer for 40 min at 37 ℃ (Coopman et al., 2010). The fluo-4 was then removed and the cells were washed twice with 100 uL of KHB. 100 µL of KHB-BSA, with or without added Ca^{2+}, was added into each well, which were then incubated at 37 ℃ for a further 5 min. Cells were then stimulated with ligands at 37 ℃ at the required concentrations and the changes in fluorescence were measured as an index of $[Ca^{2+}]_i$ using a NOVOstar microplate reader (Coopman et al., 2010). A 20 µL volume of KHB-BSA or ligand (prepared in KHB-BSA with or without added Ca^{2+}) was added into the well at 200 µL/s using the liquid-handling capability of the machine. Fluorescence was determined by excitation at 485 nm with emitted light collected at 520 nm. Data were collected at 0.5 or 1 s intervals. The protocol was modified according to each experiment as illustrated in figures in each results chapter.

When required, the $[Ca^{2+}]_i$ was calculated using **equation 2.1**. The cells were washed twice with buffer and the fluorescence was measured in 120 µL of KHB-BSA (F_{blank}) at 37 ℃. The cells were then loaded with fluo-4 in the same way as described above. After twice washing with buffer, cells were incubated in 120 µL of KHB-BSA at 37 ℃ and the fluorescence was measured again (F_{basal}). Calibration of the fluo-4 signal was performed by adding ionomycin to a final concentration of 2 µM to equilibrate the concentration of

intracellular and extracellular Ca^{2+}. The value of F_{max} was obtained firstly by manually adding 120 µL of KHB-BSA buffer with a high concentration of Ca^{2+} (4 mM), measured for 10 min at 37 ℃ and the F_{min} was then derived by replacing the buffer with 120 µL of Ca^{2+}-free KHB-BSA buffer with 2 mM EGTA with measurement for at least another 10 min at 37 ℃ (Bootman and Roderick, 2011). The calibration experiment was performed with different passages of HEK-GLP-1R cells and at various cell densities to ensure an appropriate calibration was available for use.

Equation 2.1:

$[Ca^{2+}]_i = K_d (F'-F'_{min})/(F'_{max}-F')$, where the K_d of fluo-4 was taken as 350 nM (Yamasaki-Mann et al., 2009).

The data for F' were generated from background subtraction of F. For example, $F'_{min} = F_{min} - F_{background}$.

2.8. Radioligand binding assay

A radioligand binding assay was used to measure cell-surface GLP-1R binding. To avoid ligand depletion, binding of the radioligand (^{125}I-exendin 9-39) to cells at various densities and using different volumes were tested. In the final assays, the proportion of total added that was bound was ≤ 20% in both HEK-GLP-1R and INS-1E cells. HEK-GLP-1R cells were used at 80% confluence in 8-well strips pre-coated with poly-D-lysine, along with 200 µL/well of 0.05 nM ^{125}I-exendin 9-39 amide. For INS-1E cells at 80% confluence in 24-well plates pre-coated with poly-D-lysine, 350 µL/well of 0.05 nM ^{125}I-exendin 9-39 amide was used.

HEK-GLP-1R cells or INS-1E cells were treated as required. At the end of treatment, cells were washed with acidified buffer (pH 4.0) followed by standard KHB and then incubated with 200 µL (HEK-GLP-1R) or 350 µL (INS-1E) of 0.05 nM ^{125}I-exendin 9-39 amide either with or without 1 µM exendin 9-39 amide for 16 h at 4 ℃. Cells were

then washed twice with 200 µL (HEK-GLP-1R) or 500 µL (INS-1E) of ice-cold buffer. NaOH (0.1M) was then added to each well (100 µL for HEK-GLP-1R or 200 µL for INS-1E). The plates were then washed with another 100 µL (HEK-GLP-1R) or 200 µL (INS-1E) of 0.1 M HCl. The samples were counted by liquid-scintillation spectrometry in 2 mL (HEK-GLP-1R) or 4 mL (INS-1E) Safefluor scintillant.

2.9. Western blot analysis

2.9.1. Treatment of cells and solubilisation

Cells were seeded into 24-well plates, pre-coated with 0.1% *w:v* poly-D-lysine, and cultured in required growth medium until 70-90% confluent. For HEK293 cells, the media was removed and the cells cultured in 500 µL of serum-free media for 20-24 h to serum-starve cells. After washing twice with KHB-BSA buffer, cells were treated as required at 37 ℃ as described. Reactions were terminated by placing the plates on ice and aspirating the solution immediately. Cells were solubilised by adding 100 µL of 1 × Laemmli sample buffer (62.5 mM Tris-HCl, pH 6.8, 0.1% *w:v* bromophenol blue, 2% *w:v* SDS, 10% *v:v* glycerol and 50 mM DTT) to each well. Samples were then collected into 1.5 mL tubes followed by centrifugation at 16,100 g for 1 min at 4 °C. Samples were boiled for 5 min at 100 ℃ followed by centrifugation at 16,100 g for another 1 min. Samples were then cooled down to RT and vortexed before use or stored at -20 ℃.

2.9.2. SDS-polyacrylamide gel electrophoresis (PAGE) and immunoblotting

Samples were separated using SDS-PAGE BioRad minigels which were run at 100-170 V for 60-90 min. Proteins were transferred onto polyvinylidene fluoride (PVDF) membranes at 15 V for 30 min by semi-dry blotting apparatus. When immunoblots were for lower molecular weight proteins (<100 kDa) or ECE-1 (80-120 kDa), the transfer buffer contained 48 mM Tris, 39 mM glycine, 1.3 mM SDS, 10% methanol. When immunoblotting was for higher molecular weight proteins (eg. mCherry-tagged versions of ECE-1 isoforms (100-150 kDa)), transfer buffer was used without methanol

but with a high concentration of SDS (3.5 mM). The membranes were then blocked with 5% non-fat milk powder/TBST buffer (50 mM Tris, 150 mM NaCl, 0.1% Tween-20) for 1 h at RT. The blots were then incubated in primary antibody diluted in 5% BSA/TBST buffer **(Table 2.1.)** overnight at 4 ℃ followed by 3 × 8 min washes with TBST. They were then incubated with secondary antibody diluted in 5% (*w:v*) non-fat milk powder/TBST buffer **(Table 2.1.)** for another 1 h at RT followed by another 3 × 8 min washes. Signals were developed using ECL and exposure to Film.

Table 2.1. Antibodies used in immunoblotting

Primary antibody	Secondary antibody
Mouse IgG polyclonal anti-pERK1/2 (1:2000 dilution)	Goat anti-mouse IgG, HRP-linked (1:1000 dilution)
Rabbit IgG polyclonal anti-ERK1/2 (1:3000 dilution)	Goat anti-rabbit IgG, HRP-linked (1:3000 dilution)
Mouse IgG polyclonal anti-S6 (1:20,000 dilution)	Goat anti-mouse IgG, HRP-linked (1:1000 dilution)
Rabbit IgG polyclonal anti-ECE-1 (1:1000 dilution)	Goat anti-rabbit IgG, HRP-linked (1:3000 dilution)
Mouse IgG monoclonal anti-mCherry (1:1000 dilution)	Goat anti-mouse IgG, HRP-linked (1:1000 dilution)

2.10. Immunocytochemistry

2.10.1. Sample preparation

Cells at ~80% confluence in poly-D-lysine-coated 96-well plates (for ERK detection) or 24-well plates with 12 mm cover-slips (for EEA1 detection) were washed twice with KHB-BSA and treated at 37 ℃ as required. The reactions were stopped by aspirating off the buffer or ligand and adding 50 μL (96-well plates) or 300 μL (24 well plates) of 4% paraformaldehyde immediately. After 10 min incubation at RT, the paraformaldehyde solution was removed and cells were then exposed to 50 μL (96-well plates) or 300 μL (24-well plates) of methanol (pre-cold to -20 ˚C) for 2 min at -20 ˚C for permeabilization. After immediately aspirating off the methanol, cells were washed twice with 100 μL (96-well plates) or 500 μL (24-well plates) of PBS. The cells were blocked for 90 min with 50 μL (96-well plates) or 300 μL (24-well plates) of 2% BSA in PBS on the shaker at RT. For detecting pERK, cells were incubated with mouse IgG polyclonal anti-pERK1/2 primary antibody (1:400 in PBS with 2% BSA, 30 μL/well). The wells for detecting the signal noise (ie. non-specific binding) from the secondary antibody were incubated with PBS containing 2% BSA only. For detecting EEA1, 100 μL/well of mouse IgG monoclonal anti-EEA1 primary antibody (1:500 in PBS with 2% BSA) was added in the middle of each well in a dry 24-well plate. The cover-slips from the culture plate were gently put into the dry plate inverted with cells facing to the antibody.

Following overnight incubation at 4 ˚C with shaking, the primary antibody was removed and the cells were washed three times with 100 μL (96-well plates) or 500 μL (24 well plates) of PBS. Cells were then incubated with Alexa fluor 488 anti-mouse IgG antibody (1:500 in PBS with 2% BSA, 30 μL/well for 96-well plates or 100 μL/well for 24-well plates using the method described above) or Alexa fluor 568 anti-mouse IgG antibody (1:500 in PBS with 2% BSA, 100 μL/well for 24-well plates using the method described above) for 90 min at RT with shaking. The plates were covered with foil. For pERK detection, the cells were washed once with 100 μL of PBS and then incubated

with Hoechst staining solution (1:10,000 in PBS, 50 µL/well) for 10 min at RT followed by washing twice with 100 µL of PBS. The cells remained in 100 µL PBS and plates were kept in the fridge with foil covered until scanned by an Olympus cell^R microscope with an Olympus LUCPLFLN 40 × objective lens and an excitation wavelength of either 488 nm or 350 nm for Alexa fluor 488 and Hoechst respectively. Emitted light was collected above 510 nm for the fluorescent emission of Alexa fluor 488 or above 461 nm for Hoechst. In total, 16 images/well (equal to a total area of 217×165 µm) were captured using a CCD camera. The exposure time was 4 s/image or 1 s/image for the Alexa flour 488 and Hoechst channels respectively. For EEA1 detection, the cells were then washed three times with 500 µL of PBS. The cover-slips were inverted onto mounting solution (10 µL/cover-slip) on glass slides and then sealed with nail polish. The fixed cells were either kept at -4 ℃ covered with foil until use or directly imaged following **Method 2.11.1.**.

2.10.2. Data analysis the detection of ERK activation and distribution

The images were analysed by the Olympus scan^R analysis software. The area of nucleus was determined by the intensity detection for the Hoechst signal and an area of 20 pixels around the nucleus was classified as cytoplasm. All of the signals were background-corrected by the intensity-conserving algorithm included in the software and only the signals reaching threshold were determined to minimize the inclusion of background signal. Abnormal signals, including multi-nucleated cells and any abnormal cell edge were excluded by the gates for the parameters of total intensity, area and circularity. For each cell, the background-corrected mean fluorescent intensity of either the whole cell, the cytoplasm or the nucleus and the ratio of background-corrected mean fluorescent intensity of the cytoplasm to nucleus were generated and the mean data for the population of cells in each well were determined.

2.11. Confocal imaging

2.11.1. Two dimensional (2D) images

HEK293 cells with either stable or transient expression of EGFP- or mCherry-tagged proteins were grown in monolayers on 0.1% *w:v* poly-D-lysine-coated cover-slips for 24-48 h. Cover-slips were then washed with KHB at 37 ℃ at least twice and mounted in a perfusion chamber containing 500 µL of KHB heated to 37 ℃ with a Peltier unit. The 100 µL of ligand at 6 × the required concentration was manually injected using pipet.

Both fixed and live cells were imaged using an Ultra*VIEW* confocal microscope (PerkinElmer LAS, Beaconsfield, Bucks., U.K.) with a 60 × oil-immersion objective lens and either a 488 nm or 568 nm Kr/Ar laser line for EGFP or Alexa fluor 488 nm and mCherry, rhodamine or Alexa fluor 568 nm respectively. Emitted light was collected above 510 nm for the fluorescent emission of EGFP or Alexa fluor 488 nm or above 560 nm for mCherry, rhodamine or Alexa fluor 568 nm and images were captured using a CCD camera.

For determining receptor internalisation, in an individual cell, an area in both the plasma membrane and cytosol was selected for measuring the integrated density with background correction by Fiji (free download from http://fiji.sc/Downloads) as an index of fluorescence intensity **(Fig 2.1)**. At least 2 individual cells for each experiment were measured. An index of internalization was then generated by using the following **Equation 2.2**..

Equation 2.2

Internalisation (%) = [1-(Fmt/Fct)/(Fmb/Fcb)]×100%

where Fm is background-corrected membrane fluorescence, Fc is background-corrected cytoplasmic fluorescence, t is time and b is basal (0min). Fmb and Fcb represent these parameters under basal conditions at the start of the experiment (Huang, 2010).

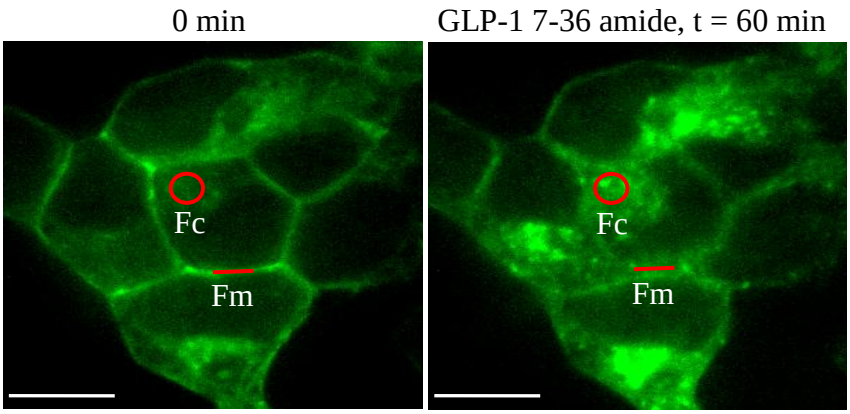

Fig 2.1. Analysis of confocal images. HEK-GLP-1R-EGFP cells were challenged with buffer (0 min) or 100 nM GLP-1 7-36 amide for 60 min. The red lines and the red circles indicate the areas on the plasma membrane and in the cytosol respectively that were used for measuring the integrated density with background correction as an index of membrane fluorescence (Fm) and cytoplasmic fluorescence (Fc). Scale bar (in the bottom left of image), 5 μm.

Where required, images were analysed (using Fiji) to determine Pearson correlation coefficients to allow the degree of co-localization between fluorophores to be quantified.

2.11.2. Three dimensional (3D) images

HEK-GLP-1R-EGFP cells were separately transfected with mCherry-tagged ECE-1 isoforms for 36-48 h. The whole cells were scanned by a Leica TCS SP5 confocal laser scanning microscope at 0.3 μm intervals using excitation at both 488 nm and 561 nm every 2 min over a 60 min period during which cells were stimulated with 100 nM GLP-1 7-36 amide. The stacks were then used for making the 3D images using Fiji.

2.12. Bacterial cell culture

2.12.1. Growth and multiplication

E. coli were cultured at 37 ℃ either on LB agar (1% *w:v* tryptone, 0.5% *w:v* yeast extract, 1% *w:v* NaCl and 1.5% *w:v* agar) plates or in Luria-Bertani (LB) broth (1% *w:v* tryptone, 0.5% *w:v* yeast extract and 1% *w:v* NaCl) with shaking at 220-230 rpm. The antibiotics, ampicillin (100 µg/mL) or kanamycin (50 µg/mL) as appropriate were used for selection following transformation of bacteria.

2.12.2. E. coli stock

For each Escherichia coli (*E.coli*) stock, 600 µL of fresh overnight culture in LB broth was gently mixed with 300 µL of 50% *v:v* glycerol in sterile 2 mL cryotubes and then stored at -80 ℃.

2.12.3. Resuscitation of E. coli

To resuscitate *E. coli*, the frozen glycerol stocks were scraped with a sterile plastic inoculating loop, which was then used to streak onto an LB agar plate containing appropriate antibiotic. The plate was transferred inverted into an incubator at 37 ℃ overnight and then stored inverted at 4 ℃ until use.

2.13. Colony polymerase chain reaction (PCR)

Colony PCR was performed by slightly touching the single colony (at least 3 individual colonies were selected) with a 200 µL of pipette tip and pipetting up and down in the pre-prepared 20 µL of standard *Taq* polymerase reaction mixture following the manufacturer's instruction. The reactions were then quickly transferred to a thermocycler following brief centrifugation (1,500 g, 1 s). The initial denaturation was performed at 96 ℃ for 1 min and 15 s for the subsequent 33 cycles. The annealing step following each cycle was set to 62 ℃ for 30 s. The extension was carried out at 68 ℃ for 30 s (1 min/kb) without final extension. The reactions were then held at 4 ℃. In this

case, the primer pair was designed to enable selection of an interested colony by simply amplifying a small fragment (322 bp), which is common to all the isoforms of ECE-1 (within the central region). The sequences of these primers are shown in **Fig 2.2.**

a. 5'~ primer for all isoforms of ECE-1
   5'- GACAGATGCCTGCTCAACAA -3'

b. 3'~ primer for all isoforms of ECE-1
   5'- CTGATTTTCGGGTTTCCTCA -3'

Fig 2.2. Primers for colony PCR. This pair of primers is able to amplify a 322 bp of ECE-1, which is located in the central region of all isoforms.

2.14. Preparation of plasmid DNA from *E. coli*

Following the colony PCR, the colony containing the interested gene was selected and grown in 3 mL of LB broth at 37˚C for 16-20 h with shaking at 220 rpm. The *E. coli* stock for the colony was made as described in **Method 2.12.2.** and kept in -80℃. The plasmid DNA was prepared using a commercial plasmid Mini-prep kit (~20 μg DNA product; Qiagen) for diagnostic digestion, sequencing or PCR. After each plasmid was confirmed, the frozen *E. coli* were resuscitated as described in **Method 2.12.3**. and a single colony was picked and grown in 3 mL of LB broth containing antibiotics at 37˚C for 16-20 h with shaking at 220 rpm. A 250 μL aliquot from 3 mL of LB broth was added into 100 mL of LB broth with appropriate antibiotics. It was incubated at 37˚C for 16-20 h with shaking at 220 rpm. A Midi-prep kit (Macherey-Nagel) was then used to generate 800~1000 μg DNA for *in-vitro* transfection into wild-type HEK293 cells or HEK-GLP-1R cells.

2.15. Quantification of DNA by absorbance

The amount and quality of plasmid DNA were determined by measuring the optical density (OD) at wavelengths of 260 nm and 280 nm. The maximum absorption of

nucleic acids is at 260 nm while that of protein is at 280 nm. According to the Beer Lambert Law, an OD_{260nm} of 1 corresponds to a concentration of 50 µg/mL for double-stranded DNA. The samples were diluted appropriately to make sure that the value of OD_{260nm} was within the linear range of 0.1-1.0 units. The ratio of OD_{260nm}/OD_{280nm} was used as an indication of nucleic acid purity. Each plasmid preparation was used for transfection, when the OD_{260nm}/OD_{280nm} was between 1.8-1.9 units indicating a relatively high quality of the DNA preparation.

2.16. Polymerase chain reaction (PCR) cloning of ECE-1a and ECE-1d sequences from ECE-1a I.M.A.G.E. DNA.

The frozen ECE-1a in pCR4-TOPO vector in *E.coli* was resuscitated and grown as described in **Method 2.12.3**.. Three colonies were tested by colony PCR **(Method 2.13.)**. A positive colony was then selected and grown in 3 mL of LB broth followed by the preparation in 20 µL of H_2O using a Miniprep kit as shown in **Method 2.14**. The amount of DNA was determined as in **Method 2.15**. For amplifying full length ECE-1a and ECE-1d, 20 ng DNA template was added into 20 µL of reaction containing 0.4 U Phusion polymerase, 0.5 µM gene-specific primers as below, 0.2 mM dNTPs and an appropriate amount of H_2O.

2.16.1. Primer design

The sequences of primers for cloning full-length ECE-1a and ECE-1d genes are shown in **Fig 2.3**. 13-16 bp of the primer sequences encode a region of ECE-1a or ECE-1d containing either the start codon (ATG) or stop codon (TAA). Start codons were flanked by a Kozak sequence, 'GCCACC' (Kozak, 1987), to increase the efficiency of translation, a restriction enzyme site and finally 2-3 additional bases. The stop codon in the common 3'-primer was flanked by a restriction enzyme site and 3 additional bases.

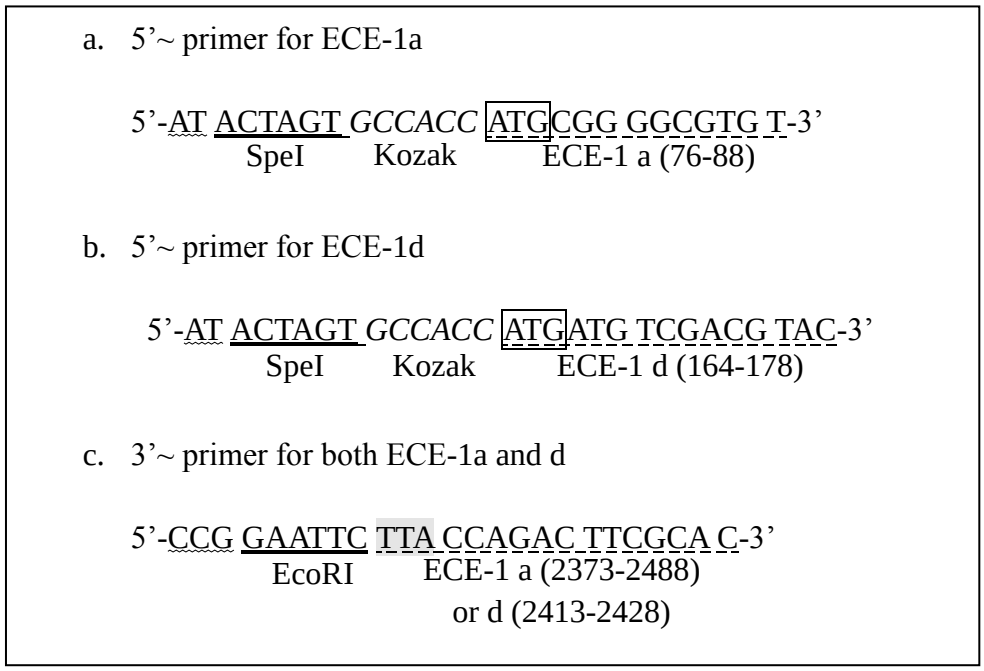

Fig 2.3. Primers for cloning full length ECE-1a and d. The bases with dashed underline are the specific coding sequences of ECE-1 a or ECE-1 d, in which the start codon and stop codon are in a hollow or shaded box. Bases in italic represent the Kozak sequence and those on a solid underline represent the RE sites as indicated. The extra bases are present on a waved underline.

2.16.2. Setting up PCRs

The reactions were set up on ice and following a brief centrifugation (1,500 g, 1 s) were quickly transferred to a thermocycler with a heated lid. The initial denaturation was performed at 98 ℃ for 30 s and subsequent for 10 s for 33 cycles. The annealing step for each cycle was 71 ℃ for 30 s based on the T_m of the primer pair for phusion polymerase calculated using the NEB T_m calculator online. The extension was carried out at 72 ℃ for 1.5 min (15-30 s/kb) for each cycle and 10 min for the final extension. The reactions were then held at 4 ℃ before identification by agarose gel or kept at -20 ℃ until use.

2.17. Agarose gel electrophoresis of DNA

To separate and identify the size of DNA fragments, agarose gel electrophoresis was carried out. Depending on the size of DNA, 0.8-2% *w:v* agarose in TBE buffer (89 mM Tris-borate, 890 mM boric acid, 2 mM EDTA) containing 0.005% *w:v* ethidium bromide was used to make the gels. Samples mixed with 10 × loading buffer (50 % *v:v* glycerol, 2 % *v:v* Ficoll (hydrophilic polysaccharide), 50 mM EDTA and 5 % *w:v* bromophenol blue prepared in sterile water). A 100 bp or 1.0 kb Plus DNA ladder (0.5 µg/lane) was used to estimate the size of the DNA fragments. The gel was run at 100-120 V for 60-100 min. The DNA in the gel was then visualized by a UV trans-illuminator and where required photographed using a digital camera.

2.18. Purification of DNA fragments from solution or agarose gel

PCR clean-up gel extraction kits (Macherey-Nagel) were used to purify DNA fragments (50 bp-~20 kb) from either solution (e.g., RE digestion reactions) or agarose gel (e.g., digested DNA fragments and PCR products). To extract DNA from an agarose gel, the band of interest was excised using a clean scalpel under low-power UV trans-illumination. DNA in the cut gel or solution was then dissolved and purified following the manufacturer's protocol. The purified DNA was finally eluted with H_2O in preparation for ligation or re-PCR reactions (using the PCR product as the template).

2.19. Restriction digests of plasmids and DNA fragments

In order to prepare samples for ligation, vectors and inserts were digested by restriction enzymes. DNA (2-3 µg of plasmid or purified PCR product) were digested at 37 ℃ for 16 h in a 50 µL reaction containing 10 U of each restriction enzyme, the recommended buffer and BSA (0.1 mg/ml) when required and an appropriate volume of H_2O. After digestion, the target DNA fragments were either directly extracted from the reaction mixture following the manufacturer's protocol or identified and separated by agarose gel electrophoresis **(Method 2.17.)** and subsequently extracted from the gel **(Method**

2.18.). Dependent of the conditions required for both of the restriction enzymes, either a double digest or sequential digest was performed. The sequential digest was carried out with a DNA separation and purification step between the two digestions.

Diagnostic digestion was performed at 37 ℃ for 2 h in a 20 µL reaction containing 0.5 µg of DNA, 2 µL 10 × buffer and 0.2 µL of 100 × BSA (10 mg/mL) where required, 4 U of enzyme and an appropriate amount of H_2O. The digested DNA was then identified by agarose gel electrophoresis **(Method 2.17.)**.

2.20. DNA ligation

The cohesive end termini of vectors and inserts digested with restriction enzymes were ligated using T4 DNA ligase with a molar ratio from 1:3 to 1:10 of vector to insert. For example, in a 10 µL of ligation reaction, ~30 ng of vector and ~120 ng of insert (estimated from DNA ladder; 2:1 of MWt ratio) were mixed with 200 U of ligase, 1 µL of 10 × ligase buffer and appropriate amount of H_2O. The mixture was mixed by gently tapping the tube and collected to the bottom by brief centrifugation (1500 g, 1 s). The reaction was carried out at RT for 3 h.

2.21. Bacterial transformation

Competent DH5α cells were prepared using the pre-established method (Willars and Challiss, 2011) and stored at -80 ℃. For each transformation, a 50 µL aliquot of competent DH5α cells was thawed on ice for ~7 min. A 5-10 ng aliquot of plasmid DNA or 8 µL of ligation reaction was added followed by gently tapping the tube and incubation on ice for 10 min. The DNA/cell mixture was then heat-shocked at 42 ℃ for 90 s and immediately transferred to ice for 3 min incubation. The cells were then incubated at 37 ℃ for 1 h in 800 µL SOC medium (0.5% *w:v* yeast extract, 2% *w:v* tryptone, 10 mM NaCl, 2.5 mM KCl, 10 mM $MgCl_2$, 10 mM $MgSO_4$, 20 mM glucose). Following incubation, 50 µL of cells transformed with 5-10 ng of plasmid DNA were spread onto a 10 cm LB agar plate containing an appropriate antibiotics and incubated

inverted at 37 ℃ overnight. For cells transformed with the products of a ligation reaction, cells were centrifuged (140 g, 4 min) followed by removal of 600 µL of supernatant. The cell pallet was then resuspended and spread onto an agar plates. Following overnight incubation, colony PCR was performed **(Method 2.13.)** or the plates were sealed with Nescofilm and stored inverted at 4 ℃ until use.

2.22. Reverse-transcription polymerase chain reaction (RT-PCR) of ECE-1 and PCR cloning of full-length ECE-1b and ECE-1c

2.22.1. Preparation of ECE-1 cDNA by RT-PCR

Following the manufacturer's instruction (Invitrogen), the first-strand cDNA of ECE-1 was synthesized by SuperScript III reverse transcriptase (200 U) and 2 pmol ECE-1 gene-specific reverse primer **(Figure 2.4.)** in 20 µL of reaction from 400 ng of mRNA of HEK-GLP-1R cells as template.

2.22.2. PCR cloning of full-length ECE-1b and ECE-1c

For amplifying full-length ECE-1b and ECE-1c, 2 µL of cDNA as the template was added into 20 µL of reaction containing 0.4 U of Phusion polymerase, 0.5 µM gene specific primers as designed below, 0.2 mM dNTPs and an appropriate amount of H_2O. For ECE-1c, re-PCR was performed using ~100 ng of PCR product as template and another pair of gene specific primers as shown below **(Fig 2.4.)**.

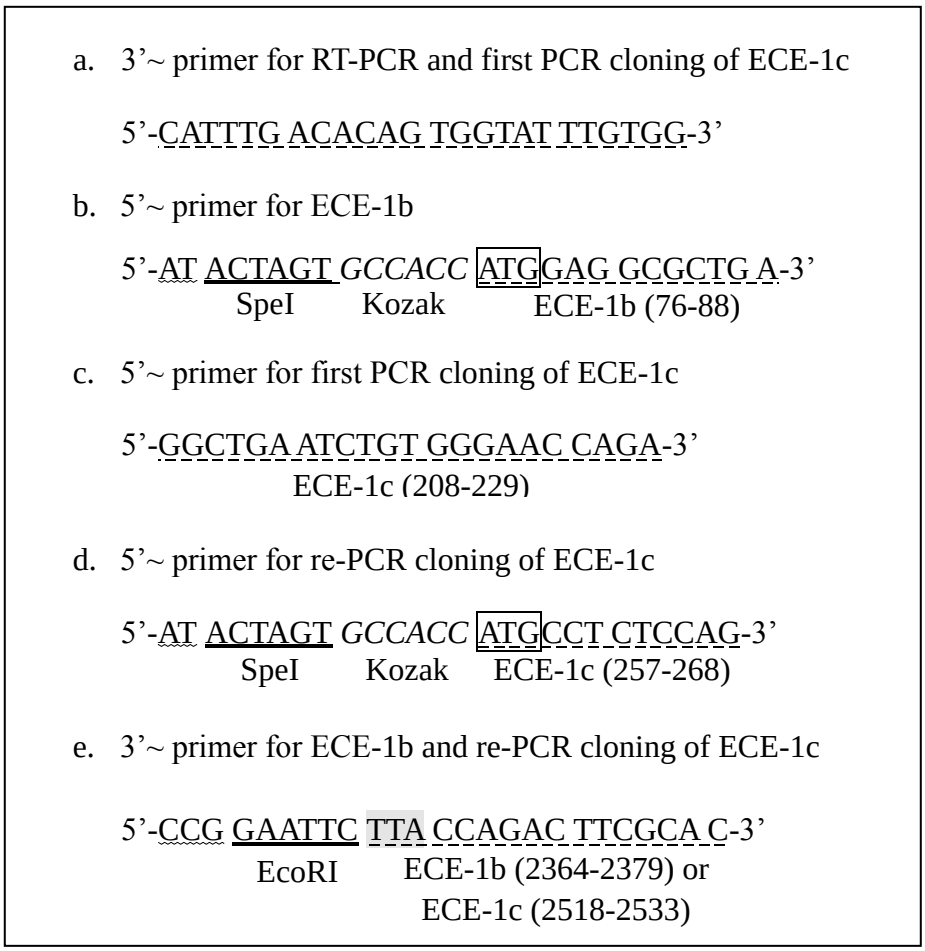

Fig 2.4. Primers for RT-PCR and cloning full length ECE-1b and ECE-1c. The bases with dashed underline are the specific coding sequences of ECE-1b or ECE-1c, in which the start codon and stop codon are in a hollow or shaded box. Bases in italic represent the Kozak sequence and those on a solid underline represent the RE sites as indicated. The extra bases are present on a waved underline.

2.23. The cloning of ECE-1a-d sequences to remove the stop codons and the mCherry sequence to remove start codon for generation of C-terminal mCherry-tagged ECE-1 a-d plasmids

In order to express mCherry tagged on the C-terminal of ECE-1 protein, the sequences of stop codon truncated ECE-1 a-d and start codon truncated mCherry were amplified.

2.23.1. The cloning of stop codon truncated ECE-1a-d sequences and start codon truncated mCherry sequence

Using the ECE-1a-d plasmids as templates, the same forward primers that were used for full length ECE-1a-d **(Fig 2.3. and Fig 2.4.)** and the reverse primer without a stop codon shown below **(Fig 2.5.)** were used. The same conditions for PCR were set up as used previously **(Fig 2.16.2. and Fig 2.22.2.)** to generate ECE-1a-d sequences minus the stop codons. The plasmid of full-length mCherry was used as the template for amplifying the mCherry sequence without a start codon by using the primers shown below **(Fig 2.5.)**.

a. 3'~ primer for stop codon truncated ECE-1a-d

5'- AAT GGTACC CCAGACTTCGCACTTG -3'
KpnI ECE-1

b. 5'~ primer for start codon truncated mCherry

5'-ATT GGTACC GTGAGCAAGGGCGA-3'
KpnI mCherry

c. 3'~ primer for mCherry

5'-CCG GAATTC TTACTTGTACAGCTCGTC-3'
EcoRI mCherry

Fig 2.5. Primers for cloning stop codon-truncated ECE-1 a-d and start codon-truncated mCherry. The bases with dashed underline are the stop codon-truncated coding sequences common for all the ECE-1 isoforms. Bases on a solid underline represent the RE sites as indicated. The extra bases are present on a waved underline.

2.23.2. Generation of C-terminal mCherry-tagged ECE-1a-d plasmids

The stop codon-truncated ECE-1a-d PCR products were digested and ligated into the digested pcDNA3.1 vector. The Miniprep from the single colony was made as described before **(Method 2.14.)**. This group of ECE-1a-d plasmids without a stop codon were

then digested at the sites after the C-terminal of ECE-1 and the start codon-truncated mCherry sequence was inserted into it.

2.24.Automated DNA sequencing

The sequences of the inserts in all recombinant plasmids were confirmed by automated DNA sequencing (Protein and Nucleic Acid Characterisation Laboratory, University of Leicester, Leicester, UK). The automated DNA sequencing was performed by a Biosystems 3730 Squencer based on fluorescently labelling DNA fragments with a circle sequencing protocol. The primers were designed to recognize the sequence located at least 50 nucleotides away from the insert in pcDNA3.1(+) as there is s poor quality of recognition in the first 15-40 bases **(Table 2.2)**.

Table 2.2. Primers for automated DNA sequencing

Sequencing direction	Sequence	Vector and location
5' to 3'	5'-AGGCGTTTTGCGCTGCTTCGC-3'	pcDNA3.1(+) (409-433)
3' to 5'	5'-ACTAGAAGGCACAGTCGAGGC-3'	pcDNA3.1(+) (1220-1201)

2.25. Data analysis.

All data obtained were analysed using Prism 6.0 (GraphPad Software Inc., San Diego, CA). Concentration-response curves were analysed using a four parameter non-linear regression analysis. Data are representative of $n \geq 3$ and are presented as mean +/± S.E.M., unless otherwise stated. Statistical analysis was performed by unpaired Student's t-test (two-tailed) for only two datasets. One-way or two-way analysis of variance (ANOVA) with Bonferroni's post-test for multiple comparisons, or Dunnett's post-test to compare each group with a single control group were used where more than two datasets were compared. All analysis was performed using Prism 6. Statistical significance was accepted at $p < 0.05$. Where statistical comparisons are shown for normalised data, the statistical analyses were performed on the raw data and shown on the normalised data for clarity.

CHAPTER 3 Desensitisation and Re-sensitisation of the GLP-1R

3.1. Introduction

GLP-1 has a variety of anti-diabetic effects including stimulating insulin release from pancreatic β-cells in a glucose-dependent manner, promoting proinsulin transcription and insulin biosynthesis, anti-apoptotic and proliferative effects on β-cells and inhibiting glucagon secretion from α-cells, reducing gastric emptying and suppressing appetite (Drucker, 2006, Doyle and Egan, 2007, Garber, 2010). These effects are mediated by binding to its receptor, the GLP-1R, which is a validated target for the treatment of type 2 diabetes. It is important therefore to understanding the function and regulation of the GLP-1R. Although G protein-coupling and aspects of the signalling of the GLP-1R have been well documented, information about desensitisation, re-sensitisation and particularly the trafficking of GLP-1R are less well explored.

During continuous subcutaneous infusion of native GLP-1 for 6 or 12 weeks to type 2 diabetic patients in order to maintain elevated levels of circulating GLP-1, the activity of GLP-1 including satiety and postprandial blood glucose-lowering and weight reduction suggest that the chronic activation of the GLP-1R is not associated with detectable receptor desensitisation (Zander et al., 2001, Meneilly et al., 2003). However, studies have demonstrated that *in vitro*, the GLP-1R undergoes both homologous and heterologous desensitisation. This has been shown for Ca^{2+} signalling and related to receptor phosphorylation in response to agonist stimulation (Widmann et al., 1996b). The phosphorylated GLP-1R may internalise with GLP-1 bound, entering into intracellular compartments through clathrin- or caveolin-1-dependent machinery dependent on the cell type (Widmann et al., 1995, Alvarez et al., 2005, Syme et al., 2006). Following desensitisation, GLP-1R-mediated Ca^{2+} signalling re-sensitises after removal of the extracellular ligand. The recovery of the GLP-1R to the cell surface shows a similar pattern to receptor re-sensitisation and appears to be independent of *de*

novo receptor synthesis in CHL fibroblast cells expressing recombinant GLP-1R (Widmann et al., 1995). However, the intracellular compartment(s) that the ligand-receptor complex targets to after internalisation and the actual mechanism of GLP-1R re-sensitisation are less clear.

The work described in this chapter extended previous work and examined the desensitisation and re-sensitisation of both cAMP and Ca^{2+} signalling pathways in either HEK293 cells stably expressing the recombinant human GLP-1R or in a pancreatic β-cell line, INS-1E, expressing native GLP-1Rs.

3.2. Results

3.2.1. Activation and desensitisation of GLP-1 7-36 amide-mediated cAMP signalling in HEK-GLP-1R cells.

In the absence of the PDE inhibitor, IBMX, challenge of HEK-GLP-1R cells with 100 nM of GLP-1 7-36 amide stimulated an increase of cAMP which increased to a maximum at 15 min. The level of cAMP was then sustained up until at least 30 min after which time there was evidence of a decrease **(Fig 3.2.1.1)**.

The GLP-1 7-36 amide-mediated cAMP response was concentration-dependent with a pEC_{50} of 9.24 ± 0.07 and Hill slope of 0.82 ± 0.17 **(Fig 3.2.1.2. A_i)**. Pre-challenge of cells with 100 nM GLP-1 7-36 amide for 30 min in the absence of IBMX was used in order to study the potential desensitisation of the GLP-1R. However, even after a 1 h recovery period following removal of GLP-1 7-36 amide, cAMP levels remained elevated above basal **(Fig 3.2.1.2.A_i)**. Under these conditions, re-challenge of cells with GLP-1 7-36 amide resulted in levels of cAMP that were higher than the control (without pre-treatment), although EC_{50} values were similar. However, basal subtraction revealed that the cAMP response to the second addition of GLP-1 7-36 amide was reduced in cells pre-exposed to the agonist **(Fig 3.2.1.2.A_{ii})**.

The markedly elevated cAMP levels that were sustained following agonist removal presented a difficulty in determining receptor desensitisation and the Ca^{2+} response was therefore used as an index of receptor activation to study GLP-1R desensitisation.

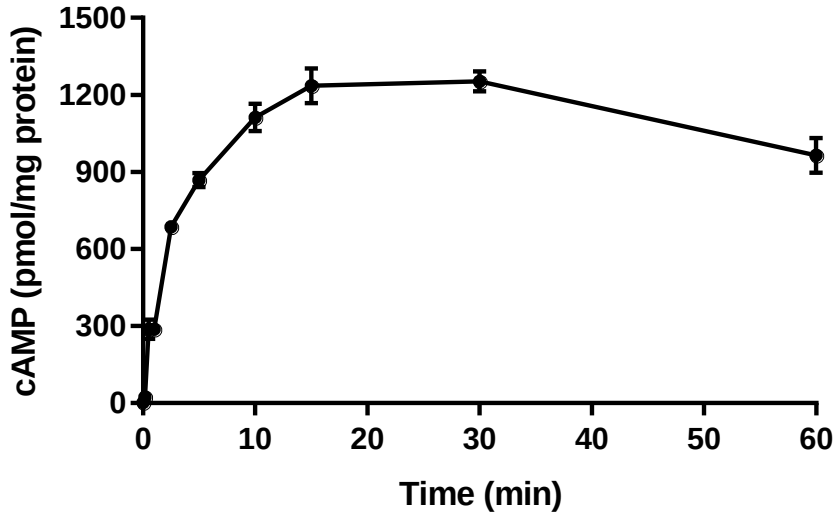

Fig 3.2.1.1. Time-course of the 100 nM GLP-1 7-36 amide-stimulated cAMP response. HEK-GLP-1R cells were stimulated with 100 nM GLP-17-36 amide for the required times (0-60 min) in the absence of IBMX. Data are mean ± S.E.M., n = 3.

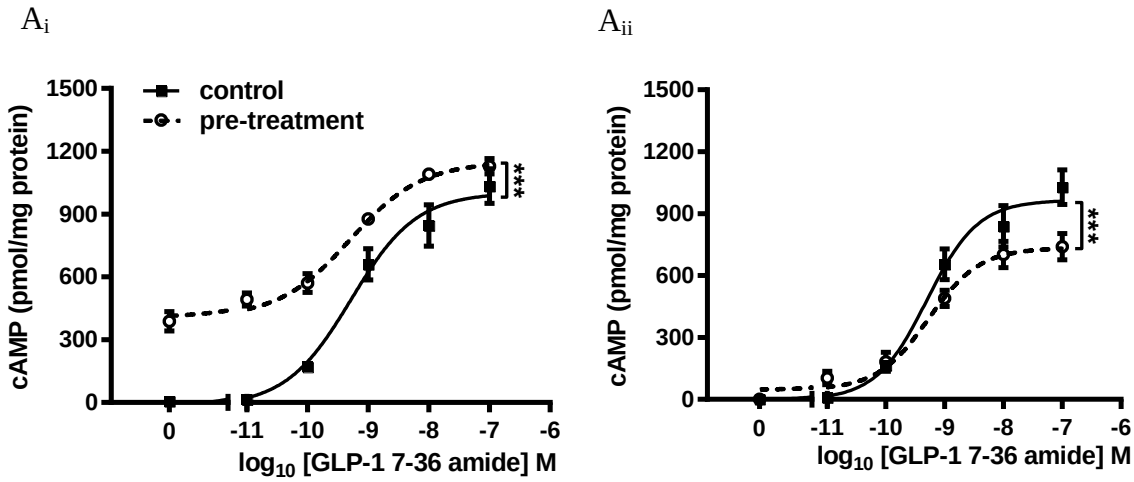

Fig 3.2.1.2. GLP-1 7-36 amide-mediated cAMP concentration-response curves in naïve cells or cells pre-exposed to GLP-1 7-36 amide. A_i. HEK-GLP-1R cells were pre-stimulated with buffer (control) or 100 nM GLP-1 7-36 amide (pre-treatment) for 30 min in the absence of IBMX followed by washing with KHB. After a 60 min period of recovery, cells were stimulated or re-stimulated with GLP-1 7-36 amide at the indicated concentrations (0-100 nM) for 15 min in the absence of IBMX. **A_{ii}.** Data from graph **A** with basal (0) subtraction. The pEC_{50} and Hill slope under control conditions were 9.24 ± 0.07 and 0.82 ± 0.17 respectively and 9.39 ± 0.17 and 0.75 ± 0.13 respectively following pre-treatment. All data are mean ± S.E.M., n = 3. ***, $p < 0.001$ (two-way ANOVA).

3.2.2. GLP-1 7-36 amide-mediated Ca^{2+} responses.

In fluo-4-loaded HEK-GLP-1R cells, GLP-1 7-36 amide produced a concentration-dependent increase in fluorescence as an index of $[Ca^{2+}]_i$. Higher concentrations of GLP-1 7-36 amide evoked a greater and more rapid increase in $[Ca^{2+}]_i$ compared with lower concentrations. For example, 10 nM GLP-1 7-36 amide evoked a Ca^{2+} response that reached a peak at ~5 s after stimulation while it took ~10 s for 1 nM GLP-1 7-36 amide and ~20 s for 0.01 nM GLP-1 7-36 amide **(Fig 3.2.2.1.A)**. The maximum increases in fluorescence were determined and used to generate concentration-response curves, which showed a pEC_{50} of 10.03 ± 0.14 **(Fig 3.2.2.1.B)**. Changes in fluorescence were calibrated as described in **Methods 2.7.** and increases in $[Ca^{2+}]_i$ calculated **(Fig 3.2.2.1.C, D)**. The peaks of calibrated Ca^{2+} traces were sharper than uncalibrated ones. Also the calibrated concentration-response curve showed GLP-1 7-36 amide to have a pEC_{50} of 9.63 ± 0.24, which was numerically lower but not significantly different to the pEC_{50} calculated from the uncalibrated fluorescence changes. The Hill slope of the calibrated curve was 1.10 ± 0.23 while it was 0.74 ± 0.15 for the uncalibrated curve ($p > 0.05$). This calibration also illustrated that the maximum concentration of GLP-1 7-36 amide (10 nM) produced an elevation of $[Ca^{2+}]_i$ from a resting value of 75 ± 6 nM to 602 ± 41 nM in HEK-GLP-1R cells **(Fig 3.2.2.1.C)**.

Removing the extracellular Ca^{2+} at 5 min before stimulation did not affect the response to GLP-1 7-36 amide, but pre-incubating the cells with an ER Ca^{2+} ATPase inhibitor, thapsigargin (2 μM, 5 min) essentially abolished the response **(Fig 3.2.2.2.)**.

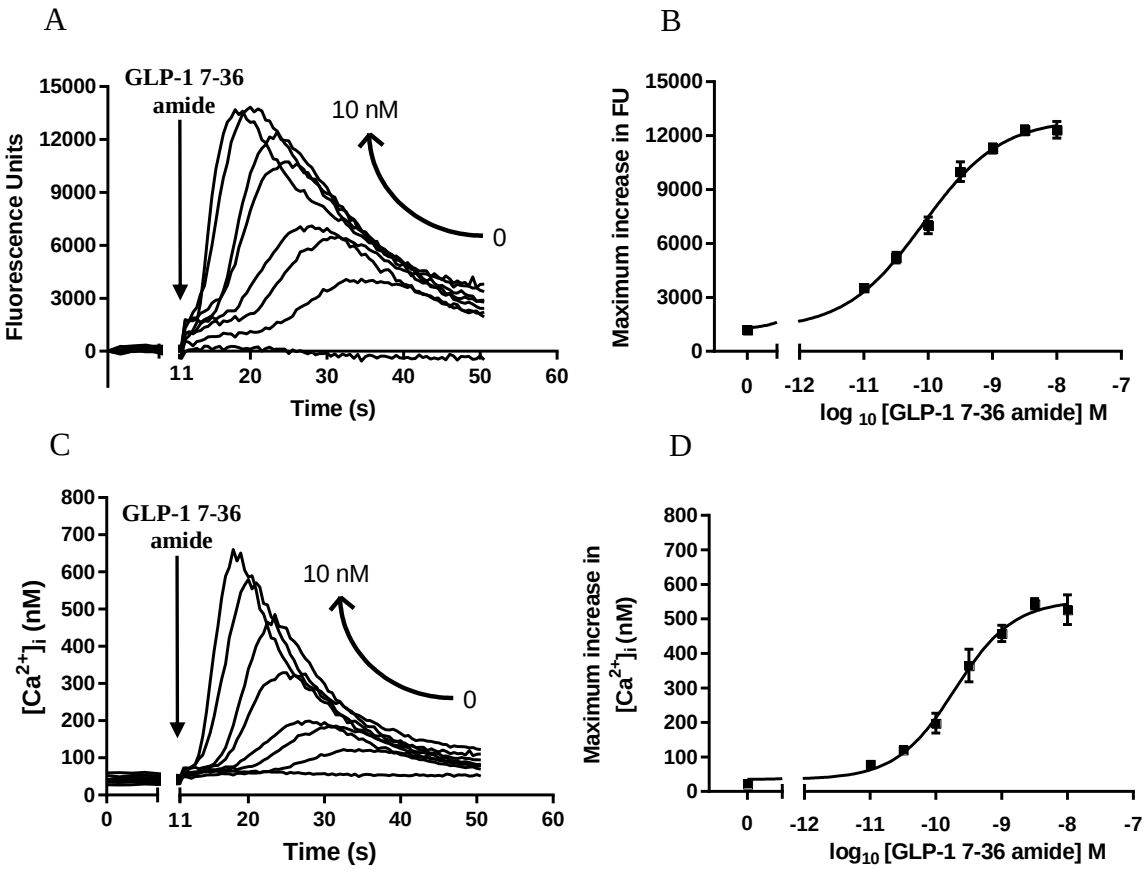

Fig 3.2.2.1. GLP-1 7-36 amide-mediated Ca^{2+} responses. Fluo-4-loaded HEK-GLP-1R cells were challenged with buffer (0) or GLP-1 7-36 amide at the indicated concentrations (0-10 nM). The changes in fluorescence were measured by a microplate reader as an index of $[Ca^{2+}]_i$. **A.** Representative traces from a single experiment showing increases in fluorescence units (basal subtracted for each trace). Fluorescence was measured for 51 s with the injection at 11 s. **B.** The maximum changes in fluorescence units (FU) were determined to generate concentration-response curves. From these, the pEC_{50} was determined as 10.03 ± 0.14 with a Hill slope of 0.74 ± 0.15. **C, D.** The $[Ca^{2+}]_i$ was calculated by calibration of the fluo-4 signal as described in **Methods 2.7.**. The concentration-response curves of GLP-1 7-36 amide-induced elevation of $[Ca^{2+}]_i$ demonstrated a pEC_{50} value of 9.63 ± 0.24 and Hill slope of 1.10 ± 0.23. Data are representative or mean ± S.E.M., n = 3.

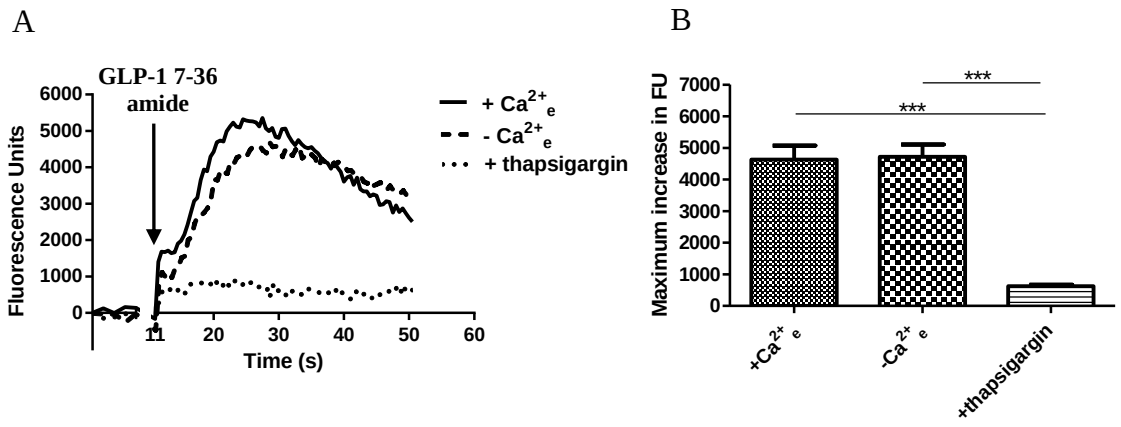

Fig 3.2.2.2. GLP-1 7-36 amide-mediated Ca^{2+} responses in HEK-GLP-1R cells are from intracellular Ca^{2+} stores. Fluo-4-loaded cells were stimulated with 10 nM GLP-1 7-36 amide in buffer either with or without extracellular Ca^{2+} (Ca^{2+}_e). Alternatively, cells were pre-incubated with 2 μM thapsigargin for 5 min followed by stimulation with 10 nM GLP-1 7-36 amide in buffer with Ca^{2+}_e. **A.** Representative traces from a single experiment showing changes in fluorescence with basal subtraction for each trace. Fluorescence was measured for 51 s with injection of ligand at 11 s. **B.** Maximum changes in fluorescence were determined in each experiment. Data are representative or mean + S.E.M., n = 3. ***, $p < 0.001$ (Bonferroni's test following one-way ANOVA).

3.2.3 Exposure of GLP-1 7-36 amide induces desensitisation of GLP-1R-mediated Ca^{2+} responses.

Pre-treatment with 10 nM (E_{max} concentration) GLP-1 7-36 amide for 1 min, followed by washing with standard KHB (pH 7.4) and a 5 min recovery period (protocol shown in **Fig 3.2.3.1.A**), resulted in a markedly reduced $[Ca^{2+}]_i$ response to re-stimulation **(Fig 3.2.3.1.B)**. In an attempt to ensure all of the GLP-1 7-36 amide was removed from the receptor before re-challenge, acidified buffers at different pH values were used to wash the cells for 20 s followed by 5 min recovery. Acid wash has been used in many studies to remove cell-surface bound ligand (Widmann et al., 1997, Haugh et al., 1999, Li et al., 2008). The response to the re-challenge increased as the pH of the washing buffer decreased **(Fig 3.2.3.1.C)** and there was no effect of the acid washes on GLP-1 7-36 amide responses in naïve cells. Washing the cells with buffer at pH 4.0 resulted in a numerical but not significant increase (~10%) in response to re-challenge with GLP-1 7-36 amide compared to the response in cells washed with standard KHB (pH 7.4) **(Fig 3.2.3.1.C_{ii})**. Moreover, washing with buffer at pH 2.0 (20 s) resulted in a further but still not significant increase (~30%) in the response to re-challenge with GLP-1 7-36 amide **(Fig 3.2.3.1.C_{ii})**.

Typically, acidified buffer at around pH 4.0 has been used to remove peptide ligands from receptors (Yu and Hinkle, 1998, Kiess et al., 1994). It is of course possible that pH 2.0 acid might damage cells, particularly on extended exposure and so, prolonging the period of washing with acidified buffer at pH 4.0 was performed in an attempt to remove more ligand from receptors. When the time of washing with acidified buffer (pH 4.0) was extended beyond 20 s up to 50 s following a 1 min pre-challenge with GLP-1 7-36 amide (protocol shown in **Fig 3.2.3.2.A**), there was a tendency for the responses to re-challenge to increase, reaching a maximal following a 40 s wash **(Fig 3.2.3.2. B, C)**. Although there were no statistically significant differences, the data normalised to controls (without pre-treatment) showed consistently that cells washed with pH 4.0 buffer for 40 s gave a maximum response to GLP-1 7-36 amide

re-challenge **(Fig 3.2.3.2.D)**. The response was, however, still significantly decreased compared to the control (without pre-treatment). Moreover, washing with acidified buffer at pH 4.0 for 40 s resulted in a response to the re-challenge with GLP-1 7-36 amide that was similar to the response following a pH 2.0 wash for 20 s or 40 s **(Fig 3.2.3.3.B)**. Washing the cells with the buffer at pH 2.0 for 40 s significantly decreased the response in naïve cells, potentially highlighting the damaging impact of a pH 2.0 wash.

Based on the data above, washing with acidified buffer at pH 4.0 for 40 s was used in the following experiment to detect the time-course of GLP-R desensitisation in the absence of continued ligand binding to the plasma membrane GLP-1Rs. Pre-exposure to 10 nM GLP-1 7-36 amide for a range of times (from 0-30 min) followed by washing with acidified buffer (pH 4.0) for 40 s (protocol shown in **Fig 3.2.3.4.A**) induced a time-dependent reduction in response to GLP-1 7-36 amide re-challenge following a 5 min recovery period. Pre-treatment for either 10 or 30 min gave similar responses on re-challenge suggesting that 10 min pre-treatment mediated a maximum desensitisation of the Ca^{2+} response **(Fig 3.2.3.4.B, C)**.

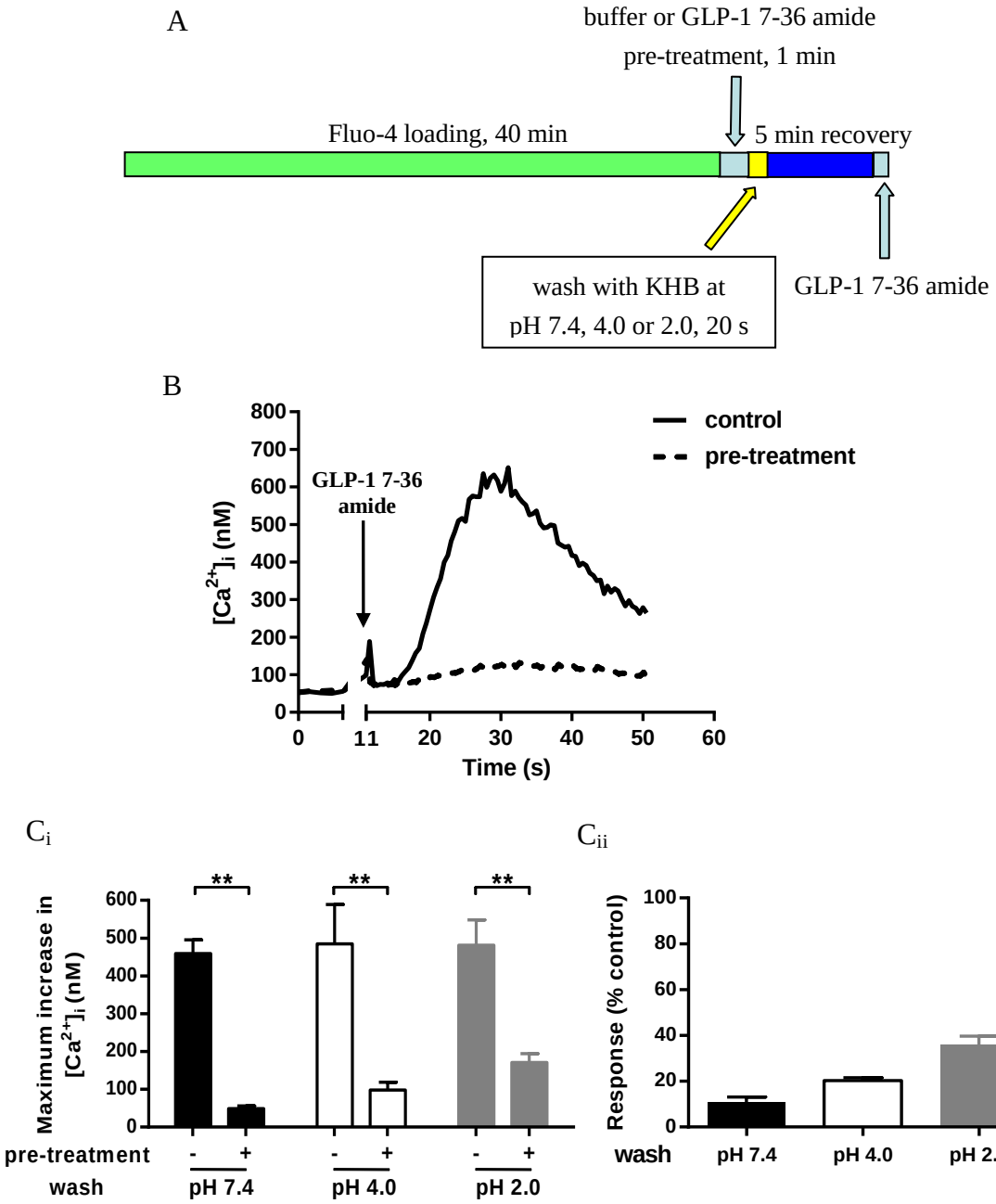
A
buffer or GLP-1 7-36 amide
pre-treatment, 1 min
Fluo-4 loading, 40 min
5 min recovery
wash with KHB at
pH 7.4, 4.0 or 2.0, 20 s
GLP-1 7-36 amide
B
control
pre-treatment
GLP-1 7-36
amide
[Ca2+]i (nM)
Time (s)
Ci
Maximum increase in
[Ca2+]i (nM)
pre-treatment
wash
pH 7.4
pH 4.0
pH 2.0
Cii
Response (% control)
wash
pH 7.4
pH 4.0
pH 2.0

Fig 3.2.3.1. Recovery of GLP-1 7-36 amide-mediated Ca^{2+} responses following pre-challenge after washing with either standard or acidified buffer. A. Experimental protocol. **B.** Representative Ca^{2+} traces. Fluo-4-loaded cells were pre-treated with buffer (control) or 10 nM GLP-1 7-36 amide for 1 min (pre-treatment) followed by washing with standard KHB (pH 7.4) for 20 s. After 5 min recovery, cells were then challenged or re-challenged with 10 nM GLP-1 7-36 amide and the changes in fluorescence were monitored and calibrated to $[Ca^{2+}]_i$. Responses were measured for 51 s with injection at 11 s. **C_i.** Fluo-4-loaded cells were pre-treated with buffer (control) or 10 nM GLP-1 7-36 amide for 1 min and then washed with buffer at different pH values (7.4, 4.0 or 2.0) for 20 s. The maximum increases in fluorescence were measured and converted to $[Ca^{2+}]_i$ when cells were challenged or re-challenged with 10 nM GLP-1 7-36 amide, following 5 min recovery. **C_{ii}.** Data were normalised to controls (without pre-treatment). Data are representative or mean + S.E.M., n $\geqslant$ 3. **, $p < 0.01$ (Bonferroni's test following two-way ANOVA. For clarity, the significance of differences between the different pH washes is not shown).

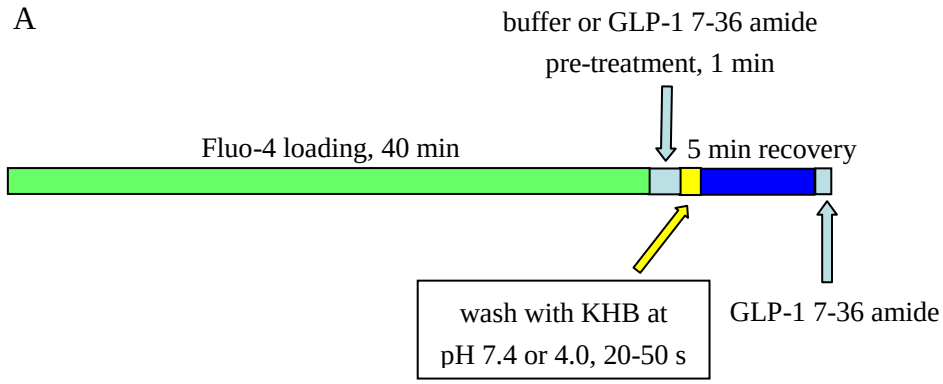
A
buffer or GLP-1 7-36 amide
pre-treatment, 1 min
Fluo-4 loading, 40 min
5 min recovery
wash with KHB at
pH 7.4 or 4.0, 20-50 s
GLP-1 7-36 amide

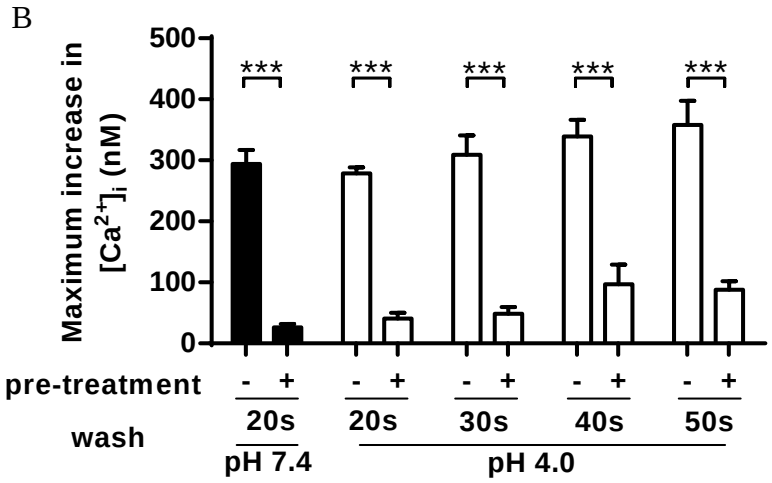
B
Maximum increase in
[Ca2+]i (nM)
500
400
300
200
100
0
***
***
***
***
***
pre-treatment
- + - + - + - + - +
wash
20s
20s
30s
40s
50s
pH 7.4
pH 4.0

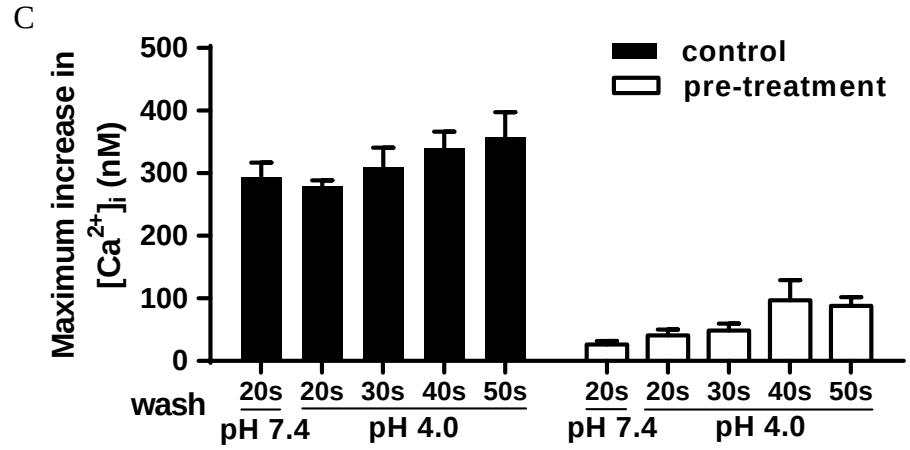
C
Maximum increase in
[Ca2+]i (nM)
500
400
300
200
100
0
control
pre-treatment
wash
20s 20s 30s 40s 50s
20s 20s 30s 40s 50s
pH 7.4 pH 4.0
pH 7.4 pH 4.0

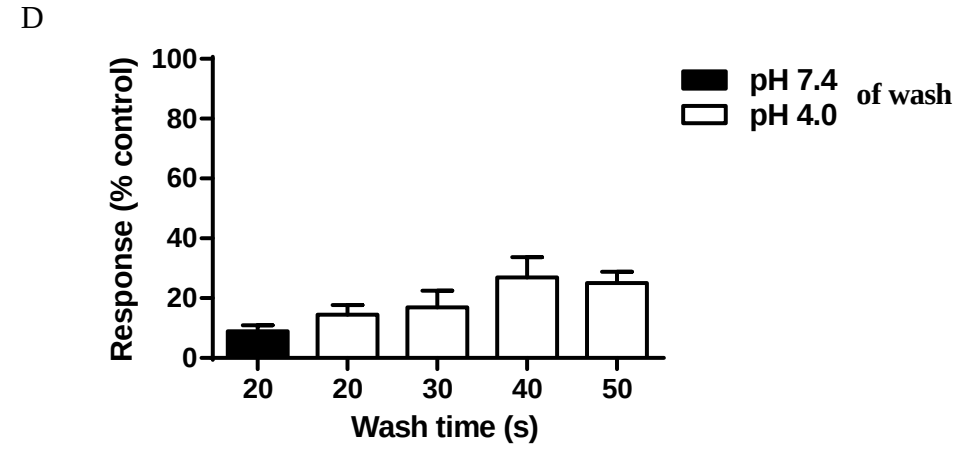
D
Response (% control)
100
80
60
40
20
0
pH 7.4
pH 4.0
of wash
20 20 30 40 50
Wash time (s)

Fig 3.2.3.2. GLP-1 7-36 amide-induced desensitisation of GLP-1R-mediated Ca^{2+} responses after washing with standard buffer or pH 4.0 buffer for various times. A. Experimental protocol. **B.** Fluo-4-loaded HEK-GLP-1R cells were pre-treated with buffer (control) or 10 nM GLP-1 7-36 amide for 1 min, followed by washing with standard KHB (pH 7.4) for 20 s or acidified buffer (pH 4.0) from 20 to 50 s as indicated. After 5 min recovery, cells were challenged or re-challenged with 10 nM GLP-1 7-36 amide and the increases in fluorescence monitored and converted to $[Ca^{2+}]_i$. **C.** The data from panel **B** were grouped to untreated (control) and GLP-1 7-36 amide pre-treated. **D.** The data in panel **B** were normalised to controls (without pre-treatment). All data are mean + S.E.M., n ≥ 3. ***, $p < 0.001$ (Bonferroni's test following one-way ANOVA. Only the differences within a pair are shown for clarity).

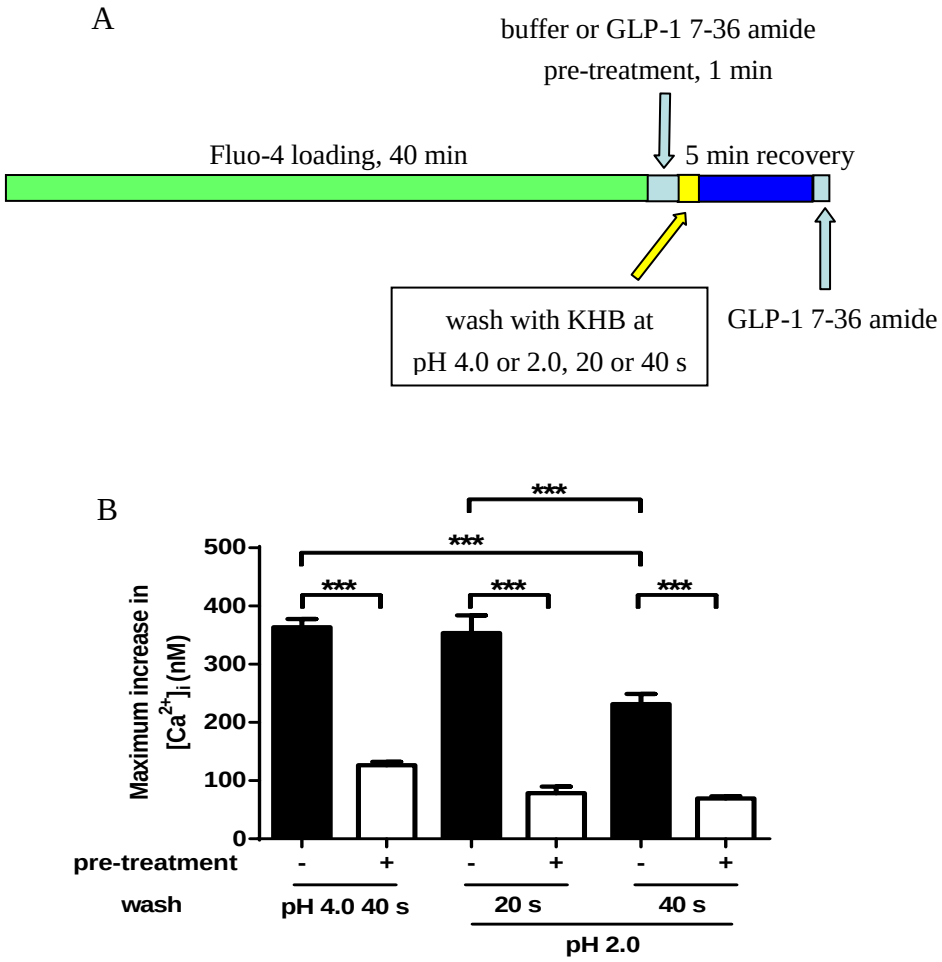

Fig 3.2.3.3. GLP-1 7-36 amide-induced desensitisation of GLP-1R-mediated Ca^{2+} responses after washing with acidified buffer at either pH 4.0 or pH 2.0. A. Experimental protocol. **B.** Fluo-4-loaded cells were pre-treated with buffer (control) or 10 nM GLP-1 7-36 amide for 1 min, followed by washing with acidified buffer at pH 4.0 for 40 s or pH 2.0 for either 20 s or 40 s. After 5 min recovery, cells were then challenged or re-challenged with 10 nM GLP-1 7-36 amide and the increases in fluorescence were determined and calibrated to $[Ca^{2+}]_i$. All data are mean + S.E.M., n > 3. ***, $p < 0.001$. (Bonferroni's test following one-way ANOVA. The differences between the pre-treatment and the controls (without pre-treatment) in different groups are not shown).

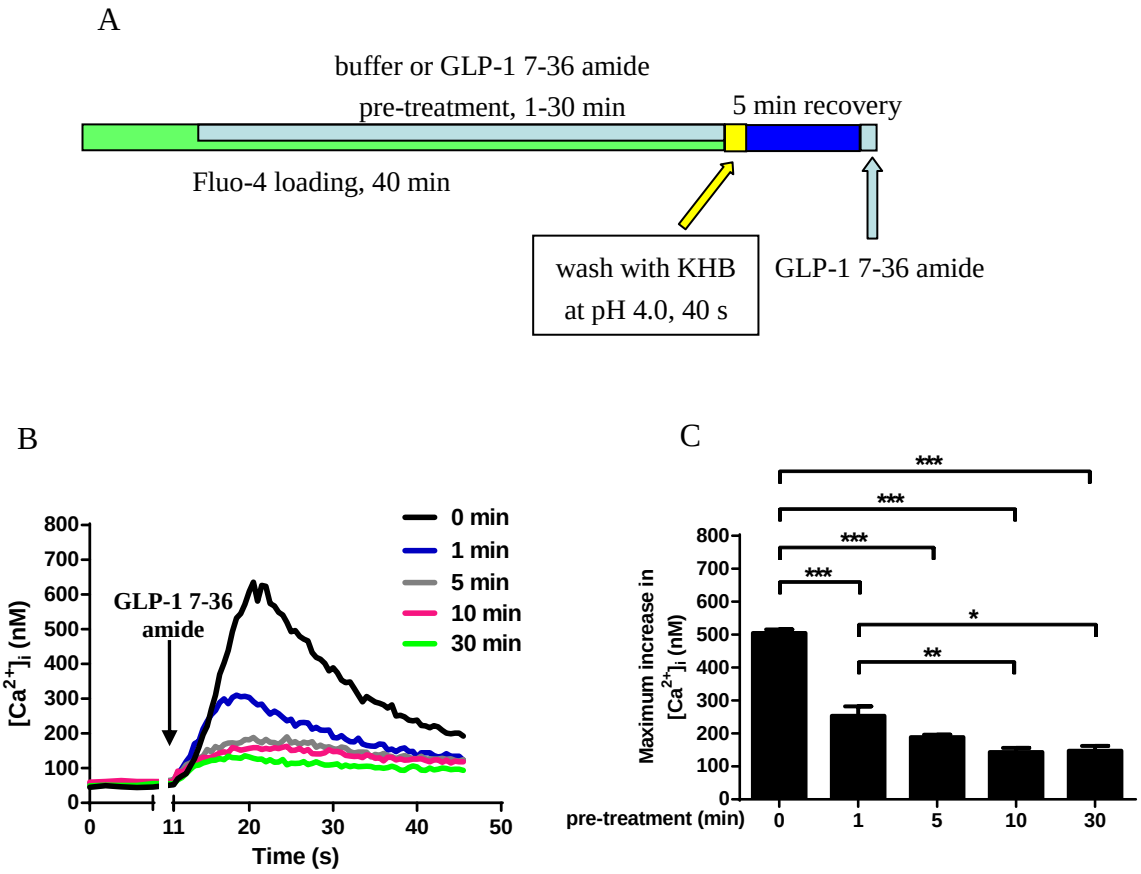

Fig 3.2.3.4. Time-dependence of GLP-1 7-36 amide-mediated desensitisation of GLP-1R signalling. A. Experimental protocol. Fluo-4-loaded cells were pre-treated with buffer (0 min) or 10 nM GLP-1 7-36 amide for 1, 5, 10 or 30 min and then washed with acidified buffer (pH 4.0) for 40 s. Cells were then challenged or re-challenged with 10 nM GLP-1 7-36 amide following 5 min recovery and changes in fluorescence were monitored and converted to $[Ca^{2+}]_i$. Responses were measured for 46 s with injection at 11 s. Both representative traces (**B**) and mean data (**C**) are shown. Data are mean + S.E.M., n = 3. *, $p < 0.05$; **, $p < 0.01$; ***, $p < 0.001$ (Bonferroni's test following one-way ANOVA).

3.2.4. GLP-1R re-sensitisation.

To mimic a more physiological environment, standard buffer (pH 7.4) instead of acidified buffer (pH 4.0) was used to wash the cells after pre-treatment to determine the time-course of GLP-1R re-sensitisation. After desensitisation induced by a 10 min pre-treatment (giving maximum desensitisation as shown in **Fig 3.2.3.4.**) with 10 nM GLP-1 7-36 amide and subsequent washing with KHB (protocol shown in **Fig 3.2.4.A**), GLP-1R-mediated Ca^{2+} signalling showed a time-dependent recovery. The response to re-challenge with GLP-1 7-36 amide was almost absent at 5 min recovery **(Fig 3.2.4.B, F)**. The Ca^{2+} response then recovered with increasing recovery times **(Fig 3.2.4.C, D, E, F)**. Indeed, after a 3 h recovery period, the response was not significantly different from the control without pre-treatment **(Fig 3.2.4.F)**, and a full concentration-response curve at this point showed a pEC_{50} and Hill slope of 8.78 $\pm$ 0.26 and 0.60 $\pm$ 0.06 respectively, which were numerical lower but not significantly different compared to the control without pre-treatment (9.40 $\pm$ 0.13 and 0.79 $\pm$ 0.08 respectively), although the curves did show a significant difference overall **(Fig 3.2.4.G)**.

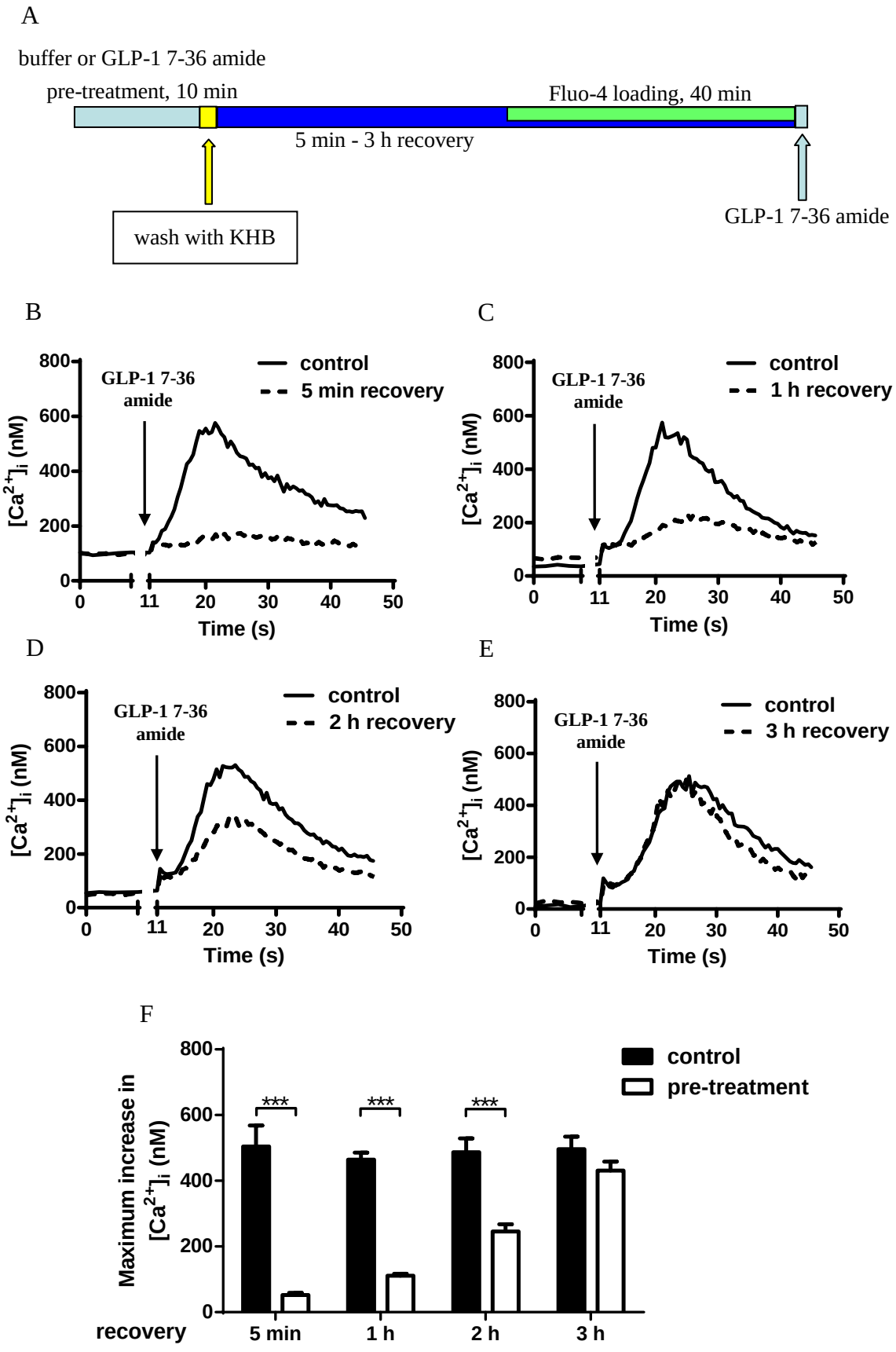
A
buffer or GLP-1 7-36 amide
pre-treatment, 10 min
Fluo-4 loading, 40 min
5 min - 3 h recovery
wash with KHB
GLP-1 7-36 amide
B
C
D
E
F
GLP-1 7-36 amide
control
5 min recovery
1 h recovery
2 h recovery
3 h recovery
[Ca2+]i (nM)
Time (s)
Maximum increase in [Ca2+]i (nM)
pre-treatment
recovery
5 min
1 h
2 h
3 h
***

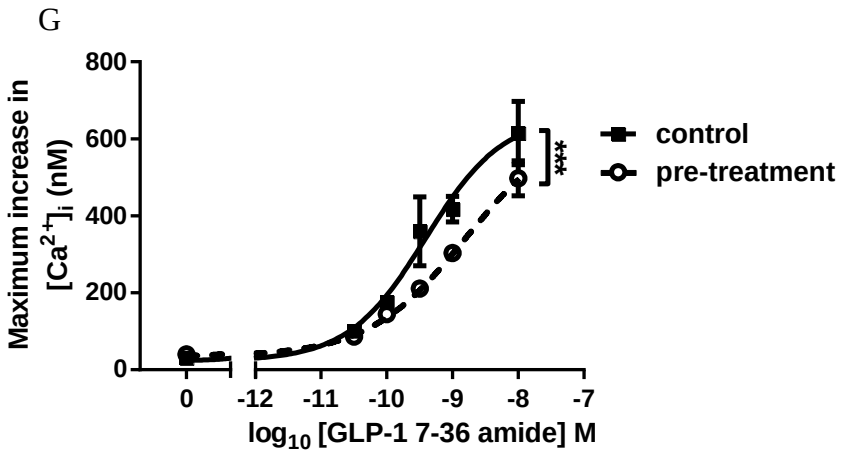

Fig 3.2.4. Re-sensitisation of GLP-1R-mediated Ca^{2+} responses. A. Experimental protocol. **B**-**E**. Representative traces. Cells were pre-treated with buffer (control) or 10 nM GLP-1 7-36 amide for 10 min followed by washing with KHB. After a 5 min **(B)**, 1 h **(C)**, 2 h **(D)** or 3 h **(E)** period of recovery, fluo-4-loaded cells were challenged or re-challenged with 10 nM GLP-1 7-36 amide. The fluorescence was monitored and calibrated to $[Ca^{2+}]_i$. Responses were measured for 46 s with the injection at 11 s. The mean data were generated **(F)**. **G**. Cells were pre-treated with buffer (control) or 10 nM GLP-1 7-36 amide (pre-treatment) for 10 min followed by washing with KHB. After 3 h recovery, fluo-4-loaded cells were stimulated or re-stimulated with GLP-1 7-36 amide at the required concentrations (0-10 nM). The pEC_{50} values were 9.40 ± 0.13 (control) and 8.79 ± 0.26 (pre-treatment) and Hill slopes were 0.79 ± 0.08 (control) and 0.60 ± 0.06 (pre-treatment). Data in **F** are mean + S.E.M., n = 4. ***, $p < 0.001$ (Bonferroni's test following two-way ANOVA. Only the differences between groups at each time point are shown for clarity). Data in **G** are mean ± S.E.M., n = 3. ***, $p < 0.0001$ (two-way ANOVA).

3.2.5. GLP-1R re-sensitisation is not dependent on protein synthesis, but dependent on receptor internalisation and endosomal acidification.

The generally accepted mechanism of receptor re-sensitisation involves receptor internalisation and receptor recycling and/or the recruitment of new receptors from the cytoplasm to the plasma membrane and/or the *de novo* synthesis of new receptors **(Fig 1.6.)**. To detect the potential mechanisms of GLP-1R re-sensitisation, a range of inhibitors were used at the concentrations previously shown to be effective in HEK293 cells (Hagen et al., 2003, Stoneham et al., 2012, Law et al., 2000). Cycloheximide (17.5 μM), a protein synthesis inhibitor, was used to inhibit new receptor synthesis. Dynasore (80 μM), an inhibitor of dynamin, was used to inhibit dynamin-dependent receptor internalisation. Monensin (50 μM) collapses proton gradients and was used as an inhibitor of endosomal acidification. The experimental protocol is shown in **Fig 3.2.5.A**. Treatment with 17.5 μM cycloheximide did not affect GLP-1R re-sensitisation **(Fig 3.2.5.B)**. This concentration of cycloheximide has previously been shown in our laboratory to block protein synthesis in HEK293 cells (Alhosaini, 2011). However, treating cells with 80 μM dynasore **(Fig 3.2.5.C)** or 50 μM monensin **(Fig 3.2.5.D)** significantly inhibited GLP-1R re-sensitisation without affecting the responses of naïve cells.

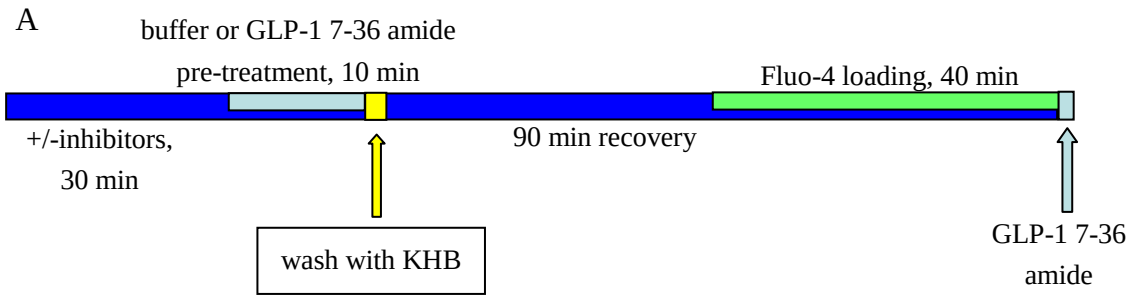
A
buffer or GLP-1 7-36 amide
pre-treatment, 10 min
Fluo-4 loading, 40 min
+/-inhibitors,
30 min
90 min recovery
wash with KHB
GLP-1 7-36
amide

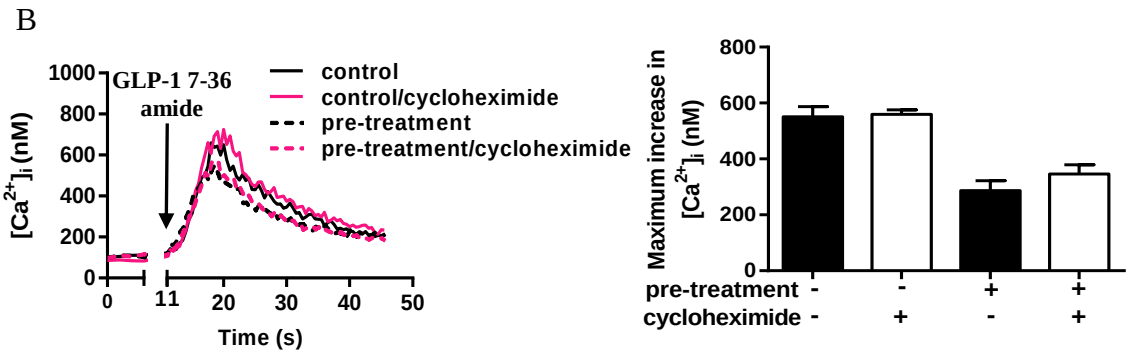
B
GLP-1 7-36
amide
control
control/cycloheximide
pre-treatment
pre-treatment/cycloheximide
[Ca2+]i (nM)
Time (s)
Maximum increase in
[Ca2+]i (nM)
pre-treatment
cycloheximide

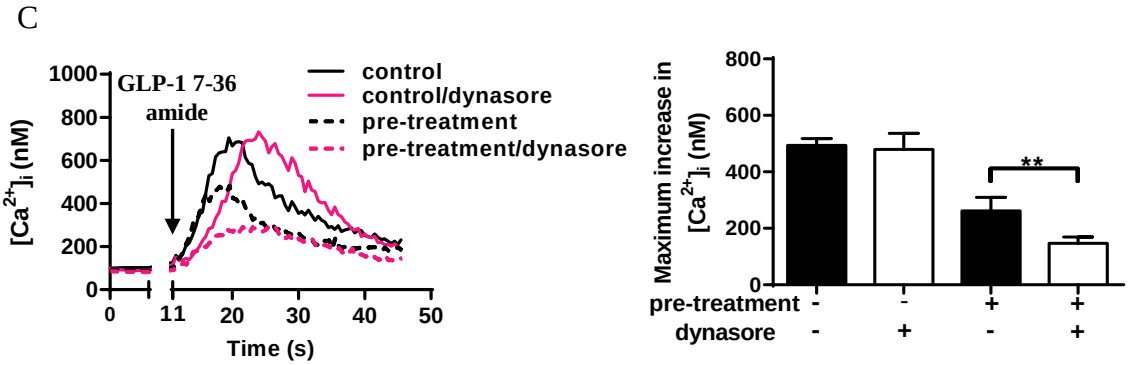
C
GLP-1 7-36
amide
control
control/dynasore
pre-treatment
pre-treatment/dynasore
[Ca2+]i (nM)
Time (s)
Maximum increase in
[Ca2+]i (nM)
**
pre-treatment
dynasore

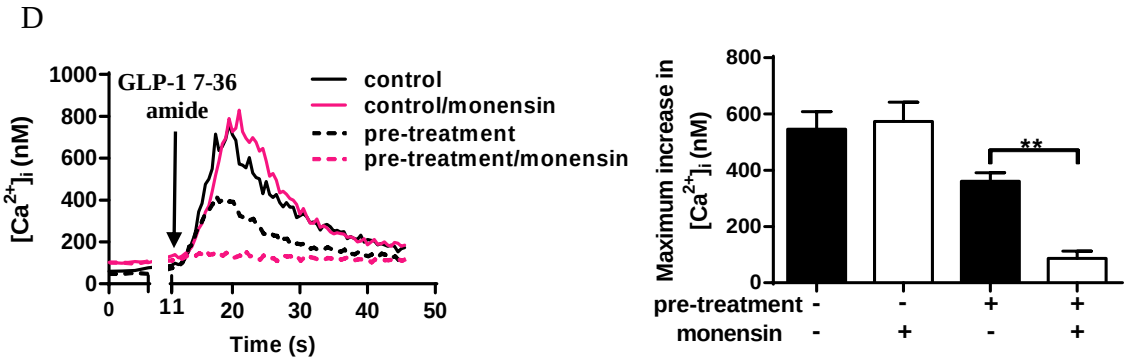
D
GLP-1 7-36
amide
control
control/monensin
pre-treatment
pre-treatment/monensin
[Ca2+]i (nM)
Time (s)
Maximum increase in
[Ca2+]i (nM)
**
pre-treatment
monensin

Fig 3.2.5. GLP-1R re-sensitisaton is not dependent on protein synthesis, but dependent on receptor internalisation and endosomal acidification. A. Experimental protocol. Cells were pre-incubated for 30 min with either buffer or buffer with inhibitors, 17.5 μM cycloheximide (**B**), 80 μM dynasore (**C**) or 50 μM monensin (**D**) (which were then included throughout). Cells were then pre-treated with buffer (control) or 10 nM GLP-1 7-36 amide for 10 min followed by washing with KHB. After a 90 min period of recovery, fluo-4-loaded cells were stimulated or re-stimulated with 10 nM GLP-1 7-36 amide. Responses were measured for 46 s with injection at 11 s. Data are representative or mean + S.E.M., n ≥ 3. **, $p < 0.01$ (Bonferroni's test following one-way ANOVA; only the differences in pre-treated cells are shown here for clarity).

3.2.6. GLP-1 7-36 amide-mediated GLP-1R internalisation with ligand bound, co-localizing with the early endosomes.

It has been reported previously in our laboratory that the signalling of a C-terminal EGFP-tagged GLP-1R (GLP-1R-EGFP) is similar to that wild-type GLP-1R when expressed in HEK293 cells. Indeed, in the HEK-GLP-1R-EGFP cell line used here to examine the real-time movement of GLP-1Rs, GLP-1 7-36 amide has similar potency on cAMP generation to that in HEK-GLP-1R cells although the E_{max} is reduced (Coopman et al., 2010). Real-time confocal imaging of live HEK-GLP-1R-EGFP cells revealed intense, continuous plasma membrane fluorescence and relatively weak intracellular fluorescence (**Fig 3.2.6.1.A, B**) demonstrating that receptors are mainly expressed on the plasma membrane with low expression in the interior of cell. Challenging cells for 60 min with GLP-1 7-36 amide at 10 nM **(Fig 3.2.6.1.A)** or 100 nM **(Fig 3.2.6.1.B)** induced the loss of this membrane fluorescence. That was associated with an increase of intracellular fluorescence in discrete puncta or large patches. Quantification of changes in both plasma membrane and intracellular fluorescence as described in **Methods 2.11.1.** indicated that GLP-1 7-36 amide induced GLP-1R internalisation in a time- and concentration-dependent manner. For example, both 10 nM and 100 nM GLP-1 7-36 amide gave maximum internalisation at ~60 min and the latter gave higher internalisation than the former **(Fig 3.2.6.1.C)**. However, pre-treatment with dynasore (80 μM, 30 min) blocked both the GLP-1 7-36 amide-induced loss of membrane fluorescence and the increase in intracellular fluorescence **(Fig 3.2.6.2.)**.

To detect whether ligand would internalise along with the GLP-1R, rhodamine-labelled GLP-1 7-36 amide (Rho-GLP-1 7-36 amide) was used along with cells expressing GLP-1R-EGFP. Treatment with 100 nM Rho-GLP-1 7-36 amide for 60 min resulted in the internalisation of both GLP-1R-EGFP and Rho-GLP-1 7-36 amide, which showed co-localization at both the plasma membrane and within the cytosol (**Fig 3.2.6.3.A**). Internalisation of both ligand and receptor was successfully blocked by 80 μM dynasore

(Fig 3.2.6.3.B). Following addition of 100 nM Rho-GLP-1 7-36 amide to HEK-GLP-1R cells, fluorescence was observed both at the cell surface and within the cytosol. Cell-surface binding and the appearance of fluorescence inside the cells were blocked by co-addition of 100 nM unlabelled GLP-1 7-36 amide **(Fig 3.2.6.3.C)**.

In a functional assay, Rho-GLP-1 7-36 amide stimulated cAMP accumulation but with a reduced potency and different Hill slope compared to GLP-1 7-36 amide in HEK-GLP-1R cells. The pEC_{50} and Hill slope for Rho-GLP-1 7-36 amide were 7.97 ± 0.04 and 1.20 ± 0.04 respectively **(Fig 3.2.6.3.D)**, both of which were significantly different to these of GLP-1 7-36 amide (pEC_{50} 9.67 ± 0.02 and Hill slope 0.86 ± 0.12). In a radioligand binding assay using intact HEK-GLP-1R cells at 4˚C, 10 nM GLP-1 7-36 amide or 10 nM Rho-GLP-1 7-36 amide was used to compete with 0.05 nM ^{125}I-exendin 9-36 amide. Both ligands inhibited ^{125}I-exendin 9-36 amide binding. However, the inhibition by GLP-1 7-36 amide was significantly higher than that of Rho-GLP-1 7-36 amide **(Fig 3.2.6.3.E)** indicating a higher affinity of GLP-1 7-36 amide. Importantly, previous research has shown that the C-terminal EGFP-tagged version of GLP-1R gives a similar potency in GLP-1 7-36 amide-mediated cAMP generation compared to the wild-type GLP-1R (Coopman et al., 2010).

The co-localization of GLP-1R-EGFP and early endosomes was then determined using immunocytochemistry of an early endosome marker, EEA1 in fixed HEK-GLP-1R-EGFP cells. As shown in live cells, in fixed cells the fluorescence of GLP-1R-EGFP was present mainly at the cell surface although some was present within the cytosol **(Fig 3.2.6.4.)**. EEA1 was present mainly in the cytosol (based on GLP-1R-EGFP defining the plasma membrane location). Under basal conditions, there was some evidence of co-localization of GLP-1R-EGFP with EEA1 within the cytosol (**Fig 3.2.6.4.**). Consistent with the data in live cells **(Fig 3.2.6.1.B)**, after 60 min stimulation with 100 nM GLP-1 7-36 amide, GLP-1R-EGFP accumulated in the interior of cells with very weak fluorescence remaining at the plasma membrane **(Fig 3.2.6.4.)**. GLP-1R-EGFP fluorescence inside of the cells was co-localized with EEA1 **(Fig**

3.2.6.4.). The Pearson correlation coefficient (r) shows that there are more co-localization between the GLP-1R-EGFP and EEA1 after simulation.

A

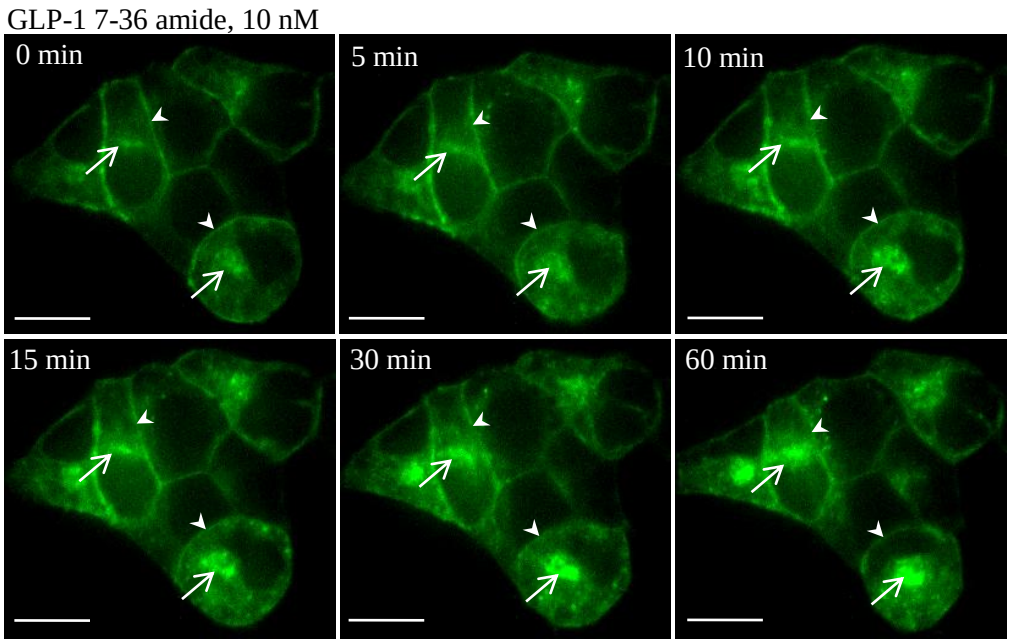
GLP-1 7-36 amide, 10 nM
0 min
5 min
10 min
15 min
30 min
60 min

B

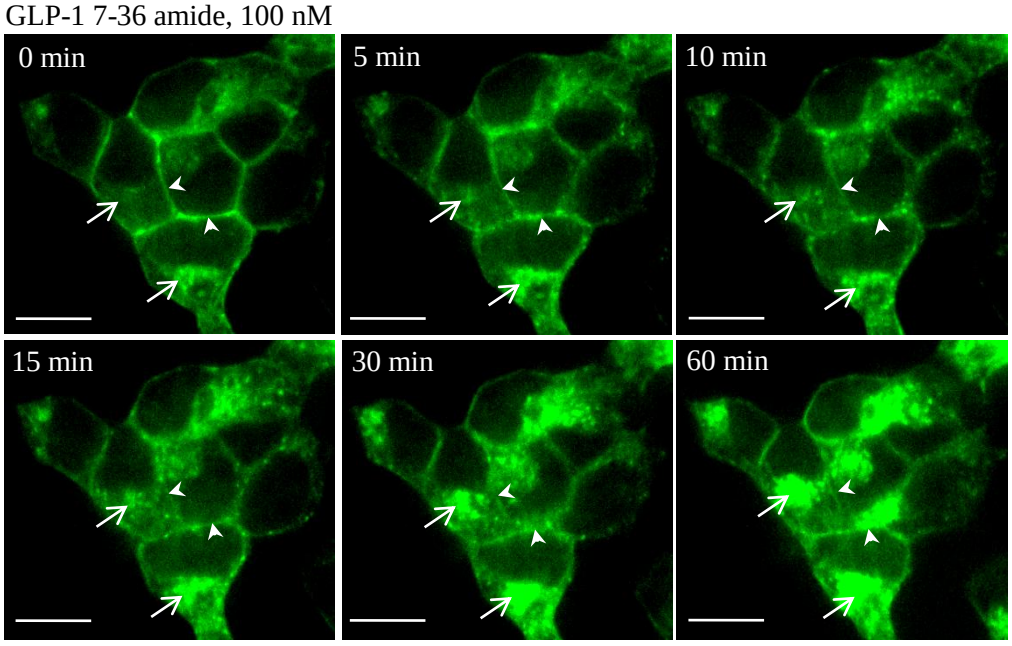
GLP-1 7-36 amide, 100 nM
0 min
5 min
10 min
15 min
30 min
60 min

C

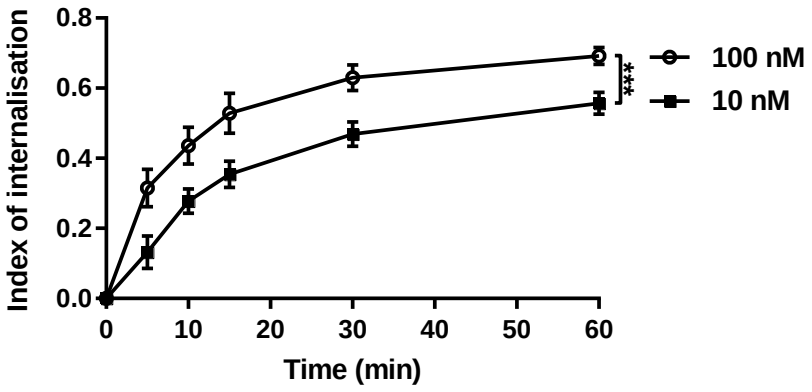
Index of internalisation
0.0
0.2
0.4
0.6
0.8
0
10
20
30
40
50
60
Time (min)
***
100 nM
10 nM

Fig 3.2.6.1. GLP-1 7-36 amide-mediated GLP-1R internalisation determined using an EGFP-tagged GLP-1R. Live HEK-GLP-1R-EGFP cells were imaged by confocal microscopy over 0-60 min period during which time they were challenged with either 10 nM GLP-1 7-36 amide (**A**) or 100 nM GLP-1 7-36 amide (**B**). **C**. Images were analysed as described in **Methods 2.11.1.**. Arrowheads and arrows indicate the distribution of GLP-1R-EGFP at the plasma membrane and in the cytosol respectively. Data are mean ± S.E.M., n = 3 (2-5 cells were analysed in each individual experiment; 10 cells in total for each data-point). ***, $p < 0.001$ (two-way ANOVA). Scale bar (in the bottom left of each image), 5 μm.

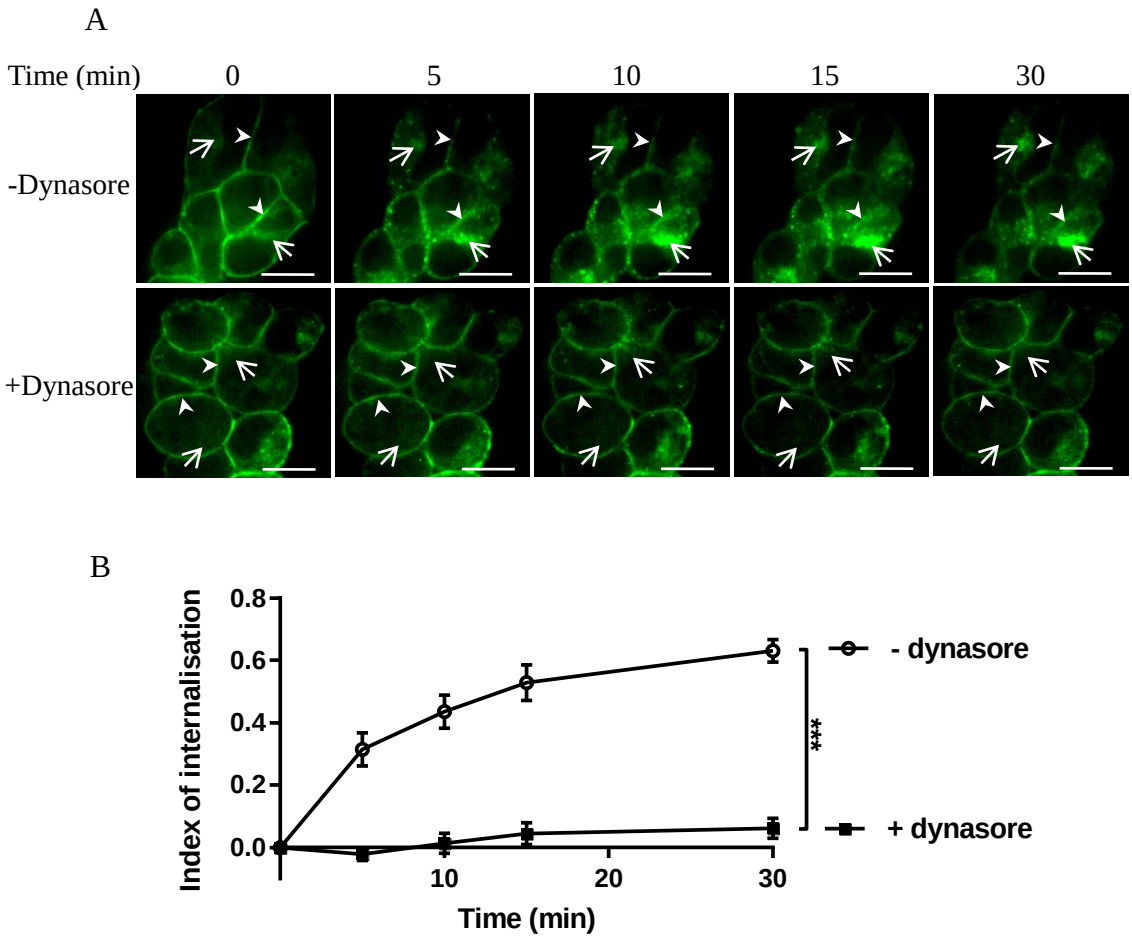

Fig 3.2.6.2. GLP-1 7-36 amide-mediated GLP-1R internalisation is blocked by dynasore. A. HEK-GLP-1R-EGFP cells were imaged by confocal microscopy over 0-30 min period during which time they were challenged with 100 nM GLP-1 7-36 amide with or without 80 μM dynasore pre-incubation for 30 min and in its continued presence or absence as appropriate. Arrowheads and arrows indicate the distribution of GLP-1R-EGFP at the plasma membrane and in the cytosol respectively. **B**. Data are mean ± S.E.M., n = 3 (2-5 cells were analysed in each individual experiment; 9 cells in total for each data-point). ***, $p < 0.001$ (two-way ANOVA). Scale bar (in the bottom right of each image), 5 μm.

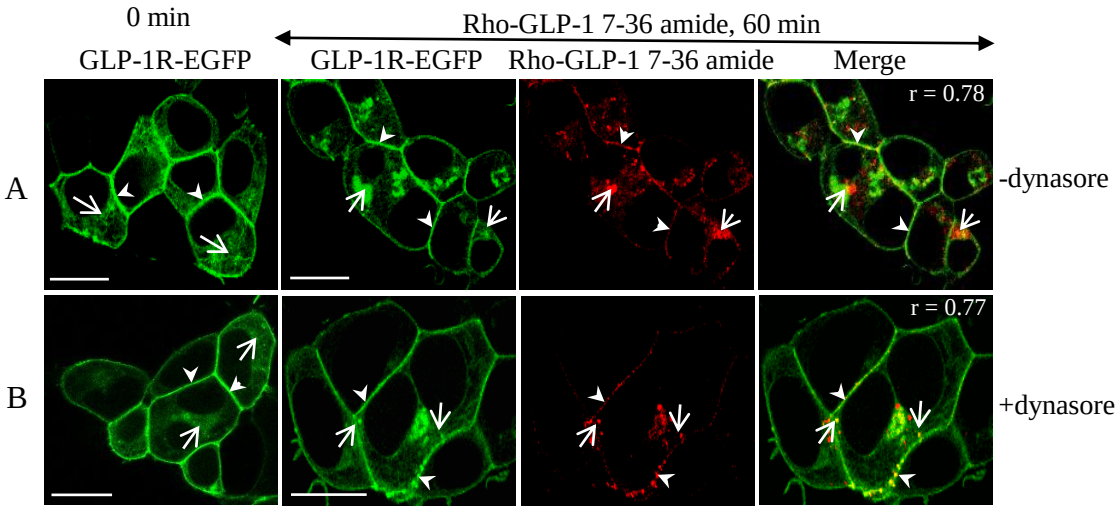
0 min
Rho-GLP-1 7-36 amide, 60 min
GLP-1R-EGFP
GLP-1R-EGFP
Rho-GLP-1 7-36 amide
Merge
r = 0.78
A
-dynasore
r = 0.77
B
+dynasore

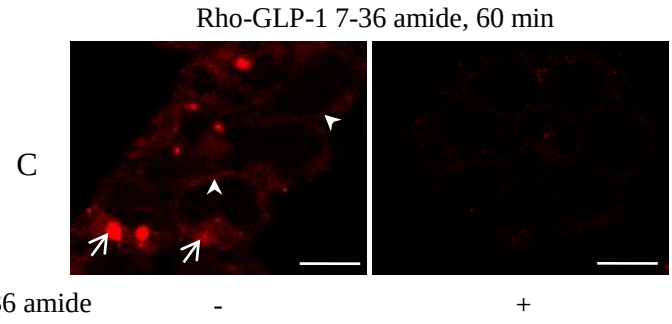
Rho-GLP-1 7-36 amide, 60 min
C
GLP-1 7-36 amide
-
+

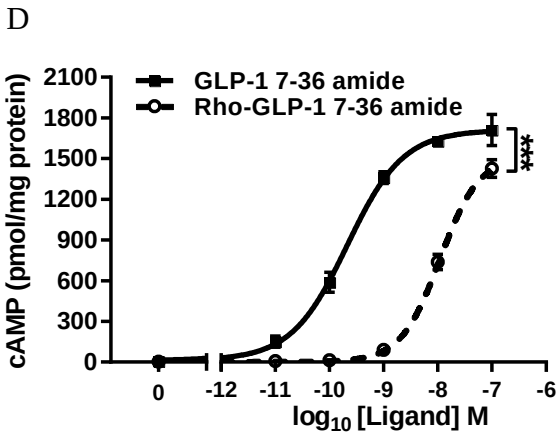
D
cAMP (pmol/mg protein)
2100
1800
1500
1200
900
600
300
0
GLP-1 7-36 amide
Rho-GLP-1 7-36 amide
***
0
-12
-11
-10
-9
-8
-7
-6
log10 [Ligand] M

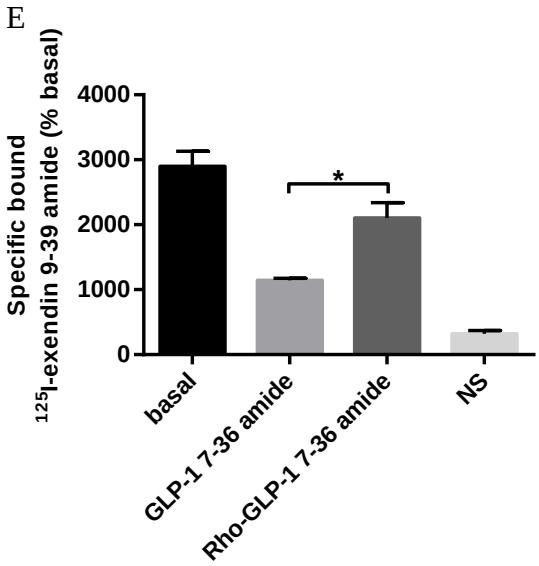
E
Specific bound
125I-exendin 9-39 amide (% basal)
4000
3000
2000
1000
0
*
basal
GLP-1 7-36 amide
Rho-GLP-1 7-36 amide
NS

Fig 3.2.6.3. Rhodamine-labelled GLP-1 7-36 amide internalises with the GLP-1R-EGFP. HEK-GLP-1R-EGFP cells were stimulated with 100 nM Rho-GLP-1 7-36 amide for 60 min in either the absence **(A)** or presence **(B)** of 80 μM dynasore. The cells were imaged by confocal microscopy either before (0 min) or after stimulation (60 min). **C.** HEK-GLP-1R cells were challenged with 100 nM Rho-GLP-1 7-36 amide alone or with 100 nM GLP-1 7-36 amide for 60 min. The cells were then imaged. **D.** HEK-GLP-1R cells were stimulated with GLP-1 7-36 amide or Rho-GLP-1 7-36 amide at the required concentrations (0-100 nM) for 15 min in the presence of IBMX. The cAMP production was then determined showing a pEC_{50} and Hill slope of 9.67 ± 0.02 and 0.86 ± 0.12 respectively for GLP-1 7-36 amide and 7.97 ± 0.04 and 1.20 ± 0.04 respectively for Rho-GLP-1 7-36 amide. **E.** HEK-GLP-1R cells were incubated with 0.05 nM ^{125}I-exendin 9-36 amide alone (basal) or with 10 nM GLP-1 7-36 amide, 10 nM Rho-GLP-1 7-36 amide or alternatively with 1 μM exendin 9-36 amide to determine non-specific binding (NSB) for 16 h at 4 ˚C. The binding of ^{125}I-exendin 9-39 amide was then assessed. The images are representative of 3 independent experiments. The arrowheads and arrows indicate the fluorescence at the plasma membrane and in the cytosol respectively. The Pearson correlation coefficient (r) was used to quantify the degree of co-localization between GLP-1R-EGFP and Rho-GLP-1 7-36 amide. Scale bar (in the bottom left or right of each image), 5 μm. Data in **D** are mean ± S.E.M., n = 3. ***, $p < 0.001$ (two-way ANOVA). Data in **E** are mean + S.E.M., n = 3. *, $p < 0.05$ (Bonferroni's test following one-way ANOVA; only the GLP-1 7-36 amide vs. Rho-GLP-1 7-36 amide comparison is shown for clarity).

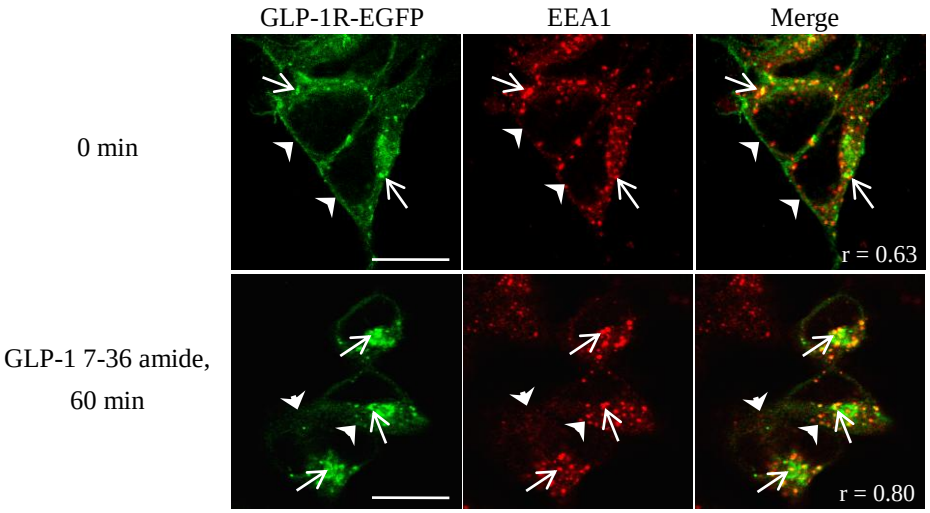

Fig 3.2.6.4. GLP-1 7-36 amide causes internalisation of the GLP-1R into early endosomes. HEK-GLP-1R-EGFP cells were un-stimulated (0 min) or challenged with 100 nM GLP-1 7-36 amide for 60 min. The cells were then fixed and permeabilized for immunostaining with anti-EEA1 antibody as described in **Methods 2.10.1.**. Cells were imaged in mounting solution using confocal microscopy. The expression of GLP-1R-EGFP or EEA1 at the plasma membrane or in the cytosol are indicated by arrowheads and arrows respectively. Representative images of 2 independent experiments. The Pearson correlation coefficient (r) was used to quantify the degree of co-localization between GLP-1R-EGFP and EEA1. Scale bar (in the bottom right of each image), 5 μm.

3.2.7. GLP-1 7-36 amide-induced reduction of cell-surface GLP-1R binding

This time- and concentration-dependent loss of cell-surface GLP-1R binding was determined using a radioligand binding assay in intact HEK-GLP-1R cells. GLP-1 7-36 amide at either 10 nM or 100 nM induced maximal reductions in binding of ^{125}I-exendin 9-39 amide at around 60 min with 100 nM causing a much greater loss than 10 nM **(Fig 3.2.7.A$_{i}$)**. For example, simulation for 60 min with 10 nM GLP-1 7-36 amide reduced binding to ~70% of that seen in the controls while it was only ~35% following 100 nM GLP-1 7-36 amide **(Fig 3.2.7.A$_{ii}$)**.

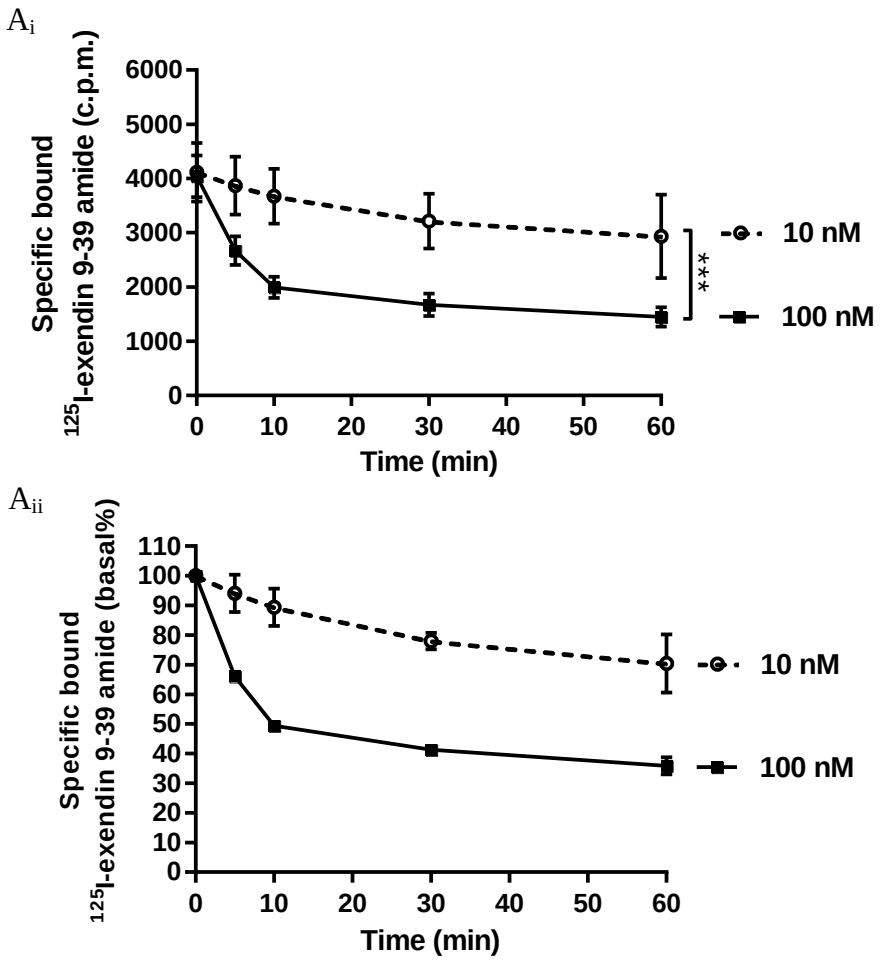

Fig 3.2.7. GLP-1 7-36 amide-mediated loss of cell-surface GLP-1R binding determined by radioligand binding assay. A_i. HEK-GLP-1R cells were stimulated with 10 nM or 100 nM GLP-1 7-36 amide for 0-60 min as indicated. Cell-surface receptor binding was then assessed as described in **Methods 2.8.**. **A_{ii}.** GLP-1R binding was normalised to that of basal (0). Data are mean ± S.E.M., n = 3. ***, $p < 0.001$ (two-way ANOVA).

3.2.8. The recovery of GLP-1R binding at the cell surface is not dependent on protein synthesis, but dependent on endosomal acidification.

To ensure that there was a reasonable window in which to detect the time-course of recovery of cell-surface GLP-1R binding using the radiobinding assay, especially when inhibitors were applied to assess their impact on recovery, 100 nM GLP-1 7-36 amide was used to induce receptor internalisation. In these experiments (protocol shown in **Fig 3.2.8.1.A**), HEK-GLP-1R cells were treated with 100 nM GLP-1 7-36 amide for 10 min which caused ~50% reduction in radioligand binding **(Fig 3.2.8.1.B)**. After removing the ligand and washing cells with KHB, GLP-1R binding recovered in a time-dependent manner. During the first one hour after ligand removal, GLP-1R binding increased rapidly from ~50% to ~75% of basal **(Fig 3.2.8.1.D)**. There was then a gradual increase in GLP-1R binding to ~80% of basal after 3 h and ~90% after 6 h recovery. Measuring the re-sensitisation of the Ca^{2+} response under the same conditions (ie 100 nM GLP-1 7-36 amide pre-treatment for 10 min), the GLP-1R response initially desensitised (~10% response of the control). The response then recovered with increasing recovery periods up to 6 h in the absence of ligand **(Fig 3.2.8.1.C, D)**.

Consistent with the functional assay demonstrating that re-sensitisation of the GLP-1R-mediated Ca^{2+} response was independent on protein synthesis **(Fig 3.2.5.B)**, cycloheximide did not inhibit the recovery of GLP-1R binding after GLP-1 7-36 amide (100 nM, 10 min) pre-challenge followed by KHB wash and 90 min recovery **(Fig 3.2.8.2.A)**. Furthermore, cycloheximide did not affect receptor binding on naïve cells. The functional assay also suggested that GLP-1R re-sensitisation is dependent on endosomal acidification **(Fig 3.2.5.D)** and the effect of monensin on the recovery of cell-surface GLP-1R binding was determined. The potential of monensin to block receptor recycling by inhibition of endosomal acidification was assessed in intact HEK-GLP-1R-EGFP cells by real-time confocal imaging. Incubation with 50 μM monensin resulted in the loss of cell-surface fluorescence and an increase in intracellular fluorescence that appeared in discrete puncta despite the absence of

receptor ligand **(Fig 3.2.8.2.B)**. However, in cells pre-treated with 80 μM dynasore, monensin did not influence either cell-surface or intracellular fluorescence **(Fig 3.2.8.2.B)**. Quantification of changes in both plasma membrane and intracellular fluorescence also illustrated that dynasore significantly inhibited the monensin-induced accumulation of GLP-1R-EGFP inside the cells **(Fig 3.2.8.2.C)**. This suggested that GLP-1R was constitutively internalised and that monensin could be used as a tool for trapping receptors within the cell.

In the radioligand binding assay, pre-treatment of HEK-GLP-1R cells with monensin and subsequent challenge with GLP-1 7-36 amide (100 nM, 10 min) followed by washing with KHB and then recovery dramatically inhibited the recovery of cell-surface binding **(Fig 3.2.8.2.D)**. The basal level of radioligand binding was also significantly reduced by ~20% following treatment with monensin which may have been a consequence of the inhibition of GLP-1R constitutive cycling **(Fig 3.2.8.2.B, C)**.

A

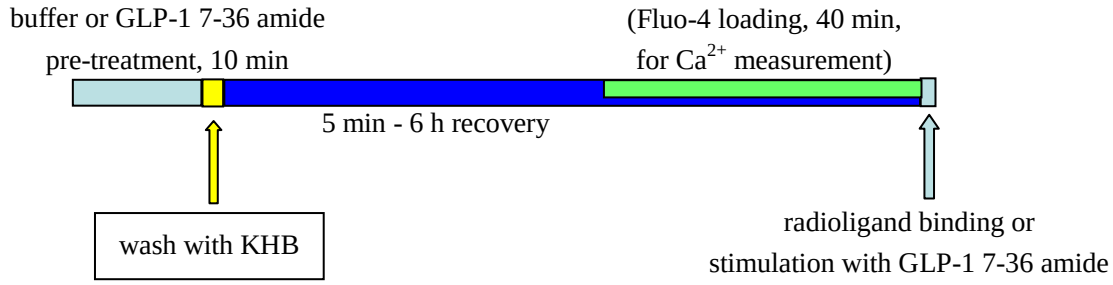
buffer or GLP-1 7-36 amide
pre-treatment, 10 min
(Fluo-4 loading, 40 min,
for Ca2+ measurement)
5 min - 6 h recovery
wash with KHB
radioligand binding or
stimulation with GLP-1 7-36 amide

B

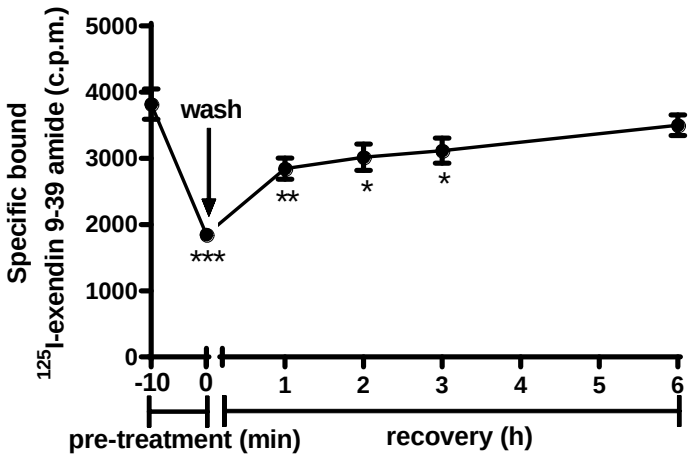
Specific bound
125I-exendin 9-39 amide (c.p.m.)
5000
4000
3000
2000
1000
0
wash
***
**
*
*
-10
0
1
2
3
4
5
6
pre-treatment (min)
recovery (h)

C

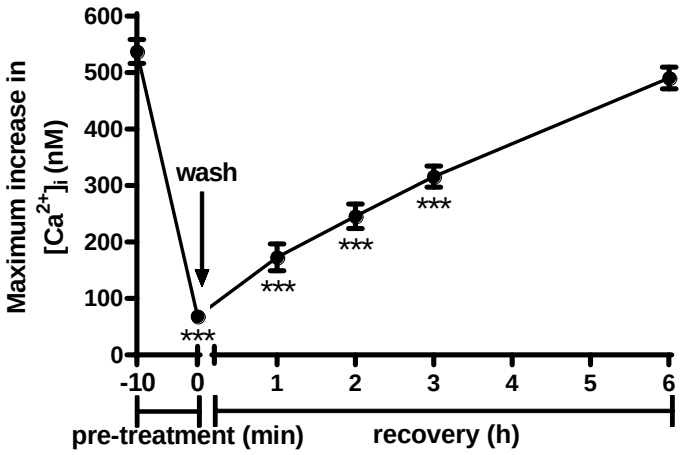
Maximum increase in
[Ca2+]i (nM)
600
500
400
300
200
100
0
wash
***
***
***
***
-10
0
1
2
3
4
5
6
pre-treatment (min)
recovery (h)

D

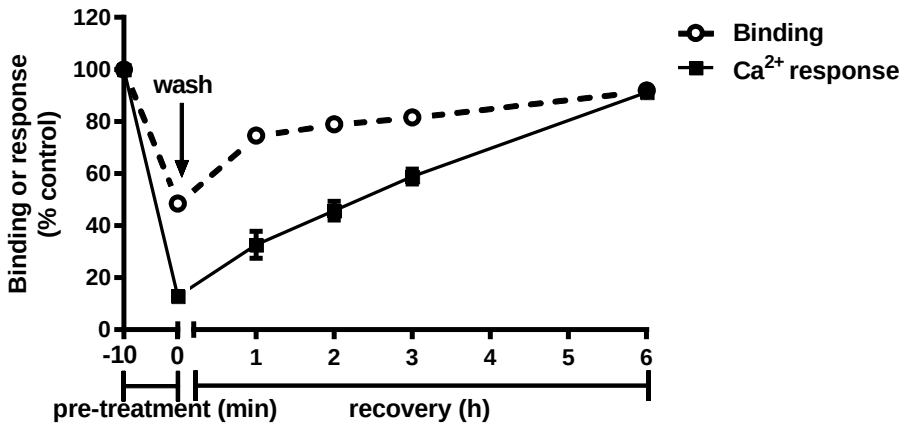
Binding or response
(% control)
120
100
80
60
40
20
0
wash
Binding
Ca2+ response
-10
0
1
2
3
4
5
6
pre-treatment (min)
recovery (h)

Fig 3.2.8.1. The recovery of cell-surface GLP-1R binding and Ca^{2+} signalling following treatment with GLP-1 7-36 amide. A. Experimental protocol. **B.** HEK-GLP-1R cells were stimulated with 100 nM GLP-1 7-36 amide for 10 min followed by washing with KHB. After 5 min-6 h recovery in serum-free DMEM, cell-surface GLP-1R binding was assessed as described in **Methods 2.8.**. **C**. Cells were treated as above but rather than determination of cell-surface binding, GLP-1R-mediated Ca^{2+} signalling was assessed. After 5 min-6 h recovery, fluo-4-loaded cells were stimulated or re-stimulated with a maximum concentration of GLP-1 7-36 amide (10 nM) and the increases in fluorescence were monitored and calibrated to $[Ca^{2+}]_i$. The mean data of maximum increase in $[Ca^{2+}]_i$ (nM) were generated. **D.** Both GLP-1R binding and the maximum increase in $[Ca^{2+}]_i$ (nM) were normalised to their controls (-10 min). All data are mean ± S.E.M., n = 4. *, $p < 0.05$; **, $p < 0.01$; ***, $p < 0.001$ vs. control (0) (Dunnett's test following one-way ANOVA).

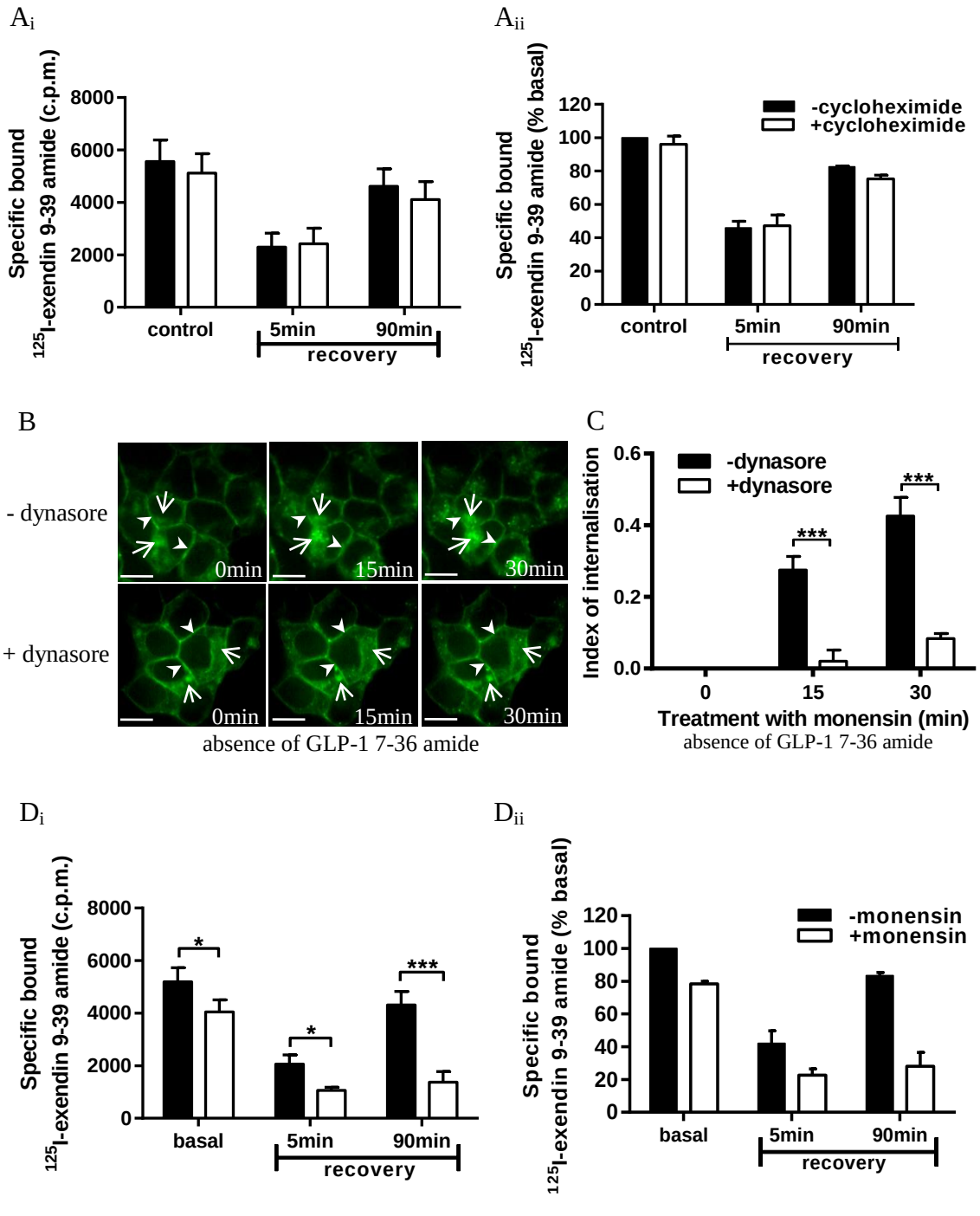
Ai
Specific bound
125I-exendin 9-39 amide (c.p.m.)
8000
6000
4000
2000
0
control
5min
90min
recovery
Aii
Specific bound
125I-exendin 9-39 amide (% basal)
120
100
80
60
40
20
0
-cycloheximide
+cycloheximide
control
5min
90min
recovery
B
- dynasore
+ dynasore
0min
15min
30min
0min
15min
30min
absence of GLP-1 7-36 amide
C
Index of internalisation
0.6
0.4
0.2
0.0
-dynasore
+dynasore
***
***
0
15
30
Treatment with monensin (min)
absence of GLP-1 7-36 amide
Di
Specific bound
125I-exendin 9-39 amide (c.p.m.)
8000
6000
4000
2000
0
*
*
***
basal
5min
90min
recovery
Dii
Specific bound
125I-exendin 9-39 amide (% basal)
120
100
80
60
40
20
0
-monensin
+monensin
basal
5min
90min
recovery

Fig 3.2.8.2. The recovery of cell-surface GLP-1R binding is independent of protein synthesis but reduced by the inhibition of endosomal acidification. HEK-GLP-1R cells were pre-incubated in the absence or presence of 17.5 μM cycloheximide **(A)** or 50 μM monensin **(D)** which was then included throughout the experiment. Cells were then stimulated with buffer (basal) or 100 nM GLP-1 7-36 amide for 10 min followed by washing with KHB. After a 5 min or 90 min period of recovery, cell-surface GLP-1R binding was measured as described in **Methods 2.8.**. GLP-1R binding was normalised to that of naïve cells **(A_{ii} and D_{ii})**. **B.** Representative images from a single experiment. HEK-GLP-1R-EGFP cells were imaged by confocal microscopy at 0, 15 and 30 min during which time they were incubated with 50 μM monensin either with or without 80 μM dynasore. Arrowheads and arrows indicate the localization of GLP-1R-EGFP at the cell surface and in the cytosol respectively. Scale bar (in the bottom left of each image), 5 μm. **C.** The images were analysed as described in **Methods 2.11.1.**. The data are mean + S.E.M., n = 3 (2-5 cells were analysed in each individual experiment.). All other data are mean + S.E.M., $n \geq 3$. *, $p < 0.05$; ***, $p < 0.001$ (Bonferroni's test following two-way ANOVA. Only the differences between groups at each time point are shown for clarity).

3.2.9. GLP-1 7-36 amide-induced loss of cell-surface GLP-1R binding and; GLP-1R desensitisation and re-sensitisation in the rat pancreatic β-cell line, INS-1E.

In INS-1E cells, 100 nM GLP-1 7-36 amide induced a rapid loss of GLP-1R binding from the cell surface in the first 5 min (reduced to ~60% of basal) **(Fig 3.2.9.1.A)**. Receptor binding then slowly decreased during further incubation reaching ~50% of basal at 60 min. Removing the ligand after 10 min of stimulation allowed recovery of GLP-1R binding at the cell surface. After 60 min recovery, receptor binding was ~80% of basal **(Fig 3.2.9.1.B)**.

The measurement of Ca^{2+} signalling using a microplate reader lacks sensitivity with these particular cells and cAMP signalling was therefore assessed to study desensitisation of the GLP-1R (protocol shown in **Fig 3.2.9.2.A**). GLP-1 7-36 amide stimulated a concentration-dependent increase in cAMP with a pEC_{50} of 9.67 ± 0.13 and Hill slope of 2.99 ± 1.14 in the presence of IBMX **(Fig 3.2.9.2.B)**. The maximum concentration of 10 nM GLP-1 7-36 amide produced an increase in cAMP to 543 ± 13 pmol/mg protein from a basal of 71 ± 3 pmol/mg protein. Pre-treatment with 100 nM GLP-1 7-36 amide (the concentration used in the radioligand binding assay to assess receptor loss from the cell surface) for 10 min resulted in desensitisation of the cAMP response on subsequent re-challenge. In contrast to HEK-GLP-1R cells **(Fig 3.2.1.2.A)**, here there was no remaining cAMP elevation from the pre-treatment **(Fig 3.2.9.2.B)**. After a 60 min period of recovery, the GLP-1 7-36 amide-mediated cAMP concentration-response curve in the pre-treated cells had a pEC_{50} of 9.55 ± 0.11 and Hill slope of 1.59 ± 0.28 in the presence of IBMX. These values were not significantly different compared to the control conditions (without pre-treatment) **(Fig 3.2.9.2.B)**. However, the E_{max} was significantly reduced in pre-treated cells. For example, re-challenge with 10 nM GLP-1 7-36 amide generated 430 ± 39 pmol/mg protein of cAMP from a basal of 62 ± 6 pmol/mg protein in the pre-treated cells compared to 543 ± 13 pmol/mg protein from a basal of 71 ± 3 pmol/mg in the control (without pre-treatment).

Following the protocol **(Fig 3.2.9.3.A)**, the cAMP response to re-challenge with GLP-1 7-36 amide after pre-challenge (100 nM GLP-1 7-36 amide, 10 min) and recovery (60 min) was not influenced by 17.5 µM cycloheximide **(Fig 3.2.9.3.B)**. However, treatment with 80 µM dynasore abolished cAMP responses in either naïve cells or pre-challenged cells **(Fig 3.2.9.3.C)**, thereby complicating interpretation. Treating cells with 50 µM monensin inhibited the cAMP response to re-stimulation by ~60% although monensin also reduced responses in naïve cells by ~30% **(Fig 3.2.9.3.D)**.

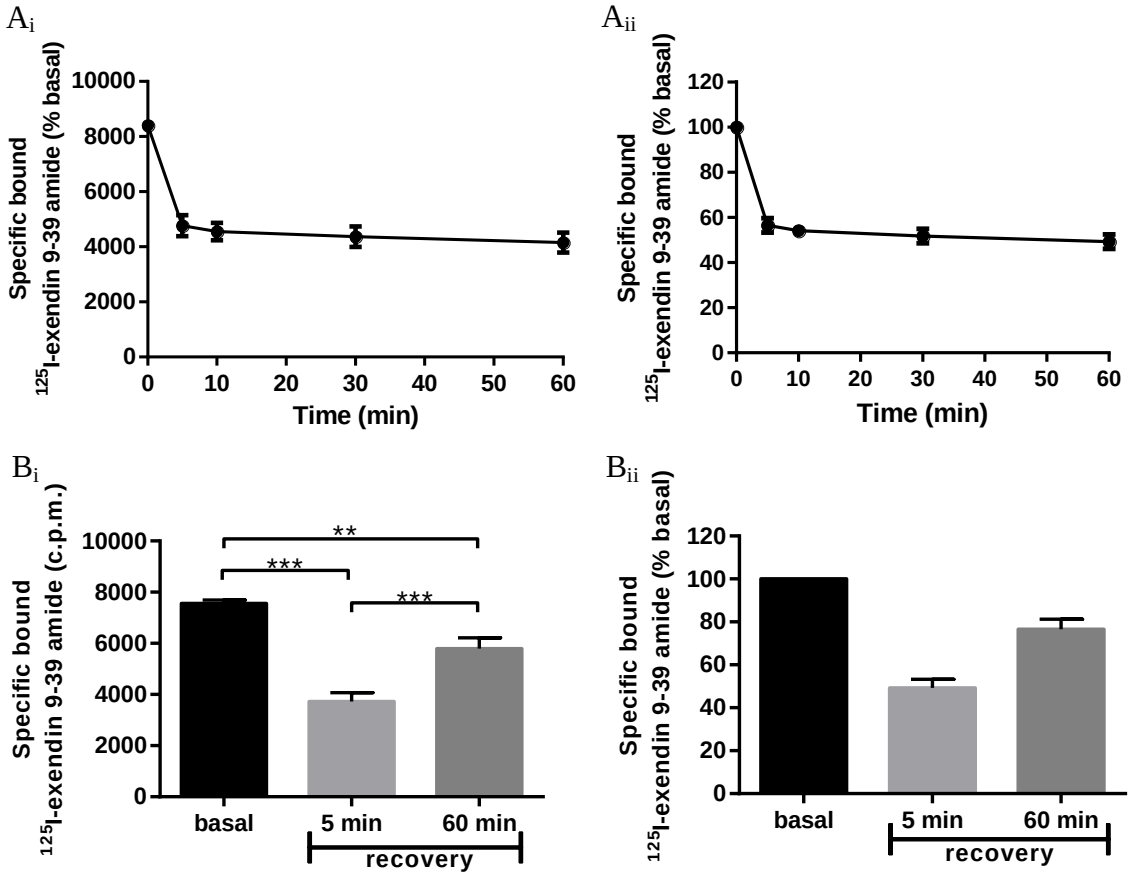

Fig 3.2.9.1. GLP-1 7-36 amide-mediated loss of cell-surface GLP-1R binding and subsequent recovery after ligand removal. A_i. INS-1E cells were stimulated with 100 nM GLP-1 7-36 amide for 0-60 min as indicated. Cell-surface GLP-1R binding was then assessed as described in **Methods 2.8.**. **A_{ii}.** GLP-1R binding was normalised to that of basal (0 min). **B_i.** INS-1E cells were stimulated with buffer (basal) or 100 nM GLP-1 7-36 amide for 10 min followed by washing with KHB. After a 5 min or 60 min period of recovery, cell-surface GLP-1R binding was measured as described in **Methods 2.8.**. **B_{ii}.** GLP-1R binding was normalised to that of basal. Data are mean ±/+ S.E.M., n = 3. Statistical analysis was performed only for data or graph **B_i**. **, $p < 0.01$; ***, $p < 0.001$ (Bonferroni's test following one-way ANOVA).

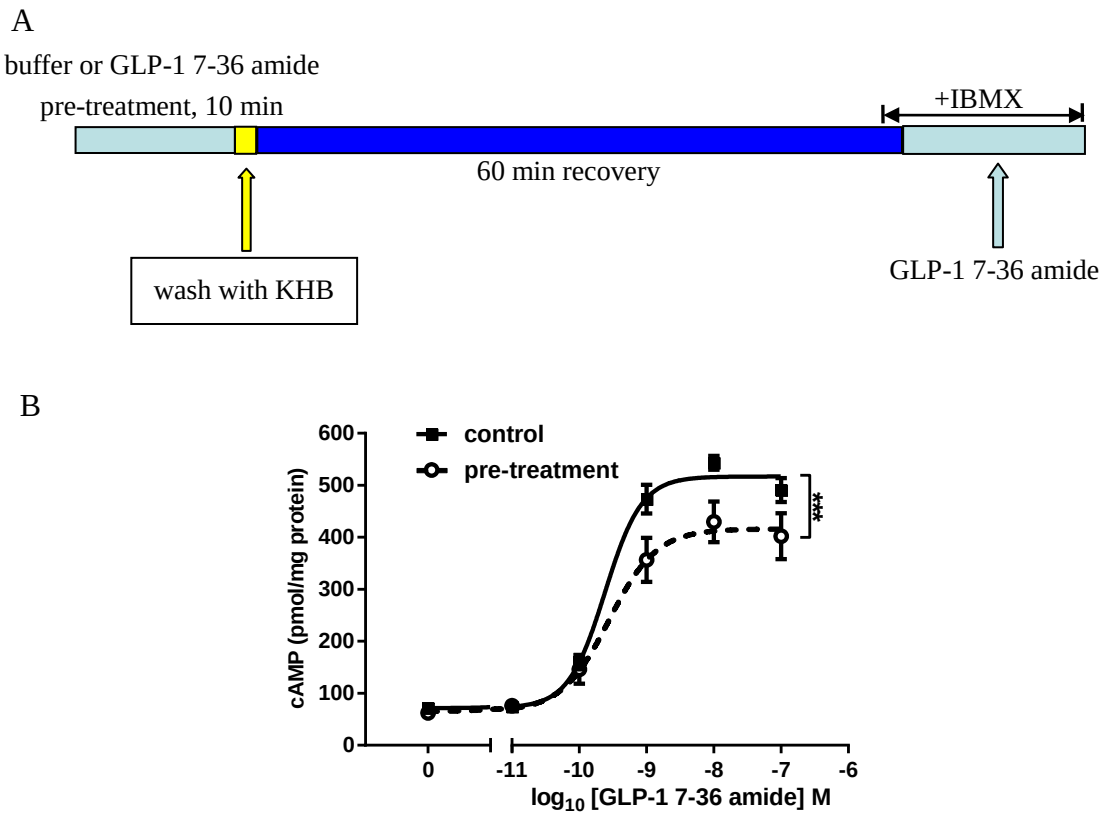

Fig 3.2.9.2. GLP-1 7-36 amide-induced cAMP responses in the absence or presence of GLP-1 7-36 amide pre-stimulation. A. Experimental protocol. **B.** In the absence of IBMX, INS-1E cells were pre-treated with buffer (control) or 100 nM GLP-1 7-36 amide (pre-treatment) for 10 min followed by washing with KHB. Following a 60 min period of recovery, cells were stimulated or re-stimulated with GLP-1 7-36 amide at the indicated concentrations (0-100 nM) for 15 min in the presence of IBMX. The cAMP generation was then determined. The concentration-response curve of the control has a pEC_{50} of 9.67 ± 0.13 and Hill slope of 2.99 ± 1.14 compared to 9.55 ± 0.11 and 1.59 ± 0.28 respectively in the pre-treated cells. Data are mean ± S.E.M., n = 4. ***, $p < 0.001$ (two-way ANOVA).

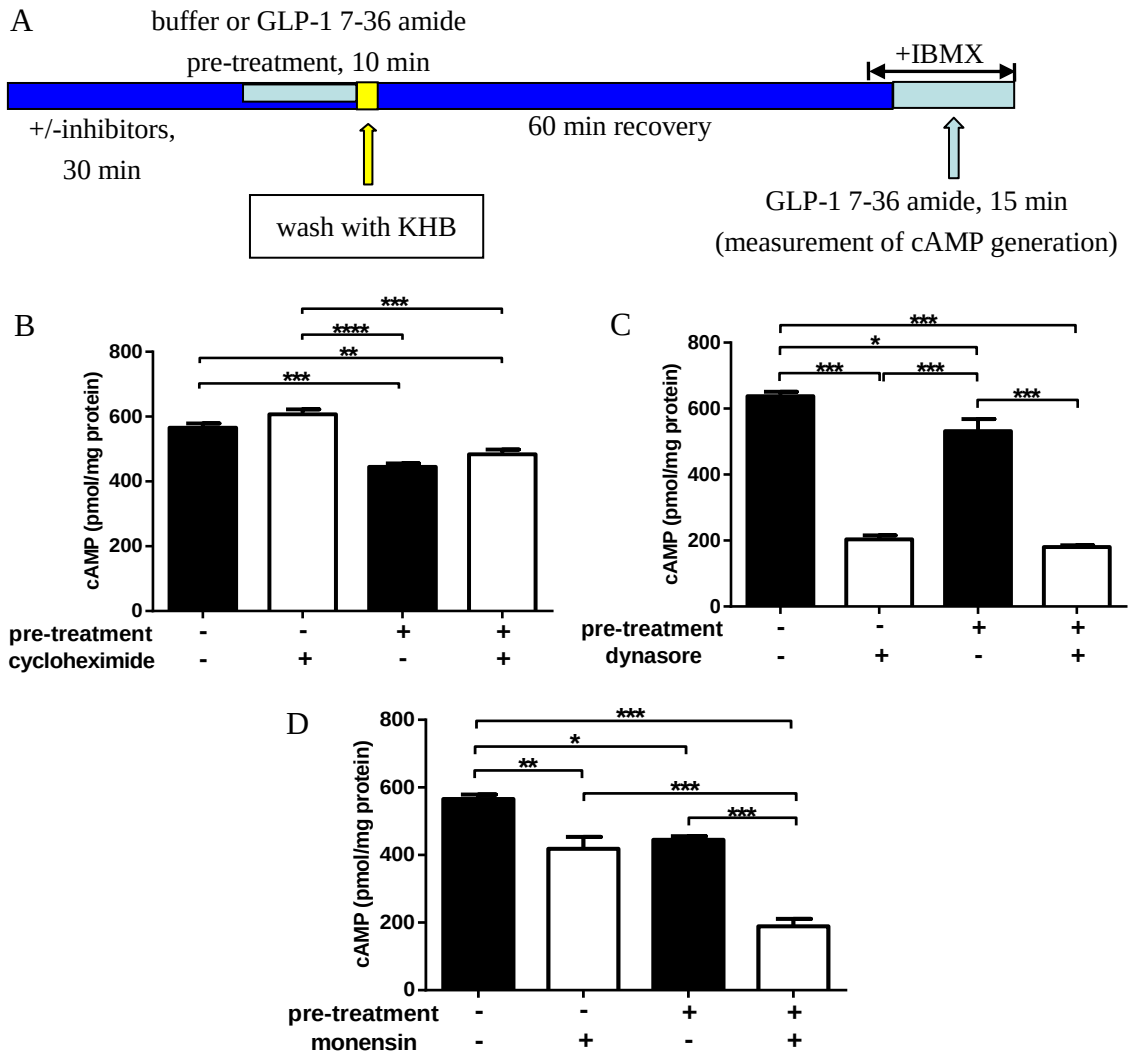

Fig 3.2.9.3. GLP-1R re-sensitisation is not dependent on protein synthesis, but reduced by the inhibition of endosomal acidification in INS-1E cells. A. Experimental protocol. Cells were pre-incubated for 30 min without or with the inhibitors, cycloheximide (17.5 µM, **B**), dynasore (80 µM, **C**) or monensin (50 µM, **D**) which were then included throughout the experiment. Cells were then pre-stimulated with buffer or 100 nM GLP-1 7-36 amide for 10 min in the absence of IBMX followed by washing with KHB. After a 60 min period of recovery, cells were stimulated or re-stimulated with GLP-1 7-36 amide in the presence of 500 µM IBMX. All data are mean + S.E.M., n ≥ 3. *, $p < 0.05$; **, $p < 0.01$; ***, $p < 0.001$ (Bonferroni's test following one-way ANOVA).

3.3. Discussion

Given that the chronic activation of GLP-1R may occur in patients with type 2 diabetes in order to provide therapeutic blood glucose control and energy homeostasis, studying the potential desensitisation and subsequent re-sensitisaton of the GLP-1R is of particular importance in both understanding the pharmacological properties and informing clinical use. The present data demonstrated that after receptor activation, the GLP-1R undergoes a process of desensitisation that is both time- and concentration-dependent. Furthermore, GLP-1 7-36 amide co-internalises with the receptor as a complex into early endosomes. The endocytosed GLP-1Rs then recycle back to the plasma membrane for a new cycle of activation after removal of the extracellular ligand. The process of GLP-1R re-sensitisation is independent of *de novo* receptor synthesis **(Fig 3.3)**.

3.3.1. GLP-1R activation

The current data show that GLP-1 7-36 amide activates the GLP-1R and stimulates both cAMP and Ca^{2+} signalling in a time- and concentration-dependent manner in HEK293 cells stably expressing recombinant human GLP-1Rs **(Fig 3.2.1.1, Fig 3.2.1.2, Fig 3.2.2.1)**. Such signalling has been reported for the GLP-1R expressed in a variety of cells, including pancreatic β-cell lines as also shown here. This suggests the HEK-GLP-1R cell line may be a suitable model to explore the desensitisation, re-sensitisation and potential trafficking of the GLP-1R. Key experiments from these studies in HEK-GLP-1R cells were confirmed in INS-1E cells expressing native GLP-1Rs, again supporting the validity of the model.

3.3.2. Constitutive cycling of the GLP-1R

Some GPCRs cycle constitutively between the cell surface and intracellular compartments in the absence of agonist. For example, in unstimulated fibroblasts and endothelial cells, PAR1 cycles between the cell surface and a cytosolic pool of receptors

which is required for receptor expression at the plasma membrane (Shapiro et al., 1996, Paing et al., 2006). The present study suggests that the GLP-1R may also undergo constitutive cycling through a dynamin-dependent mechanism **(Fig 3.2.8.2.B, C)**. This has been suggested in a previous study which also highlighted an interaction between the GLP-1R and caveolin-1 that was required for targeting the intracellular GLP-1Rs to the plasma membrane in the absence of ligand, thereby allowing efficient GLP-1R signalling (Syme et al., 2006).

3.3.3. GLP-1R desensitisation.

Although there is limited reduction of biological activity of GLP-1R upon chronic activation *in vivo* (Zander et al., 2001, Meneilly et al., 2003), consistent with previous studies the current data clearly demonstrate GLP-1R desensitisation in cellular systems. The desensitisation of GLP-1R-mediated cAMP signalling has been previously explored in pancreatic β-cell line, INS-1E (Baggio et al., 2004). In contrast to that study which showed GLP-1R desensitisation only upon prolonged GLP-1 stimulation (≥ 1 h), the present data indicated rapid GLP-1R desensitisation upon GLP-1 7-36 amide exposure in INS-1E cells **(Fig 3.2.9.2.)**. In HEK-GLP-1R cells, cAMP production in response to GLP-1 7-36 amide (100 nM) was sustained even after removal of the extracellular ligand making it difficult to assess any receptor desensitisation at the level of cAMP **(Fig 3.2.1.2.)**. Sustained cAMP production may be a consequence of a large number of cell-surface receptors in these cells compared with the endogenous level of expression in β-cells. Indeed, it has been indicated that in CHL cells expressing recombinant GLP-1R, there is a positive linear relationship between cell-surface receptor number and the activation of AC in the range of ~10,000-270,000 receptors/cell (Fehmann et al., 1998). It is also possible that there may be differences in the intracellular environment between two types of cell. For example, levels of AC and PDE, which produces and hydrolyzes cAMP respectively, may be expressed at different levels in the different cell types, thereby providing cell-specific signalling patterns. Given that the persistent cAMP response occurred in the present study, even following removal of ligand, it is

also possible that persistent signalling arose from endocytosed GLP-1Rs **(see Chapter 4)**. Despite difficulties in assessing desensitisation of cAMP signalling in HEK-GLP-1R cells, challenge with GLP-1 7-36 amide did mediate a rapid desensitisation of GLP-1R-mediated Ca^{2+} signalling in a time-dependent manner **(Fig 3.2.3.4.)**. As demonstrated, the desensitisation of GLP-1R is mediated by agonist-stimulated GLP-1R phosphorylation by GRK and/or PKC at the C-terminal tail of GLP-1R (Widmann et al., 1996a, Widmann et al., 1996b, Widmann et al., 1997). Details regarding the phosphorylation sites of the GLP-1R that critical for mediating desensitisation can be found in the **General Introductio**n **1.4.3.**.

3.3.4. GLP-1R internalisation.

The phosphorylated receptors recruit endocytic proteins such as β-arrestin to form an endocytotic vesicle leading to receptor internalisation (Gurevich and Gurevich, 2006) **(see General Introduction 1.4.2.)**. Compared with phosphorylation, internalisation is considered a slower process and has limited effect on the initiation of receptor desensitisation. However, it clearly defines the pattern of desensitisation by reducing the cell-surface receptor number and provides a route for either recycling or degradation (Ferguson, 2001). For the GLP-1R, it has been reported that phosphorylation not only mediates desensitisation but also directs internalisation in CHL fibroblast cells expressing recombinant receptors (Widmann et al., 1997). The extent to which internalisation contributes to the process of desensitisation and over what time-frame is unclear. The data presented here showed time- and concentration-dependent GLP-1R internalisation upon GLP-1 7-36 amide stimulation in both HEK-GLP-1R cells and INS-1E cells **(Fig 3.2.6.1., Fig 3.2.7. and Fig 3.2.9.1.A)**. Particularly that in HEK-GLP-1R cells the process of GLP-1R internalisation is slower than that of desensitisation. For example, GLP-1R desensitisation occurs within 1 min upon GLP-1 stimulation when internalisation is minimal **(Fig 3.2.3.4., Fig 3.2.6.1. and Fig 3.2.7.)** suggesting that at least the initial rapid desensitisation is unlikely to be through internalisation, but highly possibly to be through phosphorylation. Furthermore,

inhibition of internalisation did not prevent desensitisation **(Fig 3.2.5.C)**, again highlighting that internalisation is not required to initiate the desensitisation process.

The mechanisms mediating internalisation of the GLP-1R have not been fully elucidated although in line with other GPCRs this is generally thought to be through clathrin-dependent or -independent mechanism **(see General Introduction 1.4.2.)**. The present data highlight that the GLP-1R internalises through a dynamin-dependent mechanism upon activation by GLP-1 7-36 amide **(Fig 3.2.6.2).** Given that both clathrin- and caveolin-1-dependent pathways have been reported for GLP-1R internalisation and that both require dynamin (Widmann et al., 1995, Vazquez et al., 2005, Syme et al., 2006), it is unclear which of the pathways is involved. Evidence has suggested that the pathway engaged to mediate receptor endocytosis may be determined by the pattern of receptor phosphorylation. For example, GRK-mediated phosphorylation induces a clathrin-dependent internalisation of β_1AR whilst PKA-mediated phosphorylation triggers β_1AR internalisation through a caveolin-associated pathway (Rapacciuolo et al., 2003). The GLP-1R can be phosphorylated by both GRK and PKC upon activation but it has been suggested that PKC-dependent phosphorylation may not mediate internalisation in CHL-GLP-1R cells **(see above)**. Given that receptor phosphorylation is cell-type specific (Tobin, 2008) and indeed may be agonist-specific (Zidar et al., 2009), the mechanism of receptor endocytosis could be both cell- and ligand-dependent. Furthermore, the pathway of receptor internalisation may also depend on ligand availability. For example, when the EGFR, a receptor tyrosin kinase, is challenged with a low concentration of EGF, the receptor internalises through a clathrin-dependent mechanism and recycles back to the plasma membrane (Sigismund et al., 2005). By contrast, a high concentration of EGF triggers receptor ubiquitination, and endocytosis through both clathrin-dependent and -independent mechanisms and causes receptor degradation (Sigismund et al., 2005).

3.3.5. GLP-1R re-sensitisation requires receptor internalisation and recycling, but not de novo receptor synthesis.

Following desensitisation, GPCRs re-sensitise after removing the extracellular ligand (Anborgh et al., 2000, Tsao and von Zastrow, 2000). Receptor re-sensitisation may involve one or more of three mechanisms: receptor recycling following internalisation; *de novo* receptor synthesis or; the mobilization from a receptor pool within the cytosol **(see General Introduction, Fig 1.6)**. The present study demonstrates that re-sensitisation of the GLP-1R is independent of *de novo* receptor synthesis **(Fig 3.2.5.B, Fig 3.2.8.2.A)**, which is entirely consistent with a previous study (Widmann et al., 1995). Although under some circumstance phosphorylated receptors can be rapidly dephosphorylated at or near the cell surface (Ghosh and Schonbrunn, 2011, Murphy et al., 2011, Kliewer and Schulz, 2013), receptor internalisation is essential for many receptors dephosphorylation and therefore subsequent re-sensitisation **(see General Introduction 1.5.1.)**. For some receptors, for example the β_2AR, the internalised receptors target to endosomes where they undergo dephosphorylation by GRP(s) and are then recycled back to the plasma membrane. The inhibition of internalisation blocks β_2AR dephosphorylation and recovery (Pippig et al., 1995). Given that the dephosphorylation did not occur at pH 7.0, endosomal acidification is most likely required for such recycling process (Krueger et al., 1997). This requirement may be a consequence of the acid-induced conformational change of the protein leading to potentiated sensitivity to GRP (Davis et al., 1987, Krueger et al., 1997) and/or the low pH-induced dissociation of the ligand and receptor allowing the receptor to adopt a different conformation. The present data suggest that although internalisation may not be critical for GLP-1R desensitisation **(see above)**, it is clearly required for efficient GLP-1R re-sensitisation **(Fig 3.2.5.C).** Moreover, endosomal acidification is also required for both GLP-1R re-sensitisation and re-expression of the GLP-1Rs at the cell-surface **(Fig 3.2.5.D, Fig 3.2.8.2.D).** These data strongly suggest that GLP-1R re-sensitisation is dependent on recycling. Thus, following agonist exposure, receptors internalise in a dynamin-dependent manner and subsequent acidification of the

endosomal compartment facilitates the disassociation of ligand-receptor complex and promotes receptor dephosphorylation, recycling and re-sensitisation.

The role of an intracellular receptor pool in regulating recovery of cell-surface receptors has been shown for a thrombin receptor, PAR1 which directly targets to lysosomes for degradation following activation (Trejo and Coughlin, 1999) thereby implying mechanisms other than recycling are responsible for re-sensitisation. Indeed, in the same cell line there was a distinct distribution of the PAR1 and β_2AR with the former present at both the cell surface and within the Golgi and the latter present almost exclusively at the cell membrane (Hein et al., 1994). This implies that the intracellular receptors are located in preparation for recruitment to the cell surface and their mobilization from this reserve pool to the plasma membrane is responsible for the efficient re-sensitisation (Hein et al., 1994). PARs, for example PAR1, are cleaved by proteolytic activity of, for example, thrombin, revealing a tethered ligand which is able to interact with the receptor and provide agonism (Trejo and Coughlin, 1999). The PARs therefore represent special cases as recycling would not present an intact receptor at the plasma membrane ready for proteolysis and another round of signalling. For other receptors, it would make sense that they are able to be re-used and recycling provides a mechanism for this. Exceptions may be when receptors are subject to a high level of stimulation and as a homeostatic mechanism are trafficked for degradation to maintain a reduced cellular sensitivity and/or responsiveness to agonist. In the HEK-GLP-1R-EGFP cell line, although in the absence of agonist, GLP-1Rs were present mainly at the cell surface, there was some intracellular expression. The relative proportions in each sub-cellular compartment are unclear as is how this may be influenced by potentially artificially high expression levels. It is unclear therefore whether there is an intracellular reserve pool of GLP-1R that are able to replenish those lost from the cell-surface upon agonist stimulation.

The pattern of cell-surface GLP-1R recovery does not exactly match but is similar to that of re-sensitisation. A difference is that during the first hour of recovery period, there

is a greater proportional recovery of cell-surface receptors but a more limited proportional re-sensitisation of the Ca^{2+} response **(Fig 3.2.8.1.D)**. Given that Ca^{2+} is a much amplified signal which should provide receptor reserve for the response, receptor desensitisation should in theory shift the concentration-response curve to the right and then fall in the maximum. However, Ca^{2+} response is a non-equilibrium assay and many studies show a direct fall in the maximum without a right-shift of the curve (Gromada et al., 1996, He et al., 2002). This makes it difficult to directly correlate re-sensitisation of the Ca^{2+} response with the recovery of binding. The recycling-based mechanism of GPCR re-sensitisation suggests that dephosphorylation of the receptor generally induced by the disassociation of ligand-receptor-β-arrestin complex in endosomes which then allows receptor recycling and re-sensitisation **(see General Introduction Fig 1.5.)**. However, there are exceptions suggesting receptor dephosphorylation occurs after recycling. For example, upon exposure to SP, the NK_1R is rapidly recycled back to the cell surface in an inactive form. The re-activation of these recycled receptors requires dephosphorylation by the phosphatase, PP-2A, which occurs at the plasma membrane (Murphy et al., 2011). The location at which the GLP-1R is de-phosphorylated is, however, unclear. It is of course possible that the GLP-1R recycles back to the plasma membrane in an inactive form, which is then dephosphorylated at the cell surface therefore leading to a delayed process of re-sensitisation compared with the recovery of cell-surface receptor binding, although as mentioned above, it is difficult to address this issue using the current data.

A previous study indicated that removal of extracellular GLP-1 following receptor activation induced GLP-1R re-sensitisation within 1 h and that this was independent of ligand concentration (Gromada et al., 1996). This is somewhat counter-intuitive and indeed the present data demonstrated that a high concentration (100 nM) of agonist was associated with less efficient receptor re-sensitisation compared to a low concentration (10 nM) **(Fig 3.2.4. and Fig 3.2.8.1.C)**. Given that the proportion of receptors internalised is also dependent on the concentration of ligand **(Fig 3.2.6.1. and Fig 3.2.7.)**, it may be that the concentration-dependence of the recovery period required is

simply a consequence of the different amounts of receptor internalised. It may well be that the more receptors that are endocytosed, the longer the period required for complete recovery. However, it must be noted that at any one moment, plasma membrane receptor expression is in equilibrium between internalisation and recycling and a larger reduction of cell-surface receptor number may equate to less recycling rather than the endocytosis of more receptors. The K_D value for the binding of GLP-1 7-36 amide is around 1 nM (Schmidtler et al., 1994, Xiao et al., 2000). So there would be already ~90% of cell-surface GLP-1Rs occupied by 10 nM GLP-1 7-36 amide. However, we determined a big increase of cell-surface receptor reduction from 10 nM to 100 nM **(Fig 3.2.7.)**. It is therefore possible that different processes of recycling occur under the low and high concentrations of ligand. Particularly, different mechanisms of receptor endocytosis have been indicated for the low and high concentrations of ligand for some receptors **(see above)**. Furthermore a high concentration (10 nM) of SP induces the sequestration of NK_1R into the prenuclear sorting endosomes (long recycling pathway). By contrast, a low concentration (1 nM) of SP induces receptor internalisation into endosomes located beneath the plasma membrane (short recycling pathway) possibly due to a low level of receptor phosphorylation (Roosterman et al., 2004).

Continuous treatment of type 2 diabetic patients with either GLP-1 or exendin-4 does not result in a detectable loss of biological activity *in vivo* (Zander et al., 2001, Meneilly et al., 2003, Fineman et al., 2003). However, the present study and indeed most other studies on desensitisation of GPCRs *in vitro* are based on relatively high concentrations of agonist to investigate the potential mechanisms involved. For example, in the present study, nanomolar concentrations of GLP-1 have been used, which do not equate to those *in vivo* where for the active forms of GLP-1 circulate at picomolar levels (Henriksen et al., 1986, Henriksen et al., 1987, Bendtsen et al., 1991). Thus, the fasting plasma concentration of GLP-1 7-36 amide is < 10 pM and it rises to ~40 pM after a meal (Orskov et al., 1994, Meneilly et al., 2003), although it must be noted that the concentration of ligand at its site of action is unknown. Importantly, the level of receptor phosphorylation depends on the concentration of agonist (Tobin et al., 1995, Liu and

Schonbrunn, 2001). The extent of receptor phosphorylation *in vivo* is unknown and whether this is sufficient to generate a significant receptor desensitisation is not clear. In the present study, both receptor internalisation and re-sensitisation were concentration-dependent **(see above)** suggesting that limited receptor phosphorylation could occur *in vivo* in response to the endogenous agonist and this may result in minor desensitisation followed by rapid re-sensitisation which may not manifest as a reduction in the ability of exogenous ligands to regulate blood glucose levels. It might be worth considering whether aspects of GLP-1R function in addition to blood glucose control are equally resistant to desensitisation *in vivo*.

3.3.6. GLP-1 internalises with GLP-1R as a complex into endosomes

Many GPCRs have been shown to internalise with ligand bound (Weissman et al., 1986, Smalley et al., 2001, Pelayo et al., 2011). By using a fluorescently-tagged ligand the present data clearly show that GLP-1 co-internalises with the GLP-1R targeting to endosomes. It must be noted that this was despite the fact that the N-terminal rhodamine-labelled GLP-1 7-36 amide had both reduced affinity for the GLP-1R binding and reduced potency on cAMP generation **(Fig 3.2.6.3.)**. This is perhaps not too surprising given the critical role of the N-terminal His^7 of GLP-1 for both affinity and efficacy. Given that such peptides internalise with their receptors, the ligand has to be either recycled with the receptor or alternatively processed by the cell. Current models of receptor recycling do not adequately address the fate of the ligand. Although a number of ligands such as transforming growth factor and somatostatin-14 have been reported to recycle back to the plasma membrane (Lenferink et al., 1997, Koenig et al., 1998), it perhaps makes sense for ligands to be processed such that they are unable to re-initiate continued rounds of receptor signalling by re-binding to re-sensitised receptors at the plasma membrane when the pH returns to more favourable conditions. Indeed, the endosomal processing of a small number of peptide ligands has been reported. Thus, the zinc metalloprotease, ECE-1, has been reported to cleave SP and CGRP only in the acidic environment of the endosomal compartment, thereby

promoting disassociation of the receptor-β-arrestin complex leading to efficient receptor recycling (Roosterman et al., 2007, Padilla et al., 2007). Given that GLP-1 and its receptor internalise as a complex and target to early endosomes and that endocytosed GLP-1 has been reported to be continuously degraded in intracellular compartments (Widmann et al., 1995), it is possible that recycling of the GLP-1R and receptor re-sensitisation require such ligand processing. This will be investigated in the next Chapter.

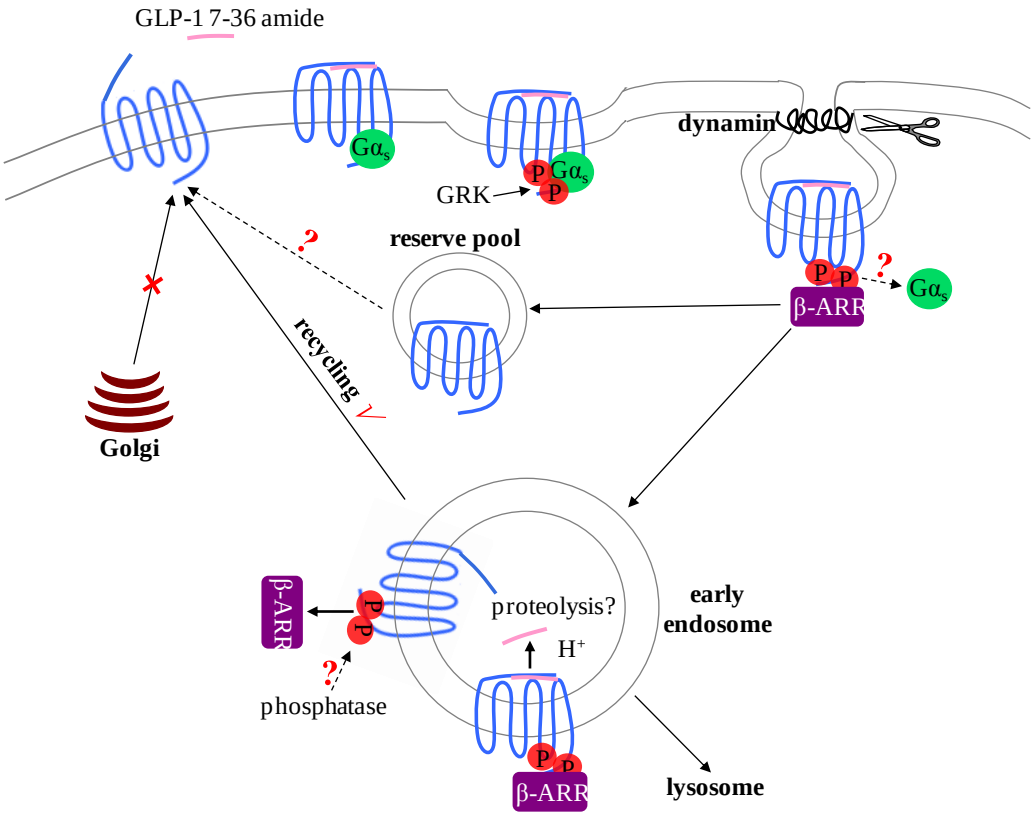

Fig 3.3. Potential mechanisms of GLP-1 7-36 amide-mediated GLP-1R re-sensitisaton. The binding of GLP-1 7-36 amide induces the activation and phosphorylation of the GLP-1R. The phosphorylated receptors recruit β-arrestin and internalise through a dynamin-dependent manner. Whether phosphorylation and β-arrestin recruitment lead to G protein disassociation is unclear **(see Chapter 4)**. The endocytosed receptors with ligand bound target to early endosomes where the pH is acidified inducing ligand disassociation which results in β-arrestin disassociation and subsequently receptor recycling. Whether the phosphorylated GLP-1R is dephosphorylated in the endosome following ligand disassociation or at the plasma membrane after recycling is unclear. The re-sensitisation of the GLP-1R is independent of the *de novo* receptor synthesis although whether it is dependent on the mobilization of a reserve pool of receptors within the cytosol is unclear. β-ARR, β-arrestin. Pathways that are unclear are shown by dashed arrows.

CHAPTER 4 ECE-1 Regulates the Signalling and Recovery of the GLP-1R

4.1. Introduction

As described in the previous chapter, there is a possibility that the processing of ligand, internalised along with the receptor, is required for the intracellular trafficking of receptors, allowing recycling back to the plasma membrane and thereby re-sensitisation. Such processing of internalised peptide ligands has been suggested to be the role of endosomally located ECE-1. In this chapter, the role of ECE-1 in regulating GLP-1R re-sensitisation will be explored. The early stage of receptor processing following agonist stimulation requires β-arrestin recruitment to the phosphorylated receptor which then mediates receptor internalisation. However, in addition to that, β-arrestin also acts as a scaffold for other intracellular effectors leading to G-protein-independent signalling. It is possible, therefore, that the stability of the receptor-β-arrestin association, which may be governed by ligand availability or stability, may influence such G-protein-independent events. It has been shown, for example, that ECE-1 regulates SP-evoked β-arrestin-dependent ERK activation which plays an important role in cell death (Cottrell et al., 2009). The recruitment of β-arrestin1 to the GLP-1R in response to GLP-1 stimulation has been demonstrated (Sonoda et al., 2008) and GLP-1R-mediated β-arrestin-dependent signalling including ERK activation and possibly cAMP generation has been shown (Sonoda et al., 2008, Quoyer et al., 2010, Kuna et al., 2013). In this chapter, the role of ECE-1 activity in regulating GLP-1R-mediated signalling has also been assessed.

4.2. Results

4.2.1. Re-sensitisation of GLP-1R-mediated Ca^{2+} signalling is promoted by washing with acidified buffer.

GLP-1 7-36 amide internalises with the receptor **(Fig 3.2.6.3.)** leading to the hypothesis that ligand processing, for example proteolysis, within the cell may be responsible for regulating GLP-1R re-sensitisation. In that case, endocytosed GLP-1Rs without ligand bound should traffic differently to those with ligand bound leading to differential rate of GLP-1R re-sensitisation. To test this hypothesis, following stimulation with GLP-1 7-36 amide, cells were washed with acidified buffer (pH 4.0) to remove cell-surface bound ligand and re-sensitisation determined (protocol shown in **Fig 4.2.1.A**). After 90 min recovery, cells washed with standard KHB following pre-treatment with GLP-1 7-36 amide (10 nM, 10 min) produced a Ca^{2+} response to re-challenge that was ~60% of control. However, this response was significantly promoted by washing with acidified buffer (pH 4.0, 40 s) (90% of control response) (**Fig 4.2.1.B, C**). Washing naïve cells with acidified buffer (pH 4.0, 40 s) did not influence the Ca^{2+} response to GLP-1 7-36 amide.

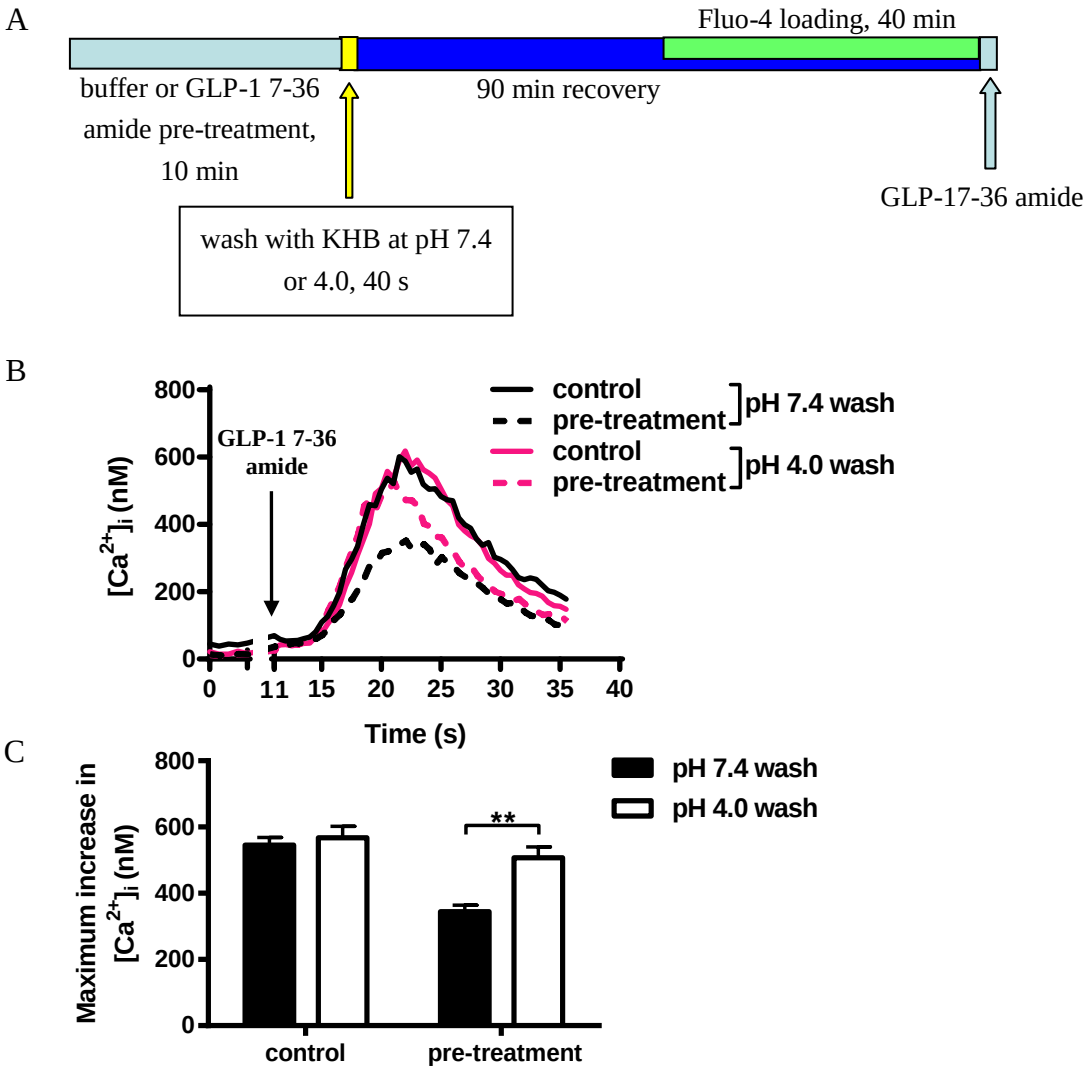

Fig 4.2.1. Washing with acidified buffer promotes GLP-1R re-sensitisation. A. Experimental protocol. HEK-GLP-1R cells were pre-treated with either buffer (control) or 10 nM GLP-1 7-36 amide (pre-treatment) for 10 min followed by either standard buffer (pH 7.4) wash or acidified buffer (pH 4.0) wash for 40 s. After 90 min recovery, fluo-4-loaded cells were stimulated or re-stimulated with 10 nM GLP-1 7-36 amide. The changes in fluorescence were monitored and calibrated to allow calculation of $[Ca^{2+}]_i$. Responses were measured for 36 s with injection of agonist at 11 s. Data are either representative **(B)** or mean + S.E.M. n = 5 **(C)**. **, $p < 0.01$ (Bonferroni's test following two-way ANOVA; only the difference within a group is shown for clarity).

4.2.2. ECE-1 activity regulates the re-sensitisation of signalling by the GLP-1R in both HEK-GLP-1R cells and INS-1E cells.

Experiments in Chapter 3 highlighted that in HEK-GLP-1R cells, pre-challenge with 10 nM GLP-1 7-36 amide for 10 min induced maximum desensitisation of the Ca^{2+} response **(Fig 3.2.3.4)** and that removing the extracellular ligand facilitated GLP-1R re-sensitisation **(Fig 3.2.4).** The 90 min recovery period allowed the subsequent re-application of GLP-1 7-36 amide to stimulate a response of ~50% of that seen in naïve cells **(Fig 3.2.5)**. In the present experiment (protocol shown in **Fig 4.2.2.1.A**), pre-incubation with the highly selective ECE-1 inhibitor, SM19712 at 10 μM (Umekawa et al., 2000), before GLP-1 7-36 amide pre-treatment (10 nM, 10 min) markedly inhibited the Ca^{2+} response to re-challege after a 90 min period of recovery **(Fig 4.2.2.1.B, D)**. Given that ECE-1 is present both at the plasma membrane and in the endosomes (Roosterman et al., 2007), it is possible that inhibition of ECE-1 at the cell surface could protect extracellular peptide from breakdown, which might in some way enhance desensitisation or prevent recovery. Thus, in these experiments, the inhibitor was added only after pre-treatment and subsequent removal of GLP-1 7-36 amide. Under these conditions SM19712 still significantly reduced the extent of re-sensitisation **(Fig 4.2.2.1.C, D)**. SM19712 did not affect the response of naïve cells to GLP-1 7-36 amide.

In further experiments, the impact of SM19712 on re-sensitisation of the GLP-1R following stimulation with exendin-4 was assessed. Exendin-4 has approximately 50% homology to GLP-1 7-36 amide and is used clinically in the treatment of type 2 diabetes, particularly as it is resistant to cleavage by DPP-IV (Sinclair and Drucker, 2005). Exendin-4 produced a concentration-dependent increase in $[Ca^{2+}]_i$ with a pEC_{50} of 10.41 ± 0.03 and Hill slope of 2.37 ± 0.12 **(Fig 4.2.2.2.A, B)**. Pre-treatment with 1 nM (E_{max}) exendin-4 for 10 min followed by wash and 5 min recovery (protocol shown in **Fig 4.2.2.2.C**) resulted in a markedly reduced Ca^{2+} increase to the re-challenge with 1 nM exendin-4 compared with that in naïve cells (without pre-treatment) **(Fig 4.2.2.2.D,**

E). After a 6 h period of recovery, the response to re-challenge significantly increased but was still much lower than that in naïve cells (without pre-treatment). Treatment with SM19712 did not influence the response in naïve cells or in the re-challenge protocol after either 5 min or 6 h recovery **(Fig 4.2.2.2.D, E)**.

HEK-GLP-1R cells were transfected with either scrambled siRNA (control) or ECE-1 siRNA. As determined by immunoblotting, ECE-1 expression was markedly reduced after 36-48 h transfection with ECE-1 siRNA (**Fig 4.2.2.3.A**). In assessment of the functional consequences of reducing ECE-1 expression (protocol shown in **Fig 4.2.2.3.B**), the reduced expression did not affect the Ca^{2+} response of naïve cells to 10 nM GLP-1 7-36 amide **(Fig 4.2.2.3.C)**. However, knock-down markedly inhibited the response to a re-challenge with GLP-1 7-36 amide after 90 min recovery in cells pre-stimulated with GLP-1 7-36 amide (10 nM, 10 min) **(Fig 4.2.2.3.C)**.

In experiments to assess the consequences of overexpression of ECE-1, HEK-GLP-1R cells were transfected with either vector alone (control) or plasmids containing one of the ECE-1 isoforms. The expression of the ECE-1 isoforms was assessed by immunoblotting with an ECE-1 antibody but which was unable to distinguish between the different isoforms. A single band at ~115 kDa was detected in the control (untransfected) cells, at which size, the overexpressed ECE-1 isoforms were also detected (**Fig 4.2.2.4.A**). Interestingly, when either ECE-1a, b or d (but not c) were overexpressed, an additional band at ~87 kDa was detected, which is the predicted molecular size of ECE-1. The overexpression of each isoform of ECE-1 significantly enhanced the Ca^{2+} response to re-challenge with 10 nM GLP-1 7-36 amide after 60 min recovery compared to the control (without ECE-1 overexpression) (protocol shown in **Fig 4.2.2.4.B**). The 60 min recovery period was selected to provide a large window to detect the promotion of re-sensitisation by the overexpression of ECE-1. In each case this enhanced recovery was sensitive to SM19712, which reduced recovery to levels that were numerically but not significantly lower than that seen in untransfected cells (**Fig 4.2.2.4.C-F**).

In INS-1E cells, as previously demonstrated **(Fig 3.2.9.2)**, pre-treatment with 100 nM GLP-1 7-36 amide for 10 min in the absence of IBMX followed by 60 min recovery (protocol shown in **Fig 4.2.2.5.A**) induced a reduction of cAMP in response to GLP-1 7-36 amide re-challenge in the presence of IBMX **(Fig 4.2.2.5.B, C)**. In cells pre-incubated with 10 μM SM19712, the cAMP concentration-response curve after 60 min recovery had a pEC_{50} of 9.64 ± 0.15, which was not significantly different from either the control (without pre-treatment, 9.67 ± 0.13) or in cells that had been pre-stimulated in the absence of SM19712 (9.55 ± 0.11, **Fig 4.2.2.5.B**). However, in cells that had been pre-stimulated with GLP-1 7-36 amide, the reduced E_{max} following the 60 min recovery period was further reduced by SM 19712 **(Fig 4.2.2.5.B, C)**.

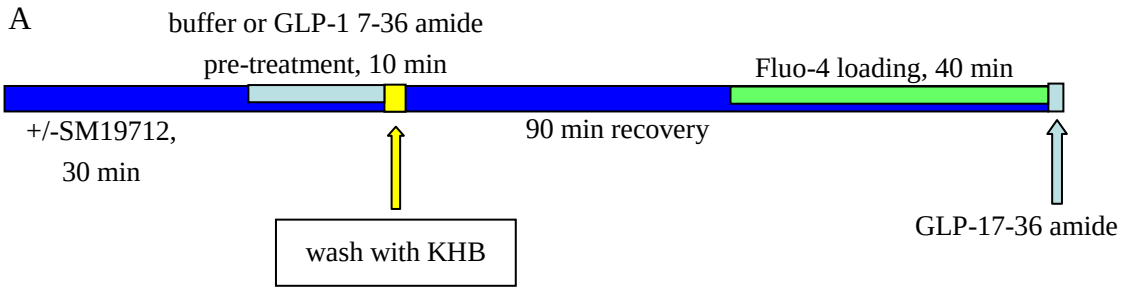
A
buffer or GLP-1 7-36 amide
pre-treatment, 10 min
Fluo-4 loading, 40 min
+/-SM19712,
30 min
90 min recovery
wash with KHB
GLP-17-36 amide

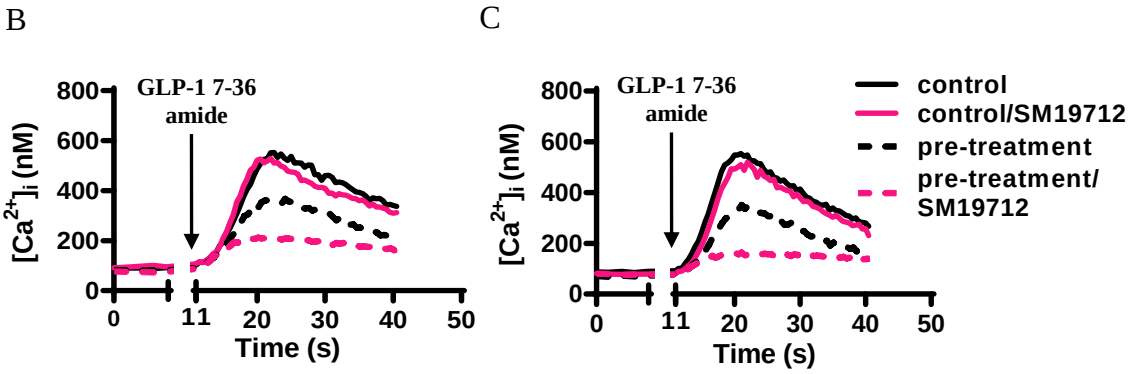
B
C
GLP-1 7-36 amide
[Ca2+]i (nM)
Time (s)
control
control/SM19712
pre-treatment
pre-treatment/ SM19712

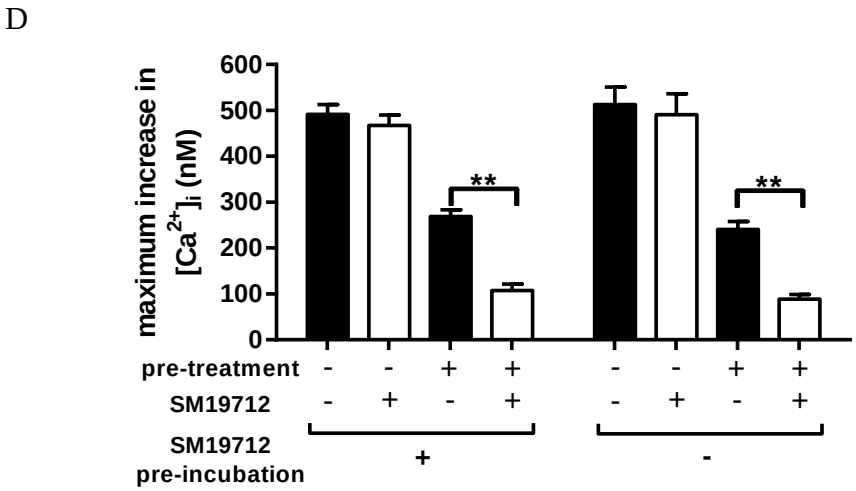
D
maximum increase in [Ca2+]i (nM)
pre-treatment
SM19712
SM19712 pre-incubation
**

Fig 4.2.2.1. SM19712 inhibits re-sensitisation of GLP-1R-mediated Ca^{2+} signalling. **A**. Experimental protocol **B.** HEK-GLP-1R cells were pre-incubated for 30 min without or with SM19712 (10 μM, which was then included throughout). Cells were then pre-treated with buffer (control) or 10 nM GLP-1 7-36 amide for 10 min (pre-treatment) followed by washing with KHB. After a 90 min period of recovery, fluo-4-loaded cells were stimulated or re-stimulated with 10 nM GLP-1 7-36 amide and the changes in fluorescence were monitored and converted to $[Ca^{2+}]_i$. Responses were measured for 41 s with the injection of agonist at 11 s. **C**. Cells were treated in the same way as shown in **B** but SM19712 was only added after GLP-1 7-36 amide pre-treatment and a KHB wash to remove free ligand. **D**. Mean data of the maximum increases in $[Ca^{2+}]_i$ from **B** and **C**. Data are either representative or mean + S.E.M., n = 3. **, $p < 0.01$ (Bonferroni's test following two-way ANOVA; only the differences between agonist-pre-treated cells are shown for clarity).

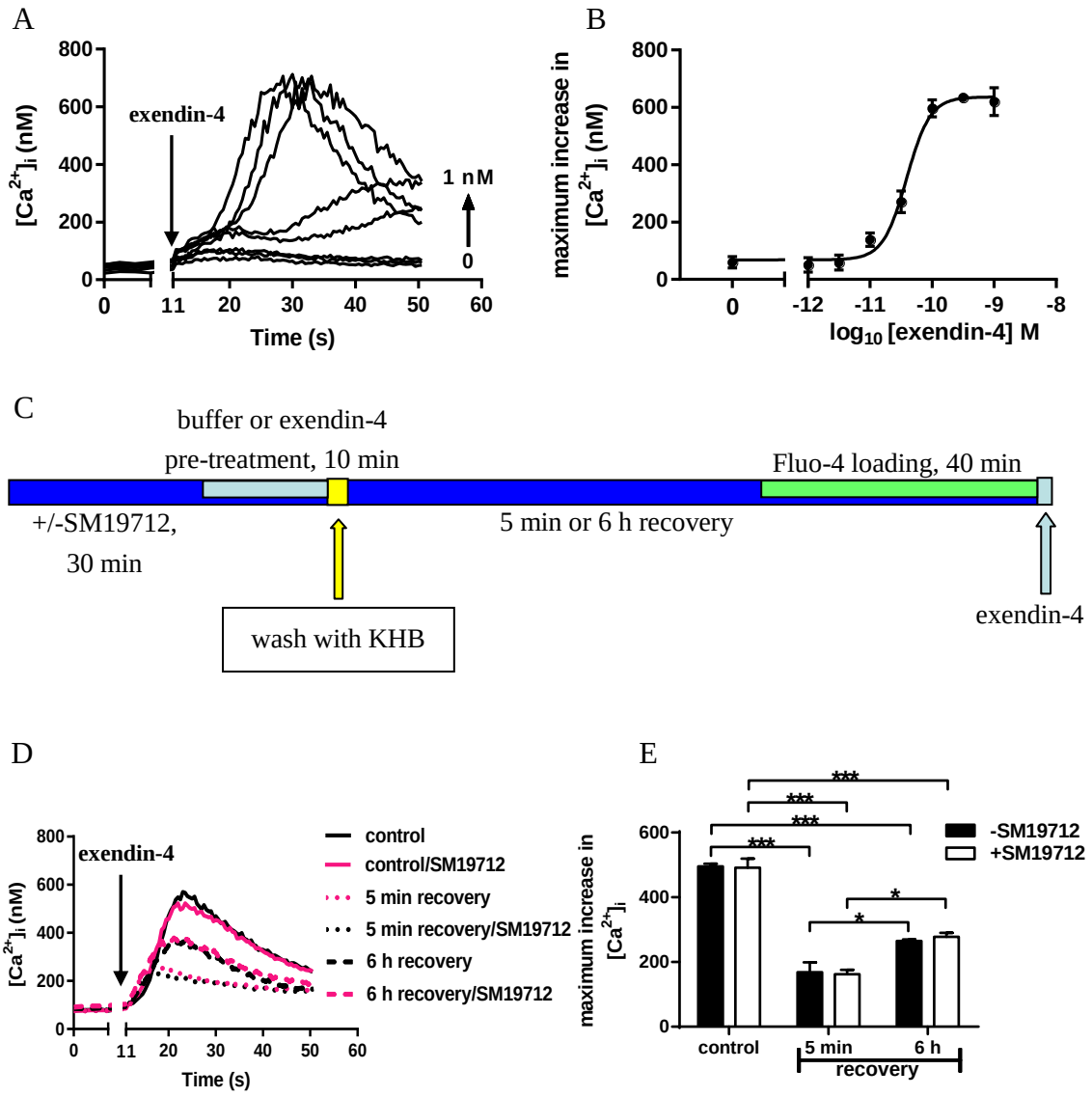

Fig 4.2.2.2. SM19712 has no effect on re-sensitisation of GLP-1R-mediated Ca^{2+} signalling following stimulation with exendin-4. A. Fluo-4-loaded HEK-GLP-1R cells were challenged with buffer (0) or exendin-4 at the indicated concentrations (0-1 nM). The changes in fluorescence were measured and calibrated to $[Ca^{2+}]_i$. Responses were measured for 51 s with the injection of agonist at 11 s. **B.** The maximum changes in $[Ca^{2+}]_i$ were determined to generate concentration-response curves which had a pEC_{50} of 10.41 ± 0.03 and Hill slope of 2.37 ± 0.12. **C**. Experimental protocol for **D** and **E**. **D.** HEK-GLP-1R cells were pre-incubated for 30 min without or with SM19712 (10 μM, which was then included throughout). Cells were then pre-treated with buffer (control) or 1 nM exendin-4 for 10 min followed by washing with KHB. After a 5 min or 6 h period of recovery in KHB or serum-free medium respectively, fluo-4-loaded cells were

stimulated or re-stimulated with 1 nM exendin-4 and the changes in fluorescence were monitored and converted to $[Ca^{2+}]_i$. Responses were measured for 51 s with the injection at 11 s. **E**. Mean data of the maximum increases in $[Ca^{2+}]_i$. Data are either representative or mean + S.E.M., n = 3. *, $p < 0.05$; ***, $p < 0.001$ (Bonferroni's test following two-way ANOVA. Only the differences within a group are shown for clarity).

A

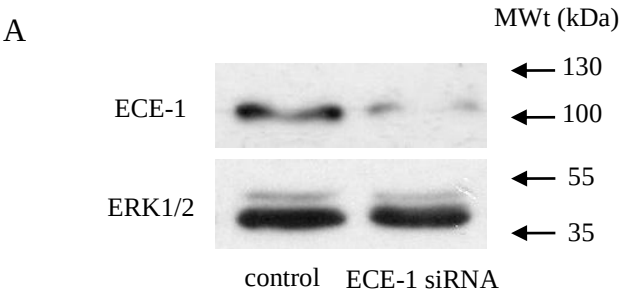
MWt (kDa)
ECE-1
ERK1/2
130
100
55
35
control
ECE-1 siRNA

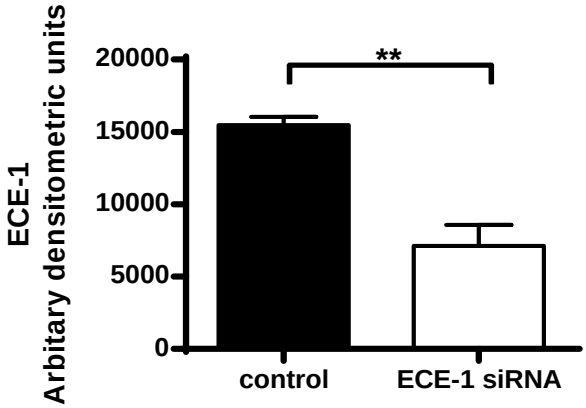
ECE-1
Arbitary densitometric units
20000
15000
10000
5000
0
**
control
ECE-1 siRNA

B

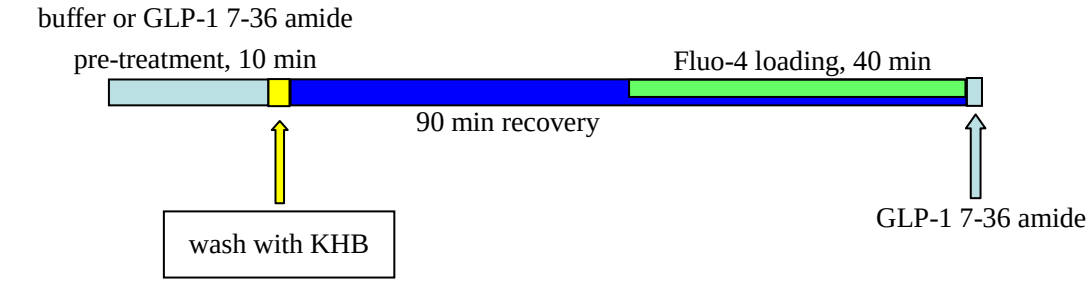
buffer or GLP-1 7-36 amide
pre-treatment, 10 min
Fluo-4 loading, 40 min
90 min recovery
wash with KHB
GLP-1 7-36 amide

C_i

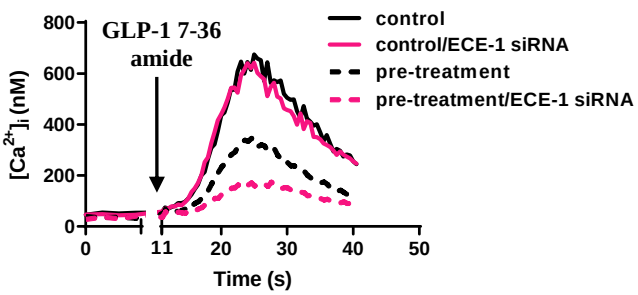
GLP-1 7-36 amide
control
control/ECE-1 siRNA
pre-treatment
pre-treatment/ECE-1 siRNA
[Ca2+]i (nM)
800
600
400
200
0
0
11
20
30
40
50
Time (s)

C_{ii}

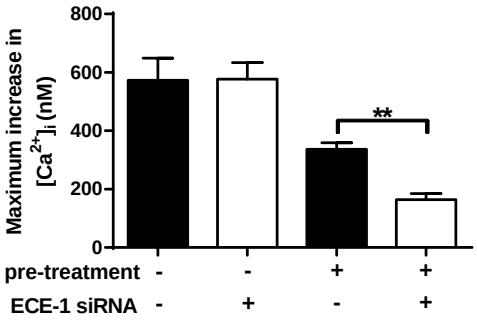
Maximum increase in [Ca2+]i (nM)
800
600
400
200
0
**
pre-treatment - - + +
ECE-1 siRNA - + - +

Fig 4.2.2.3. Knockdown of ECE-1 inhibits re-sensitisation of GLP-1R-mediated Ca^{2+} signalling. **A**. HEK-GLP-1R cells were transfected with scrambled siRNA (control) or ECE-1 siRNA as described in **Methods 2.4.2.**. The expression of ECE-1 was determined by immunoblotting. Blotting of ERK1/2 was used as a loading control. **C**. HEK-GLP-1R cells were transfected with scrambled siRNA or ECE-1 siRNA. Following the protocol **(B)**, transfected cells were pre-treated with either buffer (control) or 10 nM GLP-1 7-36 amide (pre-treatment) for 10 min followed by washing with KHB. After a 90 min period of recovery, cells were stimulated or re-stimulated with 10 nM GLP-1 7-36 amide. Responses were measured for 41 s with the injection at 11 s. Both the representative Ca^{2+} traces **(C_i)** and the mean data **(C_{ii})** are shown. Data are either representative or mean + S.E.M., $n \geq 3$. **, $p < 0.01$ (Student's t test).

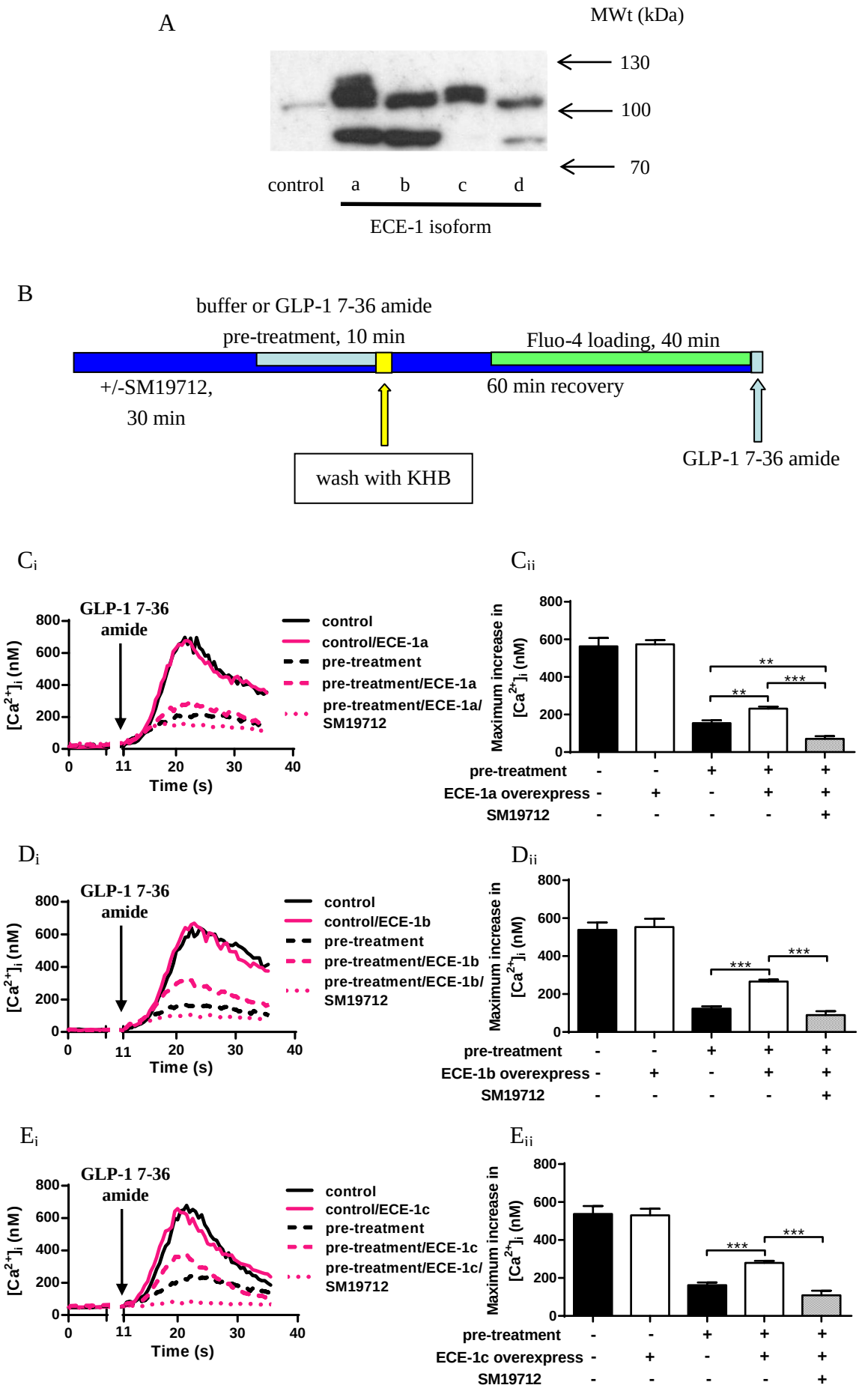
A
MWt (kDa)
130
100
70
control
a
b
c
d
ECE-1 isoform
B
buffer or GLP-1 7-36 amide
pre-treatment, 10 min
Fluo-4 loading, 40 min
+/-SM19712,
30 min
60 min recovery
wash with KHB
GLP-1 7-36 amide
Ci
GLP-1 7-36 amide
[Ca2+]i (nM)
Time (s)
control
control/ECE-1a
pre-treatment
pre-treatment/ECE-1a
pre-treatment/ECE-1a/ SM19712
Cii
Maximum increase in [Ca2+]i (nM)
pre-treatment
ECE-1a overexpress
SM19712
Di
GLP-1 7-36 amide
control
control/ECE-1b
pre-treatment
pre-treatment/ECE-1b
pre-treatment/ECE-1b/ SM19712
Dii
pre-treatment
ECE-1b overexpress
SM19712
Ei
GLP-1 7-36 amide
control
control/ECE-1c
pre-treatment
pre-treatment/ECE-1c
pre-treatment/ECE-1c/ SM19712
Eii
pre-treatment
ECE-1c overexpress
SM19712

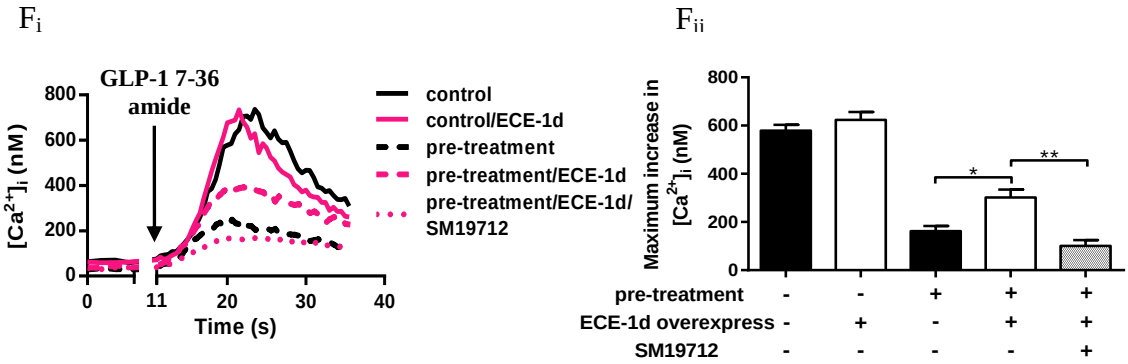

Fig 4.2.2.4. Overexpression of ECE-1 a-d promotes re-sensitisation of GLP-1R-mediated Ca^{2+} signalling. **A**. Representative blot. HEK-GLP-1R cells were transfected with either vector alone (pcDNA3.1, control) or individually with the ECE-1 isoforms as described in **Methods 2.4.1.**. The expression of ECE-1 was determined by immunoblotting using a pan-isoform antibody. **B-F.** HEK-GLP-1R cells were transfected with either vector alone or ECE-1a (**C**), ECE-1b (**D**), ECE-1c (**E**) or ECE-1d (**F**). As shown in the protocol (**B)**, the transfected cells were pre-incubated without or with 10 μM SM19712 for 30 min (which was then included throughout). Cells were then pre-treated with either buffer (control) or 10 nM GLP-1 7-36 amide for 10 min followed by washing with KHB. After a 60 min period of recovery, fluo-4-loaded cells were stimulated or re-stimulated with 10 nM GLP-1 7-36 amide. Responses were measured for 36 s with the injection at 11 s. Representative Ca^{2+} traces (**B_i, C_i, D_i, E_i**) and the mean data (**B_{ii}, C_{ii}, D_{ii}, E_{ii}**) are shown. Data are mean + S.E.M., n ≥ 3. *, $p < 0.05$; **, $p < 0.01$; ***, $p < 0.001$ (Bonferroni's test following one-way ANOVA. Only the differences in GLP-1 7-36 amide pre-treated cells are shown for clarity).

A

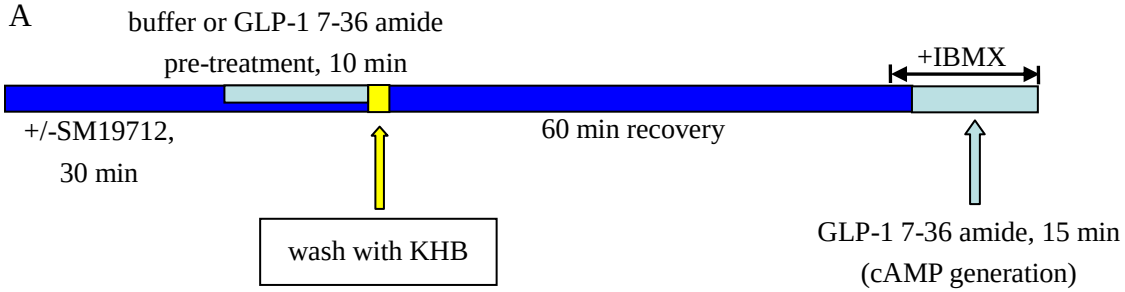
buffer or GLP-1 7-36 amide
pre-treatment, 10 min
+IBMX
+/-SM19712,
30 min
60 min recovery
wash with KHB
GLP-1 7-36 amide, 15 min
(cAMP generation)

B

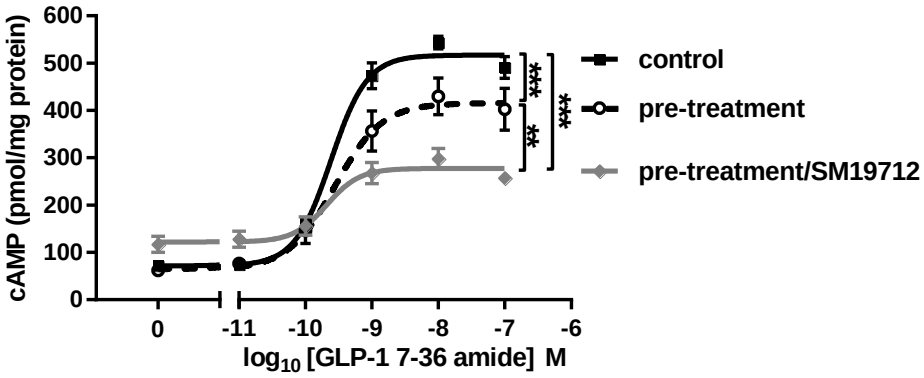
cAMP (pmol/mg protein)
600
500
400
300
200
100
0
0
-11
-10
-9
-8
-7
-6
log10 [GLP-1 7-36 amide] M
control
pre-treatment
pre-treatment/SM19712
***
**
***

C

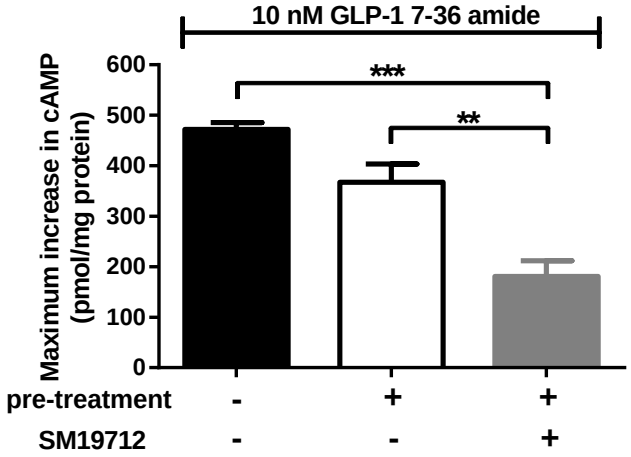
10 nM GLP-1 7-36 amide
Maximum increase in cAMP (pmol/mg protein)
600
500
400
300
200
100
0
***
**
pre-treatment - + +
SM19712 - - +

Fig 4.2.2.5. ECE-1 regulates re-sensitisation of the GLP-1R-mediated cAMP response in INS-1E cells. A. Experimental protocol. **B.** Cells were pre-incubated for 30 min in buffer with or without 10 μM SM19712 (which was then included throughout). Cells were then pre-treated in the absence of IBMX with either buffer (control) or 100 nM GLP-1 7-36 amide (pre-treatment) for 10 min followed by washing with KHB. After a 60 min period of recovery, cells were challenged or re-challenged with GLP-1 7-36 amide at the required concentrations (0-100 nM) for 15 min in the presence of IBMX. The generation of cAMP was then determined. The pEC_{50} was 9.67 ± 0.13 for the control, 9.55 ± 0.11 for pre-treated cells in the absence of SM19712 and 9.64 ± 0.15 for pre-treated cells in the presence of SM19712. Data are mean ± S.E.M., n = 3. **, $p < 0.01$; ***, $p < 0.001$ (two-way ANOVA). **C.** The maximum increases (E_{max} - E_{basal}) in cAMP were generated. Data are mean + S.E.M., n = 3. **, $p < 0.01$; ***, $p < 0.001$ (Bonferroni's test following one-way ANOVA).

4.2.3. High concentrations of glucose promote both ECE-1 expression and re-sensitisation of the GLP-1R.

There is evidence suggesting that the expression level of ECE-1 increases under high glucose conditions (Keynan et al., 2004). In the present experiment, HEK-GLP-1R cells cultured in low glucose medium (5.5 mM) for at least 7 days had a detectable level of ECE-1 expression which increased in a time-dependent manner (0-72 h) following an increase in the concentration of glucose to 25 mM (**Fig 4.2.3.1.A, B**). A similar experiment in INS-1E cells was inconclusive as multiple bands were present on the Western blot making it difficult to determine which, if any, was ECE-1.

Given the ability of a high glucose concentration to increase ECE-1 expression in HEK-GLP-1R cells, the impact of high glucose on GLP-1R re-sensitisation was determined. Thus, cells were cultured in either low glucose (5.5 mM) or high glucose (25 mM) for 48 h and the re-sensitisation of the GLP-1R-mediated Ca^{2+} response determined following desensitisation with GLP-1 7-36 amide (protocol shown in **Fig 4.2.3.2.A**). Cells cultured in low glucose (5.5 mM) displayed a small Ca^{2+} response to re-challenge with 10 nM GLP-1 7-36 amide (~30 % of control) (**Fig 4.2.3.2.B, D**) after pre-treatment (10 nM GLP-1 7-36 amide, 10 min) and recovery (90 min). However, in cells cultured at a high glucose concentration (25 mM) for 48 h, the response to re-challenge was ~60 % of control **(Fig 4.2.3.2.C, D)**. The recovery of these responses in cells cultured in either low or high glucose medium was significantly inhibited by SM19712.

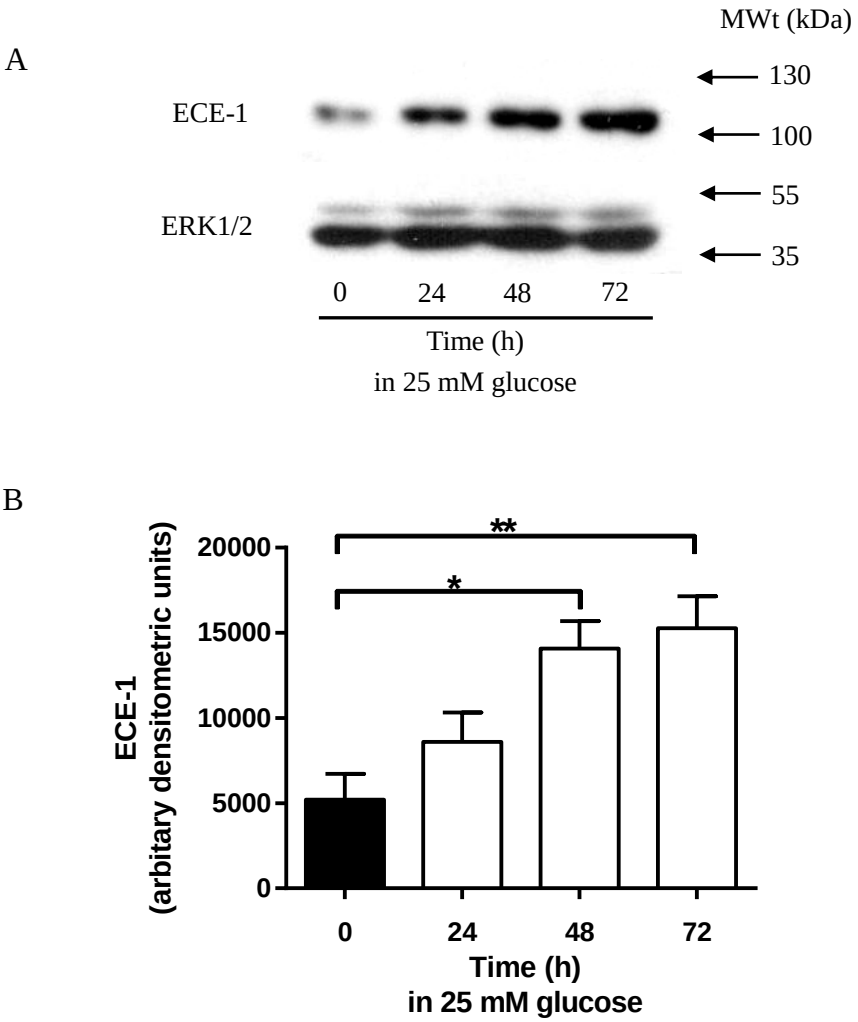

Fig 4.2.3.1. The expression level of ECE-1 is increased by culturing cells at a high glucose concentration. **A, B.** HEK-GLP-1R cells were grown in low glucose (5.5 mM) for at least 7 days. Cells were then either cultured in the same conditions or transferred to high glucose medium (25 mM) for 24-72 h. The protein concentrations were normalised and the expression of ECE-1 was determined by immunoblotting. ERK1/2 was used as a loading control. Data are either representative of 3 independent experiments **(A)** or mean + S.E.M., n = 3 **(B)**. *, $p < 0.05$; **, $p < 0.01$ (Bonferroni's test following one-way ANOVA).

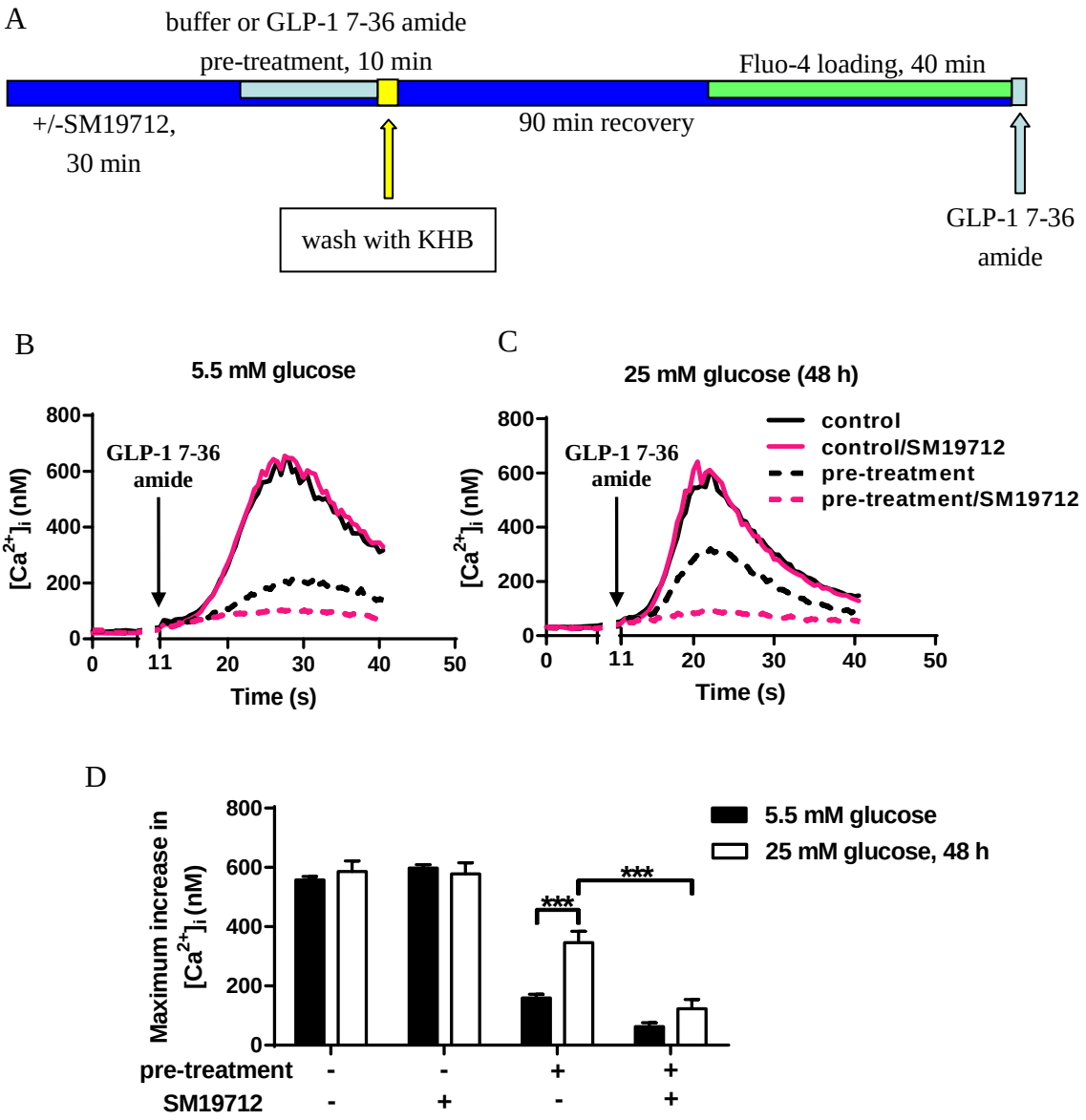

Fig 4.2.3.2. Culturing cells in a high glucose concentration promotes re-sensitisation of GLP-1R-mediated Ca^{2+} signalling. HEK-GLP-1R cells were grown in low glucose (5.5 mM) for at least 7 days. Cells were then either cultured in this medium **(B)** or transferred to a high glucose medium (25 mM, **C**) for 48 h. On the day of assay, standard KHB containing 11.7 mM glucose was used throughout. Cells were pre-incubated with buffer with or without 10 μM SM19712 for 30 min (which was then included throughout). Cells were then pre-treated with buffer (control) or 10 nM GLP-1 7-36 amide (pre-treatment) for 10 min followed by washing with KHB. After a 90 min period of recovery, fluo-4-loaded cells were stimulated or re-stimulated with 10 nM GLP-1 7-36 amide and the changes in fluorescence were monitored to allow

determination of $[Ca^{2+}]_i$. Responses were measured for 41 s with the injection at 11 s. Data are either representative **(B, C)** or mean + S.E.M., n = 4 **(D)**. ***, $p < 0.001$ (Bonferroni's test following two-way ANOVA. Not all the differences are shown for clarity).

4.2.4. mCherry-tagged ECE-1 isoforms localize with early endosomes.

Given that the commercial ECE-1 antibody is not isoform-specific, C-terminal mCherry-tagged versions of ECE-1 isoforms were generated to enable detection of distribution and potential trafficking. The expression of the ECE-1-mCherry isoforms was assessed by immunoblotting with a commercial mCherry antibody. A non-specific band was detected at around 80 kDa in non-transfected cells **(Fig 4.2.4.1.A)**. A band at around 28 kDa (predicted size of mCherry) was also detected in the cells overexpressing mCherry alone. For the cells overexpressing ECE-1-mCherry isoforms, 2-3 bands from 100-150 kDa were apparent, indicating the expression of ECE-1-mCherry isoforms **(Fig 4.2.4.1.A)**. To check the function of the mCherry-tagged ECE-1 isoforms, their ability to enhance re-sensitisation of GLP-1R-mediated Ca^{2+} signalling was determined (protocol shown in **Fig 4.2.4.1.B**). The overexpression of ECE-1b-mCherry or ECE-1c-mCherry significantly enhanced GLP-1R re-sensitisation **(Fig 4.2.4.1.D, E).** In cells overexpressing ECE-1a-mCherry or ECE-1d-mCherry, the Ca^{2+} response to re-stimulation was ~40% greater than controls (without ECE-1-mCherry overexpression), although this did not quite reach statistical significance **(Fig 4.2.5.3.C, F)**. **Table 4.1.** summarizes the findings with the wild-type and mCherry-tagged ECE-1 isoforms.

As the expression level of ECE-1 increased in response to culturing the cells at a high glucose concentration **(Fig 4.2.3.1.)**, we cultured the cells in low glucose (5.5 mM) medium to minimize the expression of endogenous ECE-1 and maximize the possibility of detecting the expression and distribution of ECE-1-mCherry isoforms. Previously we have shown that GLP-1Rs co-localized with EEA1, an early endosome marker **(Fig 3.2.6.4.)**. In the present experiment, each isoform of ECE-1-mCherry co-localized with EEA1. This was particularly apparent for ECE-1b-mCherry and ECE-1d-mCherry in HEK293 cells (in the absence of GLP-1R expression) cultured in low glucose (5.5 mM) medium **(Fig 4.2.4.2.)**.

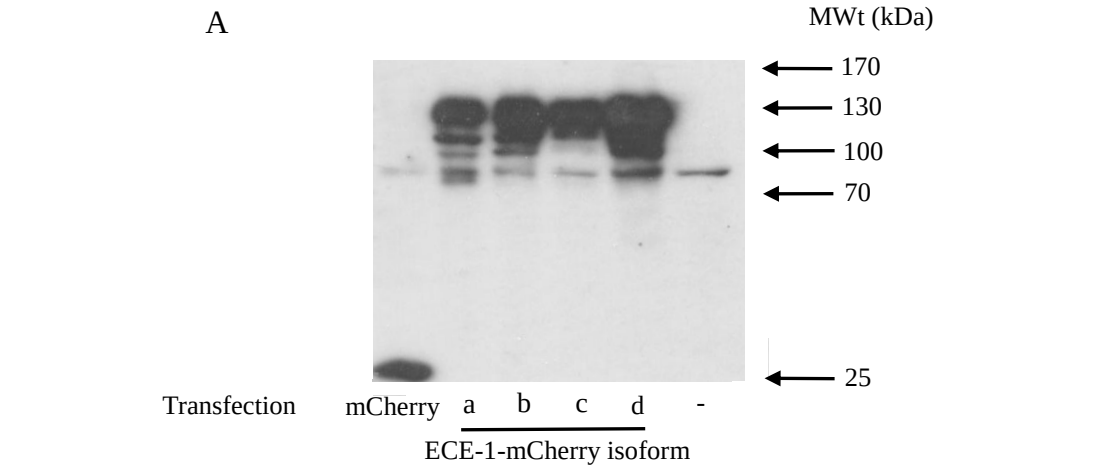
A
MWt (kDa)
170
130
100
70
25
Transfection
mCherry
a
b
c
d
-
ECE-1-mCherry isoform

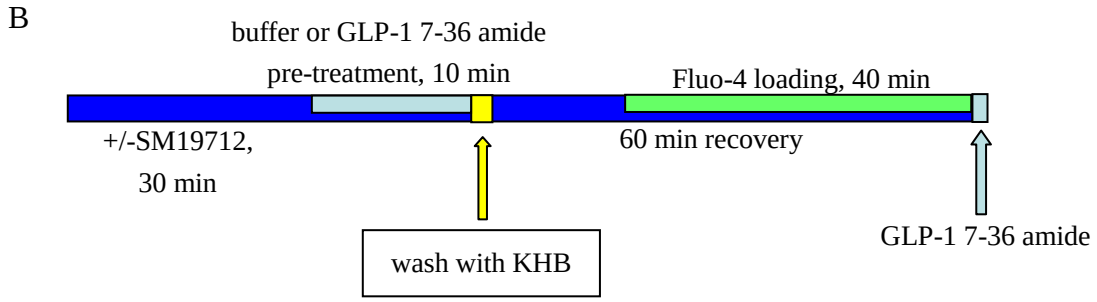
B
buffer or GLP-1 7-36 amide
pre-treatment, 10 min
Fluo-4 loading, 40 min
+/-SM19712,
30 min
60 min recovery
wash with KHB
GLP-1 7-36 amide

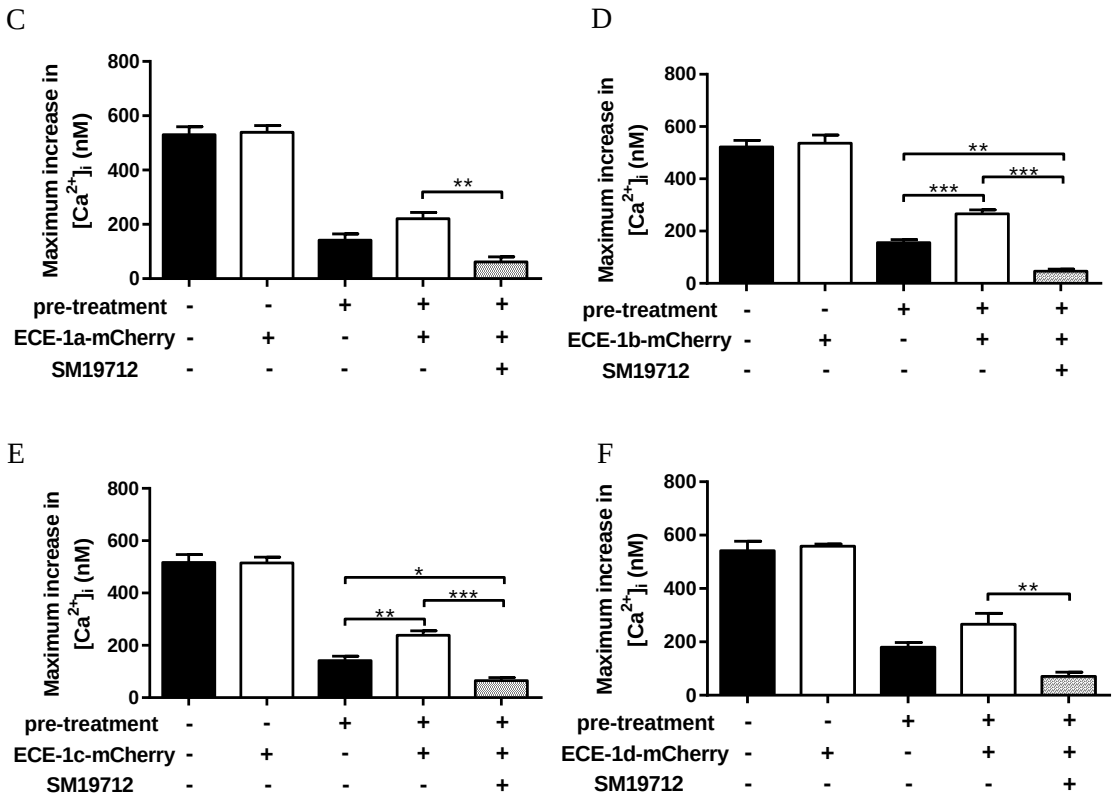
C
D
E
F
Maximum increase in [Ca2+]i (nM)
800
600
400
200
0
pre-treatment
ECE-1a-mCherry
ECE-1b-mCherry
ECE-1c-mCherry
ECE-1d-mCherry
SM19712
*
**
***

Fig 4.2.4.1. Overexpression of mCherry-tagged ECE-1 isoforms enhances re-sensitisation of GLP-1R-mediated Ca^{2+} signalling. **A.** Representative blot. HEK-GLP-1R cells were transfected with mCherry alone or ECE-1-mCherry isoforms as described in **Methods 2.4.1.**. The expression of proteins was determined by immunoblotting. **B.** Experimental protocol. **C-F.** HEK-GLP-1R cells were transfected with mCherry alone or ECE-1a-mCherry (**C**), ECE-1b-mCherry (**D**), ECE-1c-mCherry (**E**) or ECE-1d-mCherry (**F**). Following the protocol **(Fig 4.2.2.4.B)**, transfected cells were pre-incubated without or with 10 μM SM19712 for 30 min (which was then included throughout). The cells were then pre-treated with either buffer (control) or 10 nM GLP-1 7-36 amide for 10 min followed by washing with KHB. After a 60 min period of recovery, fluo-4-loaded cells were stimulated or re-stimulated with 10 nM GLP-1 7-36 amide. Data are either representative or mean + S.E.M., $n \geq 3$. *, $p < 0.05$; **, $p < 0.01$; ***, $p < 0.001$ (Bonferroni's test following one-way ANOVA. Only the differences between pre-treated cells are shown for clarity).

ECE-1 / function	a	a-mCherry	b	b-mCherry	C	c-mCherry	d	d-mCherry
re-sensitisation ↑	30% **	40% ns	50% ***	50% ***	50% ***	50% **	50% *	40% ns
SM19712 ↓	***	**	***	***	***	***	**	**

Table 4.1. Summary of the findings with the wild-type and mCherry-tagged ECE-1 isoforms. The upward arrow indicates the promotion of re-sensitisation by the overexpression of ECE-1-mCherry isoforms and the downward arrow indicates the inhibition of re-sensitisation by SM19712. The stars indicate the level of statistical significance compared to the controls (without overexpression or SM19712 treatment). *, $p < 0.05$; **, $p < 0.01$; ***, $p < 0.001$; ns, no significant difference (Bonferroni's test following one-way ANOVA).

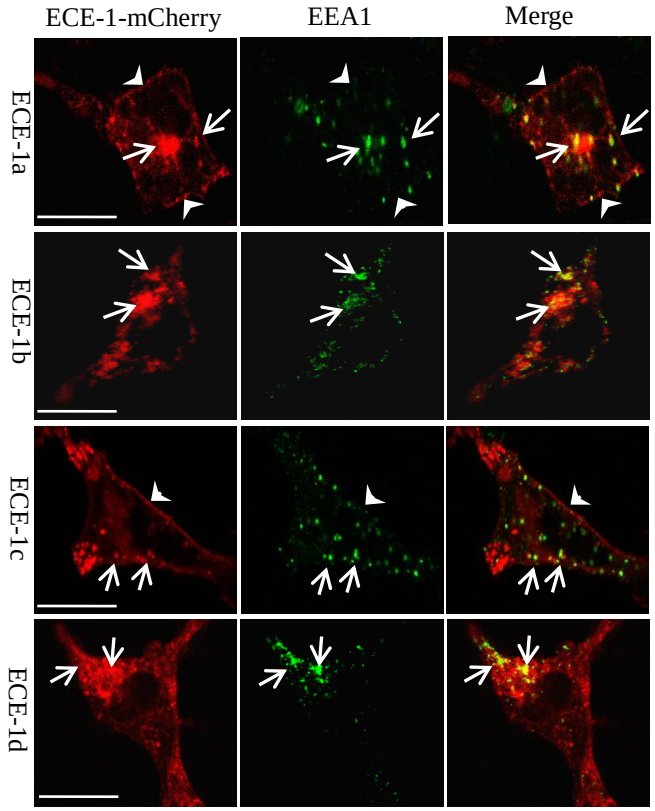

Fig 4.2.4.2. ECE-1-mCherry isoforms co-localized with early endosomes. HEK293 cells cultured under low glucose (5.5 mM) conditions for at least 7 days were transfected separately with mCherry-tagged versions of the ECE-1 isoforms. At 36-48 h following transfection, cells were washed with KHB and then fixed and permeabilized for immunostaining with EEA1. The cells were imaged in the mounting solution using confocal microscopy. The expression of ECE-1-mCherry or EEA1 at the plasma membrane or in the cytosol is indicated by arrowheads and arrows respectively. Representative images of 2 independent experiments. Scale bar (in the bottom left of image), 5 μm.

4.2.5. The co-localization of GLP-1R-EGFP and ECE-1-mCherry isoforms and the influence of GLP-1R-EGFP activation on the sub-cellular localization of ECE-1-mCherry.

In order to examine the sub-cellular distribution of GLP-1R and ECE-1, ECE-1-mCherry isoforms were imaged either before or after stimulation with GLP-1 7-36 amide in live HEK-GLP-1R-EGFP cells cultured under low glucose conditions (5.5 mM). Under basal conditions, ECE-1a-mCherry was present both at the plasma membrane and in the cytosol. ECE-1b-mCherry and ECE-1d-mCherry were distributed mainly in the cytosol and ECE-1c-mCherry was mainly at the cell surface **(Fig 4.2.5.1.)**. ECE-1a-mCherry showed little co-localization with GLP-1R-EGFP under basal (unstimulated) conditions. In contrast all the other isoforms showed substantial co-localization with GLP-1R-EGFP. ECE-1c-mCherry mainly co-localized with GLP-1R-EGFP at the plasma membrane. ECE-1b-mCherry and ECE-1d-mCherry co-localized with the receptor both at the plasma membrane and in the cytosol **(Fig 4.2.5.1.)**.

As shown previously **(Fig 3.2.6.1.)**, challenge of HEK-GLP-1R-EGFP cells with GLP-1 7-36 amide (100 nM, 60 min) resulted in the loss of plasma membrane EGFP fluorescence and an increase in intracellular EGFP fluorescence **(Fig 4.2.5.1.)**. Here, this GLP-1 7-36 amide stimulation also resulted in the accumulation of all mCherry-tagged ECE-1 isoforms into large cytosolic fluorescent patches, which co-localized with the increased intracellular fluorescence of GLP-1R-EGFP **(Fig 4.2.5.1.)**. Also the Pearson correlation coefficient (r) shows that there is more co-localization between the GLP-1R-EGFP and each ECE-1-mCherry isoform after simulation. In the absence of ECE-1-mCherry expression, but in cells expressing GLP-1R-EGFP, no fluorescence was detected using 568 nm excitation (used to image mCherry), demonstrating that these two signals did not overlap. Furthermore, in cells only expressing ECE-1-mCherry and not GLP-1R-EGFP, fluorescence was not observed using 488 nm excitation (used to image GLP-1R-EGFP) **(Fig 4.2.5.1.C, D)**.

Although the intracellular fluorescence of ECE-1-mCherry increased in response to GLP-1 7-36 amide stimulation, there was no obvious loss of fluorescence elsewhere. In order to further examine the re-distribution of ECE-1-mCherry isoforms, 3D reconstructions were made. There is some evidence of loss of cell-surface ECE-1-mCherry after 60 min stimulation with GLP-1 7-36 amide compared to basal (0 min) **(Fig 4.2.5.2)**. And the analysis of Pearson correlation coefficient (r) shows that there is more co-localization between the GLP-1R-EGFP and each ECE-1-mCherry isoform after simulation. However, it is difficult to localize the cell-surface ECE-1 based only on GLP-1R-EGFP in the 3D images.

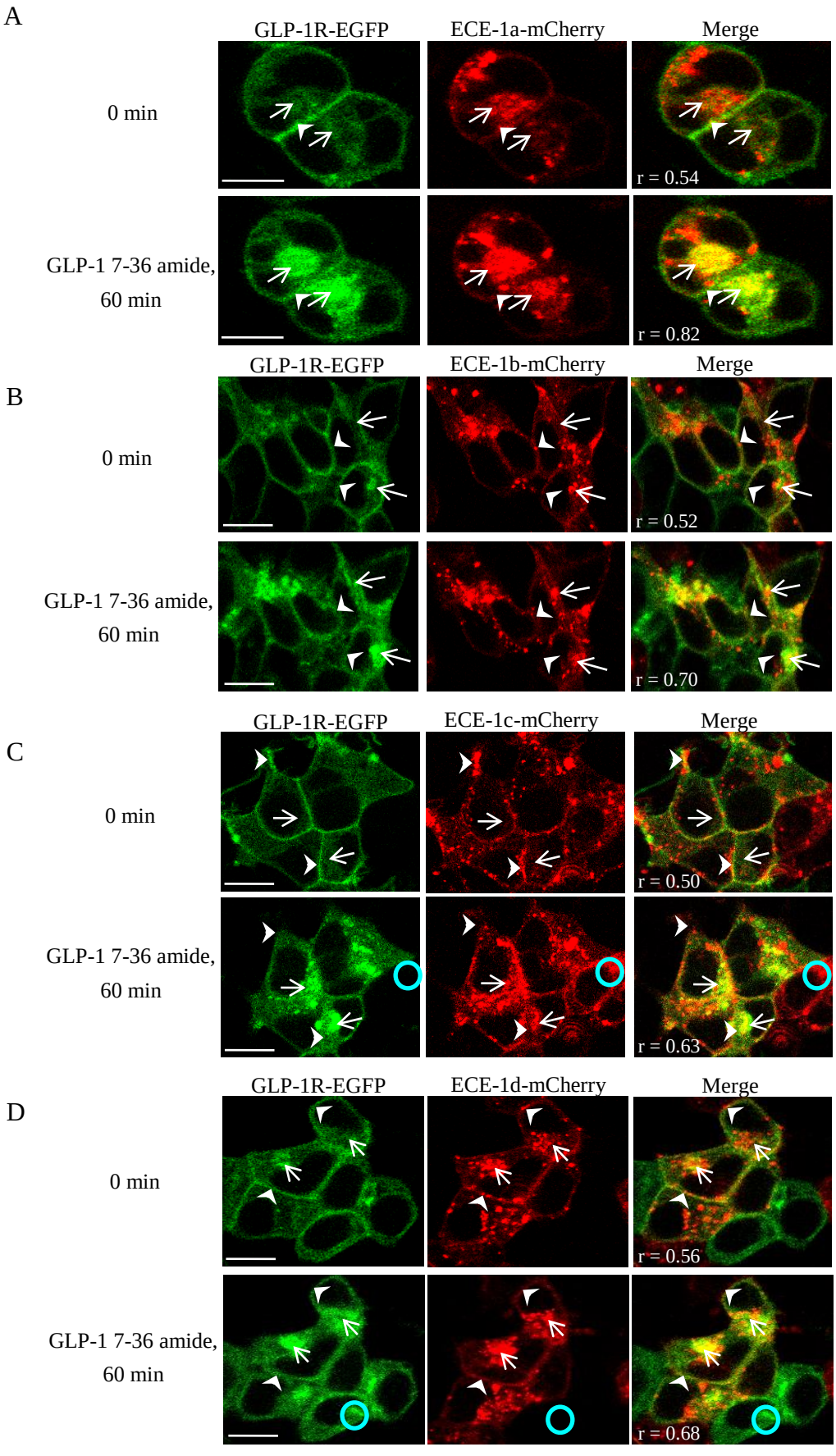
A
GLP-1R-EGFP
ECE-1a-mCherry
Merge
0 min
r = 0.54
GLP-1 7-36 amide,
60 min
r = 0.82
B
GLP-1R-EGFP
ECE-1b-mCherry
Merge
0 min
r = 0.52
GLP-1 7-36 amide,
60 min
r = 0.70
C
GLP-1R-EGFP
ECE-1c-mCherry
Merge
0 min
r = 0.50
GLP-1 7-36 amide,
60 min
r = 0.63
D
GLP-1R-EGFP
ECE-1d-mCherry
Merge
0 min
r = 0.56
GLP-1 7-36 amide,
60 min
r = 0.68

Fig 4.2.5.1. Co-localization of GLP-1R-EGFP and mCherry-tagged ECE-1 isoforms before and after challenge with GLP-1 7-36 amide. HEK-GLP-1R-EGFP cells, cultured in low glucose (5.5 mM) for at least 7 days, were transfected separately with either ECE-1a-mCherry (**A**), ECE-1b-mCherry (**B**), ECE-1c-mCherry (**C**) or ECE-1d-mCherry (**D**). Cells were challenged with 100 nM GLP-1 7-36 amide for 60 min in KHB at 37 ˚C. The images of GLP-1R-EGFP and ECE-1-mCherry were captured using confocal microscopy either before (0 min) or after stimulation with GLP-1 7-36 amide (60 min). The arrowheads and arrows indicate the localization of GLP-1R-EGFP or ECE-1-mCherry at the plasma membrane and in the cytosol respectively. The circles in images C and D indicate cells expressing only either ECE-1-mCherry or GLP-1R-EGFP. Representative images of 3 independent experiments. The Pearson correlation coefficient (r) was used to quantify the degree of co-localization between GLP-1R-EGFP and ECE-1-mCherry isoforms. Scale bar (in the bottom left of image), 5 μm.

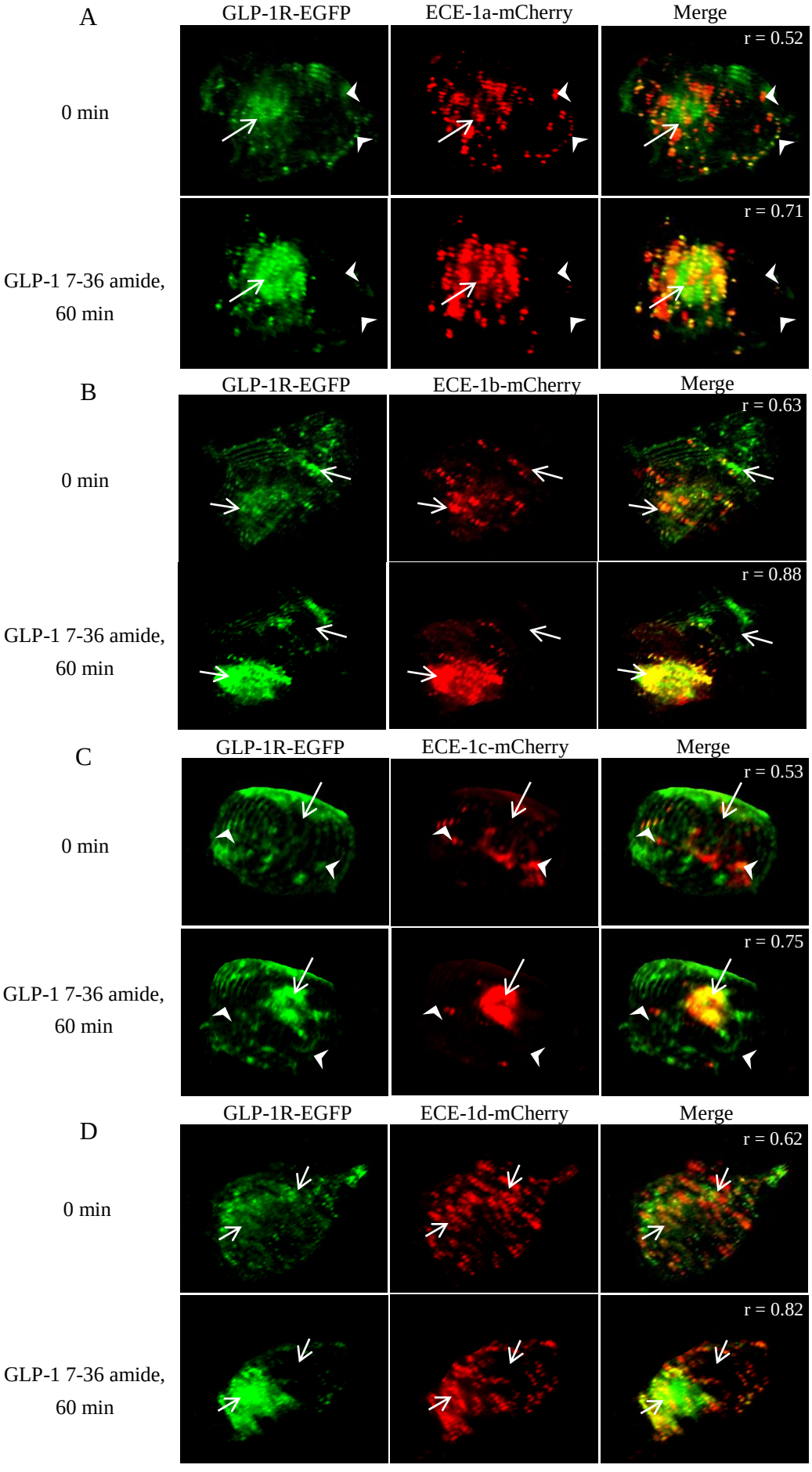
A
GLP-1R-EGFP
ECE-1a-mCherry
Merge
r = 0.52
0 min
r = 0.71
GLP-1 7-36 amide,
60 min
B
GLP-1R-EGFP
ECE-1b-mCherry
Merge
r = 0.63
0 min
r = 0.88
GLP-1 7-36 amide,
60 min
C
GLP-1R-EGFP
ECE-1c-mCherry
Merge
r = 0.53
0 min
r = 0.75
GLP-1 7-36 amide,
60 min
D
GLP-1R-EGFP
ECE-1d-mCherry
Merge
r = 0.62
0 min
r = 0.82
GLP-1 7-36 amide,
60 min

Fig 4.2.5.2. 3D images of GLP-1R-EGFP and ECE-1-mCherry before and after treatment of cells with 100 nM GLP-1 7-36 amide. HEK-GLP-1R-EGFP cells cultured in low glucose (5.5 mM) for at least 7 days were transfected with either ECE-1a-mCherry **(A)**, ECE-1b-mCherry **(B)**, ECE-1c-mCherry **(C)** or ECE-1d-mCherry **(D)**. Image stacks were generated by imaging at 0.3 μm intervals every 2 min over the 60 min period of stimulation with 100 nM GLP-1 7-36 amide. 3D images were then made as described in **Methods 2.11.2.**. Only the images of basal (0 min) and GLP-1 7-36 amide stimulation (60 min) are shown here. The arrowheads and arrows indicate the localization at the plasma membrane and in the cytosol of GLP-1R-EGFP or ECE-1-mCherry respectively. n = 1. The Pearson correlation coefficient (r) was used to quantify the degree of co-localization between GLP-1R-EGFP and ECE-1-mCherry isoforms.

4.2.6. ECE-1 activity regulates the recovery of cell-surface binding of GLP-1R in both HEK-GLP-1R cells and INS-1E cells.

Radioligand binding was conducted to assess the impact of ECE-1 activity on changes in cell-surface GLP-1R binding. Treatment with 100 nM GLP-1 7-36 amide for 10 min (a concentration used to induce a marked loss of cell-surface GLP-1R binding as assessed by radioligand binding assay **(Fig 3.2.7.)**) followed by washing with KHB and a 5 min period of recovery (protocol shown in **Fig 4.2.6.1.A**) induced ~50% reduction in GLP-1R binding in HEK-GLP-1R cells **(Fig 4.2.6.1.B)**. After a 90 min period of recovery, binding had recovered to ~80% of basal levels **(Fig 4.2.6.1.B)**. Treating cells with SM19712 significantly reduced cell-surface GLP-1R binding following either a 5 min or a 90 min period of recovery **(Fig 4.2.6.1.B)**. SM19712 did not affect binding to na ïve cells (without GLP-1 7-36 amide treatment).

Previous experiments showed that SM19712 inhibited recovery of GLP-1R-mediated Ca^{2+} signalling following treatment with 10 nM GLP-1 7-36 amide **(Fig 4.2.2.1)**. To assess whether this was also true for 100 nM GLP-1 7-36 amide, Ca^{2+} signalling was determined (protocol shown in **Fig 4.2.6.1.A**). Pre-treating the cells with 10 µM SM19712 largely inhibited the Ca^{2+} response to re-challenge with GLP-1 7-36 amide after 90 min recovery following GLP-1 7-36 amide pre-treatment (100 nM, 10 min) with no inhibition in na ïve cells (without pre-treatment, **Fig 4.2.6.1.C, D**).

As both ECE-1 expression and re-sensitisation of GLP-1R-mediated Ca^{2+} signalling were enhanced by culturing cells in a high glucose medium **(Fig 4.2.3.1. and Fig 4.2.3.2.)**, radioligand binding was performed in cells grown in either low glucose (5.5 mM) medium or high glucose (25 mM) medium for 48 h to determine the influence of glucose concentration on the recovery of cell-surface GLP-1R binding. In these experiments, cells grew faster under high glucose (25 mM) conditions than under the low glucose (5.5 mM). Therefore, here the raw data were normalised to minimize the impact of different cell numbers. In the cells grown in low glucose (5.5 mM), 100 nM

GLP-1 7-36 amide treatment for 10 min followed by a 90 min period of recovery resulted in ~80% GLP-1R binding compared to basal (without GLP-1 7-36 amide treatment) **(Fig 4.2.6.2.)**. This was enhanced to ~90% in cells grown under high glucose (25 mM) conditions although this did not reach statistical significance **(Fig 4.2.6.2.)**. SM19712 treatment markedly inhibited the recovery of cell-surface GLP-1R binding in cells grown in either low or high glucose concentrations **(Fig 4.2.6.2.)**.

In INS-1E cells, as shown previously **(Fig 3.2.9.1)**, challenge with 100 nM GLP-1 7-36 amide for 10 min followed by 5 min recovery evoked ~50% reduction of GLP-1R binding at the cell surface which increased after removal of the ligand **(Fig 4.2.6.3.A)**. Treatment with SM19712 significantly inhibited recovery of GLP-1R binding at the plasma membrane after 60 min recovery without changing the binding in naïve cells (without GLP-1 7-36 amide treatment).

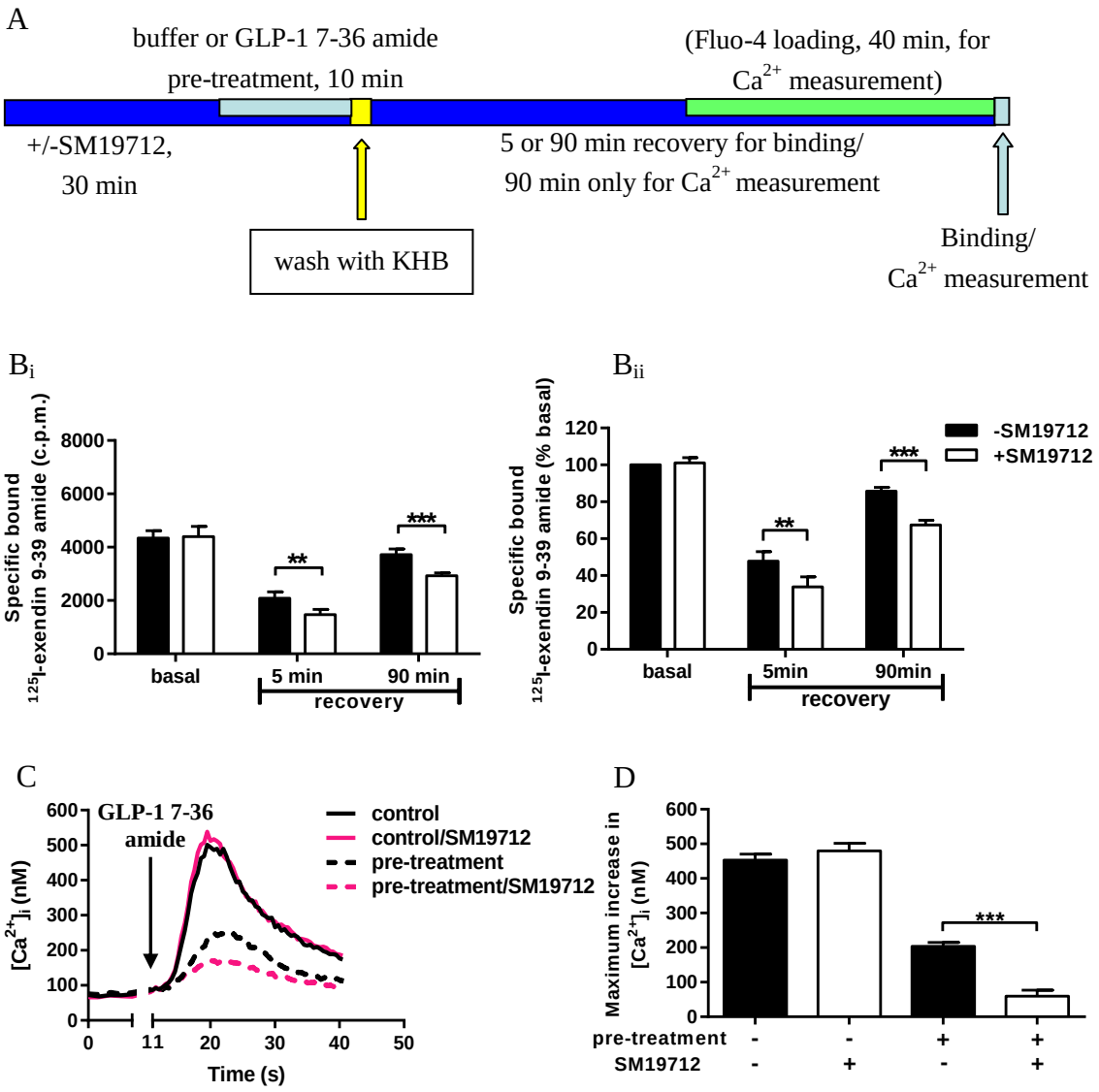

Fig 4.2.6.1. ECE-1 regulates recovery of cell-surface GLP-1R binding and GLP-1 7-36 amide-mediated Ca^{2+} responses. A. Experimental protocol. **B.** HEK-GLP-1R cells were pre-incubated without or with 10 µM SM19712 for 30 min (which was then included throughout). Cells were then challenged with buffer (control) or 100 nM GLP-1 7-36 amide for 10 min followed by washing with KHB. After either a 5 min or 90 min period of recovery, cell surface GLP-1R binding was assessed. GLP-1R binding was normalised to naïve cells **(B_{ii})**. **C.** Representative Ca^{2+} traces. HEK-GLP-1R cells were pre-incubated with or without 10 µM SM19712 for 30 min (which was then included throughout). Cells were then pre-treated with buffer (control) or 100 nM GLP-1 7-36 amide (pre-treatment) for 10 min followed by washing with KHB. After 90

min recovery, fluo-4-loaded cells were stimulated or re-stimulated with 10 nM GLP-1 7-36 amide (maximum concentration for GLP-1 7-36 amide-mediated Ca^{2+} response) and the changes in fluorescence were monitored and calibrated to $[Ca^{2+}]_i$. Responses were measured for 41 s with the injection at 11 s. **D.** The mean data of the maximum increase in $[Ca^{2+}]_i$ (nM) were generated. Data are representative or mean + S.E.M., $n \geq 3$. **, $p < 0.01$; ***, $p < 0.001$ (**B_i**. Bonferroni's test following two-way ANOVA; only the differences between groups at each time point are shown for clarity. **D.** Bonferroni's test following one-way ANOVA; only the difference in pre-treated cells is shown for clarity).

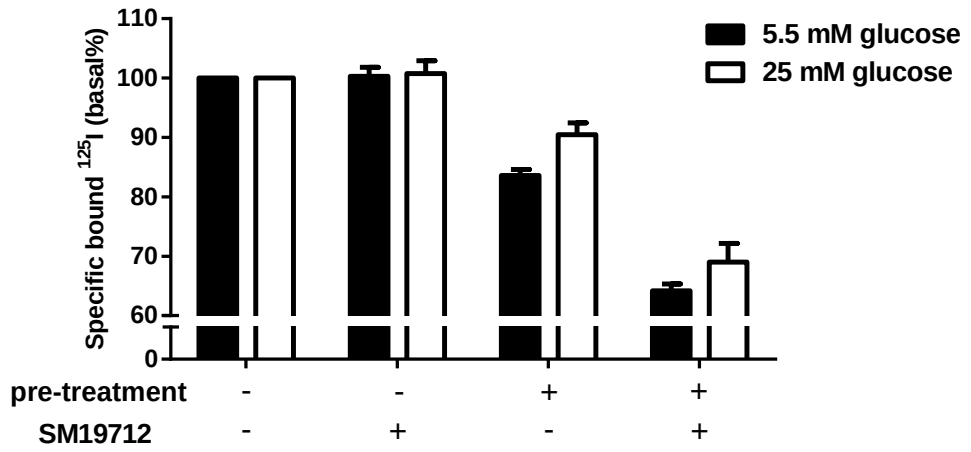

Fig 4.2.6.2. Effects of high glucose on cell-surface GLP-1R binding. HEK-GLP-1R cells were grown in low glucose medium (5.5 mM) for at least 7 days. Cells were then either cultured in the same medium (5.5 mM glucose) or exposed to high glucose medium (25 mM) for 48 h. On the day of assay, standard KHB containing 11.7 mM glucose was used throughout. Cells were pre-incubated with buffer with or without 10 μM SM19712 for 30 min (which was then included throughout). Cells were then challenged with buffer or 100 nM GLP-1 7-36 amide for 10 min followed by washing with KHB. After a 90 min period of recovery, the cell-surface GLP-1R binding was assessed. GLP-1R binding was normalised to basal (without pre-treatment). The data are mean + S.E.M., n = 3.

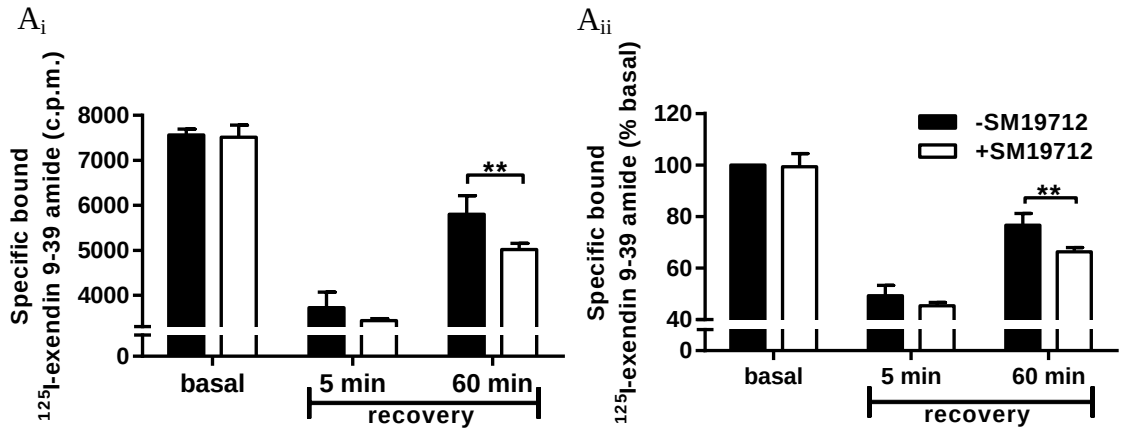

Fig 4.2.6.3. ECE-1 activity regulates the recovery of cell-surface GLP-1R binding in INS-1E cells. A_i. Cells were pre-incubated for 30 min without or with 10 μM SM19712 (which was then included throughout). Cells were then challenged with buffer (basal) or 100 nM GLP-1 7-36 amide for 10 min followed by washing with KHB. After a 5 min or 60 min period of recovery, cell-surface GLP-1R binding was assessed. **A_{ii}.** GLP-1R binding was normalised to basal. Data are mean + S.E.M., n = 3. **, $p < 0.01$ (Bonferroni's test following two-way ANOVA. Only the differences between groups at each time point are shown for clarity).

4.2.7. Sustained cAMP generation mediated by GLP-1 7-36 amide is regulated by ECE-1 in both HEK-GLP-1R and INS-1E cells.

In HEK-GLP-1R cells, in the absence of IBMX, treatment with 100 nM GLP-1 7-36 amide produced a time-dependent cAMP response which increased in the first 30 min and then slowly decreased **(Fig 4.2.7.1.A, Fig 4.2.7.2.A)**. However, in the presence of IBMX, 100 nM GLP-1 7-36 amide stimulated a marked cAMP response which was sustained for up to 60 min **(Fig 4.2.7.1.A)**. Dynasore inhibited the GLP-1 7-36 amide-stimulated cAMP response in the absence of IBMX whereas it promoted it in the presence of IBMX **(Fig 4.2.7.1.A)**. Nevertheless, the potentiation of the cAMP response by dynasore in the presence of IBMX was prevented by stimulating with and removal of GLP-1 7-36 amide **(Fig 4.2.7.1.B)**. In fact, under these conditions, dynasore prevented the continuous increase of cAMP level seen after washing **(Fig 4.2.7.1.B)**. Additionally, in the presence of IBMX, the endosomal acidification inhibitor, monensin, enhanced the 100 nM GLP-1 7-36 amide-evoked cAMP response at 60 min in the absence of dynasore without influencing the basal (0 min) or the initial stimulation (10 min). This effect was absent in the presence of dynasore **(Fig 4.2.7.1.C)**.

Treatment with SM19712 did not influence the time-course of the GLP-1 7-36 amide-mediated cAMP response **(Fig 4.2.7.2.A)**. Following removal of the extracellular GLP-1 7-36 amide after 10 min stimulation of HEK-GLP-1R cells in the absence of IBMX, cAMP production continued to increase during the next 10 min and then decreased such that at 60 min after washing, the response had decreased to ~75% of the level at 10 min stimulation. Treatment with SM19712 did not affect the response over the initial 10 min stimulation period but significantly enhanced the cAMP response following removal of the extracellular ligand **(Fig 4.2.7.2.B)**. Moreover, the reduced cAMP production after removal of ligand was also promoted by monensin without influencing the initial response **(Fig 4.2.7.1.D)**.

Similarly, in INS-1E cells, treatment with SM19712 did not influence the response of

naïve cells, but significantly enhanced the cAMP level at 60 min following removal of the extracellular ligand **(Fig 4.2.7.2.C)**.

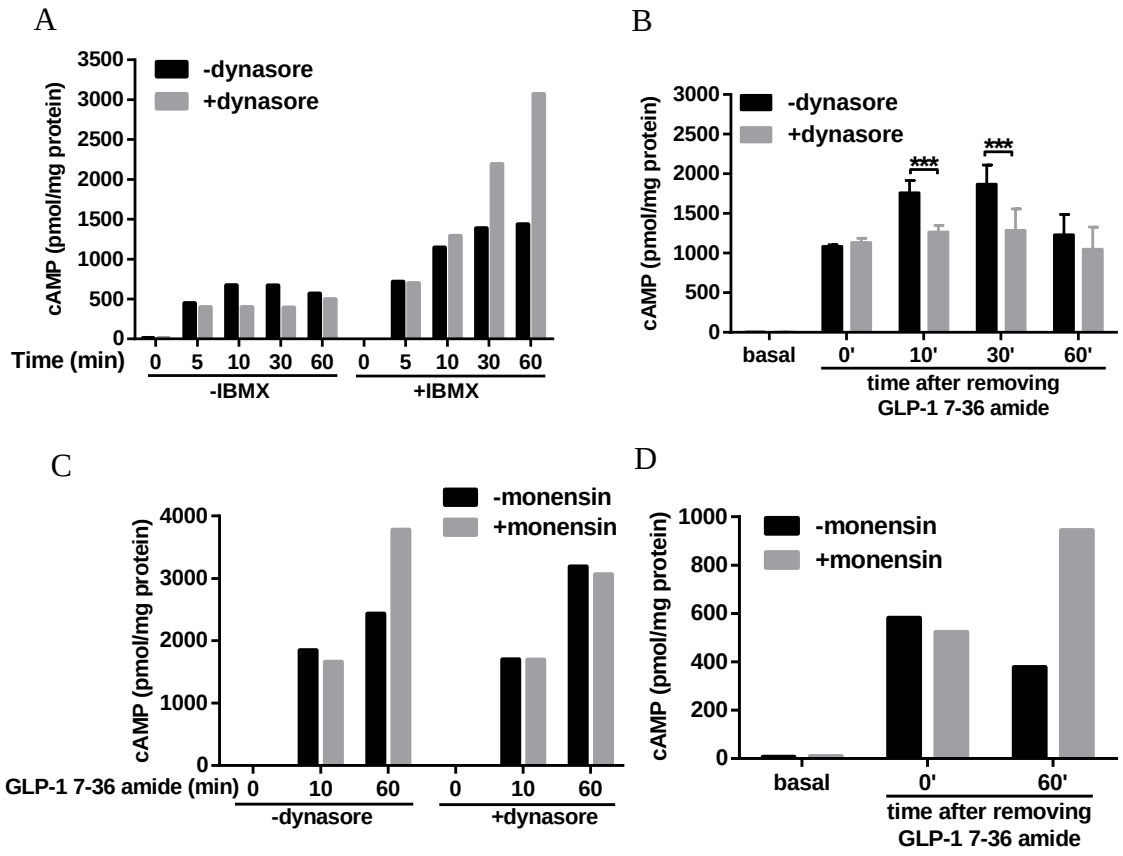

Fig 4.2.7.1. Effect of internalisation or endosomal acidification on GLP-1 7-36 amide-induced cAMP production. A. HEK-GLP-1R cells were pre-incubated without or with 80 μM dynasore for 30 min (which was then included throughout). Cells were then stimulated with 100 nM GLP-1 7-36 amide for the indicated times (0-60 min) in either the absence or presence of 500 μM IBMX. The cellular cAMP production was then determined. **B.** Cells pre-treated without or with 80 μM dynasore were challenged with buffer (basal) or 100 nM GLP-1 7-36 amide for 10 min in the presence of 500 μM IBMX followed by washing with acidified buffer (pH 4.0, 40 s). The cellular cAMP generation was then determined after 0-60 min incubation in KHB with IBMX (+/-dynasore as indicated). **C.** Cells were pre-incubated in KHB without or with 80 μM dynasore in either the absence or presence of 50 μM monensin for 30 min (which were then included throughout). Cells were then stimulated with buffer (0) or 100 nM GLP-1 7-36 amide for 10 or 60 min in the presence of 500 μM IBMX. The cellular cAMP production was then determined. **D.** Cells pretreated without or with 50 μM monensin for 30 min were challenged with buffer (basal) or 100 nM GLP-1 7-36 amide

(pre-treatment) for 10 min in the absence of 500 μM IBMX followed by washing with acidified buffer (pH 4.0, 40 s). After a 60 min period of recovery, the cellular cAMP level was determined. Data in B are n=3. ***, $p < 0.001$ (Bonferroni's test following two-way ANOVA. Only the differences between groups at each time point are shown for clarity). Other data are n=1.

A

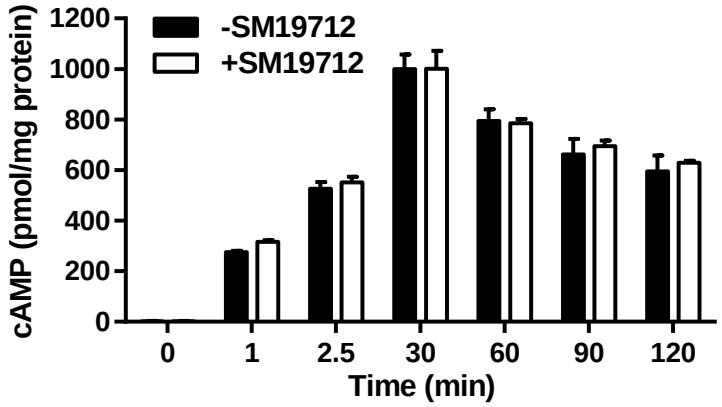
-SM19712
+SM19712
cAMP (pmol/mg protein)
1200
1000
800
600
400
200
0
0
1
2.5
30
60
90
120
Time (min)

B

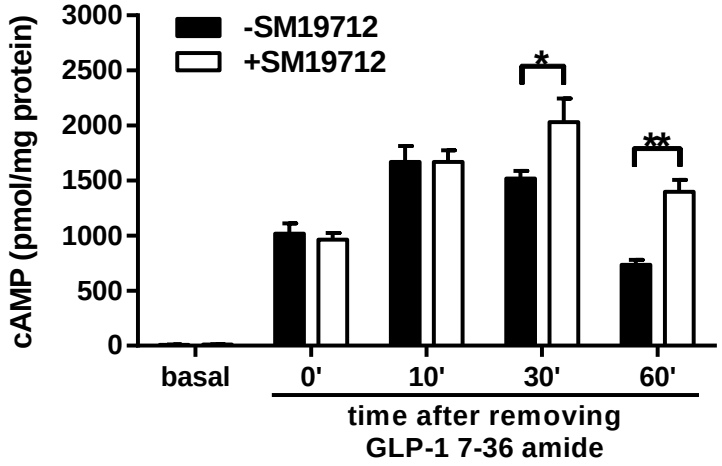
-SM19712
+SM19712
cAMP (pmol/mg protein)
3000
2500
2000
1500
1000
500
0
*
**
basal
0'
10'
30'
60'
time after removing
GLP-1 7-36 amide

C

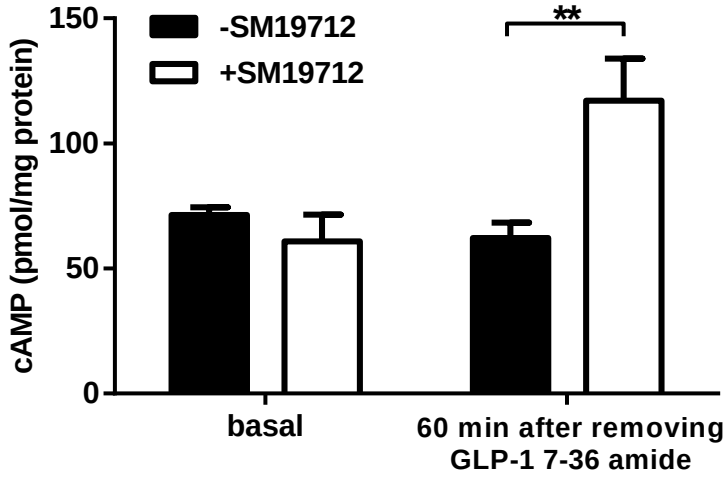
-SM19712
+SM19712
cAMP (pmol/mg protein)
150
100
50
0
**
basal
60 min after removing
GLP-1 7-36 amide

Fig 4.2.7.2. Sustained cAMP generation mediated by GLP-1 7-36 amide is regulated by ECE-1 activity. A. HEK-GLP-1R cells were pre-incubated without or with 10 μM SM19712 for 30 min (which was then included throughout). In the absence of IBMX, cells were stimulated with 100 nM GLP-1 7-36 amide for the required times (0-120 min) and cellular cAMP levels determined. **B**. HEK-GLP-1R cells, either pre-incubated with or without 10 μM SM19712, were challenged with buffer (basal) or 100 nM GLP-1 7-36 amide for 10 min in the absence of IBMX followed by washing with KHB to remove the extracellular ligand. After 0-60 min incubation (+/-SM19712), the reactions were stopped and the cellular cAMP determined. **C**. INS-1E cells were pre-incubated without or with 10 μM SM19712 for 30 min (which was then included throughout). In the absence of IBMX, the cells were stimulated with buffer (basal) or 100 nM GLP-1 7-36 amide for 10 min followed by washing with KHB. After a further 60 min incubation (+/- SM19712), the reactions were stopped and the cellular cAMP determined. All data are mean + S.E.M., $n \geq 3$. *, $p < 0.05$; **, $p < 0.01$ (Bonferroni's test following two-way ANOVA. Only the differences between groups at each time point are shown for clarity).

4.2.8. Sustained ERK activation mediated by GLP-1 7-36 amide is regulated by ECE-1 activity in both HEK-GLP-1R cells and INS-1E cells.

In HEK-GLP-1R cells, challenge with 10 nM GLP-1 7-36 amide evoked a rapid activation of ERK as determined by immunoblotting of pERK1/2. The response was maximal at 2 min and then decreased in the continued presence of agonist, returning to basal levels at 60 min. Treating the cells with SM19712 did not influence this time-course of 10 nM GLP-1 7-36 amide-mediated ERK activation **(Fig 4.2.8.1)**.

In an alternative protocol, cells were stimulated for 10 min with 10 nM GLP-1 7-36 amide, which was then removed by washing with KHB. In these circumstances, the level of pERK reduced following the wash but this reduction was significantly attenuated by SM19712 such that at 30 min, 60 min or 90 min after washing, the ERK activation in SM19712-treated cells was significantly higher than the control (without SM19712) **(Fig 4.2.8.2.)**.

In INS-1E cells, the pERK response evoked by 10 nM GLP-1 7-36 amide was more sustained than that in HEK-GLP-1R cells. A 5 min stimulation evoked a robust signal that slowly decreased over the subsequent 60 min **(Fig 4.2.8.3**) but was then relatively sustained even to 120 min **(Fig 4.2.8.4)**. Treating the cells with SM19712 did not influence the time-course of GLP-1 7-36 amide-mediated ERK activation **(Fig 4.2.8.4)**.

The sustained pERK response was prevented by removing the extracellular ligand after 10 min stimulation **(Fig 4.2.8.5.)**. Under these circumstances, the signal quickly decreased to basal levels. In cells treated with SM19712, the signal also decreased to basal levels after removing the extracellular ligand but increased again with prolonged incubation **(Fig 4.2.8.5.)**. At 90 min after washing, the ERK activation in the presence of SM19712 was significantly higher than that in the absence of SM19712 **(Fig 4.2.8.5.B)**.

A

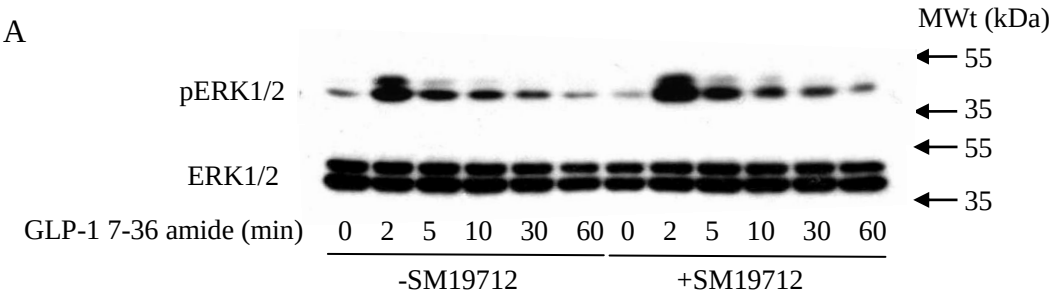

B

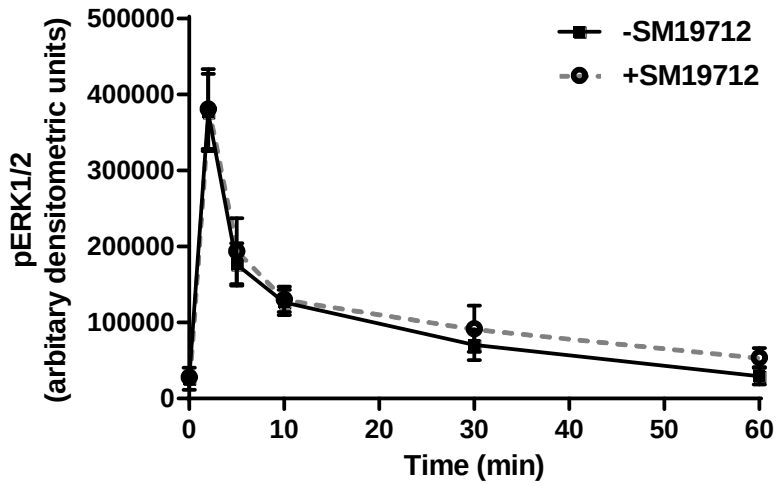

Fig 4.2.8.1. ECE-1 activity did not affect the time-course of GLP-1 7-36 amide-mediated ERK activation. HEK-GLP-1R cells were pre-incubated without or with 10 μM SM19712 for 30 min (which was then included throughout). Cells were then challenged with 10 nM GLP-1 7-36 amide for the required time (0-60 min). The expression of pERK1/2 was detected by immunoblotting. Total ERK1/2 was used as a loading control. Data are either representative **(A)** or mean ± S.E.M., n = 3 **(B)**.

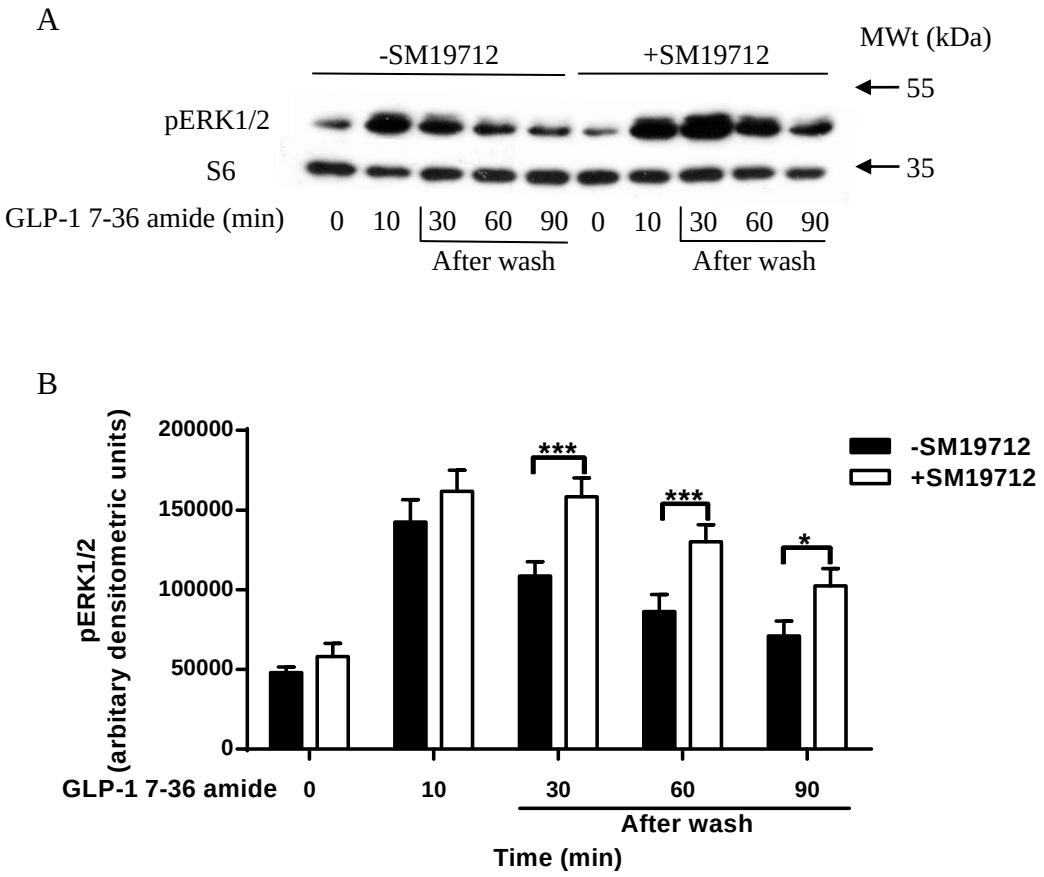

Fig 4.2.8.2. ECE-1 activity regulates the duration of ERK activation following removal of the extracellular ligand. Following pre-treatment with or without 10 μM SM19712 for 30 min (which was then included throughout), cells were challenged with buffer (0) or 10 nM GLP-1 7-36 amide for 10 min. The extracellular free ligand was then removed by washing with KHB. Cells were then incubated in buffer in the continued absence or presence of SM19712 as appropriate for the indicated times (0-90 min). The expression of pERK1/2 was then determined by immunoblotting. Ribosomal protein S6 was used as a loading control. Data are either representative **(A)** or mean + S.E.M., n = 4 **(B)**. *, $p < 0.05$; ***, $p < 0.05$ (Bonferroni's test following two-way ANOVA. Only the differences between the groups at each time point are shown for clarity).

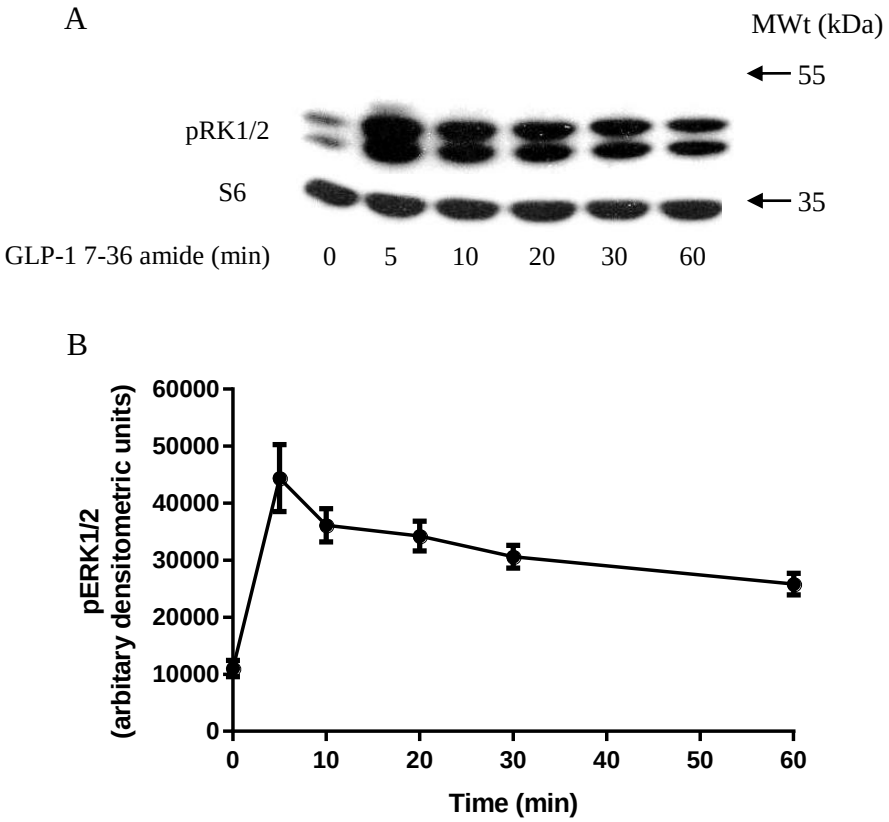

Fig 4.2.8.3. Time-course of GLP-1 7-36 amide-mediated ERK activation in INS-1E cells. Cells were pre-incubated in KHB for 120 min. Cells were then stimulated with 10 nM GLP-1 7-36 amide for the required times (0-60 min). The expression of pERK1/2 was determined by immunoblotting. S6 was used as a loading control. Data are either representative **(A)** or mean ± S.E.M., n = 3 **(B)**.

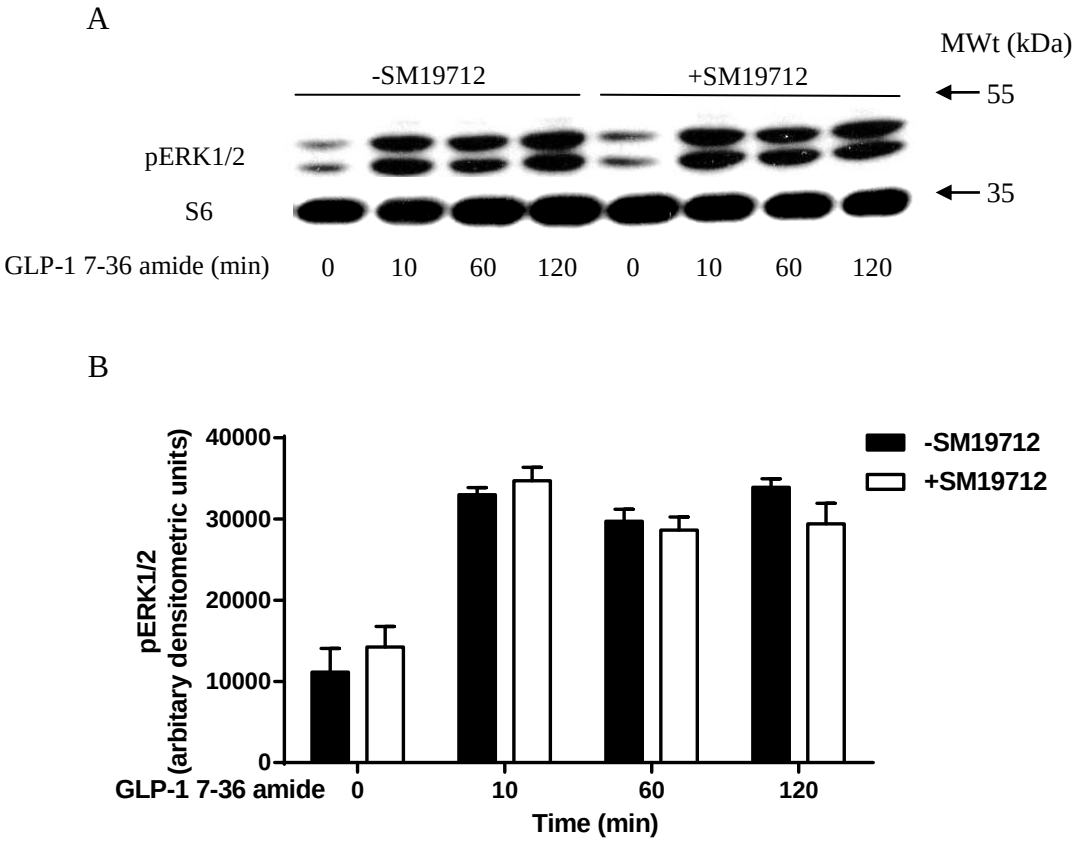

Fig 4.2.8.4. ECE-1 activity had no effect on the time course of 10 nM GLP-1 7-36 amide-induced ERK activation. INS-1E cells were pre-incubated in KHB for 90 min and then pre-treated with or without 10 μM SM19712 for another 30 min (which was then included throughout). Cells were challenged with 10 nM GLP-1 7-36 amide for the required times (0-120 min). The expression of pERK1/2 was then determined by immunoblotting. S6 was used as a loading control. Data are either representative **(A)** or mean + S.E.M., n = 3 **(B)**.

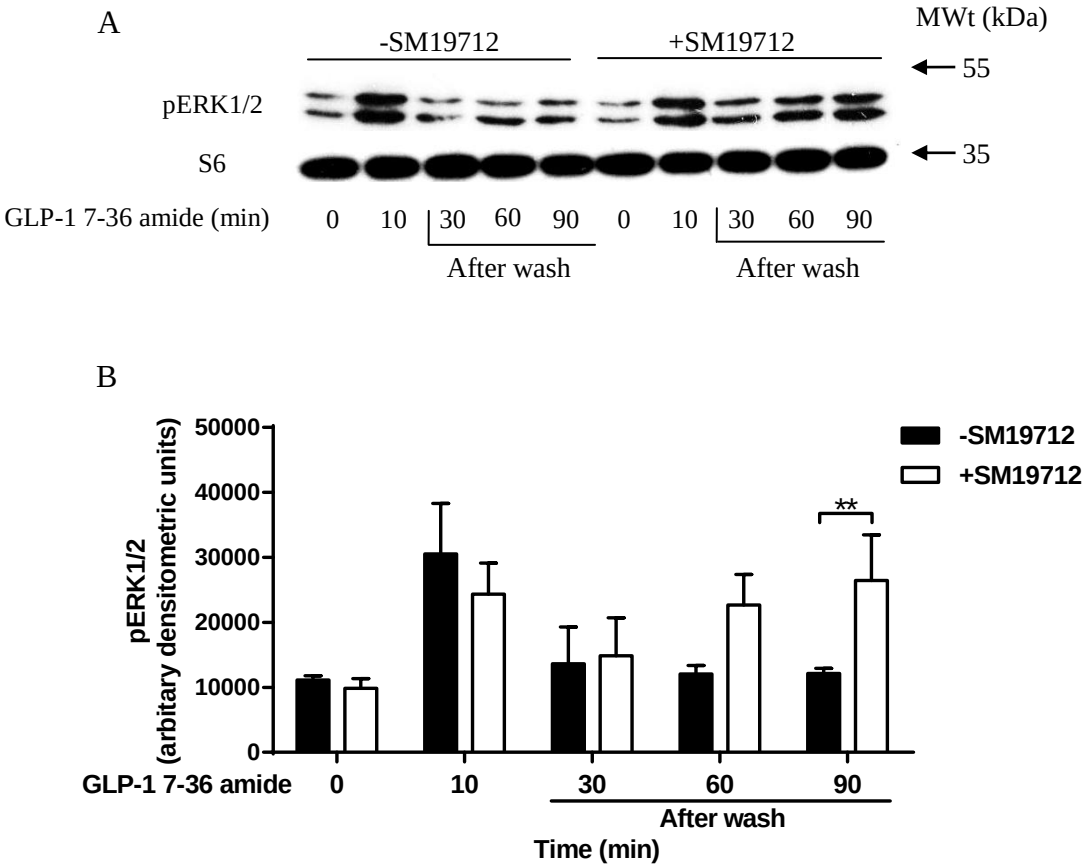

Fig 4.2.8.5. ECE-1 activity regulates ERK activation after removal of the extracellular ligand in INS-1E cells. Cells were pre-incubated in KHB for 90 min and then pre-treated with or without 10 μM SM19712 for 30 min (which was then included throughout). Cells were challenged with buffer (0) or 10 nM GLP-1 7-36 amide for 10 min followed by washing with KHB. After 30, 60 or 90 min incubation in buffer in the continued absence or presence of SM19712, the expression of pERK1/2 were detected by immunoblotting. S6 was used as a loading control. Data are either representative **(A)** or mean + S.E.M., n = 3 **(B)**. **, $p < 0.01$ (Bonferroni's test following two-way ANOVA. Only the differences between groups at each time point are shown for clarity).

4.2.9. GLP-1 7-36 amide-evoked ERK activation and sub-cellular distribution.

An immunostaining method was developed to detect both ERK activation and the sub-cellular distribution of activated ERK using HEK-GLP-1R cells **(Methods 2.10.)**. Images demonstrated that under basal conditions, pERK was present at low levels and distributed mainly in the cytoplasm **(Fig 4.2.9.1.)**. In cells stimulated with the activator of PKC, phorbol 12, 13-dibutyrate (100 nM; PDBu), for 5 min the increased intensity of fluorescence indicated an increased level of pERK. Under these conditions the fluorescence was equally distributed between the cytoplasm and nucleus. In cells stimulated with GLP-1 7-36 amide (10 nM, 5 min), levels of pERK were again elevated in both the cytoplasm and nucleus. However, in contrast to PDBu stimulation, following stimulation with GLP-1 7-36 amide the fluorescence was stronger in the cytosol compared to the nucleus. The background-corrected mean fluorescent intensity of either the whole cell, the cytoplasm or the nucleus and the ratio of background-corrected mean fluorescent intensity of cytoplasm to nucleus were generated. Quantification of the images demonstrated patterns of change that were consistent with the images **(Table 4.2.)**.

Using the same immunostaining method in INS-1E cells, pERK levels were shown to be low and mainly in the cytosol under basal conditions **(Fig 4.2.9.2.A)**. Addition of 10 nM GLP-1 7-36 amide activated ERK rapidly within 5 min and the response was sustained over 60 min **(Fig 4.2.9.2.A, B)**. Both cytosolic and nuclear pERK were increased in response to GLP-1 7-36 amide stimulation and the ratio of cytosolic fluorescence versus nuclear fluorescence declined in the first 20 min suggesting that the increase in the level of nuclear pERK was greater than that of cytosolic pERK during this time. The ratio was then sustained after 20 min **(Fig 4.2.9.2.C)**.

Following 10 min stimulation with 10 nM GLP-1 7-36 amide, extracellular ligand was removed and the cells were washed with KHB. At 90 min after removal of the ligand, the level of pERK and the sub-cellular distribution was returning to those seen under

basal conditions (0 min). Treatment with SM19712 did not affect the ERK activation and distribution under basal conditions or during the initial response (10 min). There was some evidence of enhanced ERK activation in both cytosol and nucleus at 90 min following removal of the ligand although this did not reach statistical significance **(Fig 4.2.9.3.)**.

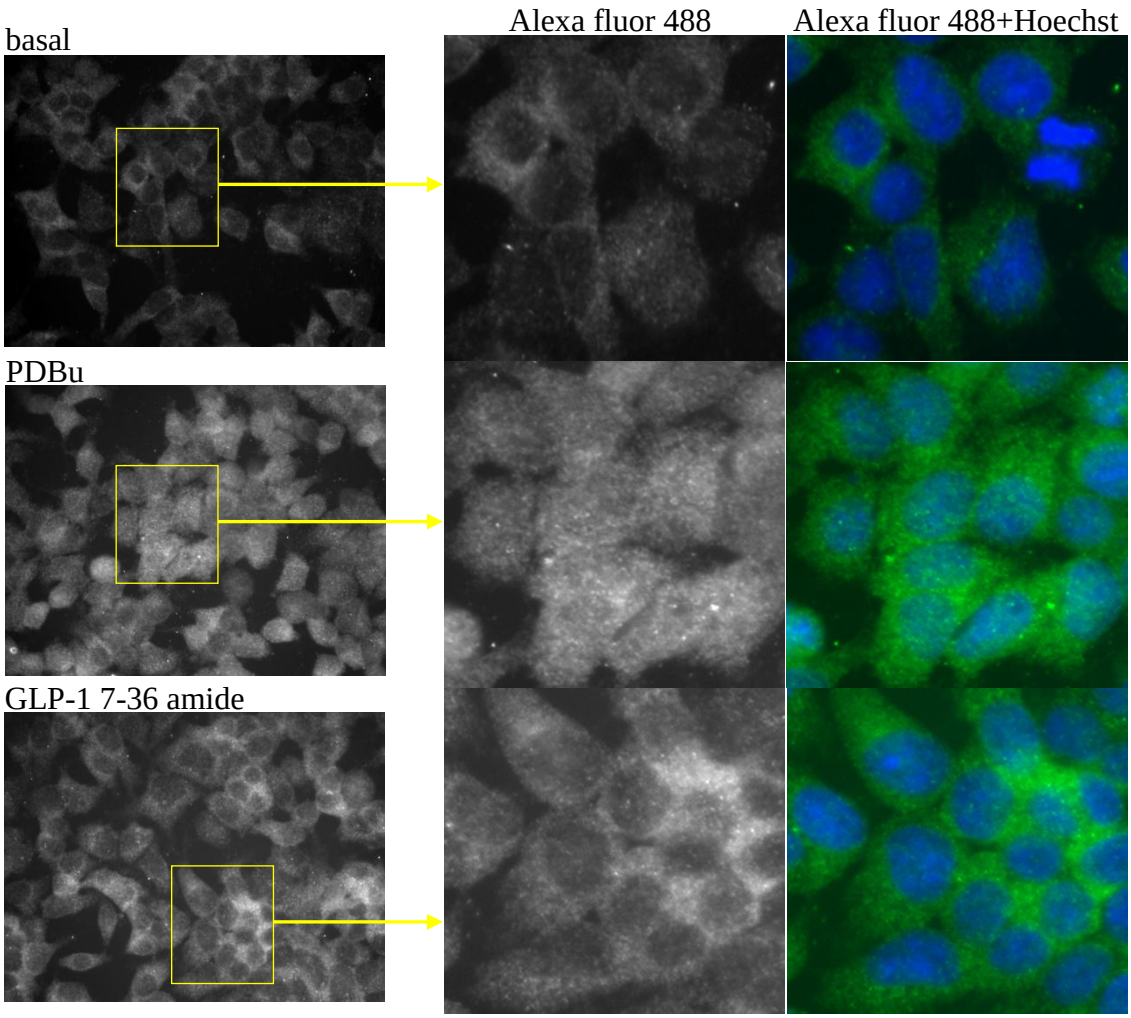

Fig 4.2.9.1. Immunostaining of pERK1/2. HEK-GLP-1R cells were challenged with buffer (basal), 100 nM PDBu or 10 nM GLP-1 7-36 amide for 5 min. Cells were fixed and permeabilized for immunostaining with a pERK1/2 antibody and nuclear staining with Hoechst as described in **Methods 2.10.1.**. Generally, 16 positions in each well (equal to at least 1,000 cells) were imaged, however only one representative image showing staining of pERK (Alexa fluor 488) alone or merged with nuclear staining (Alexa fluor 488 + Hoechst) and its distribution under each condition is presented here to directly compare the quantification alongside the image.

	Whole cell (FU)	Cytoplasm (FU)	Nucleus (FU)	Cytosolic/nuclear
Basal	**121 ± 4**	**138 ± 6**	**106 ± 5**	**1.40 ± 0.04**
PDBu	**241 ± 7**	**237 ± 6**	**247 ± 9**	**1.01 ± 0.03**
GLP-1 7-36 amide	**188 ± 7**	**220 ± 9**	**165 ± 8**	**1.47 ± 0.07**

Table 4.2. Analysis of images from immunostaining. These values were generated from the cells in the three representative images in **Fig 4.2.9.1** as described in **Methods 2.10.2..** The cell numbers are 75, 83 and 90 for basal, PDBu stimulation and GLP-1 7-36 amide stimulation respectively. The data show the mean fluorescent intensity of the whole cell, the cytoplasm, the nucleus and the ratio of cytoplasmic to nuclear fluorescence (cytosolic/nuclear). FU = fluorescence units. Data are mean ± S.E.M.

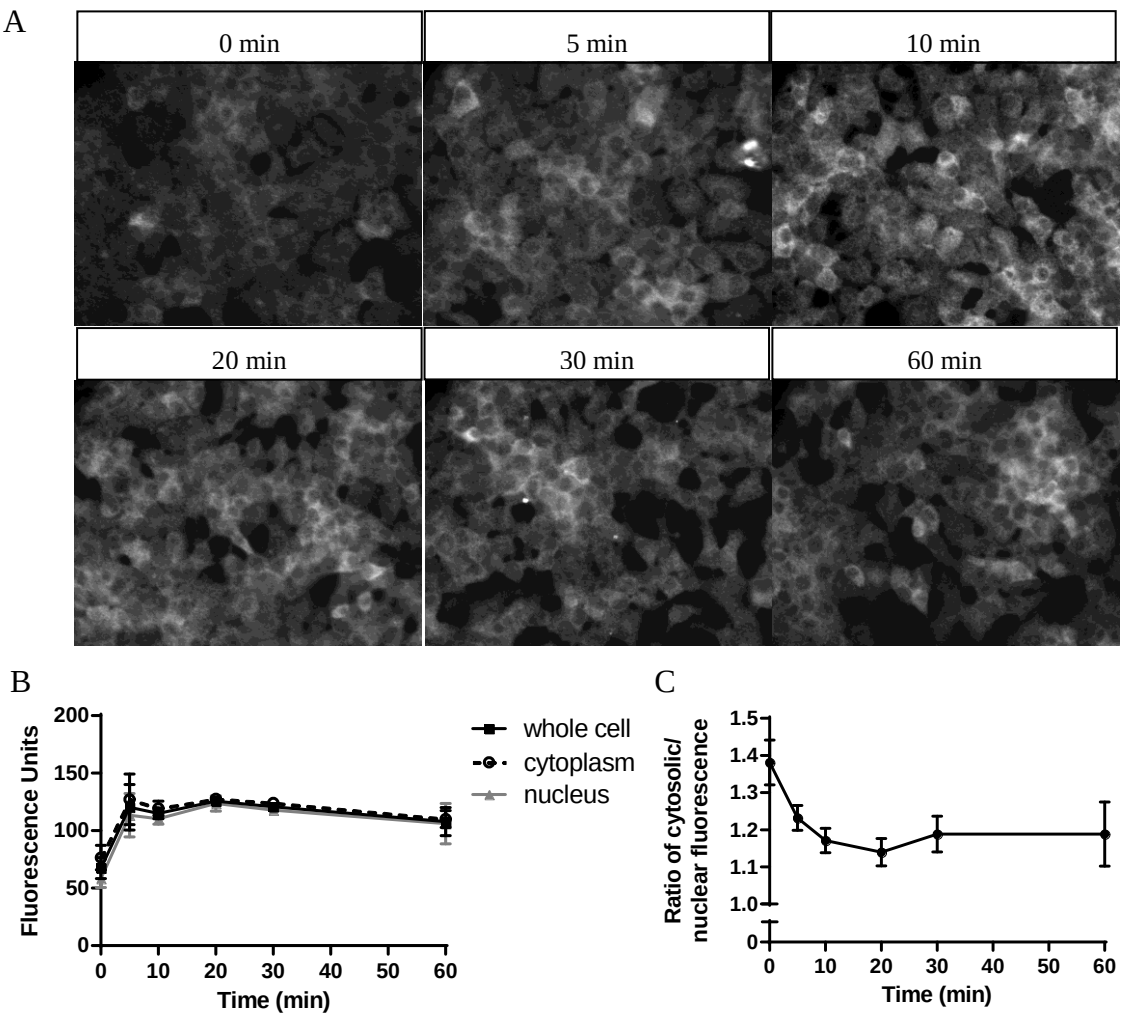

Fig 4.2.9.2. GLP-1 7-36 amide-evoked ERK activation in INS-1E cells determined by immunostaining. Cells were pre-incubated with KHB for 120 min and then stimulated with 10 nM GLP-1 7-36 amide for the required times (0-60 min). The cells were then fixed and permeabilized for immunostaining with a pERK1/2 antibody and nuclear staining with Hoechst as described in **Methods 2.10.**. **A**. Representative images from a single experiment. **B.** The background-corrected mean fluorescent intensity of either the whole cell, the cytoplasm or the nucleus were generated. **C.** The ratio of background-corrected mean fluorescent intensity of cytoplasm to nucleus. Data are either representative or mean ± S.E.M., n = 3 (with a total of at least 1,000 cells from 16 images/well for each condition in each of three independent experiments).

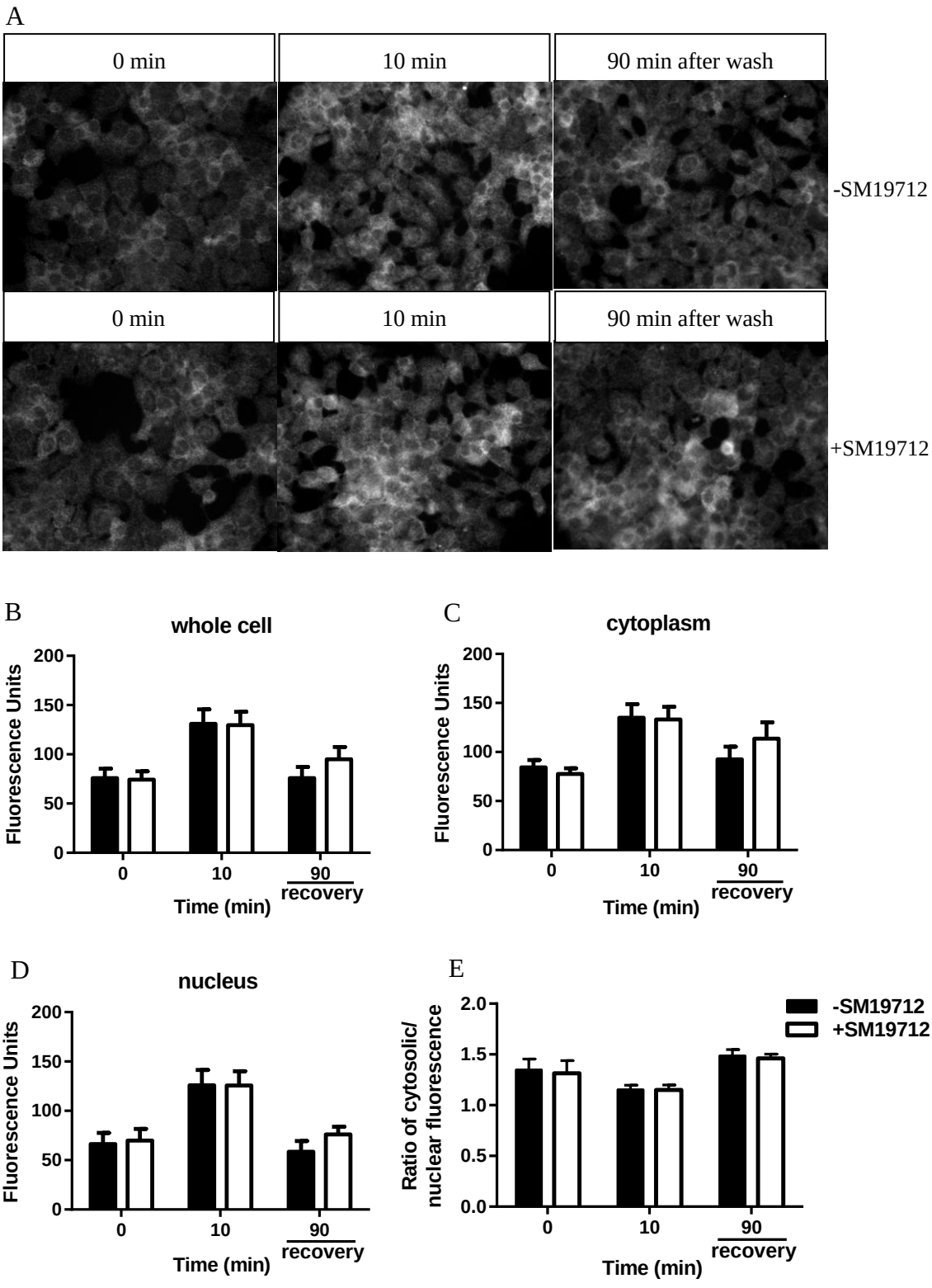
A
0 min
10 min
90 min after wash
-SM19712
0 min
10 min
90 min after wash
+SM19712
B
whole cell
Fluorescence Units
200
150
100
50
0
0
10
90
recovery
Time (min)
C
cytoplasm
Fluorescence Units
200
150
100
50
0
0
10
90
recovery
Time (min)
D
nucleus
Fluorescence Units
200
150
100
50
0
0
10
90
recovery
Time (min)
E
Ratio of cytosolic/
nuclear fluorescence
2.0
1.5
1.0
0.5
0.0
0
10
90
recovery
Time (min)
-SM19712
+SM19712

Fig 4.2.9.3. The impact of ECE-1 activity on GLP-1R-mediated ERK activation and sub-cellular distribution following ligand removal. INS-1E cells were pre-incubated with KHB for 90 min and then pre-treated with or without 10 μM SM19712 for another 30 min (which was then included throughout). Cells were then stimulated with 10 nM GLP-1 7-36 amide for 10 min prior to immunostaining of pERK or alternatively the ligand was removed after 10 min stimulation and the cells incubated for a further 90 min (+/-SM19712) prior to immunostaining for pERK. The fixation and permeabilization of cells for immunostaining with a pERK1/2 antibody and nuclear staining with Hoechst was as described in **Methods 2.10.**. **A**. Representative images from a single experiment. The background-corrected mean fluorescent intensity of either the whole cell (**B**), the cytoplasm (**C**) or nucleus (**D**) were generated. **E.** The ratio of background-corrected mean fluorescent intensity of the cytosolic to nuclear fluorescence was generated. Data are either representative or mean + S.E.M., n = 3 (with a total of at least 1,000 cells from 16 images/well for each condition in each of three independent experiments).

4.3. Discussion

Data presented in this chapter demonstrate that ECE-1 activity regulates re-sensitisation of GLP-1R-mediated signalling and aspects of GLP-1R-dependent signalling in both HEK-GLP-1R cells and INS-1E cells. Previous work has demonstrated that ECE-1 activity is responsible for the endosomal degradation of, for example, substance P (Roosterman et al., 2007) and the present data suggest that such endosomal processing of other peptide ligands may also occur. It is possible therefore that endosomal ECE-1 degrades GLP-1 7-36 amide that has internalised bound to the GLP-1R and that this facilitates the disassociation of the receptor-β-arrestin complex promoting GLP-1R recycling to the plasma membrane **(Fig 4.3.)**. The accepted model of receptor trafficking **(Fig 1.5.)** would suggest that following internalisation, the newly formed endosomal compartment undergoes acidification over a period of ~10 min (Mellman et al., 1986). This acidification to a pH of approximately 5.5 (Zen et al., 1992) is thought to promote dissociation of the ligand from the receptor and this may expose the ligand to endosomally-located proteases, particularly ECE-1. The subsequent degradation of the ligand would prevent any re-association and presumably allow the receptor to adopt a conformation that causes disassociation of the receptor-β-arrestin complex, receptor de-phosphorylation and the events required for recycling. As arrestin provides a scaffold for proteins involved in some aspects of G protein-independent signalling, including ERK activation (Lefkowitz and Shenoy, 2005), it is possible that the reduction in ERK activation seen in the presence of the ECE-1 inhibitor, SM19712, results from a reduced stability of the GLP-1R-β-arrestin complex. In addition, our data suggest ECE-1 activity also enhanced GLP-1R-mediated cAMP generation.

4.3.1. ECE-1 activity regulates GLP-1R recycling and re-sensitisation.

Work described in the previous chapter suggested that receptor recycling following internalisation is responsible for GLP-1R re-sensitisation. GLP-1 co-internalises with the receptor as a complex targeting to endosomes where the pH is around 5.5 (Mellman

et al., 1986). The acidic pH optimum in endosomes will change the charges and their distribution on amino acids leading to conformational changes of the peptide ligand and/or the receptor thereby facilitating the disassociation of ligand-receptor complex (Mellman et al., 1986). The efficiency of disassociation in endosomes has been suggested to be enhanced by the endosomal protease, ECE-1, which can cleave some peptides such as SP and CGRP in the endosomes (Roosterman et al., 2007, Padilla et al., 2007). Given there is no direct interaction between ECE-1c and CLR/RAMP1, the receptor for CGRP, (Padilla et al., 2007), ECE-1 may degrade receptor-disassociated peptide induced by the acidified conditions in the endosomes. Notably, another metalloendopeptidase, endopeptidase 24.15, interacts with the C-terminal tails of the AT_1 and bradykinin B_2 receptors at the plasma membrane and after receptor endocytosis (Shivakumar et al., 2005), implying the possibility of degradation of receptor-associated peptide by endopeptidase or at least placing the enzyme in close proximity to the ligand when it dissociates from the receptor. Alternatively, it is possible that ECE-1 is scaffolded in the vicinity of the receptor rather than directly interacting with it. Data in the present study demonstrated that removing bound ligand by an acid wash enhanced the rate of GLP-1R re-sensitisation **(Fig 4.2.1.)**. These data highlight that the presence of ligand influences GLP-1R re-sensitisation, potentially by influencing receptor recycling. Such acid washing of cells to remove bound ligand has been used in many studies to remove cell-surface bound ligand (Widmann et al., 1997, Haugh et al., 1999, Li et al., 2008) but it is unclear if the plasma membrane receptors from which ligand has been removed subsequently internalise. Evidence shows that the time constant of receptor re-sensitisation is slower than that of ligand disassociation (Chang et al., 2002) implying that the desensitised receptor remains phosphorylated even after the disassociation of agonist. It is possible therefore that receptors from which ligand has been removed still undergo internalisation. In the current experiments, some internalisation would have already occurred after pre-treatment (10 min) and the proportion of endocytosed receptors without ligand bound compared to those with ligand bound is unclear.

Inhibition of either endosomal acidification or ECE-1 markedly reduced re-sensitisation of GLP-1R-mediated cAMP generation or Ca^{2+} mobilization **(Fig 4.2.2.1. and Fig 4.2.2.5.)** highlighting that endosomal ECE-1 may regulate GLP-1R re-sensitisation by regulating receptor recycling. Given the localization of ECE-1 is at the plasma membrane and within intracellular compartments including the endosomes **(Fig 4.2.4.2.)** (Schweizer et al., 1997, Azarani et al., 1998, Valdenaire et al., 1999, Muller et al., 2003), there are at least two possible mechanisms that could explain the inhibition of GLP-1R re-sensitisation by the ECE-1 inhibitor. Firstly, cell-surface ECE-1 could degrade extracellular GLP-1 7-36 amide leading to a reduction of ligand concentration in the extracellular fluid. This might be expected to result in a greater desensitisation in the presence of SM19712 (as opposed to a reduction in re-sensitisation). If this were the case, we would also expect that addition of the ECE-1 inhibitor after the initial stimulation and ligand removal (ie. added only during the recovery period) would not have any effect. However, when the inhibitor was added after removal of the extracellular ligand the inhibition of GLP-1R re-sensitisation was equal to that seen when applying the inhibitor before pre-treatment (and remaining present in the recovery period) **(Fig 4.2.2.1)**. These observations suggest that it is the intracellular processing of ligand that may regulate GLP-1R re-sensitisation. The acidic pH in endosomes should promote GLP-1 disassociation from the receptor **(see above)** which may then provide accessibility for the degradation by endosomally located ECE-1 although the possibility of degradation of bound ligand cannot be excluded **(see above)**. The degradation of ligand by ECE-1 would prevent ligand-receptor re-association leading to conformational change of the receptor and the uncoupling of β-arrestin to allow GLP-1R recycling to the cell surface for a new cycle of activation. To further support this model, an *in vitro* assay of GLP-1 7-36 amide degradation by ECE-1 (and particularly the impact of pH) is currently being conducted in our laboratory. Preliminary data highlight that GLP-1 is certainly a substrate for recombinant human ECE-1 *in vitro* (data not shown). Whether ECE-1 activity facilitates the disassociation of the receptor-β-arrestin complex is worthy of investigation.

The data presented here also suggest that the different sensitivities of ligands to endosomal proteolysis could play an important role in determining the process of receptor re-sensitisation. Exendin-4 induced efficient desensitisation of the GLP-1R but recovery was slow and unaffected by inhibition of ECE-1. Although exendin-4 shares ~50% homology with GLP-1, it is used as a therapy in type 2 diabetes due to its insensitivity to DPP-IV which cleaves GLP-1 7-36 amide to an inactive form, GLP-1 9-36 amide (Hansen et al., 1999, Sinclair and Drucker, 2005). It is possible that within the endosome, exendin-4 may also not be a substrate for ECE-1. However, it is worthy of note that the role of ECE-1 in regulating receptor recycling and re-sensitisation may not only be ligand specific, but also concentration-dependent. For example, corticotropin-releasing factor (CRF) and urocortin 1 (Ucn1) are agonists for CRF_1 and are also both substrates for ECE-1. However, ECE-1 regulates Ucn1-induced CRF_1 recycling and re-sensitisation independent of the concentration of agonist whereas it influences CRF-induced CRF_1 trafficking at near K_D concentration but not at the higher concentration (Hasdemir et al., 2012). Given that the mechanisms of receptor endocytosis and post-endocytic trafficking are dependent on the concentration of ligand **(see Chapter 3 Discussion)**, it is possible that high concentrations of agonist result in receptor trafficking through a different route where ECE-1 is not present or alternatively another protease(s) play(s) a more prominent role in degradation. Evidence has suggested that the high concentration of CRF triggers receptor trafficking through a Rab11-associated pathway whereas it is unclear for the low concentration (Hasdemir et al., 2012). Notably, ECE-1 cleaves Ucn1 at critical residues which are responsible for ligand-receptor binding whereas the cleavage product(s) of CRF retain(s) high affinity for the receptor (Hasdemir et al., 2012). There is also the possibility that when one or more of the proteolytic products has a reduced affinity for binding to the receptor, proteolysis of the released peptide-ligand from the receptor induced by the acidic pH in endosomes prevents the re-association thereby facilitating the disassociation rate and promoting recycling. By contrast, if the product retains high affinity for the receptor, ligand proteolysis in endosomes would have less impact on preventing ligand-receptor interaction and inhibition of proteolysis may, therefore, have little or no effect on either

recycling or re-sensitisation. This indicates the importance of determining the ECE-1 cleavage site(s) within peptides and developing an understanding of their pharmacology.

4.3.2. Potential trafficking of ECE-1 upon activation of the GLP-1R.

ECE-1 isoforms have been found to constitutively internalise from the plasma membrane to the endosomes in a dynamin-dependent mechanism and recycle with kinetics that is distinct among the isoforms. Under basal conditions, although ECE-1c internalises to a greater extent than ECE-1b and d, it also rapidly recycles to the cell surface (Muller et al., 2003). Data for ECE-1a are not available. Given that ECE-1 is also constitutively phosphorylated by intracellular kinases such as CK-I, PKA and PKC in a isoform-selective manner (MacLeod et al., 2002, Smith et al., 2006, Jafri and Ergul, 2006) **(see General Introduction 1.8.3.1.)** and the phosphorylation of ECE-1 has been shown to influence its expression and trafficking (Keynan et al., 2004, Kuruppu et al., 2010, Kuruppu and Smith, 2012, Jafri and Ergul, 2006) **(see General Introduction 1.8.3.2. and 1.8.4.1.)**, it is possible that the different rates of endocytosis and recycling amongst the ECE-1 isoforms is regulated by such isoform-specific phosphorylation and dephosphorylation. It is possible therefore that receptor activation and the subsequent activation of various kinases could phosphorylate ECE-1 thereby influencing its expression, distribution and even function. So far, there is no evidence regarding potential ligand-induced phosphorylation of ECE-1.

Evidence has showed that, at least for ECE-1c, addition of a GFP tag at the N-terminus prevents phosphorylation of ECE-1 by PKC whereas addition at the C-terminus reduces its catalytic activity (Kuruppu et al., 2013). Therefore, epitope tagging ECE-1 has the potential to alter its distribution and/or function. Previous studies that have examined the sub-cellular distribution of N-terminal GFP-tagged ECE-1 isoforms have shown that GFP-ECE-1a and GFP-ECE-1c are predominantly located at the plasma membrane with low expression within the cytosol. In contrast, GFP-ECE-1b and GFP-ECE-1d mainly reside in the cytoplasm with low expression at the cell surface (Roosterman et al., 2007, Padilla et al., 2007). As the various ECE-1 isoforms differ in their N-termini and it is

thought to be these differences that account for the different sub-cellular distributions (Kuruppu et al., 2012), C-terminal mCherry-tagged versions of ECE-1 isoforms were generated in the present study. Overexpression of each isoform promoted GLP-1R re-sensitisation in the same way as the wild-type ECE-1 isoforms **(Table 4.1.)** suggesting no loss of function. This was supported by the abolition of the enhanced recovery by the ECE-1 inhibitor, SM-19712. Both ECE-1b-mCherry and ECE-1d-mCherry isoforms showed similar distributions to those reported for the N-terminal GFP-tagged versions **(Fig 4.2.5.1.)**. However, the cell-surface expression of ECE-1a-mCherry and ECE-1c-mCherry was not as strong as that suggested for the N-terminal GFP-tagged versions which is consistent with the previous study comparing the distribution of GFP-ECE-1c and ECE-1c-GFP (Kuruppu et al., 2013). It is possible that either the GFP or mCherry tag at either the C-terminus or N-terminus of ECE-1 could enhance or reduce exposure of phosphorylation sites and that this could influence the phosphorylation state even under basal conditions. This could result in different trafficking and therefore different sub-cellular localization. The HA-tagged ECE-1 isoforms have been generated in our laboratory and these could be useful in determining sub-cellular distribution by immunocytochemistry because the HA tag is considerably smaller than the fluorescent tags which should have less impact on the structure of ECE-1.

Interestingly, in response to GLP-1 7-36 amide stimulation ECE-1 especially isoform a and c re-distribute within the cell and aggregate into large patches within the cytosol **(Fig 4.2.5.1. and Fig 4.2.5.2.)**. These patches are consistent with the localization of the internalised GLP-1R. It has been suggested that ECE-1 constitutively internalises and traffics with the ligand-receptor complex into the same endosomes for CLR and CRF_1 (Padilla et al., 2007, Hasdemir et al., 2012). However, the reduction of cell-surface ECE-1c in response to CGRP stimulation was equal to the loss of cell-surface ECE-1c without ligand stimulation quantified by flow cytometry (Padilla et al., 2007). In our study, the C-terminal mCherry-tagged versions of ECE-1 did not show much cell-surface distribution which leads to the difficulty to monitor the reduction of

cell-surface ECE-1 by confocal microscopy. ECE-1 isoforms did traffic quickly between the plasma membrane and cytoplasm under basal condition without accumulating into patches in the cytosol. Given that the endocytosis of both GLP-1R and ECE-1 are through dynamin-dependent mechanisms, it is likely that in response to receptor activation, the plasma membrane invaginates and is pinched off by dynamin to form a vesicle that contains both GLP-1R and ECE-1, thereby targeting them to the same intracellular compartments. The loss of cell-surface ECE-1 could then be replenished by recycling of ECE-1 therefore producing the appearance that ECE-1 aggregates into large patches within the cytosol consistent with the localization of internalised GLP-1R. The possibility that GLP-1R activation facilitates the trafficking of ECE-1 from the plasma membrane to the endosomes requires further investigation. As suggested before, ECE-1 could be phosphorylated by kinases such as PKA and PKC that may also regulate trafficking. Given that the activation of GLP-1R activates PKA (Doyle and Egan, 2007), it is possible that the activation of GLP-1R could trigger the phosphorylation of ECE-1 isoforms therefore leading to regulation of its trafficking and function. These aspects require further investigation.

Exploring the trafficking of ECE-1 is of great importance. Notably, the catalytic ability of ECE-1 is not only substrate specific but also pH dependent **(see General Introduction 1.8.5.)**. The initial possible site of interaction between ECE-1 and peptides at the plasma membrane may have little or no effect where the enzyme has an acidic pH optimum for interaction and proteolysis. However, if the hypothesized model is true, when ECE-1 internalises with the ligand-receptor complex, resulting in trafficking into the same endosome, subsequent acidification will allow proteolysis of the peptide and limit endosomal signalling particularly through β-arrestin **(see below)**. This might be a critical physiological mechanism to limit signalling from the endocytosed receptors without influencing the cellular effects conducted from the plasma membrane.

4.3.3. ECE-1 regulates GLP-1R-mediated signalling.

It has been reported that ECE-1 cleaves SP in endosomes thereby facilitating the disassociation of the ligand-receptor complex. This releases β-arrestin from the receptor thereby terminating β-arrestin-dependent ERK activation (Roosterman et al., 2007). The recruitment of β-arrestin1/2 to the GLP-1R in response to GLP-1 stimulation has been demonstrated (Sonoda et al., 2008, Wootten et al., 2013). The coupling of β-arrestin1 mediates GLP-1R signalling during endocytosis and is responsible for insulin secretion and β-cell growth and survival (Sonoda et al., 2008, Quoyer et al., 2010, Talbot et al., 2012). In the present study, data show that in addition to regulating GLP-1R recycling and re-sensitisation, ECE-1 also regulates GLP-1R-mediated cAMP generation and ERK activation. It is possible that these are through a β-arrestin-dependent mechanism although this remains to be fully established **(see further direction)**.

In the present study, the effect of ECE-1 on GLP-1-stimulated ERK activation is absent when the ligand is continuously present **(Fig 4.2.8.4.)**. The prolonged activation of ERK in the continuous presence of GLP-1 is prevented by ligand removal **(Fig 4.2.8.5.)** implying that the recycled receptors might be re-activated and conduct G protein-dependent ERK activation when ligand is continuously present. However, when ligand has been removed this may not be possible and continued signalling would be entirely dependent on the existing ligand-receptor interactions. Signalling may be short-lived as the ligand-receptor-β-arrestin complexes disassociate. However, under these circumstances, inhibition of ECE-1 may hold receptors in endosomes, thereby enhancing any β-arrestin-dependent ERK activation. Thus, data showed that ECE-1 activity reduced ERK1/2 activation when GLP-1 7-36 amide was added but then removed indicating that ECE-1 regulates GLP-1R-mediated ERK1/2 activation, possibly through a G protein-independent but β-arrestin dependent manner. The mechanism could be that ECE-1 cleaves GLP-1 in the endosomes facilitating the disassociation of ligand-receptor complex which reduces the binding of β-arrestin thereby preventing its scaffolding function, specifically the recruitment of components

of the MAPK signalling pathway **(Fig 4.3.)**. Furthermore, the present data also provide some evidence that suggests ECE-1 regulates the extent of both cytoplasmic and nuclear ERK activation **(Fig 4.2.9.3.)**. However, in the present study the immunofluorescence experiments had relatively low sensitivity compared to immunoblotting and this may limit the ability to precisely define the sub-cellular distribution of pERK.

In the classic model of GPCR activation, the cAMP response is considered to arise as a consequence of signalling conducted from the plasma membrane which is terminated by receptor phosphorylation and β-arrestin binding which uncouples the G protein from the receptor (Lohse et al., 1990, Pippig et al., 1993). Subsequent to this PDE can be recruited to degrade cAMP at the plasma membrane (Perry et al., 2002). However, there is a growing appreciation that such signalling may arise from internalised receptors, most likely from the endosomal compartment. This has been suggested for the cAMP generation in response to activation of the thyroid-stimulating hormone (TSH) receptor, PTHR and D_1R (Calebiro et al., 2009, Ferrandon et al., 2009, Kotowski et al., 2011). The molecular mechanism suggested for PTHR is that apart from directing internalisation, the receptor-associated β-arrestin recruits Gβγ dimers upon PTH exposure, which in turn facilitates the activation of $G\alpha_s$ and stabilizes the active form of $G\alpha_s$ leading to a prolonged cAMP generation (Wehbi et al., 2013). This provides a novel model of GPCR activation. The persistent cAMP is thought to be responsible for the prolonged PTHR-mediated physiological calcemic and phosphate responses *in vivo* (Wehbi et al., 2013). In the present study, GLP-1R rapidly internalises in response to GLP-1 stimulation but there is a persistent cAMP generation in the absence of PDE inhibitor in HEK-GLP-1R cells. This persistent response is blocked by the inhibition of internalisation, consistent with a previous study in BRIN-BD11 cells (Kuna et al., 2013), and potentiated by the inhibition of endosomal acidification **(Fig 4.2.7.1.)**. Moreover, prolonged GLP-1R-mediated cAMP generation is reportedly β-arrestin1-dependent and the internalised GLP-1-GLP-1R complex has been shown to co-localize with AC (Sonoda et al., 2008, Kuna et al., 2013). Taken together, these data suggest a prolonged interaction between the endocytosed GLP-1R and G_s and it is possible that this is

through association with β-arrestin. Persistent cAMP generation by the GLP-1R is responsible for insulin secretion in pancreatic β-cells (Kuna et al., 2013) and such regulation of signalling could be essential for the anti-diabetic effects of GLP-1R activation. The present data highlight that the cAMP response may also be regulated by ECE-1 activity. By cleaving the peptide in endosomes, ECE-1 may reduce the stability of the receptor-β-arrestin complex, leading to disassociation of the G protein from the complex and thereby terminating prolonged cAMP generation. This model clearly remains to be further proven. Also whether ECE-1 regulates GLP-1-induced insulin secretion is worthy of exploration.

4.3.4. Increased levels of ECE-1 expression at high glucose concentrations could impact on GLP-1R signalling in diabetes.

Both previous work (Keynan et al., 2004) and the present study demonstrate that high glucose concentrations increase ECE-1 expression levels **(Fig 4.2.3.1.)**. Although so far, there are no *in vivo* studies showing that ECE-1 levels increase under hyperglycemic conditions, there is evidence indicating that the level of ET-1, which is the product of ECE-1 cleavage of big ET, is elevated in hyperglycemia rats (Kuwaki et al., 1990). It is possible therefore that increased levels of ECE-1 under hyperglycemia may result in abnormal signalling and trafficking of the GLP-1R and also other peptidergic receptors where ECE-1-dependent degradation of the ligand plays an important regulatory role. Indeed, the present data show that both GLP-1R recycling and re-sensitisation are potentiated under high glucose conditions **(Fig 4.2.6.2. and Fig 4.2.3.2.)**. Given that ECE-1 regulates both GLP-1R-mediated cAMP generation and ERK activation and these two signalling pathways play critical roles in GLP-1R-mediated insulin secretion and β-cell growth and survival, an impaired insulin secretion and a reduced β-cell mass associated with the progress of type 2 diabetes might be related to altered signalling of the GLP-1R under hyperglycemia as a consequence of elevated expression of ECE-1. If this is true, regulation of ECE-1 expression or activity might be beneficial in type 2 diabetes.

Due to the short half-life of GLP-1 and the problems associated with injection, many pharmaceutical companies are focusing on the development of small-molecule and orally active agonists for the GLP-1R. Given that even peptide ligands show distinct sensitivity to ECE-1 inhibition, it is possible that the use of such small-molecules could result in different time-courses or routes of receptor signalling and trafficking. Understanding such aspects may provide important information for drug design where ligands could be selected that exploit the beneficial effects of all aspects of GLP1R-mediated signalling. This is perhaps not surprising for compound 2, which is a small-molecule ligand and unlikely, therefore, to be processed by ECE-1 or indeed other proteases. Compound 2-mediated GLP-1R desensitisation and re-sensitisation will be assessed in Chapter 5. In addition, the interaction between compound 2 and orthosteric agonists of GLP-1R will also be examined.

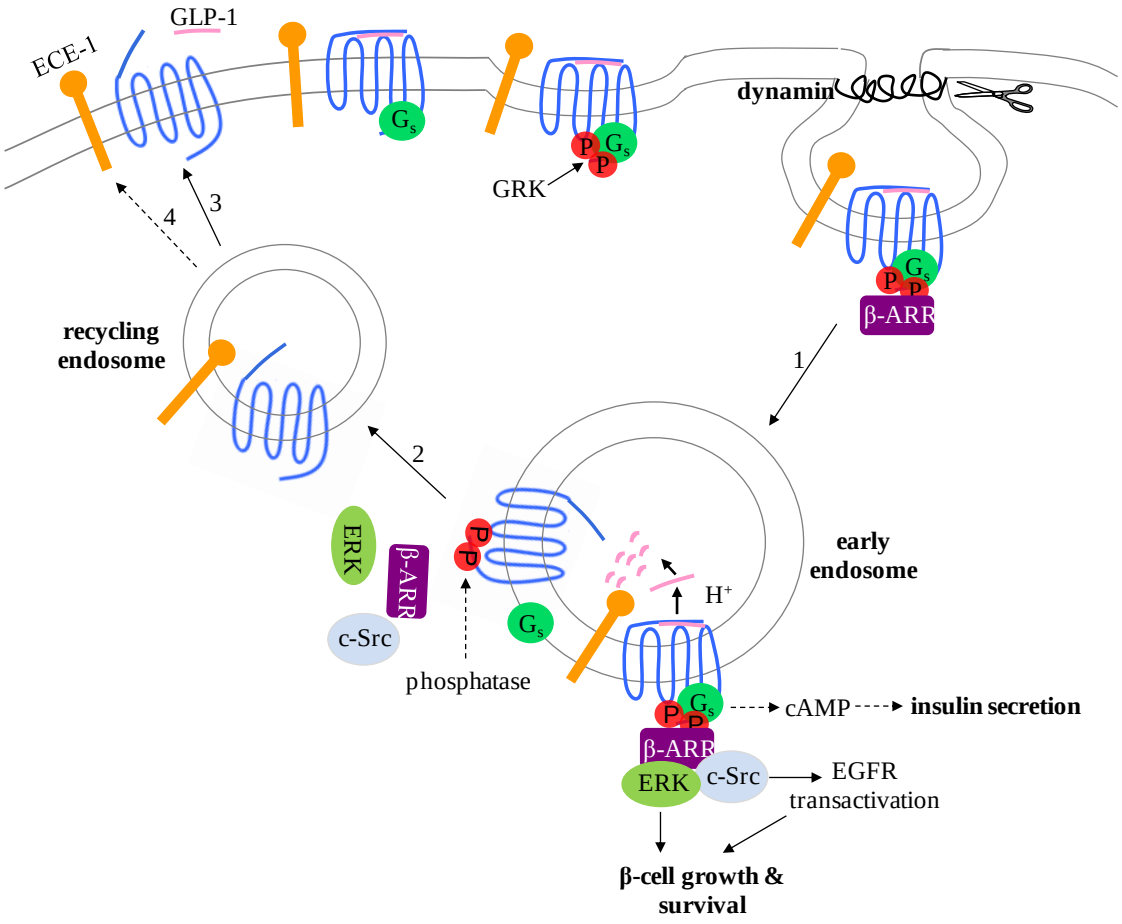

Fig 4.3. Potential role of ECE-1 in GLP-1R trafficking. 1. The activated and phosphorylated GLP-1R recruits β-arrestin and internalises into early endosomes with GLP-1 bound in a dynamin-dependent manner. G_s ($G\alpha_s$ or $G\beta\gamma$ is unclear) may also internalise with the receptor but this requires further investigation. Cell-surface ECE-1 internalises with the GLP-1R into the same early endosomes. 2. The acidified environment in the early endosome promotes the disassociation of GLP-1 from the receptor which is then hydrolyzed by ECE-1. This may prevent ligand-receptor re-association and result in disassociation of the receptor-β-arrestin complex leading to termination of β-arrestin-dependent signalling including ERK and possibly cAMP generation. ECE-1 may also regulate other β-arrestin-dependent pathways including c-Src activity although these have not been investigated in the present study. 3. The receptors then recycle back to the plasma membrane either following dephosphorylation or to be dephosphorylated at the plasma membrane in preparation for a new cycle of activation. 4. ECE-1 may also recycle back to the cell surface, but it is unclear whether

it is through the same route as GLP-1R recycling. β-ARR, β-arrestin. Pathways that are not well-investigated are shown by dashed arrows.

CHAPTER 5 Allosteric Modulation of the GLP-1R: Enhancing the Activity of GLP-1 9-36 Amide, a Major Degradation Product of GLP-1 7-36 Amide

5.1. Introduction

Compound 2 is one of an emerging number of small-molecule ligands for the GLP-1R. Aside from reportedly enhancing the affinity of the GLP-1R for GLP-1, it has intrinsic efficacy and can activate the receptor in the absence of other ligands causing responses typical of GLP-1R activation including the stimulation of insulin release in a glucose-dependent manner (Knudsen et al., 2007). Given the drive within the pharmaceutical industry to develop such compounds, it is important to address whether they behave in a similar manner to the endogenous ligand. In this chapter, aspects of compound 2 action have been explored for comparison with GLP-1 7-36 amide, the major postprandial circulating form of GLP-1 (Kreymann et al., 1987). Interestingly, previous work has demonstrated that cAMP responses to compound 2 are enhanced in the presence of the GLP-1R antagonist, exendin 9-39 amide. This is in contrast to the lack of effect of compound 2 on cAMP responses to GLP-1 7-36 amide (Coopman et al., 2010, Cheong et al., 2012). GLP-1 (GLP-1 7-37 and GLP-1 7-36 amide) is rapidly degraded by DPP-IV to generate GLP-1 9-37 or GLP-1 9-36 amide (Kieffer et al., 1995). The latter is the major postprandial circulating form of GLP-1 (Orskov et al., 1994) but the degradation by DPP-IV is considered to terminate activity, generating peptides that have been reported as inactive or even antagonists of the GLP-1R (Hansen et al., 1999). Given the reported interaction between compound 2 and exendin 9-39, work within this chapter also explored the potential interactions between compound 2 and GLP-1 9-36 amide in a variety of signalling pathways in both HEK-GLP-1R and INS-1E cells.

5.2. Results

5.2.1. GLP-1R desensitisation and re-sensitisation following challenge with GLP-1 9-36 amide and compound 2.

GLP-1 9-36 amide has 100-fold less affinity for the GLP-1R than GLP-1 7-36 amide (Knudsen and Pridal, 1996). The affinity of compound 2 is unclear although it evokes a concentration-dependent cAMP response with an E_{max} at 10 μM in HEK-GLP-1R cells (Coopman et al., 2010). In the present study in HEK-GLP-1R cells, GLP-1 9-36 amide or compound 2 (both at 10 μM) stimulated a thapsigargin-sensitive increase in $[Ca^{2+}]_i$ which were less than that evoked by 10 nM GLP-1 7-36 amide. Compound 2 also caused a much slower increase in $[Ca^{2+}]_i$ (reaching a peak at ~50 s after injection) compared to either of the orthosteric ligands (~10 s for both GLP-1 7-36 amide (10 nM) and GLP-1 9-36 amide (10 μM)). There was an immediate rapid increase in fluorescence induced by compound 2 injection but this was a result of the fluorescence of compound 2 itself **(see below)**.

Pre-treatment with GLP-1 9-36 amide (10 μM) for 10 min followed by washing with KHB and a 5 min period of recovery (protocol shown in **Fig 5.2.1.B**) resulted in a small reduction of the Ca^{2+} response to subsequent stimulation with 10 nM GLP-1 7-36 amide compared with the control (buffer) **(Fig 5.2.1.C)**. By contrast, pre-treatment with compound 2 (10 μM) evoked a markedly reduced response to a subsequent challenge with GLP-1 7-36 amide **(Fig 5.2.1.C)**. Nevertheless, when HEK-GLP-1R-EGFP cells were used to measure GLP-1R internalisation induced by either GLP-1 9-36 amide or compound 2, challenge with 10 μM GLP-1 9-36 amide for 60 min resulted in the loss of cell-surface fluorescence and an increase in the intracellular fluorescence **(Fig 5.2.1.D).** A similar effect was noted for cells treated with 10 μM compound 2 for 60 min **(Fig 5.2.1.D)**.

After a 3 h period of recovery, the Ca^{2+} response to 10 nM GLP-1 7-36 amide in the cells pre-treated with 10 μM compound 2 for 10 min (protocol shown in **Fig 5.2.1.B**) was still significantly lower than that of naïve cells (without pre-treatment) **(Fig**

5.2.1.E). However, the pre-treatment with compound 2 did not affect the response to ATP (300 μM) used as a control for effects such as toxicity **(Fig 5.2.1.E)**. Given the limited recovery of signalling following treatment with 10 μM compound 2, a lower concentration of compound 2 was used to determine any impact of ECE-1 inhibition. Pre-treatment with 1 μM compound 2 for 10 min followed by 5 min recovery caused a reduction of the Ca^{2+} response to 10 nM GLP-1 7-36 amide but which fully recovered after a 3 h period **(Fig 5.2.1.F)**. However, the recovery of the response was not influenced by treatment with the ECE-1 inhibitor, SM19712 (10 μM) **(Fig 5.2.1.F)**. By contrast, pre-treatment with 10 nM GLP-1 7-36 amide for 10 min followed by a 3 h period of recovery resulted in a similar response to the re-stimulation compared with that of naïve cells (without pre-treatment) but this was significantly reduced by SM19712 **(Fig 5.2.1.G)**.

A

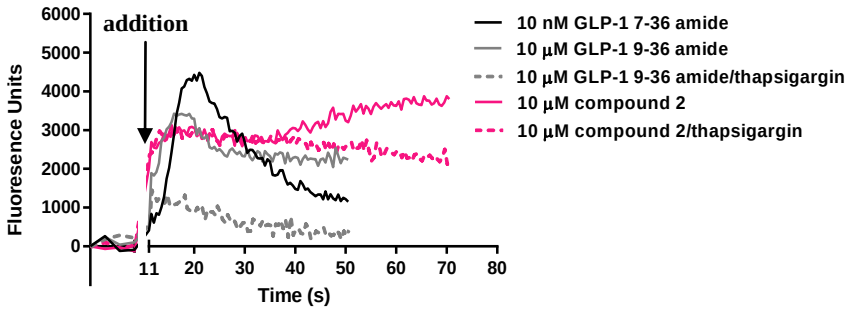
addition
Fluorescence Units
Time (s)
10 nM GLP-1 7-36 amide
10 µM GLP-1 9-36 amide
10 µM GLP-1 9-36 amide/thapsigargin
10 µM compound 2
10 µM compound 2/thapsigargin

B

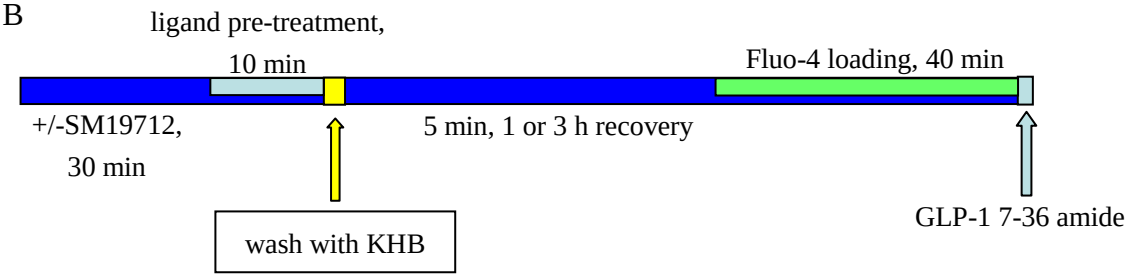
ligand pre-treatment,
10 min
Fluo-4 loading, 40 min
+/-SM19712,
30 min
5 min, 1 or 3 h recovery
wash with KHB
GLP-1 7-36 amide

C

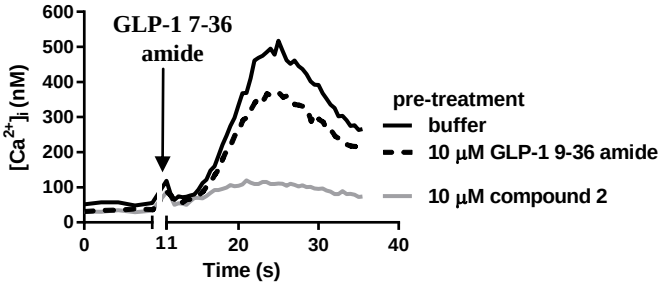
GLP-1 7-36 amide
[Ca2+]i (nM)
Time (s)
pre-treatment
buffer
10 µM GLP-1 9-36 amide
10 µM compound 2

D

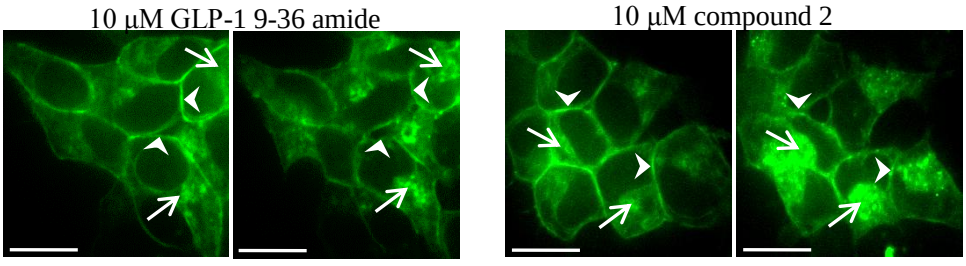
10 µM GLP-1 9-36 amide
10 µM compound 2
0 min
60 min
0 min
60 min

E

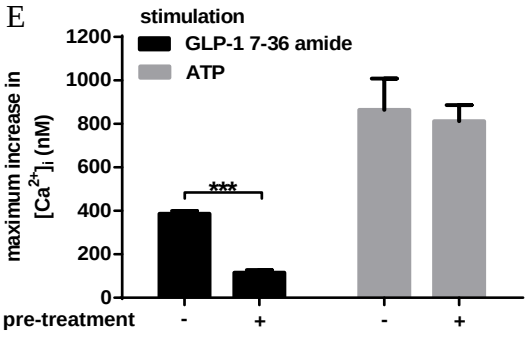
stimulation
GLP-1 7-36 amide
ATP
maximum increase in [Ca2+]i (nM)
***
pre-treatment

F

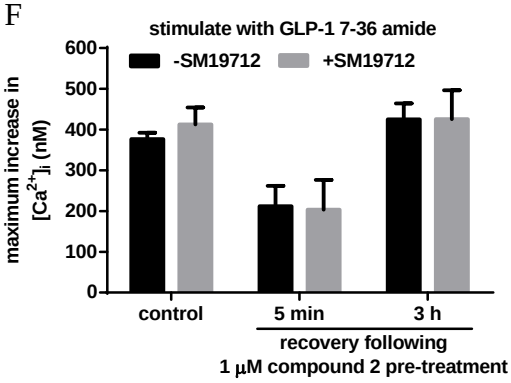
stimulate with GLP-1 7-36 amide
-SM19712
+SM19712
maximum increase in [Ca2+]i (nM)
control
5 min
3 h
recovery following
1 µM compound 2 pre-treatment

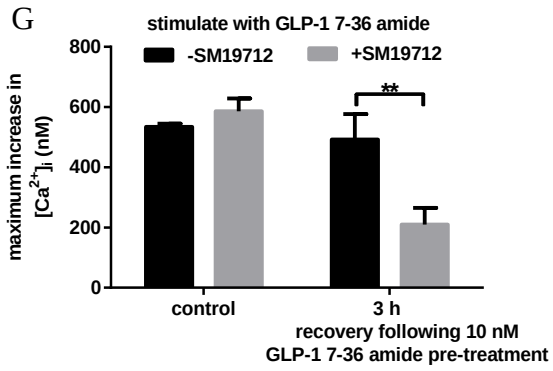

Fig 5.2.1. GLP-1R desensitisation and re-sensitisation in response to GLP-1 9-36 amide or compound 2. A. Representative fluorescence traces. Fluo-4-loaded HEK-GLP-1R cells were pre-incubated with buffer in either the absence or presence of 2 μM thapsigargin for 5 min. Cells were then stimulated with either 10 nM GLP-1 7-36 amide, 10 μM GLP-1 9-36 amide or 10 μM compound 2 and the changes in fluorescence were monitored. Responses were measured for either 51 s or 71 s with the injection of ligand at 11 s. **B.** Experimental protocol for **C**, **E**, **F** and **G**. **C**. Representative Ca^{2+} traces. HEK-GLP-1R cells were pre-treated with buffer, 10 μM GLP-1 9-36 amide or 10 μM compound 2 for 10 min followed by washing with KHB. After 5 min recovery, fluo-4-loaded cells were stimulated with 10 nM GLP-1 7-36 amide and the changes in fluorescence were monitored and calibrated to $[Ca^{2+}]_i$. Responses were measured for 36 s with the injection of ligand at 11 s. **D**. HEK-GLP-1R-EGFP cells were stimulated with 10 μM GLP-1 9-36 amide or 10 μM compound 2 for 60 min. The cells were imaged by confocal microscopy either before (0 min) or after (60 min) stimulation. The images are representative of 3 independent experiments. The arrowheads and arrows indicate the expression of GLP-1R-EGFP at the plasma membrane and in the cytosol respectively. Scale bar (in the bottom left of each image), 5 μm. **E**. HEK-GLP-1R cells were pre-treated with 10 μM compound 2 for 10 min followed by washing with KHB. After a 3 h period of recovery, fluo-4-loaded cells were stimulated with either 10 nM GLP-1 7-36 amide or 300 μM ATP. The maximum increases in fluorescence were determined and converted to $[Ca^{2+}]_i$. HEK-GLP-1R cells were pre-incubated for 30 min without or with SM19712 (10 μM,

which was then included throughout). Cells were then pre-treated with buffer (control) or either 1 μM compound 2 **(F)** or 10 nM GLP-1 7-36 amide **(G)** for 10 min followed by washing with KHB. After a 5 min or 3 h period of recovery, fluo-4-loaded cells were stimulated or re-stimulated with 10 nM GLP-1 7-36 amide and the changes in fluorescence were monitored and converted to $[Ca^{2+}]_i$. Data are representative or mean + S.E.M., n ≥ 2. **, $p < 0.01$; ***, $p < 0.001$ (Bonferroni's test following two-way ANOVA. Only the differences within a group **(E)** or between the groups at each time point **(F, G)** are shown for clarity).

5.2.2. GLP-1 9-36 amide and exendin 9-39 amide enhance compound 2-evoked cAMP production in HEK-GLP-1R cells.

In HEK-GLP-1R cells, the cAMP generation evoked by 1 nM (EC_{50}) of the GLP-1R orthosteric agonist GLP-1 7-36 amide was abolished by the co-addition with GLP-1R orthosteric antagonist, exendin 9-39 amide (1 μM). In contrast, exendin 9-39 amide significantly enhanced the cAMP response to the allosteric agonist, compound 2 (1 μM, submaximal concentration) in the presence of IBMX **(Fig 5.2.2.1.)**. This is consistent with previous findings in our laboratory (Coopman et al., 2010).

GLP-1 7-36 amide induced a concentration-dependent cAMP response with a pEC_{50} of 10.16 ± 0.11 in the presence of IBMX. GLP-1 7-36 amide (100 nM) produced an increase in cAMP to 1748 ± 73 pmol/mg protein from a basal level of 5 ± 2 pmol/mg protein. GLP-1 9-36 amide stimulated a concentration-dependent increase in cAMP with low potency (pEC_{50} 6.27 ± 0.09) and a maximal response that was ~20% of that in response to GLP-1 7-36 amide **(Fig 5.2.2.2.A)**. Although the concentration-response curve for compound 2-mediated cAMP generation was not well-defined, previous experiments in these cells gave a pEC_{50} of 6.23 and a maximal response at around 10 μM that was approximately 90% of the maximal response to GLP-1 7-36 amide (Coopman et al., 2010). Here 10 μM compound 2 evoked a cAMP response that was around 70% of the maximal response to GLP-1 7-36 amide. The co-addition of 1 μM GLP-1 9-36 amide (which alone generated 225 ± 18 pmol/mg protein cAMP, ~10% of GLP-1 7-36 amide E_{max}) and a range of concentrations of compound 2 resulted in a leftward shift of the concentration-response curve by a half log unit and demonstrated synergy. For example, 1 μM compound 2 produced 179 ± 37 pmol/mg protein of cAMP while co-stimulation with 1 μM GLP-1 9-36 amide enhanced that to 905 ± 46 pmol/mg protein which is significantly higher than the numerical addition (404 ± 55 pmol/mg protein) **(Fig 5.2.2.2.B)**.

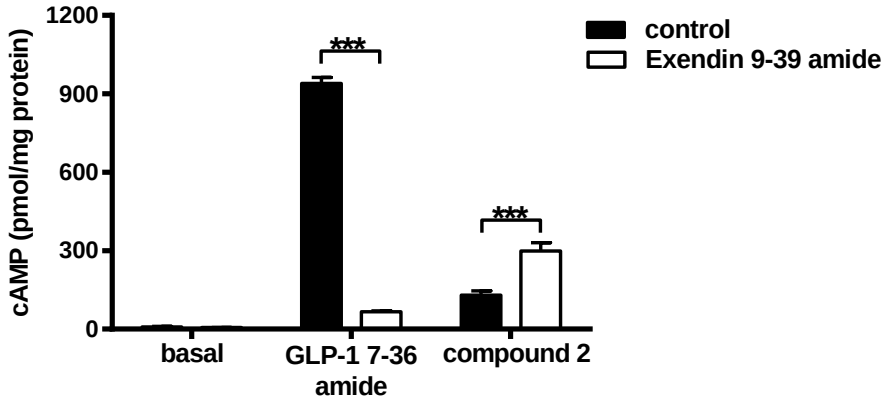

Fig 5.2.2.1. Exendin 9-39 amide inhibits GLP-1 7-36 amide-evoked cAMP generation but promotes compound 2-evoked cAMP production. In the presence of 500 μM IBMX, HEK-GLP-1R cells were stimulated with buffer (basal), 1 nM GLP-1 7-36 amide or 1 μM compound 2 in the absence (control) or presence of 1 μM exendin 9-39 amide for 15 min. Data are mean + S.E.M., n = 3. ***, $p < 0.001$ (two-way AVOVA; only the differences between groups under each condition are shown for clarity).

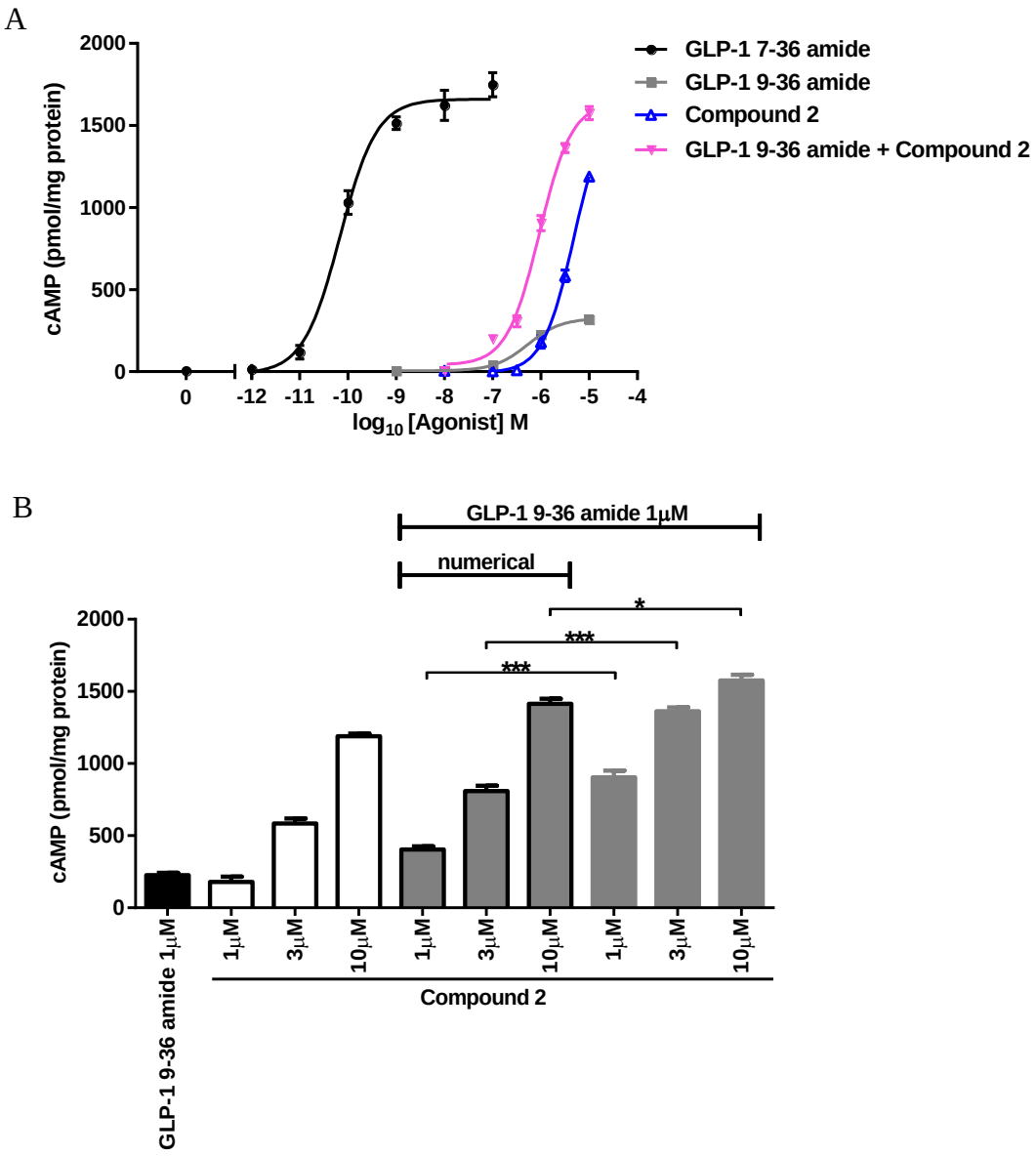

Fig 5.2.2.2. GLP-1 9-36 amide enhances the compound 2-evoked cAMP response in HEK-GLP-1R cells. A. Cells were stimulated with either vehicle (1% v/v DMSO) or various GLP-1R agonists: GLP-1 7-36 amide (from 0 to 100 nM); GLP-1 9-36 amide (from 0 to 10 μM); compound 2 (from 0 to 10 μM) or; co-stimulated with 1 μM GLP-1 9-36 amide and compound 2 (from 0-100 μM) for 15 min in the presence of 500 μM IBMX. The cAMP was then extracted and determined. The pEC_{50} and Hill slope values were 10.16 ± 0.11 and 1.14 ± 0.10 for GLP-1 7-36 amide and 6.27 ± 0.09 and 1.27 ± 0.05 for GLP-1 9-36 amide. Values could not be determined for either compound 2 alone or co-addition of compound 2 and 1 μM GLP-1 9-36 amide. The bar chart (**B**) was generated from the data in graph **A**. The numerical data were calculated from the

mathematical addition of the measured responses to 1 μM GLP-1 9-36 amide and compound 2 as indicated. All data are mean +/- S.E.M., n = 3. *, $p < 0.05$, ***, $p < 0.001$ (Student's t test).

5.2.3. GLP-1 9-36 amide enhances the compound 2-induced Ca^{2+} signalling in HEK-GLP-1R cells.

Compound 2 at 100 μM evoked a rapid increase in fluorescence at the time of injection followed by a second increase after 20 s **(Fig 5.2.3.1.A)**. Treatment with thapsigargin did not inhibit the initial, rapid increase but did abolish the later one. The initial rapid increase occurred in fluo-4-loaded wild-type HEK293 cells **(Fig 5.2.3.2.A)** and in HEK-GLP-1R cells in the absence of fluo-4-loading **(Fig 5.2.3.2.B)**. All these indicated that the initial change was a consequence of the fluorescence of compound 2 itself. The fluorescence of compound 2 prevented calibration of the Ca^{2+} signal and the responses are therefore shown as fluorescence as an index of $[Ca^{2+}]_i$. GLP-1 9-36 amide at 1 μM gave little or no detectable Ca^{2+} response **(Fig 5.2.3.1.B)**. Compound 2 at 10 μM evoked a slow and small Ca^{2+} response. In contrast, the co-injection with 10 μM compound 2 and 1 μM GLP-1 9-36 amide mediated a quicker and higher thapsigargin-sensitive increase in fluorescence **(Fig 5.2.3.1.B)**. This promotion by co-treatment was concentration-dependent **(Fig 5.2.3.1.C, D)**. The mean data generated using the area under the curve (AUC) showed that the responses given by the co-treatment with compound 2 at 10 μM or 30 μM and 1 μM GLP-1 9-36 amide were significantly higher than the numerical addition of each response alone **(Fig 5.2.3.1.D)**. The interaction between compound 2 and GLP-1 9-36 amide was not observed in fluo-4 loaded wild-type HEK293 cells **(Fig 5.2.3.2.A)**.

A

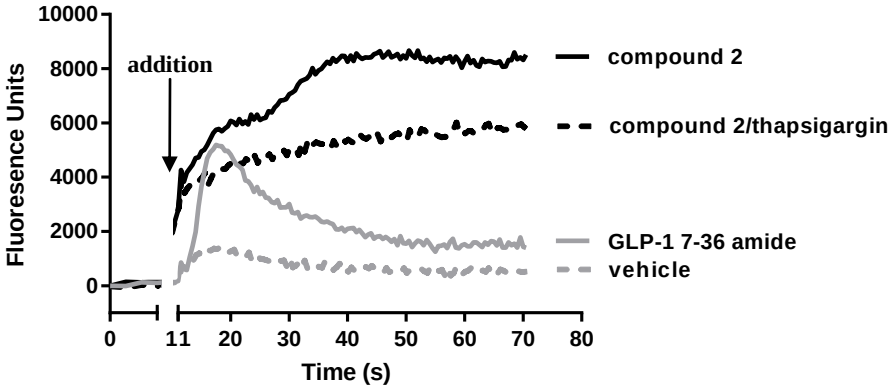
Fluoresence Units
addition
compound 2
compound 2/thapsigargin
GLP-1 7-36 amide
vehicle
Time (s)

B

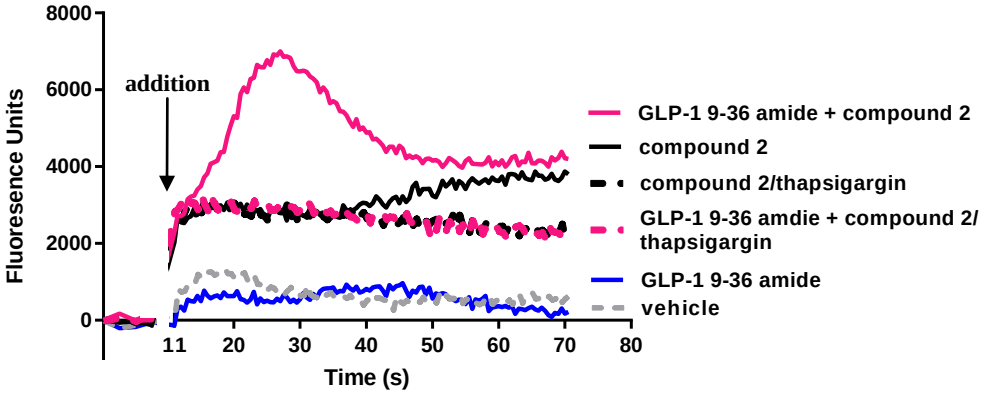
Fluoresence Units
addition
GLP-1 9-36 amide + compound 2
compound 2
compound 2/thapsigargin
GLP-1 9-36 amdie + compound 2/ thapsigargin
GLP-1 9-36 amide
vehicle
Time (s)

C

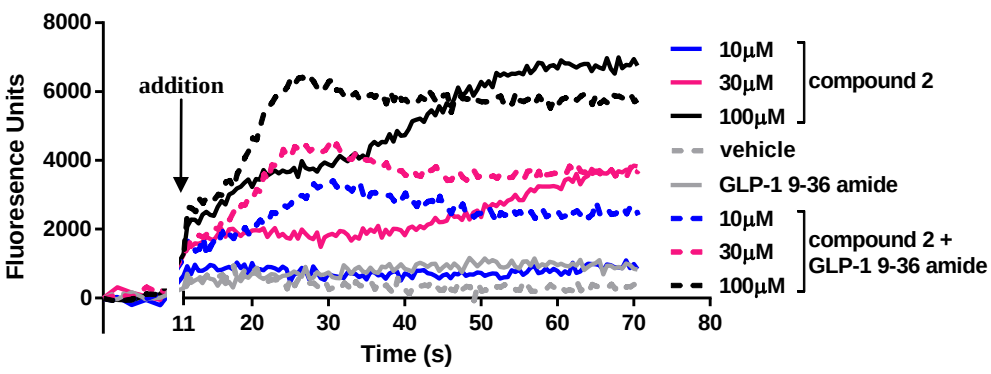
Fluoresence Units
addition
10μM
30μM
100μM
compound 2
vehicle
GLP-1 9-36 amide
10μM
30μM
100μM
compound 2 + GLP-1 9-36 amide
Time (s)

D

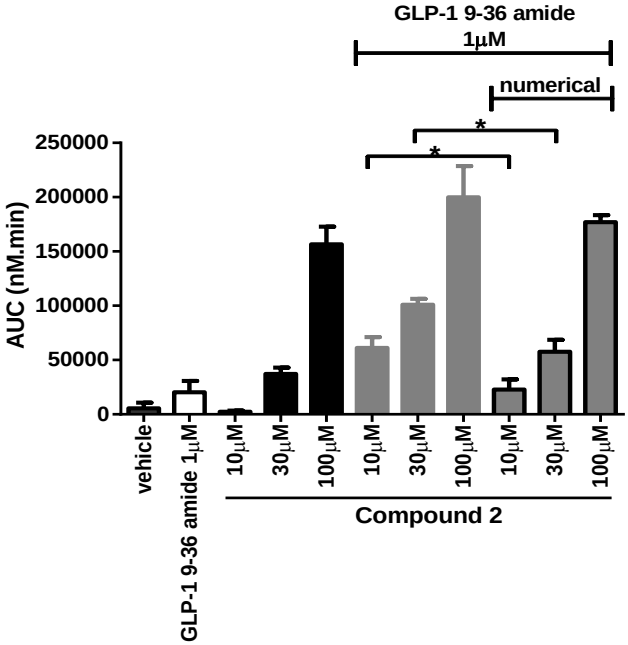
GLP-1 9-36 amide 1μM
numerical
*
*
AUC (nM.min)
vehicle
GLP-1 9-36 amide 1μM
10μM
30μM
100μM
Compound 2

Fig 5.2.3.1. Compound 2-evoked Ca^{2+} responses are promoted by co-addition with GLP-1 9-36 amide and blocked by thapsigargin. A. Fluo-4-loaded cells were pre-incubated without or with 2 μM thapsigargin for 5 min, followed by stimulation with either vehicle (1% v/v DMSO), 10 nM GLP-1 7-36 amide or 10 μM compound 2. **B.** Fluo-4-loaded cells were pre-incubated without or with 2 μM thapsigargin for 5 min, followed by stimulation with either vehicle (1% v/v DMSO) or 1 μM GLP-1 9-36 amide, 10 μM compound 2 or 1 μM GLP-1 9-36 amide and 10 μM compound 2 together. **C.** Fluo-4-loaded cells were stimulated with either vehicle (1% v/v DMSO), 1 μM GLP-1 9-36 amide, compound 2 (10 μM, 30 μM or 100 μM) or 1 μM GLP-1 9-36 amide and compound 2 (10 μM, 30 μM or 100 μM) together as indicated. The changes in fluorescence were measured for 71 s with the injection of ligand(s) at 11 s by a microplate reader as an index of $[Ca^{2+}]_i$. **D.** The bar chart of area under curve (AUC) was generated from graph **C**. The numerical data are equal to the mathematical addition of AUC of 1 μM GLP-1 9-36 amide-induced response plus AUC of the compound 2-induced response as indicated. Data are either representative or mean + S.E.M., $n \geq 3$. *, $p < 0.05$ (Student's t test).

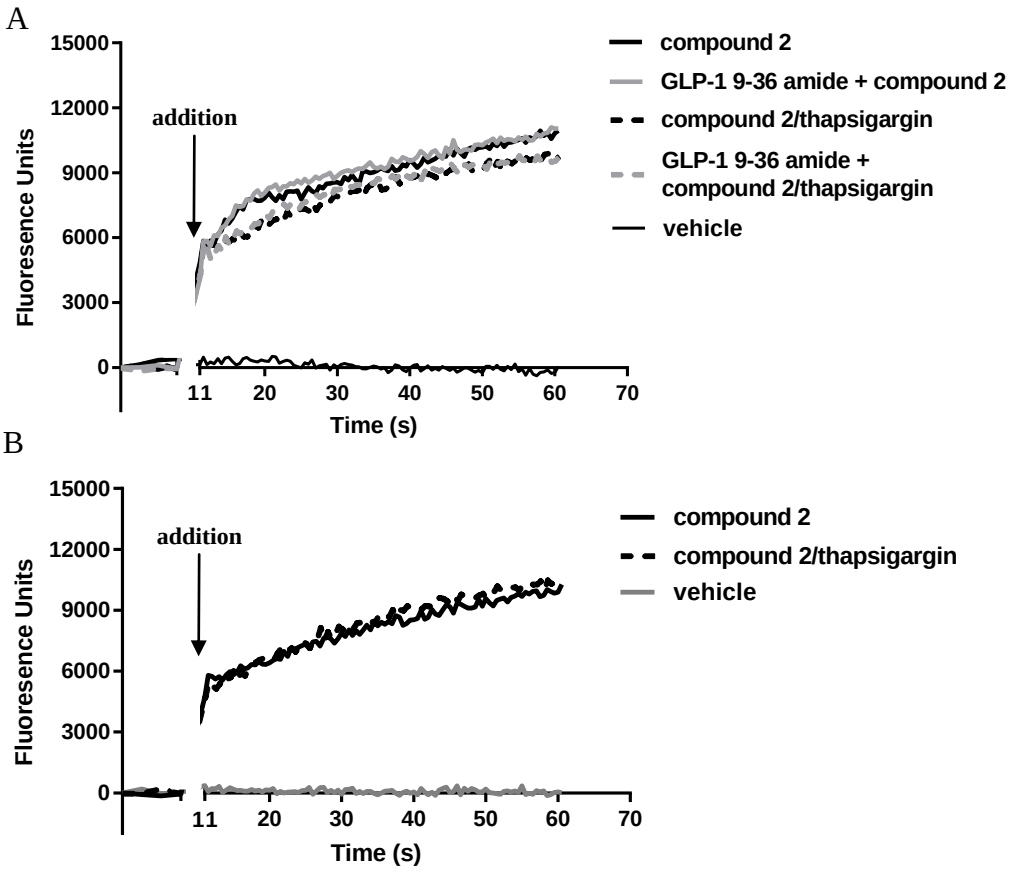

Fig 5.2.3.2. Interactions between GLP-1 9-36 amide and compound 2 does not occur in wild-type HEK293 cells or HEK-GLP-1R cells without fluo-4 loading. A. Fluo-4-loaded wild-type HEK293 cells were pre-incubated without or with 2 μM thapsigargin for 5 min, followed by stimulation with either vehicle (1% v/v DMSO) or 100 μM compound 2, or co-stimulation with 1 μM GLP-1 9-36 amide and 100 μM compound 2. **B.** HEK-GLP-1R cells in the absence of fluo-4 loading were stimulated with either vehicle (1% v/v DMSO) or 100 μM compound 2 with or without 5 min pre-incubation with 2 μM thapsigargin. The changes in fluorescence were measured for 61 s with the injection at 11 s. Representative Ca^{2+} traces from one experiment.

5.2.4. GLP-1 9-36 amide enhances compound 2-evoked cAMP production in INS-1E cells.

In INS-1E cells, GLP-1 7-36 amide stimulated a concentration-dependent increase in cAMP with a pEC_{50} of 9.39 ± 0.12 and Hill slope of 1.47 ± 0.24 in the presence of IBMX **(Fig 5.2.4.A)**. The maximum concentration of 100 nM produced an increase in cAMP to 770 ± 63 pmol/mg protein from a basal of 80 ± 16 pmol/mg. However, GLP-1 9-36 amide gave little or no cAMP response in these cells. Furthermore, compound 2 at 10 μM evoked a very low cAMP production (190 ± 31 pmol/mg protein). Co-addition of compound 2 (10 μM) with GLP-1 9-36 amide (1 μM), which alone evoked little or no cAMP response, increased the cAMP production to 490 ± 44 nmol/mg protein. This was significantly greater than the numerical addition of individual responses to 1 μM GLP-1 9-36 amide and 10 μM compound 2 **(Fig 5.2.4.B)**.

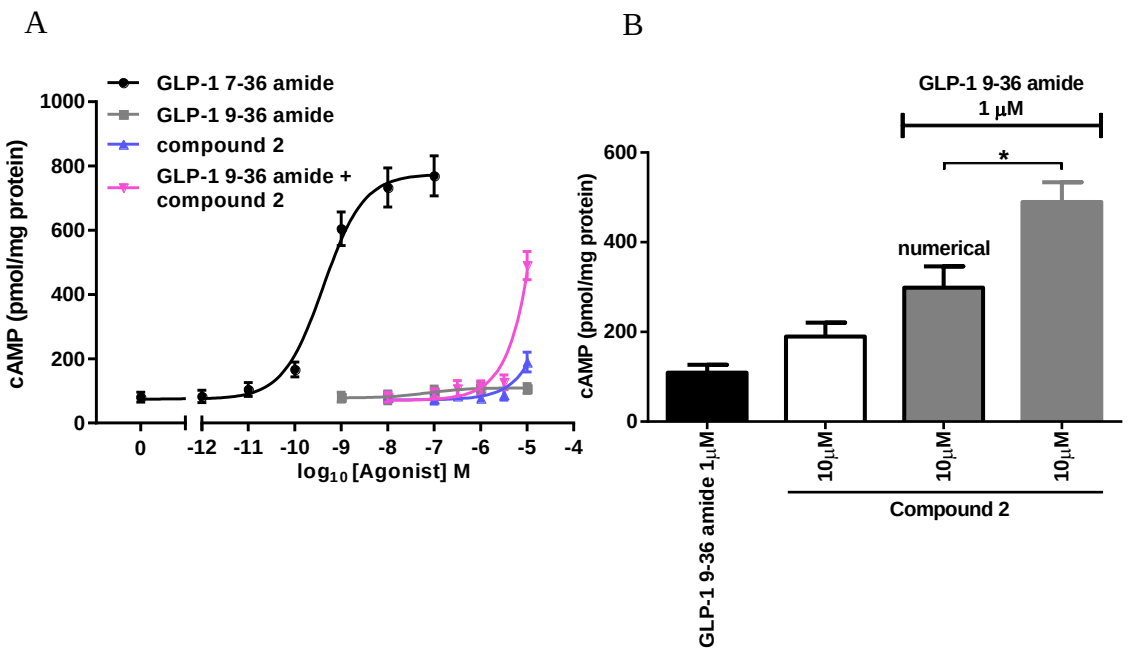

Fig 5.2.4. GLP-1 9-36 amide enhances compound 2-evoked cAMP production in INS-1E cells. A, **B**. INS-1E cells were stimulated with either vehicle (1% v/v DMSO), GLP-1 7-36 amide (0-100 nM), GLP-1 9-36 amide (0-10 µM), compound 2 (0-10 µM) or co-stimulated with 1 µM GLP-1 9-36 amide and compound 2 (0-100 µM) for 15 min in the presence of 500 µM IBMX. The cAMP was then determined showing a pEC_{50} and Hill slope of 9.39 ± 0.12 and 1.47 ± 0.24 respectively for GLP-1 7-36 amide. The bar chart (**B**) was generated from graph **A**. The numerical data are equal to the mathematical addition of responses to 1 µM GLP-1 9-36 amide and 10 µM compound 2 when added alone to the cells. Data are mean ±/+ S.E.M. n = 3. *, $p < 0.05$ (Student's t test).

5.2.5. GLP-1 9-36 amide enhances compound 2-evoked ERK activation in both HEK-GLP-1R and INS-1E cells.

In HEK-GLP-1R cells, simulation with 10 μM GLP-1 9-36 amide for 5 min evoked an ERK activation that was less than that induced by 10 nM GLP-1 7-36 amide **(Fig 5.2.5.A)**. Compound 2 mediated a concentration-dependent ERK activation and 1 μM compound 2 gave a very weak activation **(Fig 5.2.5.A)**. However, co-treatment with compound 2 at various concentrations and a concentration of GLP-1 9-36 amide (1 μM) that evoked little ERK activation by itself evoked greater ERK responses. For example, the responses to co-addition of 1 μM GLP-1 9-36 amide and compound 2 at 0.1 or 0.3 μM were significantly higher than the numerical addition of the individual responses **(Fig 5.2.5.A).**

In INS-1E cells, stimulation for 5 min with 10 μM compound 2 mediated a similar ERK response to that of 10 nM GLP-1 7-36 amide **(Fig 5.2.5.B)**. Challenge of cells with 1 μM GLP-1 9-36 amide for 5 min produced a small ERK response **(Fig 5.2.5.B)**. Co-treatment with compound 2 (3 μM) and GLP-1 9-36 amide (1 μM) significantly promoted ERK activation compared to the numerical addition of the responses to each ligand alone **(Fig 5.2.5.B)**.

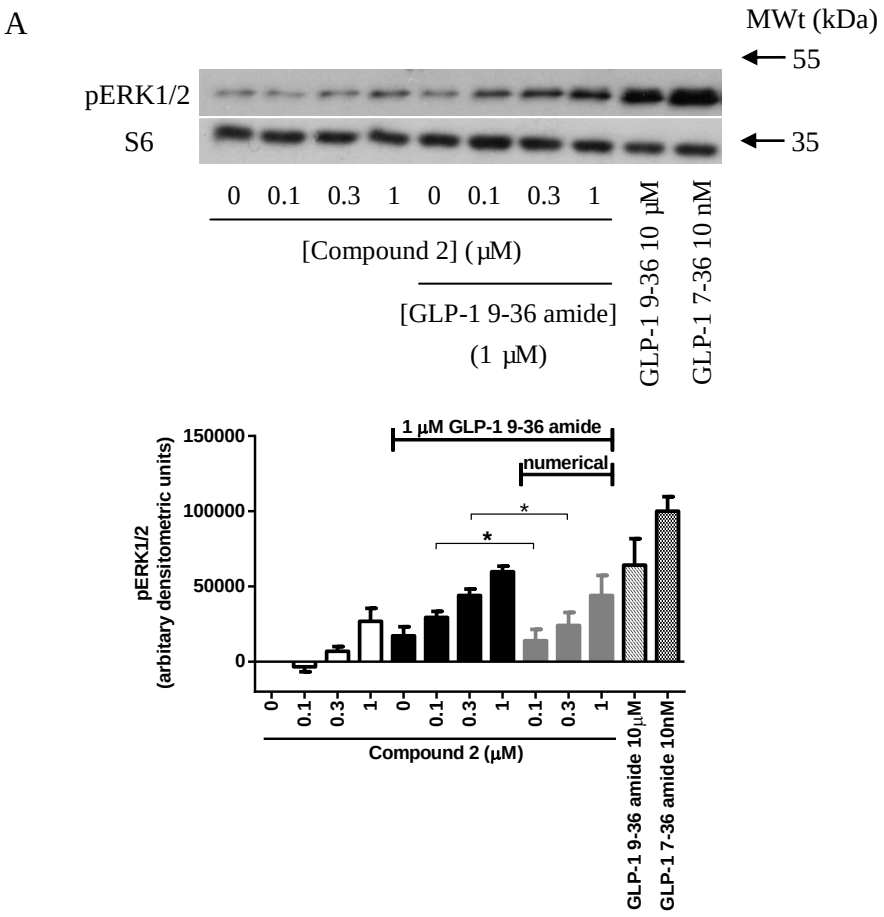
A
MWt (kDa)
55
35
pERK1/2
S6
0 0.1 0.3 1 0 0.1 0.3 1
[Compound 2] (µM)
[GLP-1 9-36 amide]
(1 µM)
GLP-1 9-36 10 µM
GLP-1 7-36 10 nM
1 µM GLP-1 9-36 amide
numerical
pERK1/2
(arbitary densitometric units)
150000
100000
50000
0
*
*
0 0.1 0.3 1 0 0.1 0.3 1 0.1 0.3 1
Compound 2 (µM)
GLP-1 9-36 amide 10µM
GLP-1 7-36 amide 10nM

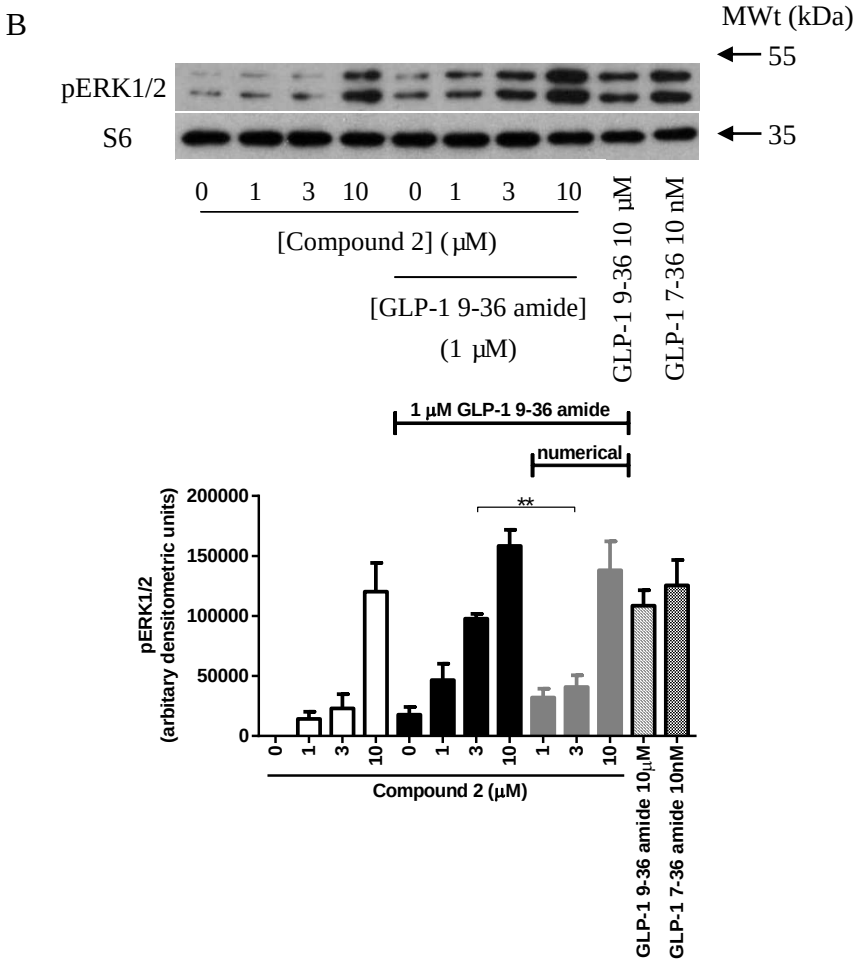
B
MWt (kDa)
55
35
pERK1/2
S6
0 1 3 10 0 1 3 10
[Compound 2] (µM)
[GLP-1 9-36 amide]
(1 µM)
GLP-1 9-36 10 µM
GLP-1 7-36 10 nM
1 µM GLP-1 9-36 amide
numerical
pERK1/2
(arbitary densitometric units)
200000
150000
100000
50000
0
**
0 1 3 10 0 1 3 10 1 3 10
Compound 2 (µM)
GLP-1 9-36 amide 10µM
GLP-1 7-36 amide 10nM

Fig 5.2.5. GLP-1 9-36 amide enhances compound 2-evoked ERK activation in both HEK-GLP-1R and INS-1E cells. HEK-GLP-1R cells (**A**) or INS-1E cells (**B**) were stimulated for 5 min with either vehicle (1% v/v DMSO), 10 nM GLP-1 7-36 amide, GLP-1 9-36 amide (1 or 10 μM), compound 2 alone at concentrations as indicated or both 1 μM GLP-1 9-36 amide and compound 2 together as indicated. The levels of pERK expression were determined by immunoblotting. Ribosomal protein S6 was used as a loading control. The data are vehicle (0) subtracted. The numerical data are equal to the mathematical addition of the responses to 1 μM GLP-1 9-36 amide and compound 2 alone at indicated concentrations. Data are either representative or mean + S.E.M., n = 3. *, $p < 0.05$, **, $p < 0.01$ (Student's t test).

5.3. Discussion

Work described in this chapter showed that the allosteric agonist compound 2 not only shows different activity in GLP-1R activation, but also mediates a different pattern of GLP-1R re-sensitisation compared to the orthosteric agonist GLP-1. The process of GLP-1R re-sensitisation following challenge with compound 2 at a high concentration was slow and insensitive to inhibition of ECE-1 which does, however, regulate re-sensitisation following challenge with GLP-1 **(see Chapter 4)**. This implies that compared with the native ligands, this small-molecule allosteric agonist not only displays different intrinsic activity but also mediates a different efficiency of receptor re-sensitisation which may imply different pathways of receptor trafficking.

Allosteric ligands can act as either negative or positive modulators to either inhibit or promote the affinity and/or efficacy of orthosteric agonists respectively (Keov et al., 2011). Compound 2 not only has intrinsic activity but also enhances the affinity of the GLP-1R for GLP-1 but does not impact on efficacy (Knudsen et al., 2007, Koole et al., 2010) showing it is an ago-allosteric agonist for the GLP-1R. The data presented here demonstrate that compound 2 potentiates both the efficacy and potency of the metabolite of GLP-1, GLP-1 9-36 amide. This may provide a novel therapeutic strategy for the treatment of type 2 diabetes.

5.3.1. Allosteric agonist-mediated GLP-1R desensitisation and re-sensitisation.

Data in the previous chapter demonstrated a ligand-dependence of GLP-1R re-sensitisation, highlighting that following GLP-1 7-36 amide stimulation, the GLP-1R re-sensitised faster than following stimulation with exendin-4. Furthermore, recovery following GLP-1 stimulation was sensitive to inhibition of ECE-1 whereas recovery following exendin-4 was not. It is possible that this difference is a consequence of the inability of endosomal ECE-1 to cleave exendin-4 (or that there is an alternative rate-limiting step). It might be predicted that the inability to process the ligand might result in a prolonged interaction between receptor and β-arrestin leading to a longer

recycling time **(see Chapter 4)** or even receptor degradation (Anborgh et al., 2000, Moore et al., 2007). The stability of the complex could also influence receptor-mediated signalling particularly that regulated by β-arrestin. Small-molecule agonists, whether orthosteric or allosteric, are generally designed to mimic the activity of the endogenous ligand. However, they would be unaffected by the activity of proteases able to degrade peptide ligands and could, therefore, behave differently in respect of aspects such as signalling, receptor trafficking and re-sensitisation. The experiments described in this chapter determined GLP-1R desensitisation and re-sensitisation mediated by the small-molecule and allosteric agonist, compound 2. Although compound 2 (10 μM) mediated a reduced level of cAMP generation and Ca^{2+} mobilization compared to GLP-1 7-36 amide **(Fig 5.2.1.A and Fig 5.2.2.2.)**, it caused a marked desensitisation and internalisation of the GLP-1R **(Fig 5.2.1.C, D)** (Coopman et al., 2010). Although it is unclear if compound 2 can internalise with the receptor, fluorescence of compound 2 could be detected inside cells after stimulation (data not shown). Further, despite reduced signalling compared to GLP-1, re-sensitisation of the GLP-1R after removal of extracellular compound 2 was minimal after 3 h compared to full recovery following stimulation with GLP-1 without influencing cell viability **(Fig 5.2.1.C, D, E and Fig 5.2.1.E).** The slower recovery is consistent with observations that compound 2 is biased for β-arrestin1 and β-arrestin2 recruitment relative to Ca^{2+} and cAMP responses (Wootten et al., 2013) and this may be the cause of the reduced rate of re-sensitisation. Given that receptor phosphorylation by different kinases may generate different functional consequences including different downstream signalling and the differential recruitment of proteins such as β-arrestin (Tobin, 2008), compound 2 may expose different phosphorylation sites on the GLP-1R compared to GLP-1. Thus, compared with the endogenous agonists, a potentially different profile of phosphorylation triggered by the small-molecule agonists together with a lack of requirement for proteases such as ECE-1 activity could result in different patterns of receptor signalling, desensitisation, re-sensitisation and possibly trafficking.

5.3.2. The interaction between GLP-1 9-36 amide and compound 2

GLP-1 binds to the receptor following a 'two domain model' whereas the binding sites for the allosteric ligands are unclear. Compound 2 does not compete with the binding of GLP-1 (Knudsen et al., 2007) and it maintains the activity on the N-terminal truncated version of GLP-1R (Huang, 2010) suggesting compound 2 interacts with the core domain of the GLP-1R without overlapping with the orthosteric binding site. Compound 2 enhances the affinity of the GLP-1R for GLP-1 but does not affect the potency or efficacy showing its positive modulation of orthosteric ligand binding (Knudsen et al., 2007, Coopman et al., 2010, Koole et al., 2010). However, work in our laboratory has showed that the GLP-1R antagonist, exendin 9-39 amide, which markedly inhibits the activity of orthosteric agonists, actually promotes compound 2-mediated cAMP generation (Coopman et al., 2010) **(Fig 5.2.2.1.)**. In the present study, we further explored the interaction between compound 2 and the metabolite of GLP-1 7-36 amide, GLP-1 9-36 amide. In the body, once GLP-1 is released it is rapidly metabolized resulting in the bulk of circulating GLP-1 being the major metabolic product, GLP-1 9-36 amide (Deacon et al., 1995). Studies around the function of GLP-1 9-36 amide suggested that it has no insulinotropic effects and even shows antagonism under some circumstance (Deacon et al., 2002, Rolin et al., 2004, Knudsen and Pridal, 1996, Wettergren et al., 1998) although this would also be consistent with its weak partial agonism shown in the present study. Compound 2 is able to induce insulin secretion in a glucose-dependent manner *in vitro* (Knudsen et al., 2007) and the present data highlight that compound 2 enhances both the potency and efficacy of GLP-1 9-36 amide.

Following GLP-1R activation in pancreatic β-cells, signalling events downstream of cAMP mediate insulin secretion **(see General Introduction 1.3.3.2.)**. Although GLP-1 9-36 amide has no effect on the level of insulin *in vivo* (Rolin et al., 2004), it was able to stimulate a low level of cAMP generation in HEK-GLP-1R cells **(Fig 5.2.2.2.)**. However, this was not apparent in INS-1E cells **(Fig 5.2.4.)** suggesting that weak partial

agonism of a large number of receptors in HEK-GLP-1R cells may be responsible. Similar to GLP-1, compound 2 couples the GLP-1R to cellular signalling through the activation of G_s (Coopman et al., 2010). The efficiency of compound 2-mediated cAMP generation was higher than that of GLP-1 9-36 amide but lower than that of GLP-1 7-36 amide in both cell lines **(Fig 5.2.2.2 and Fig 5.2.4.)** indicating its partial agonism in cAMP generation. Interestingly, compound 2 synergistically increased the efficacy of GLP-1 9-36 amide-induced cAMP generation such that maximal levels were similar to those evoked by GLP-1 7-36 amide. Such interactions between allosteric ligands and GLP-1 9-36 amide has also been reported elsewhere. Thus, the GLP-1R allosteric ligands compound 2 or compound B enhanced GLP-1 9-36 amide-mediated cAMP generation in a cell line expressing recombinant GLP-1R (Wootten et al., 2012).

The increase of $[Ca^{2+}]_i$ either directly or indirectly stimulates the acute insulin release in pancreatic β-cells **(see General Introduction 1.3.3.2.)**, therefore whether the interaction of GLP-1 9-36 amide and compound 2 would also be shown in GLP-1R-mediated Ca^{2+} signalling is important. Similar as cAMP generation, GLP-1 9-36 amide only evoked a lower Ca^{2+} response at high concentrations (>1 μM) **(Fig 5.2.1.A)**. In contrast, compound 2 (≥10 μM) evoked a long-lasting thapsigargin-sensitive Ca^{2+} response **(Fig 5.2.3.1.A, C)**. Although it is difficult to compare its efficacy with GLP-1 7-36 amide, the time course of compound 2-mediated increase of $Ca^{2+}{}_i$ is certainly different compared with the orthosteric agonists. However, when GLP-1 9-36 amide and compound 2 were used in combination, the Ca^{2+} response was more rapid and elevated and more similar to the GLP-1 7-36 amide-mediated response **(Fig 5.2.3.1.B, C)**. Therefore compound 2 also potentiates GLP-1 9-36 amide-induced Ca^{2+} mobilization. Although this phenomenon is conflicting with a recent study (Wootten et al., 2012), the potentiated increase in fluorescence as an index of Ca^{2+} was thapsigargin sensitive and was not apparent in the wild-type HEK293 cells (without the expression of GLP-1R) or in HEK-GLP-1R cells in the absence of fluo-4 loading **(Fig 5.2.3.2.)**. Given that Ca^{2+} responses in HEK293 cells appear to be dependent on cAMP and compound 2 shows agonism in cAMP generation, it would be expected that compound 2 should evoke Ca^{2+}

response. However the kinetics and/or sub-cellular localization of cAMP in response to the different agonists could be different thereby changing the Ca^{2+} responses. Moreover, literature has showed that compound 2 is able to stimulate an acute insulin release in isolated rat islets (Knudsen et al., 2007) which is generally considered to be through a Ca^{2+}-dependent mechanism in pancreatic β-cells **(see General Introduction 1.3.3.2.4.)**. Whether the interaction actually potentiates GLP-1R-mediated insulin release in pancreatic β-cells is unclear. However, interaction between GLP-1 9-36 amide and the allosteric agonist compound B did potentiate the release of insulin in isolated rat islets (Wootten et al., 2012).

Aside from mediating acute insulin secretion, GLP-1 also promotes insulin synthesis and secretion through the regulation of transcription factors activity. One mechanism is through the activation of ERK which also has beneficial effects on β-cell proliferation and survival (Briaud et al., 2003, Costes et al., 2006, Lawrence et al., 2005). Although GLP-1 9-36 amide is relatively poor at stimulating cAMP generation and Ca^{2+} mobilization, it was more efficient on ERK activation, particularly in INS-1E cells. Indeed, 10 μM GLP-1 9-36 amide although not evoking a cAMP response, activated ERK to a similar extent as 10 nM GLP-1 7-36 amide **(Fig 5.2.5.B)**. The same was also true for compound 2. Thus, in INS-1E cells, compound 2 (10 μM) stimulated 6-fold lower cAMP generation than GLP-1 7-36 amide (10 nM) **(Fig 5.2.4.)** whereas at least with 5 min stimulation, it activated ERK to a level comparable to that mediated by GLP-1 7-36 amide **(Fig 5.2.5.B).** This effect was less clear in HEK-GLP-1R cells. A recent study also indicated that the potency of compound 2-mediated ERK1/2 activation is higher than cAMP generation (Wootten et al., 2013). Given that compound 2 may show preference for β-arrestin recruitment **(see above)**, the phenomenon raises the question as to whether compound 2 shows bias for β-arrestin-dependent ERK activation relative to cAMP/PKA-dependent ERK activation. Again, compound 2 could also positively influence GLP-1 9-36 amide-induced ERK activation. To date there is no information relating to other potential actions of compound 2 such as β-cell growth and survival. Whether the interaction between compound 2 and GLP-1 9-36 amide actually

shows benefits in those aspects is unknown but clearly worth exploring.

The allosteric modulation of receptors in the presence of metabolites of endogenous ligands has been reported for non-peptide receptors. Thus, both choline and inosine, the metabolites of acetylcholine and adenosine respectively, have much lower activity than their parent ligands for their receptors, M_2 muscarinic acetylcholine receptor and adenosine A_1 receptor respectively, but the activity of each can be potentiated by an allosteric ligand (Wootten et al., 2012). Here, compound 2 potentiates the activity of GLP-1 metabolite, GLP-1 9-36 amide. Therefore, allosteric ligands have the potential ability to modulate the activity of peptide metabolites. However the mechanism is unclear. Compound 2 is not able to enhance the affinity of GLP-1 9-36 amide (Wootten et al., 2012) suggesting that potentiation is likely to be the result of enhanced efficacy, possibly through stabilization of specific receptor conformations. Thus, the structure of the receptor occupied at the same time by the two ligands may be different to that induced by single occupancy. This could expose different phosphorylation sites thereby facilitating differential coupling to effectors. Given that the signalling by the combination of compound 2 and GLP-1 9-36 amide is similar as that by GLP-1 7-36 amide, the structure may be close to that stabilized by the parent ligand although the signalling mechanisms and the full range of effectors activated would need to be defined to establish this.

Notably, although GLP-1 9-36 amide has 100-fold lower affinity at the GLP-1R compared to intact GLP-1 (Knudsen and Pridal, 1996), it is actually present at ~10-fold higher levels in the circulation (Orskov et al., 1994), although clearly the relative concentrations at the sites of action are unknown. Interestingly, GLP-1 9-36 amide is cleared by the kidney (Meier et al., 2004) whereas GLP-1 7-36 amide is of course cleared in the circulation by DPP-IV. Thus, in conditions where kidney function may be compromised (eg. diabetes), circulating levels of the metabolite may reach even higher levels (Nolin, 2008, Arnouts et al., 2013). Work in our laboratory shows that compound 2 enhances the potency of GLP-1 9-36 amide by 100-fold (Li et al., 2012), suggesting

that the modulation of metabolite activity may be a therapeutic possibility. Whether enhanced activity of the metabolite by an allosteric agonist would be beneficial *in vivo* is worthy of exploration both for GLP-1R activity and for that of other peptidergic receptors.

CHAPTER 6 Final Discussion

6.1. Overview

As a therapeutic target for the treatment of type 2 diabetes, the GLP-1R has been widely investigated in many aspects of its structure and signalling although studies of its desensitisation, re-sensitisation and particularly the trafficking are limited. The current models suggest that following receptor activation, internalisation occurs and that the subsequent trafficking processes may regulate the rate and efficiency of receptor re-sensitisation. It is now clear that such processes will also regulate signalling not only by removing receptors from the cell surface where it may engage a specific set of signalling pathways but also by regulating any signalling functions of the endocytosed receptor. Moreover, different agonists may trigger different rates of receptor trafficking, potentially even engaging different mechanisms, which may lead to distinct patterns of receptor re-sensitisation and possibly different signalling and physiological outcomes. This is particularly important as novel ligands are developed in an effort to exploit the functions of the GLP-1R. Furthermore, these findings may extend to receptors other than the GLP-1R.

The present data show that activation of the GLP-1R results in receptor desensitisation and internalisation through a dynamin-dependent mechanism. Data also indicated that the endocytosed GLP-1Rs target to early endosomes with GLP-1 bound. The model of receptor trafficking following endocytosis suggests that the endocytosed receptors in early endosomes are subsequently targeted to either recycling endosomes which traffic receptors back to the cell surface or late endosomes for degradation in lysosomes **(Fig 1.5)**. The mechanisms deciding receptor trafficking are complex (Moore et al., 2007). Lysosomal sorting of GPCRs generally requires covalent tagging of receptors with ubiquitin (Wojcikiewicz, 2004). There is evidence suggesting some GLP-1Rs sort to lysosome for degradation in BRIN-BD11 cells (Kuna et al., 2013). The mechanisms driving some GLP-1Rs to lysosomes are unclear. However, the present study showed

that upon GLP-1 stimulation followed by ligand removal, a large proportion of GLP-1Rs could then re-sensitise with the recovery of cell-surface receptor number in both HEK-GLP-1R and INS-1E cells. Receptor recovery requires internalisation and endosomal acidification but not *de novo* receptor synthesis suggesting receptor recycling is involved. The rate of receptor recycling is regulated by many factors. A very important aspect is the stability of receptor-β-arrestin complex which will be determined by several factors including the nature of the ligand, the phosphorylation pattern and status of the receptor and the stability of β-arrestin ubiquitination **(see General Introduction 1.5.2.)**. Protease degradation of peptides in endosomes has also been shown play a role in regulating receptor recycling. For example, bradykinin and EGF can be degraded by endopeptidase 24.15 and cathepsin B respectively in endosomes which facilitates receptor recycling (Norman et al., 2003, Authier et al., 1999). The present study showed that re-sensitisation of the GLP-1R is dependent on receptor internalisation and subsequent recycling. ECE-1 activity, most likely within the endosomal compartment, promotes GLP-1R re-sensitisation through facilitating recycling to the plasma membrane. It may be that ECE-1 degrades GLP-1 in the early endosomes either preventing ligand-receptor re-association or facilitating dissociation of the ligand-receptor complex. The current models would suggest that this would promote the disassociation of the receptor-β-arrestin complex leading to receptor dephosphorylation and recycling. By contrast, recovery of signalling following GLP-1R stimulation with either exendin-4 or the small-molecule allosteric agonist, compound 2, was slow and insensitive to ECE-1 inhibition. This highlights different ligands may behave differently in regulating GLP-1R trafficking. In addition to regulating GLP-1R recycling and re-sensitisation, ECE-1 regulates GLP-1R-mediated signalling. The inhibition of ECE-1 potentiates both GLP-1 7-36 amide-mediated cAMP generation and ERK activation which may be through a G protein-independent/β-arrestin-dependent mechanism. Thus, our finding provides the novel mechanism of regulating GLP-1R signalling and re-sensitisation.

Re-sensitisation of the GLP-1R displays differences that are dependent upon the ligand

used for activation. Furthermore, there is evidence to suggest ligand-preference in the activation of downstream signalling. Thus, the metabolite of GLP-1 7-36 amide, GLP-1 9-36 amide, is a weak agonist for cAMP generation and Ca^{2+} mobilization whereas it is a strong activator of ERK. The allosteric agonist, compound 2, although showing greater cAMP generation and Ca^{2+} mobilization than GLP-1 9-36 amide, is also less active than GLP-1 7-36 amide. However, it causes comparable ERK activation to that in response to GLP-1 7-36 amide. Interestingly, compound 2 synergically potentiates the activity of GLP-1 9-36 amide but not GLP-1 7-36 amide in respect of either cAMP generation, Ca^{2+} mobilization or ERK activation. GLP-1 9-36 amide is actually the major circulating form of GLP-1 in body but has no influence on plasma glucose level in patients with type 2 diabetes (Zander et al., 2006). However compound 2 stimulates glucose-dependent insulin release in isolated rat islets (Knudsen et al., 2007). Our findings suggest a new therapeutic strategy for the treatment of type 2 diabetes by modulation of essentially inactive metabolites by small molecule and allosteric agonists.

6.2. Future directions

Biased agonism has been reported at a number of GPCRs suggesting that different ligands stabilize distinct receptor conformations (Rajagopal et al., 2010). For example, ligands can display bias for different G proteins or between G protein- and β-arrestin-dependent signalling. These latter two signalling events often show both temporal and spatial differences and can, therefore, mediate unique cellular and physiological consequences (DeWire et al., 2007, Luttrell and Gesty-Palmer, 2010). Presently, drugs are developed generally based on a limited number of cellular outputs and indeed it is often unknown which signalling events are therapeutically advantageous. Although such a strategy has been effective, it may not fully exploit the possibilities or result in adverse effects. For example, in the heart, the β_1AR mediates β-arrestin1- and 2-dependent signalling, mediating transactivation of a cardioprotective EGFR (Noma et al., 2007), which could be beneficial for therapy in this case, whereas chronic activation of β_1AR-mediated G protein-dependent signalling is cardiotoxic (Lohse et al., 2003). By

contrast, β-arrestin mediates both morphine-triggered opioid receptor desensitisation and tolerance *in vivo* (Bohn et al., 1999, Bohn et al., 2000). Thus, a G protein-biased ligand inducing an elevated and prolonged analgesia is highly desirable. For the NK_1R activated by SP, inhibition of ECE-1 results in retention of the ligand-receptor-β-arrestin complex in endosomes leading to an ERK2-mediated increase in the expression and phosphorylation of the nuclear death receptor Nur77, promoting cell death (Cottrell et al., 2009). This is a clear example where signalling of the receptor from an endosomal compartment provides a distinct cellular function compared to signalling from the plasma membrane. The nature and rate of receptor trafficking and endosomal signalling may therefore regulate important cellular functions. Previous researches have shown that β-arrestin1/2 is recruited to the GLP-1R upon GLP-1 stimulation, although this might occur cell-type dependently (Sonoda et al., 2008, Wootten et al., 2013, Syme et al., 2006). The stability of the receptor-β-arrestin complex is a critical factor regulating GPCR trafficking and signalling (Oakley et al., 2001, Anborgh et al., 2000, Shenoy and Lefkowitz, 2005). The current study raises a potential mechanism whereby ECE-1 could regulate the stability of the GLP-1R-β-arrestin complex thereby regulating β-arrestin-dependent signalling pathways, including ERK activation and possibly also cAMP generation. Whether β-arrestin bound to the GLP-1R is targeted to early endosomes remains to be determined. In addition, the role of ECE-1 in regulating both the stability of the GLP-1R-β-arrestin complex and β-arrestin-dependent signalling requires further investigation. Further, β-arrestin-dependent signalling could be involved in controlling important GLP-1R-mediated functions, such as insulin secretion and the regulation of β-cell mass through anti-apoptotic and pro-proliferative effects. Whether ECE-1 plays a role in the regulation of these cellular functions is certainly worth prioritizing for further exploration. Given that the level of ECE-1 expression may increase under high glucose levels it might also be interesting to explore potential changes in the diabetic state and whether such changes could influence GLP-1R signalling or regulation. The discovery of β-arrestin-dependent signalling clearly broadens the scope of therapeutic approaches, but also brings great challenges to drug discovery which requires much more thought about the pharmacology of potential

therapeutic ligands.

Along with other studies (Roosterman et al., 2004, Sigismund et al., 2005), the present study highlights that receptor desensitisation is more pronounced and takes longer to recover with higher concentrations of agonist. Such regulation may be important in limiting receptor activation. This is not novel but while the concentration-dependence may simply be due to greater receptor endocytosis, it is possible that the trafficking of GLP-1R is differentially influenced by the concentration of ligand **(see Chapter 3 and 4)**. GLP-1 7-36 amide evokes similar maximal response of Ca^{2+} as exendin-4 and both of them mediate a comparable extent of GLP-1R desensitisation whereas the latter agonist clearly mediates a much slower process of re-sensitisation. Additionally, the allosteric agonist, compound 2 shows partial agonism in cAMP generation, but mediates similar desensitisation and internalisation as the orthosteric agonists. However, recovery is markedly prolonged compared to that following GLP-1 7-36 amide. The insensitivity of re-sensitisation following desensitisation by exendin-4 or compound 2 to inhibition of ECE-1 also highlights that receptor trafficking, particularly the rate limiting steps, may be agonist-specific. Such differences could have major implications to the signalling outputs. Exendin-4 is used clinically in the treatment of type 2 diabetes and although it displays similar functions to GLP-1 including reducing blood glucose levels, promoting weight loss and providing some β-cell protection (DeFronzo et al., 2005, Li et al., 2013b, Abe et al., 2013), it does have a range of unexpected and unwanted functions such as gastrointestinal side effects and an increased risk of pancreatitis. The mechanisms by which these effects occur are unknown. The *in vivo* activity of compound 2 is unclear, but it appears to show bias for β-arrestin-mediated scaffolding function **(see Chapter 5)** (Wootten et al., 2013). Taken together, GLP-1R trafficking might be highly regulated by both the nature of the ligand and its concentration. These may well dictate cellular and physiological functions and are worthy of further exploration.

Presently there is a desire for small molecule agonists of the GLP-1R given the

problems associated with using peptide ligands. Importantly, the present study shows that the allosteric agonist, compound 2, potentiates the activity of the metabolite of GLP-1 7-36 amide, GLP-1 9-36 amide, in a variety of signalling pathways. Considering that the combination of GLP-1 9-36 amide and compound 2 resulted in the activation of GLP-1R-mediated signalling pathways similar to that induced by GLP-1 7-36 amide, it might be expected that the combination may have similar physiological functions to GLP-1 7-36 amide. Indeed, a recent study demonstrated that such allosteric-orthosteric interactions positively regulate insulin release in rats (Wootten et al., 2012). Whether this also regulates other anti-diabetic effects such as improving β-cell mass and weight reduction needs to be further explored.

In summary, the present study suggested a role for endosomal ECE-1 activity in regulating GLP-1-induced signalling and trafficking of the GLP-1R. Different ligands showed different sensitivities to ECE-1 inhibition both in re-sensitisation and in aspects of signalling. Additionally, the data showed that an allosteric agonist of the GLP-1R could potentiate the activity of GLP-1 9-36 amide, a metabolite of GLP-1 7-36 amide. These data highlight the possibility of different and more targeted approaches to the design of ligands at the GLP-1R and indeed other receptors that may provide improved or novel therapeutic strategies.

REFERENCE

ABE, H., UCHIDA, T., HARA, A., MIZUKAMI, H., KOMIYA, K., KOIKE, M., SHIGIHARA, N., TOYOFUKU, Y., OGIHARA, T., UCHIYAMA, Y., YAGIHASHI, S., FUJITANI, Y. & WATADA, H. 2013. Exendin-4 improves β-cell function in autophagy-deficient β-cells. *Endocrinology,* 154**,** 4512-24.

ADAMS, J. M. & CORY, S. 2007. Bcl-2-regulated apoptosis: mechanism and therapeutic potential. *Curr Opin Immunol,* 19**,** 488-96.

AHN, K., SISNEROS, A. M., HERMAN, S. B., PAN, S. M., HUPE, D., LEE, C., NIKAM, S., CHENG, X. M., DOHERTY, A. M., SCHROEDER, R. L., HALEEN, S. J., KAW, S., EMOTO, N. & YANAGISAWA, M. 1998. Novel selective quinazoline inhibitors of endothelin converting enzyme-1. *Biochem Biophys Res Commun,* 243**,** 184-90.

AL-SABAH, S. & DONNELLY, D. 2003. A model for receptor-peptide binding at the glucagon-like peptide-1 (GLP-1) receptor through the analysis of truncated ligands and receptors. *Br J Pharmacol,* 140**,** 339-46.

ALHOSAINI, K. A. 2011. *Signalling, Desensitization and Resensitization of Neuromedin U Receptors*, University of Leicester.

ALVAREZ, E., MARTINEZ, M. D., RONCERO, I., CHOWEN, J. A., GARCIA-CUARTERO, B., GISPERT, J. D., SANZ, C., VAZQUEZ, P., MALDONADO, A., DE CACERES, J., DESCO, M., POZO, M. A. & BLAZQUEZ, E. 2005. The expression of GLP-1 receptor mRNA and protein allows the effect of GLP-1 on glucose metabolism in the human hypothalamus and brainstem. *J Neurochem,* 92**,** 798-806.

ANBORGH, P. H., SEACHRIST, J. L., DALE, L. B. & FERGUSON, S. S. 2000. Receptor/beta-arrestin complex formation and the differential trafficking and resensitization of beta2-adrenergic and angiotensin II type 1A receptors. *Mol Endocrinol,* 14**,** 2040-53.

ARAÚJO, T. G., OLIVEIRA, A. G. & SAAD, M. J. 2013. Insulin-Resistance-Associated Compensatory Mechanisms of Pancreatic Beta Cells: A Current Opinion. *Front Endocrinol (Lausanne),* 4**,** 146.

ARNETTE, D., GIBSON, T. B., LAWRENCE, M. C., JANUARY, B., KHOO, S., MCGLYNN, K., VANDERBILT, C. A. & COBB, M. H. 2003. Regulation of ERK1 and ERK2 by glucose and peptide hormones in pancreatic beta cells. *J Biol Chem,* 278**,** 32517-25.

ARNOUTS, P., BOLIGNANO, D., NISTOR, I., BILO, H., GNUDI, L., HEAF, J. & BIESEN, W. V. 2013. Glucose-lowering drugs in patients with chronic kidney

disease: a narrative review on pharmacokinetic properties. *Nephrol Dial Transplant*.

ASSOCIATION, A. D. 2011. Diagnosis and classification of diabetes mellitus. *Diabetes Care,* 34 Suppl 1**,** S62-9.

AUTHIER, F., MÉTIOUI, M., BELL, A. W. & MORT, J. S. 1999. Negative regulation of epidermal growth factor signaling by selective proteolytic mechanisms in the endosome mediated by cathepsin B. *J Biol Chem,* 274**,** 33723-31.

AZARANI, A., BOILEAU, G. & CRINE, P. 1998. Recombinant human endothelin-converting enzyme ECE-1b is located in an intracellular compartment when expressed in polarized Madin-Darby canine kidney cells. *Biochem J,* 333 (Pt 2)**,** 439-48.

BAGGER, J. I., KNOP, F. K., LUND, A., VESTERGAARD, H., HOLST, J. J. & VILSBØLL, T. 2011. Impaired regulation of the incretin effect in patients with type 2 diabetes. *J Clin Endocrinol Metab,* 96**,** 737-45.

BAGGIO, L. L., KIM, J. G. & DRUCKER, D. J. 2004. Chronic exposure to GLP-1R agonists promotes homologous GLP-1 receptor desensitization in vitro but does not attenuate GLP-1R-dependent glucose homeostasis in vivo. *Diabetes,* 53 Suppl 3**,** S205-14.

BARNETT, A. H. 2005. Preventing renal complications in diabetic patients: the Diabetics Exposed to Telmisartan And enalaprIL (DETAIL) study. *Acta Diabetol,* 42 Suppl 1**,** S42-9.

BAZARSUREN, A., GRAUSCHOPF, U., WOZNY, M., REUSCH, D., HOFFMANN, E., SCHAEFER, W., PANZNER, S. & RUDOLPH, R. 2002. In vitro folding, functional characterization, and disulfide pattern of the extracellular domain of human GLP-1 receptor. *Biophys Chem,* 96**,** 305-18.

BENDTSEN, F., SCHIFTER, S. & HENRIKSEN, J. H. 1991. Increased circulating calcitonin gene-related peptide (CGRP) in cirrhosis. *J Hepatol,* 12**,** 118-23.

BERGMANN, A. 2002. Survival signaling goes BAD. *Dev Cell,* 3**,** 607-8.

BERNAL-MIZRACHI, E., WEN, W., STAHLHUT, S., WELLING, C. M. & PERMUTT, M. A. 2001. Islet beta cell expression of constitutively active Akt1/PKB alpha induces striking hypertrophy, hyperplasia, and hyperinsulinemia. *J Clin Invest,* 108**,** 1631-8.

BLAIS, V., FUGÈRE, M., DENAULT, J. B., KLARSKOV, K., DAY, R. & LEDUC, R. 2002. Processing of proendothelin-1 by members of the subtilisin-like pro-protein convertase family. *FEBS Lett,* 524**,** 43-8.

BOHN, L. M., GAINETDINOV, R. R., LIN, F. T., LEFKOWITZ, R. J. & CARON, M. G. 2000. Mu-opioid receptor desensitization by beta-arrestin-2 determines morphine tolerance but not dependence. *Nature,* 408**,** 720-3.

BOHN, L. M., LEFKOWITZ, R. J., GAINETDINOV, R. R., PEPPEL, K., CARON, M. G. & LIN, F. T. 1999. Enhanced morphine analgesia in mice lacking beta-arrestin 2. *Science,* 286**,** 2495-8.

BOOTMAN, M. D. & RODERICK, H. L. 2011. Using Calcium Imaging as a Readout of GPCR Activation. *Methods Mol Biol,* 746**,** 277-96.

BRIAUD, I., LINGOHR, M. K., DICKSON, L. M., WREDE, C. E. & RHODES, C. J. 2003. Differential activation mechanisms of Erk-1/2 and p70(S6K) by glucose in pancreatic beta-cells. *Diabetes,* 52**,** 974-83.

BROWN, B. L., ALBANO, J. D., EKINS, R. P. & SGHERZI, A. M. 1971. A simple and sensitive saturation assay method for the measurement of adenosine 3':5'-cyclic monophosphate. *Biochem J,* 121**,** 561-2.

BROWN, J. C. & PEDERSON, R. A. 1970. Cleavage of a gastric inhibitory polypeptide with cyanogen bromide and the physiological action of the C-terminal fragment. *J Physiol,* 210**,** 52P-53P.

BUTEAU, J., FOISY, S., JOLY, E. & PRENTKI, M. 2003. Glucagon-like peptide 1 induces pancreatic beta-cell proliferation via transactivation of the epidermal growth factor receptor. *Diabetes,* 52**,** 124-32.

BUTLER, A. E., JANSON, J., BONNER-WEIR, S., RITZEL, R., RIZZA, R. A. & BUTLER, P. C. 2003. Beta-cell deficit and increased beta-cell apoptosis in humans with type 2 diabetes. *Diabetes,* 52**,** 102-10.

CALEBIRO, D., NIKOLAEV, V. O., GAGLIANI, M. C., DE FILIPPIS, T., DEES, C., TACCHETTI, C., PERSANI, L. & LOHSE, M. J. 2009. Persistent cAMP-signals triggered by internalized G-protein-coupled receptors. *PLoS Biol,* 7**,** e1000172.

CAMPS, M., CAROZZI, A., SCHNABEL, P., SCHEER, A., PARKER, P. J. & GIERSCHIK, P. 1992. Isozyme-selective stimulation of phospholipase C-beta 2 by G protein beta gamma-subunits. *Nature,* 360**,** 684-6.

CASTRO-OBREGÓN, S., RAO, R. V., DEL RIO, G., CHEN, S. F., POKSAY, K. S., RABIZADEH, S., VESCE, S., ZHANG, X. K., SWANSON, R. A. & BREDESEN, D. E. 2004. Alternative, nonapoptotic programmed cell death: mediation by arrestin 2, ERK2, and Nur77. *J Biol Chem,* 279**,** 17543-53.

CHAI, T. F., HONG, S. Y., HE, H., ZHENG, L., HAGEN, T., LUO, Y. & YU, F. X. 2012. A potential mechanism of metformin-mediated regulation of glucose

homeostasis: inhibition of Thioredoxin-interacting protein (Txnip) gene expression. *Cell Signal,* 24**,** 1700-5.

CHANDRA, R. & LIDDLE, R. A. 2012. Neurohormonal regulation of pancreatic secretion. *Curr Opin Gastroenterol,* 28**,** 483-7.

CHANG, Y., GHANSAH, E., CHEN, Y., YE, J. & WEISS, D. S. 2002. Desensitization mechanism of GABA receptors revealed by single oocyte binding and receptor function. *J Neurosci,* 22**,** 7982-90.

CHEN, D., LIAO, J., LI, N., ZHOU, C., LIU, Q., WANG, G., ZHANG, R., ZHANG, S., LIN, L., CHEN, K., XIE, X., NAN, F., YOUNG, A. A. & WANG, M. W. 2007. A nonpeptidic agonist of glucagon-like peptide 1 receptors with efficacy in diabetic db/db mice. *Proc Natl Acad Sci U S A,* 104**,** 943-8.

CHEONG, Y. H., KIM, M. K., SON, M. H. & KAANG, B. K. 2012. Two small molecule agonists of glucagon-like peptide-1 receptor modulate the receptor activation response differently. *Biochem Biophys Res Commun,* 417**,** 558-63.

CHIASSON, J. L. 2009. Early insulin use in type 2 diabetes: what are the cons? *Diabetes Care,* 32 Suppl 2**,** S270-4.

COOPER, D. M. 2003. Regulation and organization of adenylyl cyclases and cAMP. *Biochem J,* 375**,** 517-29.

COOPMAN, K., HUANG, Y., JOHNSTON, N., BRADLEY, S. J., WILKINSON, G. F. & WILLARS, G. B. 2010. Comparative effects of the endogenous agonist glucagon-like peptide-1 (GLP-1)-(7-36) amide and the small-molecule ago-allosteric agent "compound 2" at the GLP-1 receptor. *J Pharmacol Exp Ther,* 334**,** 795-808.

COOPMAN, K., WALLIS, R., ROBB, G., BROWN, A. J., WILKINSON, G. F., TIMMS, D. & WILLARS, G. B. 2011. Residues within the transmembrane domain of the glucagon-like peptide-1 receptor involved in ligand binding and receptor activation: modelling the ligand-bound receptor. *Mol Endocrinol,* 25**,** 1804-18.

COSTES, S., BROCA, C., BERTRAND, G., LAJOIX, A. D., BATAILLE, D., BOCKAERT, J. & DALLE, S. 2006. ERK1/2 control phosphorylation and protein level of cAMP-responsive element-binding protein: a key role in glucose-mediated pancreatic beta-cell survival. *Diabetes,* 55**,** 2220-30.

COTTRELL, G. S., PADILLA, B. E., AMADESI, S., POOLE, D. P., MURPHY, J. E., HARDT, M., ROOSTERMAN, D., STEINHOFF, M. & BUNNETT, N. W. 2009. Endosomal endothelin-converting enzyme-1: a regulator of beta-arrestin-dependent ERK signaling. *J Biol Chem,* 284**,** 22411-25.

DATTA, S. R., KATSOV, A., HU, L., PETROS, A., FESIK, S. W., YAFFE, M. B. & GREENBERG, M. E. 2000. 14-3-3 proteins and survival kinases cooperate to inactivate BAD by BH3 domain phosphorylation. *Mol Cell,* 6**,** 41-51.

DAVIS, C. G., GOLDSTEIN, J. L., SÜDHOF, T. C., ANDERSON, R. G., RUSSELL, D. W. & BROWN, M. S. 1987. Acid-dependent ligand dissociation and recycling of LDL receptor mediated by growth factor homology region. *Nature,* 326**,** 760-5.

DE BEER, K., MICHAEL, S., THACKER, M., WYNNE, E., PATTNI, C., GOMM, M., BALL, C., WALSH, D., THOMLINSON, A. & ULLAH, K. 2008. Diabetic ketoacidosis and hyperglycaemic hyperosmolar syndrome - clinical guidelines. *Nurs Crit Care,* 13**,** 5-11.

DE ROOIJ, J., ZWARTKRUIS, F. J., VERHEIJEN, M. H., COOL, R. H., NIJMAN, S. M., WITTINGHOFER, A. & BOS, J. L. 1998. Epac is a Rap1 guanine-nucleotide-exchange factor directly activated by cyclic AMP. *Nature,* 396**,** 474-7.

DEACON, C. F. & AHRÉN, B. 2011. Physiology of incretins in health and disease. *Rev Diabet Stud,* 8**,** 293-306.

DEACON, C. F., JOHNSEN, A. H. & HOLST, J. J. 1995. Degradation of glucagon-like peptide-1 by human plasma in vitro yields an N-terminally truncated peptide that is a major endogenous metabolite in vivo. *J Clin Endocrinol Metab,* 80**,** 952-7.

DEACON, C. F., PLAMBOECK, A., MØLLER, S. & HOLST, J. J. 2002. GLP-1-(9-36) amide reduces blood glucose in anesthetized pigs by a mechanism that does not involve insulin secretion. *Am J Physiol Endocrinol Metab,* 282**,** E873-9.

DEFEA, K. A., VAUGHN, Z. D., O'BRYAN, E. M., NISHIJIMA, D., DERY, O. & BUNNETT, N. W. 2000. The proliferative and antiapoptotic effects of substance P are facilitated by formation of a beta -arrestin-dependent scaffolding complex. *Proc Natl Acad Sci U S A,* 97**,** 11086-91.

DEFRONZO, R. A., RATNER, R. E., HAN, J., KIM, D. D., FINEMAN, M. S. & BARON, A. D. 2005. Effects of exenatide (exendin-4) on glycemic control and weight over 30 weeks in metformin-treated patients with type 2 diabetes. *Diabetes Care,* 28**,** 1092-100.

DELMEIRE, D., FLAMEZ, D., HINKE, S. A., CALI, J. J., PIPELEERS, D. & SCHUIT, F. 2003. Type VIII adenylyl cyclase in rat beta cells: coincidence signal detector/generator for glucose and GLP-1. *Diabetologia,* 46**,** 1383-93.

DENAULT, J. B., D'ORLÉANS-JUSTE, P., MASAKI, T. & LEDUC, R. 1995. Inhibition of convertase-related processing of proendothelin-1. *J Cardiovasc Pharmacol,* 26 Suppl 3**,** S47-50.

DEWIRE, S. M., AHN, S., LEFKOWITZ, R. J. & SHENOY, S. K. 2007. Beta-arrestins and cell signaling. *Annu Rev Physiol,* 69**,** 483-510.

DIABETES, U.K. 2012. *http://www.diabetes.org.uk/About_us/News_Landing_Page/NHS-spending-on-diabetes-to-reach-169-billion-by-2035/* [Online].

DING, W. G. & GROMADA, J. 1997. Protein kinase A-dependent stimulation of exocytosis in mouse pancreatic beta-cells by glucose-dependent insulinotropic polypeptide. *Diabetes,* 46**,** 615-21.

DOYLE, M. E. & EGAN, J. M. 2007. Mechanisms of action of glucagon-like peptide 1 in the pancreas. *Pharmacol Ther,* 113**,** 546-93.

DRUCKER, D. J. 2006. The biology of incretin hormones. *Cell Metab,* 3**,** 153-65.

DYACHOK, O. & GYLFE, E. 2004. Ca(2+)-induced Ca(2+) release via inositol 1,4,5-trisphosphate receptors is amplified by protein kinase A and triggers exocytosis in pancreatic beta-cells. *J Biol Chem,* 279**,** 45455-61.

DYACHOK, O., ISAKOV, Y., SÅGETORP, J. & TENGHOLM, A. 2006. Oscillations of cyclic AMP in hormone-stimulated insulin-secreting beta-cells. *Nature,* 439**,** 349-52.

EBERT, R., UNGER, H. & CREUTZFELDT, W. 1983. Preservation of incretin activity after removal of gastric inhibitory polypeptide (GIP) from rat gut extracts by immunoadsorption. *Diabetologia,* 24**,** 449-54.

ECKEL, R. H., KAHN, S. E., FERRANNINI, E., GOLDFINE, A. B., NATHAN, D. M., SCHWARTZ, M. W., SMITH, R. J. & SMITH, S. R. 2011. Obesity and type 2 diabetes: what can be unified and what needs to be individualized? *J Clin Endocrinol Metab,* 96**,** 1654-63.

EDELMAN, S. V., LAAKSO, M., WALLACE, P., BRECHTEL, G., OLEFSKY, J. M. & BARON, A. D. 1990. Kinetics of insulin-mediated and non-insulin-mediated glucose uptake in humans. *Diabetes,* 39**,** 955-64.

EDWARDS, C. M., TODD, J. F., MAHMOUDI, M., WANG, Z., WANG, R. M., GHATEI, M. A. & BLOOM, S. R. 1999. Glucagon-like peptide 1 has a physiological role in the control of postprandial glucose in humans: studies with the antagonist exendin 9-39. *Diabetes,* 48**,** 86-93.

EMOTO, N. & YANAGISAWA, M. 1995. Endothelin-converting enzyme-2 is a membrane-bound, phosphoramidon-sensitive metalloprotease with acidic pH optimum. *J Biol Chem,* 270**,** 15262-8.

FAHNOE, D. C., KNAPP, J., JOHNSON, G. D. & AHN, K. 2000. Inhibitor potencies

and substrate preference for endothelin-converting enzyme-1 are dramatically affected by pH. *J Cardiovasc Pharmacol,* 36**,** S22-5.

FARILLA, L., BULOTTA, A., HIRSHBERG, B., LI CALZI, S., KHOURY, N., NOUSHMEHR, H., BERTOLOTTO, C., DI MARIO, U., HARLAN, D. M. & PERFETTI, R. 2003. Glucagon-like peptide 1 inhibits cell apoptosis and improves glucose responsiveness of freshly isolated human islets. *Endocrinology,* 144**,** 5149-58.

FARILLA, L., HUI, H., BERTOLOTTO, C., KANG, E., BULOTTA, A., DI MARIO, U. & PERFETTI, R. 2002. Glucagon-like peptide-1 promotes islet cell growth and inhibits apoptosis in Zucker diabetic rats. *Endocrinology,* 143**,** 4397-408.

FEHMANN, H. C., PRACHT, A. & GÖKE, B. 1998. High-level expression of the GLP-I receptor results in receptor desensitization. *Pancreas,* 17**,** 309-14.

FERGUSON, S. S. 2001. Evolving concepts in G protein-coupled receptor endocytosis: the role in receptor desensitization and signaling. *Pharmacol Rev,* 53**,** 1-24.

FERGUSON, S. S., MENARD, L., BARAK, L. S., KOCH, W. J., COLAPIETRO, A. M. & CARON, M. G. 1995. Role of phosphorylation in agonist-promoted beta 2-adrenergic receptor sequestration. Rescue of a sequestration-defective mutant receptor by beta ARK1. *J Biol Chem,* 270**,** 24782-9.

FERRANDON, S., FEINSTEIN, T. N., CASTRO, M., WANG, B., BOULEY, R., POTTS, J. T., GARDELLA, T. J. & VILARDAGA, J. P. 2009. Sustained cyclic AMP production by parathyroid hormone receptor endocytosis. *Nat Chem Biol,* 5**,** 734-42.

FINEMAN, M. S., BICSAK, T. A., SHEN, L. Z., TAYLOR, K., GAINES, E., VARNS, A., KIM, D. & BARON, A. D. 2003. Effect on glycemic control of exenatide (synthetic exendin-4) additive to existing metformin and/or sulfonylurea treatment in patients with type 2 diabetes. *Diabetes Care,* 26**,** 2370-7.

FONG, D. S., AIELLO, L. P., FERRIS, F. L. & KLEIN, R. 2004. Diabetic retinopathy. *Diabetes Care,* 27**,** 2540-53.

FORBES, J. M. & COOPER, M. E. 2013. Mechanisms of diabetic complications. *Physiol Rev,* 93**,** 137-88.

FUKURODA, T., NOGUCHI, K., TSUCHIDA, S., NISHIKIBE, M., IKEMOTO, F., OKADA, K. & YANO, M. 1990. Inhibition of biological actions of big endothelin-1 by phosphoramidon. *Biochem Biophys Res Commun,* 172**,** 390-5.

GANCEDO, J. M. 2013. Biological roles of cAMP: variations on a theme in the different kingdoms of life. *Biol Rev Camb Philos Soc,* 88**,** 645-68.

GARBER, A. J. 2010. Incretin-based therapies in the management of type 2 diabetes: rationale and reality in a managed care setting. *Am J Manag Care,* 16**,** S187-94.

GHOSH, M. & SCHONBRUNN, A. 2011. Differential temporal and spatial regulation of somatostatin receptor phosphorylation and dephosphorylation. *J Biol Chem,* 286**,** 13561-73.

GLOERICH, M. & BOS, J. L. 2010. Epac: defining a new mechanism for cAMP action. *Annu Rev Pharmacol Toxicol,* 50**,** 355-75.

GOMEZ, E., PRITCHARD, C. & HERBERT, T. P. 2002. cAMP-dependent protein kinase and Ca2+ influx through L-type voltage-gated calcium channels mediate Raf-independent activation of extracellular regulated kinase in response to glucagon-like peptide-1 in pancreatic beta-cells. *J Biol Chem,* 277**,** 48146-51.

GRADY, E. F., GARLAND, A. M., GAMP, P. D., LOVETT, M., PAYAN, D. G. & BUNNETT, N. W. 1995. Delineation of the endocytic pathway of substance P and its seven-transmembrane domain NK1 receptor. *Mol Biol Cell,* 6**,** 509-24.

GRIBBLE, F. M., WILLIAMS, L., SIMPSON, A. K. & REIMANN, F. 2003. A novel glucose-sensing mechanism contributing to glucagon-like peptide-1 secretion from the GLUTag cell line. *Diabetes,* 52**,** 1147-54.

GROMADA, J., BROCK, B., SCHMITZ, O. & RORSMAN, P. 2004. Glucagon-like peptide-1: regulation of insulin secretion and therapeutic potential. *Basic Clin Pharmacol Toxicol,* 95**,** 252-62.

GROMADA, J., DING, W. G., BARG, S., RENSTRÖM, E. & RORSMAN, P. 1997. Multisite regulation of insulin secretion by cAMP-increasing agonists: evidence that glucagon-like peptide 1 and glucagon act via distinct receptors. *Pflugers Arch,* 434**,** 515-24.

GROMADA, J., DISSING, S. & RORSMAN, P. 1996. Desensitization of glucagon-like peptide 1 receptors in insulin-secreting beta TC3 cells: role of PKA-independent mechanisms. *Br J Pharmacol,* 118**,** 769-75.

GROOP, L. & POCIOT, F. 2014. Genetics of diabetes - Are we missing the genes or the disease? *Mol Cell Endocrinol,* 382**,** 726-39.

GROVER, G. J., SLEPH, P. G., FOX, M. & TRIPPODO, N. C. 1992. Role of endothelin-1 and big endothelin-1 in modulating coronary vascular tone, contractile function and severity of ischemia in rat hearts. *J Pharmacol Exp Ther,* 263**,** 1074-82.

GUREVICH, V. V. & GUREVICH, E. V. 2006. The structural basis of arrestin-mediated regulation of G-protein-coupled receptors. *Pharmacol Ther,* 110**,** 465-502.

GÖKE, R., WAGNER, B., FEHMANN, H. C. & GÖKE, B. 1993. Glucose-dependency of the insulin stimulatory effect of glucagon-like peptide-1 (7-36) amide on the rat pancreas. *Res Exp Med (Berl),* 193**,** 97-103.

HAGEN, T., TAYLOR, C. T., LAM, F. & MONCADA, S. 2003. Redistribution of intracellular oxygen in hypoxia by nitric oxide: effect on HIF1alpha. *Science,* 302**,** 1975-8.

HANSEN, L., DEACON, C. F., ORSKOV, C. & HOLST, J. J. 1999. Glucagon-like peptide-1-(7-36)amide is transformed to glucagon-like peptide-1-(9-36)amide by dipeptidyl peptidase IV in the capillaries supplying the L cells of the porcine intestine. *Endocrinology,* 140**,** 5356-63.

HASDEMIR, B., MAHAJAN, S., BUNNETT, N. W., LIAO, M. & BHARGAVA, A. 2012. Endothelin-converting enzyme-1 actions determine differential trafficking and signaling of corticotropin-releasing factor receptor 1 at high agonist concentrations. *Mol Endocrinol,* 26**,** 681-95.

HASHIGUCHI, H., NAKAZAKI, M., KORIYAMA, N., FUKUDOME, M., ASO, K. & TEI, C. 2006. Cyclic AMP/cAMP-GEF pathway amplifies insulin exocytosis induced by Ca2+ and ATP in rat islet beta-cells. *Diabetes Metab Res Rev,* 22**,** 64-71.

HAUGH, J. M., SCHOOLER, K., WELLS, A., WILEY, H. S. & LAUFFENBURGER, D. A. 1999. Effect of epidermal growth factor receptor internalization on regulation of the phospholipase C-gamma1 signaling pathway. *J Biol Chem,* 274**,** 8958-65.

HAUSDORFF, W. P., CARON, M. G. & LEFKOWITZ, R. J. 1990. Turning off the signal: desensitization of beta-adrenergic receptor function. *FASEB J,* 4**,** 2881-9.

HE, M. L., KOSHIMIZU, T. A., TOMIĆ, M. & STOJILKOVIC, S. S. 2002. Purinergic P2X(2) receptor desensitization depends on coupling between ectodomain and C-terminal domain. *Mol Pharmacol,* 62**,** 1187-97.

HEIN, L., ISHII, K., COUGHLIN, S. R. & KOBILKA, B. K. 1994. Intracellular targeting and trafficking of thrombin receptors. A novel mechanism for resensitization of a G protein-coupled receptor. *J Biol Chem,* 269**,** 27719-26.

HELLER, R. S., KIEFFER, T. J. & HABENER, J. F. 1996. Point mutations in the first and third intracellular loops of the glucagon-like peptide-1 receptor alter intracellular signaling. *Biochem Biophys Res Commun,* 223**,** 624-32.

HENRIKSEN, J. H., STAUN-OLSEN, P., BORG MOGENSEN, N. & FAHRENKRUG, J. 1986. Circulating endogenous vasoactive intestinal polypeptide (VIP) in patients with uraemia and liver cirrhosis. *Eur J Clin Invest,* 16**,** 211-6.

HENRIKSEN, J. H., TRONIER, B. & BÜLOW, J. B. 1987. Kinetics of circulating endogenous insulin, C-peptide, and proinsulin in fasting nondiabetic man. *Metabolism,* 36**,** 463-8.

HIRST, J. A., FARMER, A. J., ALI, R., ROBERTS, N. W. & STEVENS, R. J. 2012. Quantifying the effect of metformin treatment and dose on glycemic control. *Diabetes Care,* 35**,** 446-54.

HOANG, M. V. & TURNER, A. J. 1997. Novel activity of endothelin-converting enzyme: hydrolysis of bradykinin. *Biochem J,* 327 (Pt 1)**,** 23-6.

HOARE, S. R. 2005. Mechanisms of peptide and nonpeptide ligand binding to Class B G-protein-coupled receptors. *Drug Discov Today,* 10**,** 417-27.

HUANG, Y. 2010. *Exploring the Structure, Function & Regulation of the Human Glucagon-Like Peptide-1 Receptor*, University of Leicester.

HÄLLBRINK, M., HOLMQVIST, T., OLSSON, M., OSTENSON, C. G., EFENDIC, S. & LANGEL, U. 2001. Different domains in the third intracellular loop of the GLP-1 receptor are responsible for Galpha(s) and Galpha(i)/Galpha(o) activation. *Biochim Biophys Acta,* 1546**,** 79-86.

IKEDA, S. R. 1996. Voltage-dependent modulation of N-type calcium channels by G-protein beta gamma subunits. *Nature,* 380**,** 255-8.

IKEGAWA, R., MATSUMURA, Y., TSUKAHARA, Y., TAKAOKA, M. & MORIMOTO, S. 1990. Phosphoramidon, a metalloproteinase inhibitor, suppresses the secretion of endothelin-1 from cultured endothelial cells by inhibiting a big endothelin-1 converting enzyme. *Biochem Biophys Res Commun,* 171**,** 669-75.

JAFRI, F. & ERGUL, A. 2006. Phosphorylation of endothelin converting enzyme-1 isoforms: relevance to subcellular localization. *Exp Biol Med (Maywood),* 231**,** 713-7.

JANG, H. J., KOKRASHVILI, Z., THEODORAKIS, M. J., CARLSON, O. D., KIM, B. J., ZHOU, J., KIM, H. H., XU, X., CHAN, S. L., JUHASZOVA, M., BERNIER, M., MOSINGER, B., MARGOLSKEE, R. F. & EGAN, J. M. 2007. Gut-expressed gustducin and taste receptors regulate secretion of glucagon-like peptide-1. *Proc Natl Acad Sci U S A,* 104**,** 15069-74.

JHALA, U. S., CANETTIERI, G., SCREATON, R. A., KULKARNI, R. N., KRAJEWSKI, S., REED, J., WALKER, J., LIN, X., WHITE, M. & MONTMINY, M. 2003. cAMP promotes pancreatic beta-cell survival via CREB-mediated induction of IRS2. *Genes Dev,* 17**,** 1575-80.

JOHNSON, G. D., STEVENSON, T. & AHN, K. 1999. Hydrolysis of peptide hormones

by endothelin-converting enzyme-1. A comparison with neprilysin. *J Biol Chem,* 274**,** 4053-8.

JUHL, C. B., HOLLINGDAL, M., STURIS, J., JAKOBSEN, G., AGERSØ, H., VELDHUIS, J., PØRKSEN, N. & SCHMITZ, O. 2002. Bedtime administration of NN2211, a long-acting GLP-1 derivative, substantially reduces fasting and postprandial glycemia in type 2 diabetes. *Diabetes,* 51**,** 424-9.

KADAMUR, G. & ROSS, E. M. 2013. Mammalian phospholipase C. *Annu Rev Physiol,* 75**,** 127-54.

KANG, G., CHEPURNY, O. G., RINDLER, M. J., COLLIS, L., CHEPURNY, Z., LI, W. H., HARBECK, M., ROE, M. W. & HOLZ, G. G. 2005. A cAMP and Ca2+ coincidence detector in support of Ca2+-induced Ca2+ release in mouse pancreatic beta cells. *J Physiol,* 566**,** 173-88.

KANG, G., JOSEPH, J. W., CHEPURNY, O. G., MONACO, M., WHEELER, M. B., BOS, J. L., SCHWEDE, F., GENIESER, H. G. & HOLZ, G. G. 2003. Epac-selective cAMP analog 8-pCPT-2'-O-Me-cAMP as a stimulus for Ca2+-induced Ca2+ release and exocytosis in pancreatic beta-cells. *J Biol Chem,* 278**,** 8279-85.

KAWASAKI, H., SPRINGETT, G. M., MOCHIZUKI, N., TOKI, S., NAKAYA, M., MATSUDA, M., HOUSMAN, D. E. & GRAYBIEL, A. M. 1998. A family of cAMP-binding proteins that directly activate Rap1. *Science,* 282**,** 2275-9.

KELLY, E., BAILEY, C. P. & HENDERSON, G. 2008. Agonist-selective mechanisms of GPCR desensitization. *Br J Pharmacol,* 153 Suppl 1**,** S379-88.

KEOV, P., SEXTON, P. M. & CHRISTOPOULOS, A. 2011. Allosteric modulation of G protein-coupled receptors: a pharmacological perspective. *Neuropharmacology,* 60**,** 24-35.

KEYNAN, S., KHAMAISI, M., DAHAN, R., BARNES, K., JACKSON, C. D., TURNER, A. J. & RAZ, I. 2004. Increased expression of endothelin-converting enzyme-1c isoform in response to high glucose levels in endothelial cells. *J Vasc Res,* 41**,** 131-40.

KHAN, S. M., SLENO, R., GORA, S., ZYLBERGOLD, P., LAVERDURE, J. P., LABBÉ, J. C., MILLER, G. J. & HÉBERT, T. E. 2013. The expanding roles of Gβγ subunits in G protein-coupled receptor signaling and drug action. *Pharmacol Rev,* 65**,** 545-77.

KHOO, S., GRIFFEN, S. C., XIA, Y., BAER, R. J., GERMAN, M. S. & COBB, M. H. 2003. Regulation of insulin gene transcription by ERK1 and ERK2 in pancreatic beta cells. *J Biol Chem,* 278**,** 32969-77.

KIEFFER, T. J., MCINTOSH, C. H. & PEDERSON, R. A. 1995. Degradation of glucose-dependent insulinotropic polypeptide and truncated glucagon-like peptide 1 in vitro and in vivo by dipeptidyl peptidase IV. *Endocrinology,* 136**,** 3585-96.

KIESS, W., KESSLER, U., FUNK, B. & HOEFLICH, A. 1994. Perturbation of C6 glial cells by acetate leads to modulation of [125I]IGF-II binding to the IGF-II/M6P receptor: implications for ligand internalization studies. *Biochim Biophys Acta,* 1223**,** 179-84.

KLIEWER, A. & SCHULZ, S. 2013. Differential regulation of somatostatin receptor dephosphorylation by β-arrestin1 and β-arrestin2. *Naunyn Schmiedebergs Arch Pharmacol,* 387, 263-9.

KNIP, M., VEIJOLA, R., VIRTANEN, S. M., HYÖTY, H., VAARALA, O. & AKERBLOM, H. K. 2005. Environmental triggers and determinants of type 1 diabetes. *Diabetes,* 54 Suppl 2**,** S125-36.

KNUDSEN, L. B., KIEL, D., TENG, M., BEHRENS, C., BHUMRALKAR, D., KODRA, J. T., HOLST, J. J., JEPPESEN, C. B., JOHNSON, M. D., DE JONG, J. C., JORGENSEN, A. S., KERCHER, T., KOSTROWICKI, J., MADSEN, P., OLESEN, P. H., PETERSEN, J. S., POULSEN, F., SIDELMANN, U. G., STURIS, J., TRUESDALE, L., MAY, J. & LAU, J. 2007. Small-molecule agonists for the glucagon-like peptide 1 receptor. *Proc Natl Acad Sci U S A,* 104**,** 937-42.

KNUDSEN, L. B. & PRIDAL, L. 1996. Glucagon-like peptide-1-(9-36) amide is a major metabolite of glucagon-like peptide-1-(7-36) amide after in vivo administration to dogs, and it acts as an antagonist on the pancreatic receptor. *Eur J Pharmacol,* 318**,** 429-35.

KOENIG, J. A., KAUR, R., DODGEON, I., EDWARDSON, J. M. & HUMPHREY, P. P. 1998. Fates of endocytosed somatostatin sst2 receptors and associated agonists. *Biochem J,* 336 (Pt 2)**,** 291-8.

KOMMADDI, R. P. & SHENOY, S. K. 2013. Arrestins and protein ubiquitination. *Prog Mol Biol Transl Sci,* 118**,** 175-204.

KOOLE, C., WOOTTEN, D., SIMMS, J., MILLER, L. J., CHRISTOPOULOS, A. & SEXTON, P. M. 2012. Second extracellular loop of human glucagon-like peptide-1 receptor (GLP-1R) has a critical role in GLP-1 peptide binding and receptor activation. *J Biol Chem,* 287**,** 3642-58.

KOOLE, C., WOOTTEN, D., SIMMS, J., VALANT, C., SRIDHAR, R., WOODMAN, O. L., MILLER, L. J., SUMMERS, R. J., CHRISTOPOULOS, A. & SEXTON, P. M. 2010. Allosteric ligands of the glucagon-like peptide 1 receptor (GLP-1R) differentially modulate endogenous and exogenous peptide responses in a

pathway-selective manner: implications for drug screening. *Mol Pharmacol,* 78**,** 456-65.

KORTH, P., BOHLE, R. M., CORVOL, P. & PINET, F. 1999. Cellular distribution of endothelin-converting enzyme-1 in human tissues. *J Histochem Cytochem,* 47**,** 447-62.

KOTOWSKI, S. J., HOPF, F. W., SEIF, T., BONCI, A. & VON ZASTROW, M. 2011. Endocytosis promotes rapid dopaminergic signaling. *Neuron,* 71**,** 278-90.

KOZAK, M. 1987. An analysis of 5'-noncoding sequences from 699 vertebrate messenger RNAs. *Nucleic Acids Res,* 15**,** 8125-48.

KREYMANN, B., WILLIAMS, G., GHATEI, M. A. & BLOOM, S. R. 1987. Glucagon-like peptide-1 7-36: a physiological incretin in man. *Lancet,* 2**,** 1300-4.

KRUEGER, K. M., DAAKA, Y., PITCHER, J. A. & LEFKOWITZ, R. J. 1997. The role of sequestration in G protein-coupled receptor resensitization. Regulation of beta2-adrenergic receptor dephosphorylation by vesicular acidification. *J Biol Chem,* 272**,** 5-8.

KUBALE, V., ABRAMOVIĆ, Z., POGACNIK, A., HEDING, A., SENTJURC, M. & VRECL, M. 2007. Evidence for a role of caveolin-1 in neurokinin-1 receptor plasma-membrane localization, efficient signaling, and interaction with beta-arrestin 2. *Cell Tissue Res,* 330**,** 231-45.

KUKKOLA, P. J., SAVAGE, P., SAKANE, Y., BERRY, J. C., BILCI, N. A., GHAI, R. D. & JENG, A. Y. 1995. Differential structure-activity relationships of phosphoramidon analogues for inhibition of three metalloproteases: endothelin-converting enzyme, neutral endopeptidase, and angiotensin-converting enzyme. *J Cardiovasc Pharmacol,* 26 Suppl 3**,** S65-8.

KUNA, R. S., GIRADA, S. B., ASALLA, S., VALLENTYNE, J., MADDIKA, S., PATTERSON, J. T., SMILEY, D. L., DIMARCHI, R. D. & MITRA, P. 2013. Glucagon-like peptide-1 receptor-mediated endosomal cAMP generation promotes glucose-stimulated insulin secretion in pancreatic β-cells. *Am J Physiol Endocrinol Metab,* 305**,** E161-70.

KURUPPU, S. & SMITH, A. I. 2012. Endothelin Converting Enzyme-1 phosphorylation and trafficking. *FEBS Lett,* 586**,** 2212-7.

KURUPPU, S., TOCHON-DANGUY, N. & SMITH, A. I. 2010. Role of Protein Kinase C in Endothelin Converting Enzyme-1 trafficking and shedding from endothelial cells. *Biochem Biophys Res Commun,* 398**,** 173-7.

KURUPPU, S., TOCHON-DANGUY, N. & SMITH, A. I. 2012. Protein Kinase C

recognition sites in the cytoplasmic domain of Endothelin Converting Enzyme-1c. *Biochem Biophys Res Commun,* 427**,** 606-10.

KURUPPU, S., TOCHON-DANGUY, N. & SMITH, A. I. 2013. Applicability of green fluorescence protein in the study of endothelin converting enzyme-1c trafficking. *Protein Sci,* 22**,** 306-13.

KUWAKI, T., KOSHIYA, N., CAO, W. H., TAKAHASHI, H., TERUI, N. & KUMADA, M. 1990. Modulatory effects of endothelin-1 on central cardiovascular control in rats. *Jpn J Physiol,* 40**,** 827-41.

KWON, G., MARSHALL, C. A., PAPPAN, K. L., REMEDI, M. S. & MCDANIEL, M. L. 2004. Signaling elements involved in the metabolic regulation of mTOR by nutrients, incretins, and growth factors in islets. *Diabetes,* 53 Suppl 3**,** S225-32.

LANG, J. 1999. Molecular mechanisms and regulation of insulin exocytosis as a paradigm of endocrine secretion. *Eur J Biochem,* 259**,** 3-17.

LAPANE, K. L., YANG, S., BROWN, M. J., JAWAHAR, R., PAGLIASOTTI, C. & RAJPATHAK, S. 2013. Sulfonylureas and risk of falls and fractures: a systematic review. *Drugs Aging,* 30**,** 527-47.

LAW, P. Y., ERICKSON, L. J., EL-KOUHEN, R., DICKER, L., SOLBERG, J., WANG, W., MILLER, E., BURD, A. L. & LOH, H. H. 2000. Receptor density and recycling affect the rate of agonist-induced desensitization of mu-opioid receptor. *Mol Pharmacol,* 58**,** 388-98.

LAWLOR, M. A. & ALESSI, D. R. 2001. PKB/Akt: a key mediator of cell proliferation, survival and insulin responses? *J Cell Sci,* 114**,** 2903-10.

LAWRENCE, M., SHAO, C., DUAN, L., MCGLYNN, K. & COBB, M. H. 2008. The protein kinases ERK1/2 and their roles in pancreatic beta cells. *Acta Physiol (Oxf),* 192**,** 11-7.

LAWRENCE, M. C., BHATT, H. S., WATTERSON, J. M. & EASOM, R. A. 2001. Regulation of insulin gene transcription by a Ca(2+)-responsive pathway involving calcineurin and nuclear factor of activated T cells. *Mol Endocrinol,* 15**,** 1758-67.

LAWRENCE, M. C., MCGLYNN, K., PARK, B. H. & COBB, M. H. 2005. ERK1/2-dependent activation of transcription factors required for acute and chronic effects of glucose on the insulin gene promoter. *J Biol Chem,* 280**,** 26751-9.

LEE, Y. S. & JUN, H. S. 2014. Anti-diabetic actions of glucagon-like peptide-1 on pancreatic beta-cells. *Metabolism,* 63**,** 9-19.

LEFKOWITZ, R. J., PITCHER, J., KRUEGER, K. & DAAKA, Y. 1998. Mechanisms of beta-adrenergic receptor desensitization and resensitization. *Adv Pharmacol,* 42**,** 416-20.

LEFKOWITZ, R. J. & SHENOY, S. K. 2005. Transduction of receptor signals by beta-arrestins. *Science,* 308**,** 512-7.

LENFERINK, A. E., KRAMER, R. H., VAN VUGT, M. J., KÖNIGSWIESER, M., DI FIORE, P. P., VAN ZOELEN, E. J. & VAN DE POLL, M. L. 1997. Superagonistic behaviour of epidermal growth factor/transforming growth factor-alpha chimaeras: correlation with receptor routing after ligand-induced internalization. *Biochem J,* 327 (Pt 3)**,** 859-65.

LI, C., LIU, C., NISSIM, I., CHEN, J., CHEN, P., DOLIBA, N., ZHANG, T., DAIKHIN, Y., STOKES, D., YUDKOFF, M., BENNETT, M. J., STANLEY, C. A., MATSCHINSKY, F. M. & NAJI, A. 2013a. Regulation of glucagon secretion in normal and diabetic human islets by γ-hydroxybutyrate and glycine. *J Biol Chem,* 288**,** 3938-51.

LI, N., HILL, K. S. & ELFERINK, L. A. 2008. Analysis of receptor tyrosine kinase internalization using flow cytometry. *Methods Mol Biol,* 457**,** 305-17.

LI, N., LU, J. & WILLARS, G. B. 2012. Allosteric modulation of the activity of the glucagon-like peptide-1 (GLP-1) metabolite GLP-1 9-36 amide at the GLP-1 receptor. *PLoS One,* 7**,** e47936.

LI, S., SEITZ, R. & LISANTI, M. P. 1996. Phosphorylation of caveolin by src tyrosine kinases. The alpha-isoform of caveolin is selectively phosphorylated by v-Src in vivo. *J Biol Chem,* 271**,** 3863-8.

LI, Y., CAO, X., LI, L. X., BRUBAKER, P. L., EDLUND, H. & DRUCKER, D. J. 2005. beta-Cell Pdx1 expression is essential for the glucoregulatory, proliferative, and cytoprotective actions of glucagon-like peptide-1. *Diabetes,* 54**,** 482-91.

LI, Z., ZHOU, Z., HUANG, G., HU, F., XIANG, Y. & HE, L. 2013b. Exendin-4 protects mitochondria from reactive oxygen species induced apoptosis in pancreatic Beta cells. *PLoS One,* 8**,** e76172.

LIGHT, P. E., MANNING FOX, J. E., RIEDEL, M. J. & WHEELER, M. B. 2002. Glucagon-like peptide-1 inhibits pancreatic ATP-sensitive potassium channels via a protein kinase A- and ADP-dependent mechanism. *Mol Endocrinol,* 16**,** 2135-44.

LIU, Q. & SCHONBRUNN, A. 2001. Agonist-induced phosphorylation of somatostatin receptor subtype 1 (sst1). Relationship to desensitization and internalization. *J Biol Chem,* 276**,** 3709-17.

LOHSE, M. J., BENOVIC, J. L., CODINA, J., CARON, M. G. & LEFKOWITZ, R. J. 1990. beta-Arrestin: a protein that regulates beta-adrenergic receptor function. *Science,* 248**,** 1547-50.

LOHSE, M. J., ENGELHARDT, S. & ESCHENHAGEN, T. 2003. What is the role of beta-adrenergic signaling in heart failure? *Circ Res,* 93**,** 896-906.

LONGUET, C., BROCA, C., COSTES, S., HANI, E. H., BATAILLE, D. & DALLE, S. 2005. Extracellularly regulated kinases 1/2 (p44/42 mitogen-activated protein kinases) phosphorylate synapsin I and regulate insulin secretion in the MIN6 beta-cell line and islets of Langerhans. *Endocrinology,* 146**,** 643-54.

LU, Z. & XU, S. 2006. ERK1/2 MAP kinases in cell survival and apoptosis. *IUBMB Life,* 58**,** 621-31.

LUTTRELL, L. M. & GESTY-PALMER, D. 2010. Beyond desensitization: physiological relevance of arrestin-dependent signaling. *Pharmacol Rev,* 62**,** 305-30.

LÓPEZ DE MATURANA, R. & DONNELLY, D. 2002. The glucagon-like peptide-1 receptor binding site for the N-terminus of GLP-1 requires polarity at Asp198 rather than negative charge. *FEBS Lett,* 530**,** 244-8.

LÓPEZ DE MATURANA, R., WILLSHAW, A., KUNTZSCH, A., RUDOLPH, R. & DONNELLY, D. 2003. The isolated N-terminal domain of the glucagon-like peptide-1 (GLP-1) receptor binds exendin peptides with much higher affinity than GLP-1. *J Biol Chem,* 278**,** 10195-200.

MACDONALD, P. E., EL-KHOLY, W., RIEDEL, M. J., SALAPATEK, A. M., LIGHT, P. E. & WHEELER, M. B. 2002a. The multiple actions of GLP-1 on the process of glucose-stimulated insulin secretion. *Diabetes,* 51 Suppl 3**,** S434-42.

MACDONALD, P. E., SALAPATEK, A. M. & WHEELER, M. B. 2002b. Glucagon-like peptide-1 receptor activation antagonizes voltage-dependent repolarizing K(+) currents in beta-cells: a possible glucose-dependent insulinotropic mechanism. *Diabetes,* 51 Suppl 3**,** S443-7.

MACLEOD, K. J., HUSAIN, R. D., GAGE, D. A. & AHN, K. 2002. Constitutive phosphorylation of human endothelin-converting enzyme-1 isoforms. *J Biol Chem,* 277**,** 46355-63.

MAECHLER, P. 2012. Mitochondrial signal transduction in pancreatic β-cells. *Best Pract Res Clin Endocrinol Metab,* 26**,** 739-52.

MAGALHAES, A. C., DUNN, H. & FERGUSON, S. S. 2012. Regulation of GPCR activity, trafficking and localization by GPCR-interacting proteins. *Br J Pharmacol,* 165**,** 1717-36.

MAHAVADI, S., BHATTACHARYA, S., KIM, J., FAYED, S., AL-SHBOUL, O., GRIDER, J. R. & MURTHY, K. S. 2013. Caveolae-dependent internalization and homologous desensitization of VIP/PACAP receptor, $VPAC_2$, in gastrointestinal smooth muscle. *Peptides,* 43**,** 137-45.

MANNUCCI, E. & ROTELLA, C. M. 2008. Future perspectives on glucagon-like peptide-1, diabetes and cardiovascular risk. *Nutr Metab Cardiovasc Dis,* 18**,** 639-45.

MATHI, S. K., CHAN, Y., LI, X. & WHEELER, M. B. 1997. Scanning of the glucagon-like peptide-1 receptor localizes G protein-activating determinants primarily to the N terminus of the third intracellular loop. *Mol Endocrinol,* 11**,** 424-32.

MATSUMURA, Y., HISAKI, K., TAKAOKA, M. & MORIMOTO, S. 1990. Phosphoramidon, a metalloproteinase inhibitor, suppresses the hypertensive effect of big endothelin-1. *Eur J Pharmacol,* 185**,** 103-6.

MATSUMURA, Y., IKEGAWA, R., SUZUKI, Y., TAKAOKA, M., UCHIDA, T., KIDO, H., SHINYAMA, H., HAYASHI, K., WATANABE, M. & MORIMOTO, S. 1991. Phosphoramidon prevents cerebral vasospasm following subarachnoid hemorrhage in dogs: the relationship to endothelin-1 levels in the cerebrospinal fluid. *Life Sci,* 49**,** 841-8.

MEIER, J. J., NAUCK, M. A., KRANZ, D., HOLST, J. J., DEACON, C. F., GAECKLER, D., SCHMIDT, W. E. & GALLWITZ, B. 2004. Secretion, degradation, and elimination of glucagon-like peptide 1 and gastric inhibitory polypeptide in patients with chronic renal insufficiency and healthy control subjects. *Diabetes,* 53**,** 654-62.

MELLMAN, I., FUCHS, R. & HELENIUS, A. 1986. Acidification of the endocytic and exocytic pathways. *Annu Rev Biochem,* 55**,** 663-700.

MENEILLY, G. S., GREIG, N., TILDESLEY, H., HABENER, J. F., EGAN, J. M. & ELAHI, D. 2003. Effects of 3 months of continuous subcutaneous administration of glucagon-like peptide 1 in elderly patients with type 2 diabetes. *Diabetes Care,* 26**,** 2835-41.

MINSHALL, R. D., TIRUPPATHI, C., VOGEL, S. M., NILES, W. D., GILCHRIST, A., HAMM, H. E. & MALIK, A. B. 2000. Endothelial cell-surface gp60 activates vesicle formation and trafficking via G(i)-coupled Src kinase signaling pathway. *J Cell Biol,* 150**,** 1057-70.

MOJSOV, S. 1992. Structural requirements for biological activity of glucagon-like peptide-I. *Int J Pept Protein Res,* 40**,** 333-43.

MOJSOV, S., WEIR, G. C. & HABENER, J. F. 1987. Insulinotropin: glucagon-like

peptide I (7-37) co-encoded in the glucagon gene is a potent stimulator of insulin release in the perfused rat pancreas. *J Clin Invest,* 79**,** 616-9.

MONTROSE-RAFIZADEH, C., AVDONIN, P., GARANT, M. J., RODGERS, B. D., KOLE, S., YANG, H., LEVINE, M. A., SCHWINDINGER, W. & BERNIER, M. 1999. Pancreatic glucagon-like peptide-1 receptor couples to multiple G proteins and activates mitogen-activated protein kinase pathways in Chinese hamster ovary cells. *Endocrinology,* 140**,** 1132-40.

MONTROSE-RAFIZADEH, C., YANG, H., RODGERS, B. D., BEDAY, A., PRITCHETTE, L. A. & ENG, J. 1997. High potency antagonists of the pancreatic glucagon-like peptide-1 receptor. *J Biol Chem,* 272**,** 21201-6.

MOORE, C. A., MILANO, S. K. & BENOVIC, J. L. 2007. Regulation of receptor trafficking by GRKs and arrestins. *Annu Rev Physiol,* 69**,** 451-82.

MOORE, M. C., COATE, K. C., WINNICK, J. J., AN, Z. & CHERRINGTON, A. D. 2012. Regulation of hepatic glucose uptake and storage in vivo. *Adv Nutr,* 3**,** 286-94.

MOORE, R. H., TUFFAHA, A., MILLMAN, E. E., DAI, W., HALL, H. S., DICKEY, B. F. & KNOLL, B. J. 1999. Agonist-induced sorting of human beta2-adrenergic receptors to lysosomes during downregulation. *J Cell Sci,* 112 (Pt 3)**,** 329-38.

MORAHAN, G. 2012. Insights into type 1 diabetes provided by genetic analyses. *Curr Opin Endocrinol Diabetes Obes,* 19**,** 263-70.

MULLER, L., BARRET, A., ETIENNE, E., MEIDAN, R., VALDENAIRE, O., CORVOL, P. & TOUGARD, C. 2003. Heterodimerization of endothelin-converting enzyme-1 isoforms regulates the subcellular distribution of this metalloprotease. *J Biol Chem,* 278**,** 545-55.

MULLERSHAUSEN, F., ZECRI, F., CETIN, C., BILLICH, A., GUERINI, D. & SEUWEN, K. 2009. Persistent signaling induced by FTY720-phosphate is mediated by internalized S1P1 receptors. *Nat Chem Biol,* 5**,** 428-34.

MURPHY, J. E., PADILLA, B. E., HASDEMIR, B., COTTRELL, G. S. & BUNNETT, N. W. 2009. Endosomes: a legitimate platform for the signaling train. *Proc Natl Acad Sci U S A,* 106**,** 17615-22.

MURPHY, J. E., ROOSTERMAN, D., COTTRELL, G. S., PADILLA, B. E., FELD, M., BRAND, E., CEDRON, W. J., BUNNETT, N. W. & STEINHOFF, M. 2011. Protein phosphatase 2A mediates resensitization of the neurokinin 1 receptor. *Am J Physiol Cell Physiol,* 301**,** C780-91.

MZHAVIA, N., PAN, H., CHE, F. Y., FRICKER, L. D. & DEVI, L. A. 2003. Characterization of endothelin-converting enzyme-2. Implication for a role in

the nonclassical processing of regulatory peptides. *J Biol Chem,* 278**,** 14704-11.

MÉNARD, L., FERGUSON, S. S., ZHANG, J., LIN, F. T., LEFKOWITZ, R. J., CARON, M. G. & BARAK, L. S. 1997. Synergistic regulation of beta2-adrenergic receptor sequestration: intracellular complement of beta-adrenergic receptor kinase and beta-arrestin determine kinetics of internalization. *Mol Pharmacol,* 51**,** 800-8.

NAOMI, S., IWAOKA, T., DISASHI, T., INOUE, J., KANESAKA, Y., TOKUNAGA, H. & TOMITA, K. 1998. Endothelin-1 inhibits endothelin-converting enzyme-1 expression in cultured rat pulmonary endothelial cells. *Circulation,* 97**,** 234-6.

NAUCK, M. A., HOMBERGER, E., SIEGEL, E. G., ALLEN, R. C., EATON, R. P., EBERT, R. & CREUTZFELDT, W. 1986. Incretin effects of increasing glucose loads in man calculated from venous insulin and C-peptide responses. *J Clin Endocrinol Metab,* 63**,** 492-8.

NIE, Y., NAKASHIMA, M., BRUBAKER, P. L., LI, Q. L., PERFETTI, R., JANSEN, E., ZAMBRE, Y., PIPELEERS, D. & FRIEDMAN, T. C. 2000. Regulation of pancreatic PC1 and PC2 associated with increased glucagon-like peptide 1 in diabetic rats. *J Clin Invest,* 105**,** 955-65.

NISWENDER, K. D. 2011. Basal insulin: beyond glycemia. *Postgrad Med,* 123**,** 27-37.

NOLIN, T. D. 2008. Altered nonrenal drug clearance in ESRD. *Curr Opin Nephrol Hypertens,* 17**,** 555-9.

NOMA, T., LEMAIRE, A., NAGA PRASAD, S. V., BARKI-HARRINGTON, L., TILLEY, D. G., CHEN, J., LE CORVOISIER, P., VIOLIN, J. D., WEI, H., LEFKOWITZ, R. J. & ROCKMAN, H. A. 2007. Beta-arrestin-mediated beta1-adrenergic receptor transactivation of the EGFR confers cardioprotection. *J Clin Invest,* 117**,** 2445-58.

NORMAN, M. U., REEVE, S. B., DIVE, V., SMITH, A. I. & LEW, R. A. 2003. Endopeptidases 3.4.24.15 and 24.16 in endothelial cells: potential role in vasoactive peptide metabolism. *Am J Physiol Heart Circ Physiol,* 284**,** H1978-84.

OAKLEY, R. H., LAPORTE, S. A., HOLT, J. A., BARAK, L. S. & CARON, M. G. 1999. Association of beta-arrestin with G protein-coupled receptors during clathrin-mediated endocytosis dictates the profile of receptor resensitization. *J Biol Chem,* 274**,** 32248-57.

OAKLEY, R. H., LAPORTE, S. A., HOLT, J. A., BARAK, L. S. & CARON, M. G. 2001. Molecular determinants underlying the formation of stable intracellular G protein-coupled receptor-beta-arrestin complexes after receptor endocytosis*. *J Biol Chem,* 276**,** 19452-60.

OAKLEY, R. H., LAPORTE, S. A., HOLT, J. A., CARON, M. G. & BARAK, L. S. 2000. Differential affinities of visual arrestin, beta arrestin1, and beta arrestin2 for G protein-coupled receptors delineate two major classes of receptors. *J Biol Chem,* 275**,** 17201-10.

ORSKOV, C., RABENHØJ, L., WETTERGREN, A., KOFOD, H. & HOLST, J. J. 1994. Tissue and plasma concentrations of amidated and glycine-extended glucagon-like peptide I in humans. *Diabetes,* 43**,** 535-9.

ORZECHOWSKI, H. D., GÜNTHER, A., MENZEL, S., FUNKE-KAISER, H., RICHTER, M., BOHNEMEIER, H. & PAUL, M. 1998. Endothelial expression of endothelin-converting enzyme-1 beta mRNA is regulated by the transcription factor Ets-1. *J Cardiovasc Pharmacol,* 31 Suppl 1**,** S55-7.

ORZECHOWSKI, H. D., GÜNTHER, A., MENZEL, S., ZIMMERMANN, A., FUNKE-KAISER, H., REAL, R., SUBKOWSKI, T., ZOLLMANN, F. S. & PAUL, M. 2001. Transcriptional mechanism of protein kinase C-induced isoform-specific expression of the gene for endothelin-converting enzyme-1 in human endothelial cells. *Mol Pharmacol,* 60**,** 1332-42.

PACHECO-QUINTO, J., HERDT, A., ECKMAN, C. B. & ECKMAN, E. A. 2013. Endothelin-converting enzymes and related metalloproteases in Alzheimer's disease. *J Alzheimers Dis,* 33 Suppl 1**,** S101-10.

PADILLA, B. E., COTTRELL, G. S., ROOSTERMAN, D., PIKIOS, S., MULLER, L., STEINHOFF, M. & BUNNETT, N. W. 2007. Endothelin-converting enzyme-1 regulates endosomal sorting of calcitonin receptor-like receptor and beta-arrestins. *J Cell Biol,* 179**,** 981-97.

PAING, M. M., JOHNSTON, C. A., SIDEROVSKI, D. P. & TREJO, J. 2006. Clathrin adaptor AP2 regulates thrombin receptor constitutive internalization and endothelial cell resensitization. *Mol Cell Biol,* 26**,** 3231-42.

PANTEN, U., SCHWANSTECHER, M. & SCHWANSTECHER, C. 1996. Sulfonylurea receptors and mechanism of sulfonylurea action. *Exp Clin Endocrinol Diabetes,* 104**,** 1-9.

PATEL, T. B. 2004. Single transmembrane spanning heterotrimeric g protein-coupled receptors and their signaling cascades. *Pharmacol Rev,* 56**,** 371-85.

PELAYO, J. C., POOLE, D. P., STEINHOFF, M., COTTRELL, G. S. & BUNNETT, N. W. 2011. Endothelin-converting enzyme-1 regulates trafficking and signalling of the neurokinin 1 receptor in endosomes of myenteric neurones. *J Physiol,* 589**,** 5213-30.

PERFETTI, R. & MERKEL, P. 2000. Glucagon-like peptide-1: a major regulator of pancreatic beta-cell function. *Eur J Endocrinol,* 143**,** 717-25.

PERRY, S. J., BAILLIE, G. S., KOHOUT, T. A., MCPHEE, I., MAGIERA, M. M., ANG, K. L., MILLER, W. E., MCLEAN, A. J., CONTI, M., HOUSLAY, M. D. & LEFKOWITZ, R. J. 2002. Targeting of cyclic AMP degradation to beta 2-adrenergic receptors by beta-arrestins. *Science,* 298**,** 834-6.

PETRIE, J. R. 2013. The cardiovascular safety of incretin-based therapies: a review of the evidence. *Cardiovasc Diabetol,* 12**,** 130.

PINHAS-HAMIEL, O. & ZEITLER, P. 2007. Acute and chronic complications of type 2 diabetes mellitus in children and adolescents. *Lancet,* 369**,** 1823-31.

PIPPIG, S., ANDEXINGER, S., DANIEL, K., PUZICHA, M., CARON, M. G., LEFKOWITZ, R. J. & LOHSE, M. J. 1993. Overexpression of beta-arrestin and beta-adrenergic receptor kinase augment desensitization of beta 2-adrenergic receptors. *J Biol Chem,* 268**,** 3201-8.

PIPPIG, S., ANDEXINGER, S. & LOHSE, M. J. 1995. Sequestration and recycling of beta 2-adrenergic receptors permit receptor resensitization. *Mol Pharmacol,* 47**,** 666-76.

PRESLEY, J. F., MAYOR, S., MCGRAW, T. E., DUNN, K. W. & MAXFIELD, F. R. 1997. Bafilomycin A1 treatment retards transferrin receptor recycling more than bulk membrane recycling. *J Biol Chem,* 272**,** 13929-36.

PUFF, R., DAMES, P., WEISE, M., GÖKE, B., SEISSLER, J., PARHOFER, K. G. & LECHNER, A. 2011. Reduced proliferation and a high apoptotic frequency of pancreatic beta cells contribute to genetically-determined diabetes susceptibility of db/db BKS mice. *Horm Metab Res,* 43**,** 306-11.

PÖLL, F., DOLL, C. & SCHULZ, S. 2011. Rapid dephosphorylation of G protein-coupled receptors by protein phosphatase 1β is required for termination of β-arrestin-dependent signaling. *J Biol Chem,* 286**,** 32931-6.

QUALMANN, C., NAUCK, M. A., HOLST, J. J., ORSKOV, C. & CREUTZFELDT, W. 1995. Insulinotropic actions of intravenous glucagon-like peptide-1 (GLP-1) [7-36 amide] in the fasting state in healthy subjects. *Acta Diabetol,* 32**,** 13-6.

QUOYER, J., LONGUET, C., BROCA, C., LINCK, N., COSTES, S., VARIN, E., BOCKAERT, J., BERTRAND, G. & DALLE, S. 2010. GLP-1 mediates antiapoptotic effect by phosphorylating Bad through a beta-arrestin 1-mediated ERK1/2 activation in pancreatic beta-cells. *J Biol Chem,* 285**,** 1989-2002.

RAFIQ, I., KENNEDY, H. J. & RUTTER, G. A. 1998. Glucose-dependent translocation of insulin promoter factor-1 (IPF-1) between the nuclear periphery and the nucleoplasm of single MIN6 beta-cells. *J Biol Chem,* 273**,** 23241-7.

RAJAGOPAL, S., RAJAGOPAL, K. & LEFKOWITZ, R. J. 2010. Teaching old

receptors new tricks: biasing seven-transmembrane receptors. *Nat Rev Drug Discov,* 9**,** 373-86.

RAPACCIUOLO, A., SUVARNA, S., BARKI-HARRINGTON, L., LUTTRELL, L. M., CONG, M., LEFKOWITZ, R. J. & ROCKMAN, H. A. 2003. Protein kinase A and G protein-coupled receptor kinase phosphorylation mediates beta-1 adrenergic receptor endocytosis through different pathways. *J Biol Chem,* 278**,** 35403-11.

REAVEN, G. M. 2013. What do we learn from measurements of HOMA-IR? *Diabetologia,* 56**,** 1867-8.

ROLIN, B., DEACON, C. F., CARR, R. D. & AHRÉN, B. 2004. The major glucagon-like peptide-1 metabolite, GLP-1-(9-36)-amide, does not affect glucose or insulin levels in mice. *Eur J Pharmacol,* 494**,** 283-8.

ROOSTERMAN, D., COTTRELL, G. S., PADILLA, B. E., MULLER, L., ECKMAN, C. B., BUNNETT, N. W. & STEINHOFF, M. 2007. Endothelin-converting enzyme 1 degrades neuropeptides in endosomes to control receptor recycling. *Proc Natl Acad Sci U S A,* 104**,** 11838-43.

ROOSTERMAN, D., COTTRELL, G. S., SCHMIDLIN, F., STEINHOFF, M. & BUNNETT, N. W. 2004. Recycling and resensitization of the neurokinin 1 receptor. Influence of agonist concentration and Rab GTPases. *J Biol Chem,* 279**,** 30670-9.

RORSMAN, P. & RENSTRÖM, E. 2003. Insulin granule dynamics in pancreatic beta cells. *Diabetologia,* 46**,** 1029-45.

SAWAMURA, T., KIMURA, S., SHINMI, O., SUGITA, Y., KOBAYASHI, M., MITSUI, Y., YANAGISAWA, M., GOTO, K. & MASAKI, T. 1990. Characterization of endothelin converting enzyme activities in soluble fraction of bovine cultured endothelial cells. *Biochem Biophys Res Commun,* 169**,** 1138-44.

SCHMIDTLER, J., DEHNE, K., ALLESCHER, H. D., SCHUSDZIARRA, V., CLASSEN, M., HOLST, J. J., POLACK, A. & SCHEPP, W. 1994. Rat parietal cell receptors for GLP-1-(7-36) amide: northern blot, cross-linking, and radioligand binding. *Am J Physiol,* 267**,** G423-32.

SCHWEIZER, A., VALDENAIRE, O., NELBOCK, P., DEUSCHLE, U., DUMAS MILNE EDWARDS, J. B., STUMPF, J. G. & LOFFLER, B. M. 1997. Human endothelin-converting enzyme (ECE-1): three isoforms with distinct subcellular localizations. *Biochem J,* 328 (Pt 3)**,** 871-7.

SEINO, S., TAKAHASHI, H., FUJIMOTO, W. & SHIBASAKI, T. 2009. Roles of cAMP signalling in insulin granule exocytosis. *Diabetes Obes Metab,* 11 Suppl

4**,** 180-8.

SELWAY, J., RIGATTI, R., STOREY, N., LU, J., WILLARS, G. B. & HERBERT, T. P. 2012. Evidence that Ca2+ within the microdomain of the L-type voltage gated Ca2+ channel activates ERK in MIN6 cells in response to glucagon-like peptide-1. *PLoS One,* 7**,** e33004.

SHAJAHAN, A. N., TIRUPPATHI, C., SMRCKA, A. V., MALIK, A. B. & MINSHALL, R. D. 2004. Gbetagamma activation of Src induces caveolae-mediated endocytosis in endothelial cells. *J Biol Chem,* 279**,** 48055-62.

SHAPIRO, M. J. & COUGHLIN, S. R. 1998. Separate signals for agonist-independent and agonist-triggered trafficking of protease-activated receptor 1. *J Biol Chem,* 273**,** 29009-14.

SHAPIRO, M. J., TREJO, J., ZENG, D. & COUGHLIN, S. R. 1996. Role of the thrombin receptor's cytoplasmic tail in intracellular trafficking. Distinct determinants for agonist-triggered versus tonic internalization and intracellular localization. *J Biol Chem,* 271**,** 32874-80.

SHEIKH-ALI, M., RAHEJA, P. & BORJA-HART, N. 2013. Medical management and strategies to prevent coronary artery disease in patients with type 2 diabetes mellitus. *Postgrad Med,* 125**,** 17-33.

SHENOY, S. K. 2007. Seven-transmembrane receptors and ubiquitination. *Circ Res,* 100**,** 1142-54.

SHENOY, S. K. 2014. Deubiquitinases and their emerging roles in β-arrestin-mediated signaling. *Methods Enzymol,* 535**,** 351-70.

SHENOY, S. K., BARAK, L. S., XIAO, K., AHN, S., BERTHOUZE, M., SHUKLA, A. K., LUTTRELL, L. M. & LEFKOWITZ, R. J. 2007. Ubiquitination of beta-arrestin links seven-transmembrane receptor endocytosis and ERK activation. *J Biol Chem,* 282**,** 29549-62.

SHENOY, S. K. & LEFKOWITZ, R. J. 2003. Trafficking patterns of beta-arrestin and G protein-coupled receptors determined by the kinetics of beta-arrestin deubiquitination. *J Biol Chem,* 278**,** 14498-506.

SHENOY, S. K. & LEFKOWITZ, R. J. 2005. Receptor-specific ubiquitination of beta-arrestin directs assembly and targeting of seven-transmembrane receptor signalosomes. *J Biol Chem,* 280**,** 15315-24.

SHENOY, S. K., MCDONALD, P. H., KOHOUT, T. A. & LEFKOWITZ, R. J. 2001. Regulation of receptor fate by ubiquitination of activated beta 2-adrenergic receptor and beta-arrestin. *Science,* 294**,** 1307-13.

SHENOY, S. K., MODI, A. S., SHUKLA, A. K., XIAO, K., BERTHOUZE, M., AHN, S., WILKINSON, K. D., MILLER, W. E. & LEFKOWITZ, R. J. 2009. Beta-arrestin-dependent signaling and trafficking of 7-transmembrane receptors is reciprocally regulated by the deubiquitinase USP33 and the E3 ligase Mdm2. *Proc Natl Acad Sci U S A,* 106**,** 6650-5.

SHIVAKUMAR, B. R., WANG, Z., HAMMOND, T. G. & HARRIS, R. C. 2005. EP24.15 interacts with the angiotensin II type I receptor and bradykinin B2 receptor. *Cell Biochem Funct,* 23**,** 195-204.

SIGISMUND, S., WOELK, T., PURI, C., MASPERO, E., TACCHETTI, C., TRANSIDICO, P., DI FIORE, P. P. & POLO, S. 2005. Clathrin-independent endocytosis of ubiquitinated cargos. *Proc Natl Acad Sci U S A,* 102**,** 2760-5.

SINCLAIR, E. M. & DRUCKER, D. J. 2005. Proglucagon-derived peptides: mechanisms of action and therapeutic potential. *Physiology (Bethesda),* 20**,** 357-65.

SINGH, D. K., WINOCOUR, P. & FARRINGTON, K. 2011. Oxidative stress in early diabetic nephropathy: fueling the fire. *Nat Rev Endocrinol,* 7**,** 176-84.

SINGH, S., BHAT, J. & WANG, P. H. 2013. Cardiovascular effects of anti-diabetic medications in type 2 diabetes mellitus. *Curr Cardiol Rep,* 15**,** 327.

SLOOP, K. W., WILLARD, F. S., BRENNER, M. B., FICORILLI, J., VALASEK, K., SHOWALTER, A. D., FARB, T. B., CAO, J. X., COX, A. L., MICHAEL, M. D., GUTIERREZ SANFELICIANO, S. M., TEBBE, M. J. & COGHLAN, M. J. 2010. Novel small molecule glucagon-like peptide-1 receptor agonist stimulates insulin secretion in rodents and from human islets. *Diabetes,* 59**,** 3099-107.

SMALLEY, K. S., KOENIG, J. A., FENIUK, W. & HUMPHREY, P. P. 2001. Ligand internalization and recycling by human recombinant somatostatin type 4 (h sst(4)) receptors expressed in CHO-K1 cells. *Br J Pharmacol,* 132**,** 1102-10.

SMITH, A. I., LEW, R. A., THOMAS, W. G. & TOCHON-DANGUY, N. 2006. Protein Kinase C Regulates the Cell Surface Activity of Endothelin-Converting Enzyme-1. *Int J Pept Res Ther,* 12**,** 291-295.

SMITH, J. M., SALAMANGO, D. J., LESLIE, M. E., COLLINS, C. A. & HEESE, A. 2013. Sensitivity to flg22 is modulated by ligand-induced degradation and de novo synthesis of the endogenous flagellin-receptor FLS2. *Plant Physiol*.

SONODA, N., IMAMURA, T., YOSHIZAKI, T., BABENDURE, J. L., LU, J. C. & OLEFSKY, J. M. 2008. Beta-Arrestin-1 mediates glucagon-like peptide-1 signaling to insulin secretion in cultured pancreatic beta cells. *Proc Natl Acad Sci U S A,* 105**,** 6614-9.

SOWA, M. E., HE, W., WENSEL, T. G. & LICHTARGE, O. 2000. A regulator of G protein signaling interaction surface linked to effector specificity. *Proc Natl Acad Sci U S A,* 97**,** 1483-8.

STEVENS, R. C., CHEREZOV, V., KATRITCH, V., ABAGYAN, R., KUHN, P., ROSEN, H. & WÜTHRICH, K. 2013. The GPCR Network: a large-scale collaboration to determine human GPCR structure and function. *Nat Rev Drug Discov,* 12**,** 25-34.

STOFFERS, D. A., KIEFFER, T. J., HUSSAIN, M. A., DRUCKER, D. J., BONNER-WEIR, S., HABENER, J. F. & EGAN, J. M. 2000. Insulinotropic glucagon-like peptide 1 agonists stimulate expression of homeodomain protein IDX-1 and increase islet size in mouse pancreas. *Diabetes,* 49**,** 741-8.

STONEHAM, C. A., HOLLINSHEAD, M. & HAJITOU, A. 2012. Clathrin-mediated endocytosis and subsequent endo-lysosomal trafficking of adeno-associated virus/phage. *J Biol Chem,* 287**,** 35849-59.

SU, H., HE, M., LI, H., LIU, Q., WANG, J., WANG, Y., GAO, W., ZHOU, L., LIAO, J., YOUNG, A. A. & WANG, M. W. 2008. Boc5, a non-peptidic glucagon-like Peptide-1 receptor agonist, invokes sustained glycemic control and weight loss in diabetic mice. *PLoS One,* 3**,** e2892.

SULLIVAN, S. K., MCGRATH, D. A., GRIGORIADIS, D. & BACON, K. B. 1999. Pharmacological and signaling analysis of human chemokine receptor CCR-7 stably expressed in HEK-293 cells: high-affinity binding of recombinant ligands MIP-3beta and SLC stimulates multiple signaling cascades. *Biochem Biophys Res Commun,* 263**,** 685-90.

SYME, C. A., ZHANG, L. & BISELLO, A. 2006. Caveolin-1 regulates cellular trafficking and function of the glucagon-like Peptide 1 receptor. *Mol Endocrinol,* 20**,** 3400-11.

TAKAHASHI, A., NAGASHIMA, K., HAMASAKI, A., KUWAMURA, N., KAWASAKI, Y., IKEDA, H., YAMADA, Y., INAGAKI, N. & SEINO, Y. 2007. Sulfonylurea and glinide reduce insulin content, functional expression of K(ATP) channels, and accelerate apoptotic beta-cell death in the chronic phase. *Diabetes Res Clin Pract,* 77**,** 343-50.

TAKAHASHI, M., FUKUDA, K., SHIMADA, K., BARNES, K., TURNER, A. J., IKEDA, M., KOIKE, H., YAMAMOTO, Y. & TANZAWA, K. 1995. Localization of rat endothelin-converting enzyme to vascular endothelial cells and some secretory cells. *Biochem J,* 311 (Pt 2)**,** 657-65.

TAKHAR, S., GYOMOREY, S., SU, R. C., MATHI, S. K., LI, X. & WHEELER, M. B. 1996. The third cytoplasmic domain of the GLP-1[7-36 amide] receptor is required for coupling to the adenylyl cyclase system. *Endocrinology,* 137**,**

2175-8.

TALBOT, J., JOLY, E., PRENTKI, M. & BUTEAU, J. 2012. β-Arrestin1-mediated recruitment of c-Src underlies the proliferative action of glucagon-like peptide-1 in pancreatic β INS832/13 cells. *Mol Cell Endocrinol,* 364**,** 65-70.

TANG, W. J. & GILMAN, A. G. 1991. Type-specific regulation of adenylyl cyclase by G protein beta gamma subunits. *Science,* 254**,** 1500-3.

TESMER, J. J. 2009. Structure and function of regulator of G protein signaling homology domains. *Prog Mol Biol Transl Sci,* 86**,** 75-113.

TOBIN, A. B. 2008. G-protein-coupled receptor phosphorylation: where, when and by whom. *Br J Pharmacol,* 153 Suppl 1**,** S167-76.

TOBIN, A. B., WILLARS, G. B., BURFORD, N. T. & NAHORSKI, S. R. 1995. Relationship between agonist binding, phosphorylation and immunoprecipitation of the m3-muscarinic receptor, and second messenger responses. *Br J Pharmacol,* 116**,** 1723-8.

TREJO, J. & COUGHLIN, S. R. 1999. The cytoplasmic tails of protease-activated receptor-1 and substance P receptor specify sorting to lysosomes versus recycling. *J Biol Chem,* 274**,** 2216-24.

TRÜMPER, J., ROSS, D., JAHR, H., BRENDEL, M. D., GÖKE, R. & HÖRSCH, D. 2005. The Rap-B-Raf signalling pathway is activated by glucose and glucagon-like peptide-1 in human islet cells. *Diabetologia,* 48**,** 1534-40.

TSAO, P. I. & VON ZASTROW, M. 2000. Type-specific sorting of G protein-coupled receptors after endocytosis. *J Biol Chem,* 275**,** 11130-40.

TSURUMI, Y., FUJIE, K., NISHIKAWA, M., KIYOTO, S. & OKUHARA, M. 1995. Biological and pharmacological properties of highly selective new endothelin converting enzyme inhibitor WS79089B isolated from Streptosporangium roseum No. 79089. *J Antibiot (Tokyo),* 48**,** 169-74.

TUTTLE, R. L., GILL, N. S., PUGH, W., LEE, J. P., KOEBERLEIN, B., FURTH, E. E., POLONSKY, K. S., NAJI, A. & BIRNBAUM, M. J. 2001. Regulation of pancreatic beta-cell growth and survival by the serine/threonine protein kinase Akt1/PKBalpha. *Nat Med,* 7**,** 1133-7.

UMEKAWA, K., HASEGAWA, H., TSUTSUMI, Y., SATO, K., MATSUMURA, Y. & OHASHI, N. 2000. Pharmacological characterization of a novel sulfonylureid-pyrazole derivative, SM-19712, a potent nonpeptidic inhibitor of endothelin converting enzyme. *Jpn J Pharmacol,* 84**,** 7-15.

UMPIERREZ, G. E. & KITABCHI, A. E. 2003. Diabetic ketoacidosis: risk factors and

management strategies. *Treat Endocrinol,* 2**,** 95-108.

VALDENAIRE, O., LEPAILLEUR-ENOUF, D., EGIDY, G., THOUARD, A., BARRET, A., VRANCKX, R., TOUGARD, C. & MICHEL, J. B. 1999. A fourth isoform of endothelin-converting enzyme (ECE-1) is generated from an additional promoter molecular cloning and characterization. *Eur J Biochem,* 264**,** 341-9.

VAN NESS-OTUNNU, R. & HACK, J. B. 2013. Hyperglycemic crisis. *J Emerg Med,* 45**,** 797-805.

VAZQUEZ, P., RONCERO, I., BLAZQUEZ, E. & ALVAREZ, E. 2005. The cytoplasmic domain close to the transmembrane region of the glucagon-like peptide-1 receptor contains sequence elements that regulate agonist-dependent internalisation. *J Endocrinol,* 186**,** 221-31.

VEMULAPALLI, S., CHIU, P. J., CHINTALA, M. & BERNARDINO, V. 1993. Attenuation of ischemic acute renal failure by phosphoramidon in rats. *Pharmacology,* 47**,** 188-93.

VILSBØLL, T., KRARUP, T., DEACON, C. F., MADSBAD, S. & HOLST, J. J. 2001. Reduced postprandial concentrations of intact biologically active glucagon-like peptide 1 in type 2 diabetic patients. *Diabetes,* 50**,** 609-13.

VILSBØLL, T., KRARUP, T., MADSBAD, S. & HOLST, J. J. 2002. Defective amplification of the late phase insulin response to glucose by GIP in obese Type II diabetic patients. *Diabetologia,* 45**,** 1111-9.

VIRALLY, M., BLICKLÉ, J. F., GIRARD, J., HALIMI, S., SIMON, D. & GUILLAUSSEAU, P. J. 2007. Type 2 diabetes mellitus: epidemiology, pathophysiology, unmet needs and therapeutical perspectives. *Diabetes Metab,* 33**,** 231-44.

WANG, X., ZHOU, J., DOYLE, M. E. & EGAN, J. M. 2001. Glucagon-like peptide-1 causes pancreatic duodenal homeobox-1 protein translocation from the cytoplasm to the nucleus of pancreatic beta-cells by a cyclic adenosine monophosphate/protein kinase A-dependent mechanism. *Endocrinology,* 142**,** 1820-7.

WANG, Y., PENNOCK, S., CHEN, X. & WANG, Z. 2002. Endosomal signaling of epidermal growth factor receptor stimulates signal transduction pathways leading to cell survival. *Mol Cell Biol,* 22**,** 7279-90.

WEHBI, V. L., STEVENSON, H. P., FEINSTEIN, T. N., CALERO, G., ROMERO, G. & VILARDAGA, J. P. 2013. Noncanonical GPCR signaling arising from a PTH receptor-arrestin-Gβγ complex. *Proc Natl Acad Sci U S A,* 110**,** 1530-5.

WEI, Y. & MOJSOV, S. 1995. Tissue-specific expression of the human receptor for

glucagon-like peptide-I: brain, heart and pancreatic forms have the same deduced amino acid sequences. *FEBS Lett,* 358**,** 219-24.

WEISSMAN, A. M., HARFORD, J. B., SVETLIK, P. B., LEONARD, W. L., DEPPER, J. M., WALDMANN, T. A., GREENE, W. C. & KLAUSNER, R. D. 1986. Only high-affinity receptors for interleukin 2 mediate internalization of ligand. *Proc Natl Acad Sci U S A,* 83**,** 1463-6.

WETTERGREN, A., WØJDEMANN, M. & HOLST, J. J. 1998. The inhibitory effect of glucagon-like peptide-1 (7-36)amide on antral motility is antagonized by its N-terminally truncated primary metabolite GLP-1 (9-36)amide. *Peptides,* 19**,** 877-82.

WHALLEY, N. M., PRITCHARD, L. E., SMITH, D. M. & WHITE, A. 2011. Processing of proglucagon to GLP-1 in pancreatic α-cells: is this a paracrine mechanism enabling GLP-1 to act on β-cells? *J Endocrinol,* 211**,** 99-106.

WHITE, M. F. 2003. Insulin signaling in health and disease. *Science,* 302**,** 1710-1.

WIDMANN, C., DOLCI, W. & THORENS, B. 1995. Agonist-induced internalization and recycling of the glucagon-like peptide-1 receptor in transfected fibroblasts and in insulinomas. *Biochem J,* 310 (Pt 1)**,** 203-14.

WIDMANN, C., DOLCI, W. & THORENS, B. 1996a. Desensitization and phosphorylation of the glucagon-like peptide-1 (GLP-1) receptor by GLP-1 and 4-phorbol 12-myristate 13-acetate. *Mol Endocrinol,* 10**,** 62-75.

WIDMANN, C., DOLCI, W. & THORENS, B. 1996b. Heterologous desensitization of the glucagon-like peptide-1 receptor by phorbol esters requires phosphorylation of the cytoplasmic tail at four different sites. *J Biol Chem,* 271**,** 19957-63.

WIDMANN, C., DOLCI, W. & THORENS, B. 1997. Internalization and homologous desensitization of the GLP-1 receptor depend on phosphorylation of the receptor carboxyl tail at the same three sites. *Mol Endocrinol,* 11**,** 1094-102.

WIERNSPERGER, N. F. & BAILEY, C. J. 1999. The antihyperglycaemic effect of metformin: therapeutic and cellular mechanisms. *Drugs,* 58 Suppl 1**,** 31-9; discussion 75-82.

WILLARS, G. & CHALLISS, R. 2011. *Editors "Receptor Signal Transduction Protocols" 3rd Edition,* Methods in Molecular Biology, Humana Press Inc., Totowa, USA.

WOJCIKIEWICZ, R. J. 2004. Regulated ubiquitination of proteins in GPCR-initiated signaling pathways. *Trends Pharmacol Sci,* 25**,** 35-41.

WOOTTEN, D., SAVAGE, E. E., VALANT, C., MAY, L. T., SLOOP, K. W.,

FICORILLI, J., SHOWALTER, A. D., WILLARD, F. S., CHRISTOPOULOS, A. & SEXTON, P. M. 2012. Allosteric modulation of endogenous metabolites as an avenue for drug discovery. *Mol Pharmacol,* 82**,** 281-90.

WOOTTEN, D., SAVAGE, E. E., WILLARD, F. S., BUENO, A. B., SLOOP, K. W., CHRISTOPOULOS, A. & SEXTON, P. M. 2013. Differential activation and modulation of the glucagon-like peptide-1 receptor by small molecule ligands. *Mol Pharmacol,* 83**,** 822-34.

XIAO, K., MCCLATCHY, D. B., SHUKLA, A. K., ZHAO, Y., CHEN, M., SHENOY, S. K., YATES, J. R. & LEFKOWITZ, R. J. 2007. Functional specialization of beta-arrestin interactions revealed by proteomic analysis. *Proc Natl Acad Sci U S A,* 104**,** 12011-6.

XIAO, K., SUN, J., KIM, J., RAJAGOPAL, S., ZHAI, B., VILLEN, J., HAAS, W., KOVACS, J. J., SHUKLA, A. K., HARA, M. R., HERNANDEZ, M., LACHMANN, A., ZHAO, S., LIN, Y., CHENG, Y., MIZUNO, K., MA'AYAN, A., GYGI, S. P. & LEFKOWITZ, R. J. 2010. Global phosphorylation analysis of beta-arrestin-mediated signaling downstream of a seven transmembrane receptor (7TMR). *Proc Natl Acad Sci U S A,* 107**,** 15299-304.

XIAO, Q., JENG, W. & WHEELER, M. B. 2000. Characterization of glucagon-like peptide-1 receptor-binding determinants. *J Mol Endocrinol,* 25**,** 321-35.

XU, D., EMOTO, N., GIAID, A., SLAUGHTER, C., KAW, S., DEWIT, D. & YANAGISAWA, M. 1994. ECE-1: a membrane-bound metalloprotease that catalyzes the proteolytic activation of big endothelin-1. *Cell,* 78**,** 473-85.

YAMASAKI-MANN, M., DEMURO, A. & PARKER, I. 2009. cADPR stimulates SERCA activity in Xenopus oocytes. *Cell Calcium,* 45**,** 293-9.

YANG, E., ZHA, J., JOCKEL, J., BOISE, L. H., THOMPSON, C. B. & KORSMEYER, S. J. 1995. Bad, a heterodimeric partner for Bcl-XL and Bcl-2, displaces Bax and promotes cell death. *Cell,* 80**,** 285-91.

YU, R. & HINKLE, P. M. 1998. Signal transduction, desensitization, and recovery of responses to thyrotropin-releasing hormone after inhibition of receptor internalization. *Mol Endocrinol,* 12**,** 737-49.

ZANDER, M., MADSBAD, S., DEACON, C. F. & HOLST, J. J. 2006. The metabolite generated by dipeptidyl-peptidase 4 metabolism of glucagon-like peptide-1 has no influence on plasma glucose levels in patients with type 2 diabetes. *Diabetologia,* 49**,** 369-74.

ZANDER, M., TASKIRAN, M., TOFT-NIELSEN, M. B., MADSBAD, S. & HOLST, J. J. 2001. Additive glucose-lowering effects of glucagon-like peptide-1 and metformin in type 2 diabetes. *Diabetes Care,* 24**,** 720-5.

ZEN, K., BIWERSI, J., PERIASAMY, N. & VERKMAN, A. S. 1992. Second messengers regulate endosomal acidification in Swiss 3T3 fibroblasts. *J Cell Biol,* 119**,** 99-110.

ZHANG, Z., APSE, K., PANG, J. & STANTON, R. C. 2000. High glucose inhibits glucose-6-phosphate dehydrogenase via cAMP in aortic endothelial cells. *J Biol Chem,* 275**,** 40042-7.

ZIDAR, D. A., VIOLIN, J. D., WHALEN, E. J. & LEFKOWITZ, R. J. 2009. Selective engagement of G protein coupled receptor kinases (GRKs) encodes distinct functions of biased ligands. *Proc Natl Acad Sci U S A,* 106**,** 9649-54.